NUMERICAL MODELING OF GROUNDWATER FLOW IN MULTI LAYER AQUIFERS AT COASTAL ENVIRONMENT

JANUARY, 2009

MUHAMMAD RAMLI

ABSTRACT

Tremendous increasing density of population in coastal area has led to effect the increasing groundwater exploitation to meet water demand. Subsequently, many cities in the world have a highly vulnerability to suffer from seawater intrusion problem. In order to sustain the groundwater supply, the development of groundwater resources requires anticipating this seawater encroachment through a good understanding of the phenomena of freshwater-seawater interface.

Numerical model of finite element method is an efficient and an important tool for this purpose. However, this method is not without shortcoming. Mesh generation is well known as time consuming and formidable task for analysts. Meanwhile, physical system of multi-layer aquifer that has significant influence to the phenomena of the interface requires a huge number of elements to represent it. Furthermore, requirement of fine meshes in suppressing the numerical dispersion and spurious oscillation problem rises the mesh generation to be more difficult task. To overcome the mesh generation difficulty by implementing mesh free method faces problem of the imposition of essential boundary conditions. Therefore, development of code by employing Cartesian mesh system seems more effective. A hybridization of the finite element method and the finite difference method employing Cartesian mesh system has been developed in this study by choosing SUTRA (Version 2003) as a basis of numerical code. This technique acquires two advantages: the mesh generation can be performed easily, and the essential boundary conditions can be imposed simply.

Through understanding the phenomena of the interface, groundwater resources can be assessed and then is used as basic information in groundwater management. The various hydraulic conductance of material present a unique interface form comparing with if it is analyzed by a single layer of aquifer. The implementation of the developed code on a field problem was demonstrated by modeling of groundwater in coastal aquifer at Semarang, Indonesia. Representing of the hydrogeological system considered to employ multi layer aquifers system. The simulation results provide a satisfactory interface form comparing to observed data. Continuing the existing groundwater development policy will produce a more severe intrusion problem on the area. In order to sustain groundwater development, mitigation processes were also proposed with various scenarios. Prevention of the seawater problem on this area is effectively to be carried out by managing of surface recharge and hydraulic barrier.

ACKNOWLEDGMENTS

I gratefully acknowledge financial support from Monbukagusho Scholarships of Japanese Government, which made it possible to pursue study at Kyoto University. The process of research and writing this doctoral thesis accumulated many debts of honor. It is necessary to say that my life in Japan has given me a lot of wonderful memories and experiences that will influence the rest of my life. Many persons have supported me during the time, backed me up by great moral, technical assistance, and financial help.

I am deeply indebted to my honorable advisor, Professor Yuzo OHNISHI, for giving me opportunity to work on this research project, and for all his support, guidance, and help. His encouragement and unfailing support have been most valuable to me during these years. Without those, this dissertation has never been completed.

I would like also to express my gratitude to members of my thesis committee: Professor Hajime MASE and Associate Professor Satoshi NISHIYAMA for their constructive comments, valuable advises and suggestion of this dissertation. I also gratefully acknowledge to Professor Hiroyasu OHTSU, Associate Professor Katsuyuki SUZUKI, Assistant Professor Sin-Ichi Uehara and Assistant Professor Tomofumi KOYAMA for their valuable advises. It is necessary to acknowledge the cheery encouragement and moral support of Mr. Takao YANO, Ms. Eriko ITO, and Ms. Fumiko NOMURA. Warm thanks go to student of Geofront Environmental Engineering Laboratory of Kyoto University for their friendship and support. Special thanks to Dr. Kenji TAKAHASHI and Ms. S. TACHIBANA for their useful data.

Finally, my deepest gratitude goes to my wife, Virta, for doing this journey with me and always encourages me. My life would not be complete without three lovely daughters Khalida, Amirah, and Rhaida. I am also thankful to my families and friends for all their support.

December 25, 2008

Muhammad Ramli

TABLE OF CONTENTS

LIST OF FIGURES

LIST OF TABLES

CHAPTER 1

INTRODUCTION

1.1. GROUNDWATER ISSUES

Groundwater plays numbers of very important roles for environments and economics, supplying approximately one-third of water demand of the world's population. The groundwater provides water for human consumption, irrigation, and industry, particularly where surface water resources are contaminated or restricted in volume. In many countries, the abstraction of the groundwater is growing up due to some advantages of the groundwater to make it a good choice for water supply compared with surface water. However, issues of groundwater quantity and quality have received far less attention than the surface water, particularly in some developing countries. In addition, due to its existence in subsurface, the issues of groundwater are often not a problem arises until it comes to public attention such as quality and quantity degradation, land subsidence, etc.

Like the other water resources, the groundwater is at risk for pollution, even though under natural of hydrological cycle. With surface water infiltration, pollution can be flushed through soil and rock into aquifer from a diffuse source or a point source. Impacts of the pollution reaching on aquifer depend on its chemical concentration, nature of the aquifer, and distance form source to discharge point. Some pollutants may degrade naturally by aquifer matrix when they flow with the groundwater. Others contaminant may persistent and come to the surface again. On the other hand, the contaminant movement may also occur with a rising water table. The rising groundwater level reaching an entrapped the contaminant in unsaturated zone may flow out to bring quality problems to the surface.

Modifying the natural hydro-geological cycle by increasing of human activities may also trigger a number of side effects to the environment. In the groundwater

development area, the increasing of water demand can lead to effects of uncontrolled groundwater exploitation yielding a heavy and a concentrated withdrawal. The abstraction exceeding the local recharge will continue to decline water level over many years and to spread out to a wider area. Consequently, this heavy exploitation produces major changes in the hydraulic head distribution within the aquifer system. Such kind of evidence has been accumulating substantial and widespread drawdown of aquifer water levels in many Asian cities since the early 1980s.

The lowering of the groundwater level will be accompanied with a number of environmental problems. In groundwater study, hydro-geologists mainly concern to three categories of side effect: seawater intrusion, land subsidence, and induced pollution. Severity and frequency of their occurrences depend on the hydro-geological condition summarized in table 1.1.

Table 1.1. Susceptibility of hydrogeological environments to adverse side effects during uncontrolled exploitation (Foster et al., 1998).

Hydrogeological Setting	**Type of Side-Effect**		
	Saline Intrusion	**Land Subsidence**	**Induced Pollution**
Major alluvial formation			
- *Coastal*	**	(some cases)**	**
- *Inland*	(few areas)*	(few cases)*	**
Intermontane valley fill			
- *With lacustrine deposits*	(some areas)**	(most cases)**	*
- *Without lacustrine deposits*	(few areas)*	(few cases)*	*
Consolidated sedimentary aquifers	(some areas)**	---	(few cases)*
Recent coastal limestone	**	---	*
Glacial deposits	---	(few cases)*	*
Weathered basement	---	---	*
Loess-covered plateaus	---	(few cases)*	---

* *occurrence known,*
** *major effects*
--- *not applicable or rare*

Regarding to these three side effects; this study focused on investigation of the seawater intrusion problem related to behavior of freshwater-seawater interface. The seawater intrusion problem constitutes the most common quality impact of inadequately controlled aquifer exploitation in coastal areas. A highly population accommodated in coastal area, in which is approximated 50 % of the world population lives within 60 km of the shoreline (Oude Essink, 2001), increases the groundwater abstraction. The increasing concentration of human settlements, agricultural development, and economics activities in this zone, will impose the shortage of fresh groundwater. Many coastal regions in the world have experienced extensive seawater intrusion resulting in severe deterioration of quality of the groundwater resource. Moreover, the effect of saline intrusion in most aquifer types is quasi-irreversible. Once salinity has diffused into the pore water of fine-grained aquifer matrix, its elution will take decades or centuries, even when a coastward flow of freshwater groundwater is re-established (Foster et al., 1998).

The other issue as trigger of the shortage of groundwater resources is global warming. The global warming could raise sea level by several tens of centimeters in the next fifty years, about one meter in the century, and several meters in the next few centuries by expanding ocean water (Bobba, 1998). Direct influences of sea-level rise on water resources are: new or accelerated coastal erosion; more extensive coastal inundation and higher levels of sea flooding; increases in the landward reach of sea waves and storm surges; seawater intrusion into surface waters and coastal aquifers; and further encroachment of tidal waters into estuaries and coastal river systems (Hay and Mimura, 2005). Combination between the rise of seawater level and the intensive groundwater extraction at coastal aquifer become a serious environmental problem to coastal subsurface water systems around the world.

1.2. PROBLEMS STATEMENT AND RESEARCH OBJECTIVES

Preservation and conservation of the groundwater in coastal zone has become an important issue for a long time ago. Researches have addressed numerous difference approaches in multi development stages of the groundwater study. The complexity of

the problem and the shortcoming of technology remain some unsolved problems. However, a good understanding of basin water balance and of groundwater flow behavior is realized that as one of the basic requirement in the groundwater management. This basic requirement, efficiently and effectively, can be learn by using a numerical model.

Recently, the groundwater modeling has focused on Finite Element Method (FEM) due to some provision comparing with Finite Difference Method (FDM), even though this method is more abstract and difficult to code (Wang and Anderson, 1982). Furthermore, modeling of seawater intrusion phenomena poses an interesting numerical challenge, particularly because the groundwater flow on a system is non-linear problem (Boufadel at al., 1999). Under fully saturated density-dependent flow conditions, the non-linearity in the system arises due to the presence of density in both the groundwater flow and the solute transport. The problem is more complicated in case of variable saturated condition. The non-linear relationship becomes more complex between fluid pressure and moisture content, as well as fluid pressure and unsaturated hydraulic conductivity of the medium. Simulation of these phenomena numerically suffers easily from numerical dispersion. In order to suppress this numerical problem, modelers need to perform simulation by using an enough fine meshes.

The mesh generation for input data of the FEM code is well known as a formidable task and time consuming for analysts. To overcome of the mesh generation proposition, numerous automatic mesh generation codes have been developed. Since the mesh generation codes are often used as “black box” code, integrating of a mesh generation code with other code is sometimes difficult and user gives up control (Person, 2005). In some specific fields, the interest of mesh free method (MFM) has grown rapidly. Despite of the MFM has shown an excellent performance in some fields; this method has not succeeded to replace the FEM completely. This is due to the weakness of the MFM in representing a complex shape boundary (Yagawa, 2004), and the necessity of a special technique in imposing of an essential boundary condition (Park and Youn, 2001; Babuska and Melenk, 1997).

With regard to above-mentioned problems on the numerical modeling, the first objective of this study is to develop a simple and a practical code. A new numerical

code of Finite Element Method (FEM) integrated with code of automatic mesh generation has been created. This developed code can accomplished two advantages:

a. The mesh can be generated easily; particularly for practical modeling of variable density groundwater flow that may need some mesh adjustment to avoid numerical dispersion.
b. The essential boundary conditions can be imposed in a simple way. Since this method employ conventional finite element, so that the imposition of the boundary condition without a special technique such in mesh free methods.

The second objective is to apply the developed code in constructing a reliable groundwater model of Semarang aquifer. This analysis was based on a variable density of freshwater-seawater interface to predict changes in saltwater intrusion into the groundwater system as effect of the existing groundwater development policy. Since this area has shown a severe seawater encroachment into aquifer during the simulation period, the mitigation of the problem was addressed also in this numerical investigation as the third objective. Numerical investigation is important tool to evaluate various prevention scenarios before implementing in the real condition.

Furthermore, the residents and government of Semarang City can use the results of this study to make decision for long-term water resource management in order to sustain groundwater supply. More generally, the developed code and results of this study may be of value to similar coastal groundwater development area that needs planning for future fresh water requirements.

In spite of the numerical model is realized as the best and an important tool to understand the groundwater flow behavior on a hydrogeological system, their input data associates with high uncertainty. The data requirement on the groundwater flow modeling classified into four categories:

1. Aquifer stress factor; including effective recharge, pumping volume, groundwater-surface water flow exchange, etc that imposed on the model through the boundary conditions.
2. Aquifer strata geometry; that can be determined appropriately by using geological information (maps and cross sections).

3. Hydrogeological parameters; consisting of hydraulic conductivity, storage coefficient, dispersivity, can be obtained based on field observation or interpretation of geological conditions.
4. Main measured variables; are hydraulic head and contaminant concentration.

Performing of simulation by using available data collected from many sources may produce some discrepancy with the real condition. Therefore, for a certain modeling purpose, the simulation requires calibration to ensure that representation of the system can produce the main measured variable with certain of accuracy.

The model calibration is mainly done by adjusting the stress factor of recharge rate and the hydrogeological parameters to produce the field measured values. Setting both recharge rate and the hydrogeological parameters to produce hydraulic head and contaminant concentration cannot be carried out at the same time. Large scales of the hydrogeological parameters values are usually known with even less accuracy than recharge. Consequently, the calibrated quantity is usually for hydrogeological parameter, and recharge must come from other methods (Kinzelbach, 2002). Nevertheless, hydrologists fail to reach an agreement about the most reliable recharge estimation method. Therefore, a part of this thesis provides a short discussion for future studies in representing of recharge rate into a numerical groundwater flow modeling more accurately than the most common technique used by modelers nowadays.

1.3. SCOPE OF RESEARCH

1.3.1. Physical System

Numerical modeling is generally carried out by building a conceptual model of a hydrogeological system through a simplification of field condition. This is due to the limitation of computer memory demand that can be supported by hardware and difficulty in arrangement of hydrogeological data. In many cases, modeling of aquifer in coastal area is simplified as single layer in which may be represented as either homogeneous or heterogeneous layer. When the modeling area composed of multi layer of aquifers with a significant difference in value of hydrogeological parameters,

assuming with single layer of aquifer system may produce a significant discrepancy on numerical approximation comparing to observed field data.

Representing of this complex problem into a modeling task should be based on the geological material layer constructed from a number of borehole data. The characteristics of geological material composing a hydrogeological system related to ability to transmitting groundwater can be categorized, broadly, into aquifers and aquitards. The aquifer has a range of transmissivity value depends on many variables, such as grain size, compaction, coefficient of uniformity, chemical composition, etc. The configuration of alternating these aquifers and aquitards layers can affect the environmental problem in which may be emerged on a groundwater development area. Variation of the parameter values and the discontinuity of the material stratification have an important role for prediction of seawater invasion into coastal aquifer (Frind, 1982; Rastogi and Ukarande, 2002).

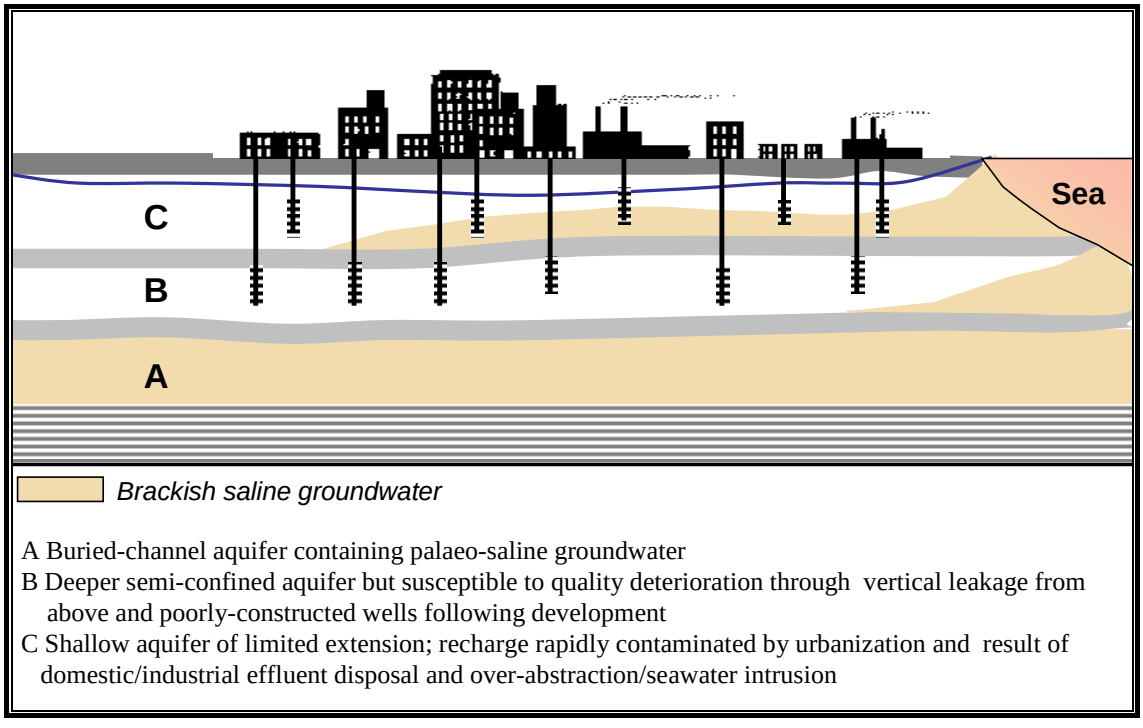

Figure 1.1. The seawater invasion into multi-layer of aquifers due to overexploitation of groundwater resources (modified from Foster et al., 1998).

This study took concern in performing numerical simulation of Semarang coastal aquifer by representing the hydrogeological system in multi layer aquifers. Beside the

layer sequences, the modeling also considered to present the inclination (strike/dip) of the geological stratum according to its existence in the field. This modeling effort differs from other modeling work in which simplification of the geological stratum as a horizontal layer, because difficulty in mesh generation particularly for 3D-model. Therefore, numerical code development accommodated problems of technique of data preparation for numerical simulation (described in the next section). The important to represent the hydrogeological system as multi layer of material is illustrated in figure (1.1) with a coastal area has three layers of aquifer. The seawater intrusion on these aquifers shows different depth of invasion for each aquifer. This figure (1.1) reflects the existence of aquitard between aquifers gives a contrast of interface form to them.

1.3.2. Numerical Code for Seawater Intrusion Problem

Numerous numerical codes of the Finite Element Method for groundwater flow and solute transport have been developed. However, a simple code for mesh generation of Cartesian mesh system that can be integrated directly to the groundwater flow and solute transport code has not been found. Therefore, development of a mesh generation code and modification of a groundwater flow and solute transport code was carried out in this study. Since the Cartesian mesh system is the simplest grid, in which time for meshing is very short and interconnectivity between nodes uses a simple arithmetic operation, this mesh system is applied in this mesh generation code.

The mesh generation code was organized to prepare an easy way for input data on the groundwater flow code. Since the groundwater flow code is rather complicated, integration both code uses loose coupling system. As loose coupling system, the mesh generation code provides some output files that will be used as input files to the numerical groundwater flow code.

Development of the numerical groundwater flow code has chosen SUTRA Version 2003 or SUTRA2D3D (Saturated Unsaturated TRAnsport for 2D and 3D model) as basis code. The SUTRA2D3D (Voss and Provost, 2003) is upgraded code of SUTRA. The SUTRA Version 1984 code regards that it has been accepted over the world and successful in application for various types of seawater intrusion profiles, which was

demonstrated in a large number of publications of Voss and Sousa (Oude Essink, 2001). In this study, the SUTRA2D3D code was modified to enhance ability to perform simulation by using either FEM mesh or Cartesian mesh system. Moreover, the complexity problem that can be solved by the SUTRA2D3D code was, then, simplified for simulating problem of variable saturated-density of groundwater flow only, particularly for seawater intrusion phenomena. The thermal equation that available on the original code was excluded in this modified code.

1.3.3. Groundwater Development System

Groundwater exploitation will increase to follow population growth, particularly in urban area. To assess environmental impact of the exploitation, numerical simulation is widely implemented. In this study, it has also been performed a simulation of the groundwater behavior at Semarang aquifer. Simulation was done by using both 2D-profile model and 3D-model to investigate the dynamic of the freshwater-seawater interface as a response to the existing groundwater development policy. Beside to learn the interface dynamics, the 2D-model also provided some supporting data to the 3D-model. Therefore, the 2D-model was run with a high accuracy to produce calibrated parameters.

Some previous research in this area reported that the seawater intrusion problem has already occurred. Some wells around coastline cannot be used to provide water demand with high salinity concentration. Therefore, in order to sustain groundwater exploitation in this area, prevention technique should be introduced. For this purpose, dynamic of the interface was investigated numerically as an impact of the prevention scheme.

1.3.4. Representing Recharge Rate on Groundwater Modeling

Since there is no agreement among hydrologist about specific method to find out the net recharge reliably, many recharge estimation methods have been developed. A number of stochastic parameters associated with the recharge quantification bring the estimation results ends with different value, and shows that each method has own limitation and

strength. In the groundwater study, the estimation of groundwater recharge based on groundwater level is widely applied (Sophocleous, 2002).

Defining an accurate of recharge estimation result for groundwater flow modeling is an important part in modeling calibration. Moreover, underground flow recharge is mainly underestimated its effect into hydrogeological system by determine the underflow recharge boundary as constant head boundary. This technique is developed by considering that the position of the boundary should be located quite far from the problem interest, so that running model in a period of time will not have a contact with the boundary. However, this procedure may not effective to simulate physical and chemical process on the system. Therefore, this study provides a discussion in handling this problem by integrating recharge estimation model with the groundwater flow model.

1.4. THESIS OUTLINE

The dissertation text is organized into seven chapters including the introductory and the conclusion. Chapter 1 covers the issues of groundwater development in coastal area, problems statements, research objectives, scope of the research, and overview of thesis content.

Chapter 2 gives some literatures review from related prior works, and numerical code development. This chapter is not intended to give a complete revise of the problem in groundwater flow at coastal environment, but it is only to provide standard references of the general idea of the research scope.

In chapter 3 explains code development of the mesh generation, and the groundwater flow and solute transport. The mesh generation code uses Cartesian mesh system for domain discretization. The numerical coding employs variable saturated-density groundwater flow and chooses the SUTRA2D3D code as basis of development. Because some modification on structure of the code and numerical solver was done from the original code, code verification is represented in the end of this chapter.

Verification code considers benchmark problems of Henry's seawater intrusion problem, Elder problem, and Circular Island problem.

Chapter 4 represents the numerical simulation of the groundwater flow at Semarang aquifer in 2D profile and 3D model. The simulation figures out the freshwater-seawater movement as impact of the groundwater development. To ensure ability in representing physical and chemical process within the hydrogeological system, the model was calibrated by using observed data. Sensitivity analysis was also carried out to seek understanding how important each model parameter to the interface dynamics.

Chapter 5 consists of mitigation effort to control seawater intrusion problem. An overview of some prevention techniques that have been successful to be implemented in other places are given here. Concerning to modeling area, prevention methods were designed by considering artificial recharge. This numerical analysis was performed to investigate six prevention schemes.

Chapter 6 describes future study for incorporating recharge estimation model to represent boundary condition for numerical groundwater flow model. This chapter provides some idea about the problem with simple data of field case study.

Finally, chapter 7 gives the overall conclusions of this research.

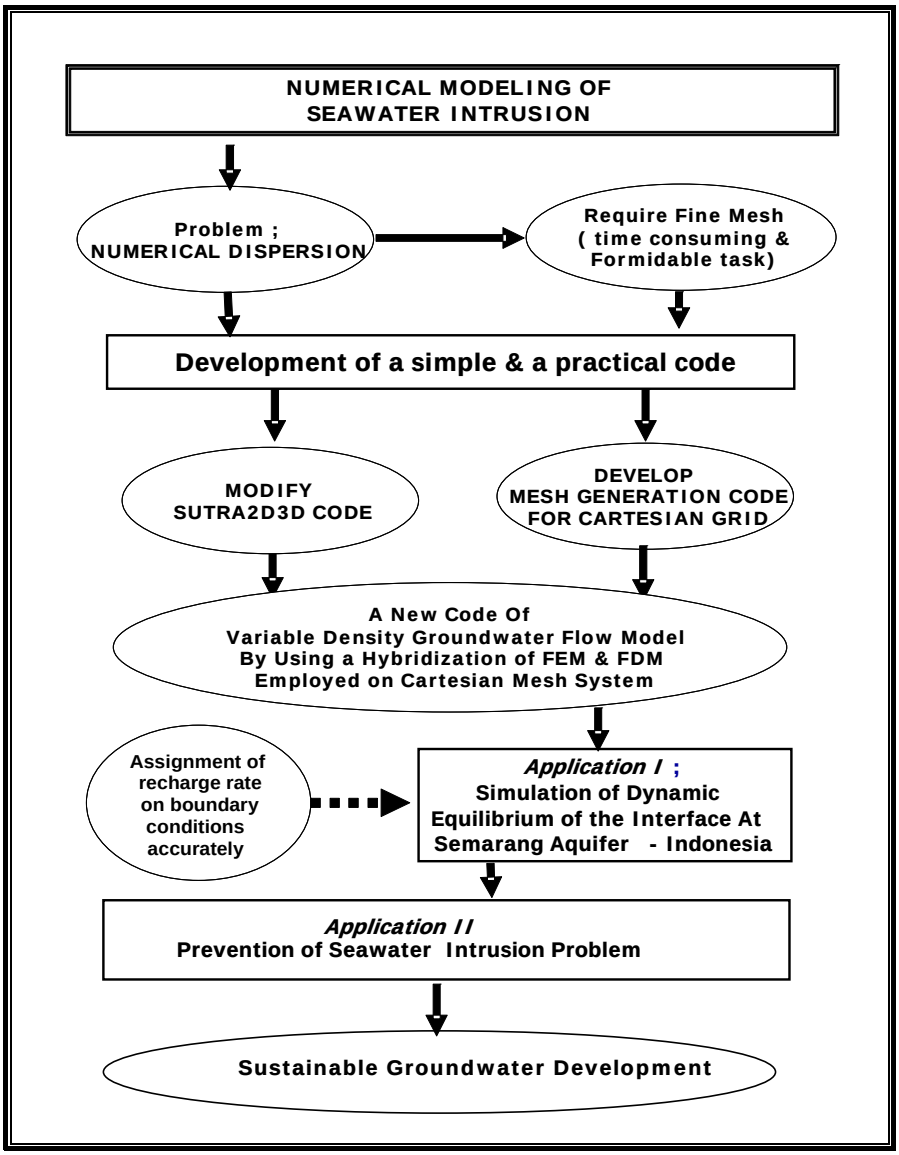

Figure 1.2. Thesis Flowchart.

REFERENCES

Anderson MP., and Woessner MW., 2002, *Applied Groundwater Modeling*, Simulation of flow and advective transport, Academic Press, INC, New York.

Babuska I., and Melenk J.M., 1997, The Partition of Unity Method, *International Journal for Numerical Methods in Engineering*, Vol. 40, pp.727-758.

Bobba, A.G., 1998, Application of a numerical model to predict freshwater depth in islands due to climate change: Agatti island, India, *Journal of Environmental Hydrology,* Vol. 6.

Boufadel, M.C., Suidan, M.T., and Venosa, A.D., 1999, A numerical model for density-and-viscosity-dependent flows in two-dimensional variably saturated porous media, *Journal of Contaminant Hydrology*, Vol. 37, pp. 1-20.

Fetter, C.W., 1992, *Contaminant Hydrogeology*, Macmillan Publishing Company, New York.

Foster S., Lawrence A., and Morris B., 1998, Groundwater in Urban Development, Assessing management needs and formulating policy strategies, *World Bank Technical Paper* No. 390.

Gogu R.C., Carabin G., Hallet V., Peters V., and Dassargues A., 2001, GIS-Based Hydrogeological Databases and Groundwater Modelling, *Hydrogeology Journal*, Springer-Verlag,

Hay, J.E., and Mimura, N., 2005, Sea level rise: Implication for water resources management, *Mitigation and Adaptation Strategies for Global Change*, Vol. 10, pp. 717-737.

Oude Essink G.H.P., 2001, Improving Fresh Groundwater Supply – problems and solutions, *Ocean and Coastal Management* 44 pp 429-449.

Park S.H., and Youn S.K., 2001, The Least-Square Meshfree Method, *International Journal for Numerical Methods in Engineering*, 52, pp. 997-1012.

Persson P.O., 2005, *Mesh Generation for Implicit Geometries*, PhD Thesis Massachusetts Institute of Technology.

Rastogi A.K., and Ukarande S.K., 2002, Parametric studies on the effect of field parameters on seawater intrusion in multi-layered coastal aquifers, *Proceeding of the international groundwater conference on sustainable development and management of groundwater resources in semi-arid region with special reference to hard rocks*, pp. 211-220.

Schwartz F.W., and Zhang H., 2003, *Fundamental of Groundwater*, John Wiley & Sons, Inc, New York.

Tsutsumi A., Jinno K., and Berndtsson R., 2004, Surface and subsurface water balance estimation by the groundwater recharge model and a 3-D two-phase flow model, *Hydrological Sciences*; 49(2), pp. 205-226.

Utomo E.P., and Sudarsono U., 2003, Groundwater resources in Java island, Indonesia, *Proceeding of the international symposium on safe and sustainable exploitation of soil and groundwater resources in Asia*, Okayama University, pp. 61-76.

Voss C.I., and Provost, A.M., 2003, *SUTRA*, A Model for Saturated-Unsaturated Variable-Density Ground-water Flow with Solute or Energy Transport, *Water-Resources Investigation Report* 02-4231, U.S. Geological Survey, published online on internet at http://water.usgs.gov/nrp/gwsoftware.

Wang H.F., and Anderson, MP., 1982, *Introduction to Groundwater Modeling*, W.H Freeman and company, San Fransisco.

Xu Y., and Tonder G.J., 2001, Estimation of recharge using a revised CRD method, *Water SA*, Vol. 27 No. 3.

Yagawa G., 2004, Node-by-Node Parallel Finite Elements; a virtually meshless method, *International Journal for Numerical Method in Engineering*, Vol. 60, pp. 69-102.

Zalik B., Clapworthy G., and Oblosenk C., 1997, An Efficient Code-Based Voxel-Transversing Algorithm, *Computer Graphics Forum*, Vol. 16, no. 2, pp. 119-129.

CHAPTER 2

LITERATURES REVIEW

2.1. GENERAL REMARKS

Modeling of groundwater flow at coastal environment is mainly focused on freshwater-seawater interface behavior. The interface is studied by using two assumptions; sharp form and transition zone. For simplicity, the sharp form of Ghyben-Herzberg relation can be accepted that is based on hydrostatic equilibrium by assuming the interface is formed from the no-mixing fluids; seawater and freshwater. Since the interface at a real condition is a dispersion zone, the sharp approach is too abrupt. The concept of transition zone or variable density is more realistic to be implemented. In the past, the behavior of density dependent groundwater flow has been investigated by analytical models. However, since computational technology appeared, numerical models gained ground.

At present, a large number of numerical code are available, which has capability in handling fresh and saline groundwater flow in aquifer systems. Each of the available code has strength and weakness, so that those available codes are being improved and another code is also coming up. Fortunately, with those available codes, numerous researches of seawater intrusion problem have been published. This chapter provides a brief of literatures review of the basic idea of density dependent flow of groundwater at coastal environment; the existing numerical code; and some related published result from prior works of the numerical simulation of groundwater behavior at coastal aquifers.

2.2. GROUNDWATER IN COASTAL AQUIFER

2.2.1. The Freshwater-Seawater Interface

The understanding of behavior of the freshwater-seawater interaction on aquifer is a substantial requirement in assessment of groundwater resources at coastal zone. Under undisturbed conditions, an equilibrium gradient exists within an aquifer, with excess freshwater discharging to the sea. Within each aquifer, a layered system of variably density of groundwater exists with a wedge of denser saltwater beneath the freshwater and the toe of the wedge pointing inland. This mixing zone between two fluids, sometimes, is called the *zone of diffusion* or the *interface of freshwater-seawater*. The mixing zone is the result of molecular diffusion together with mixing caused by fluctuations of tidal and of fresh water heads.

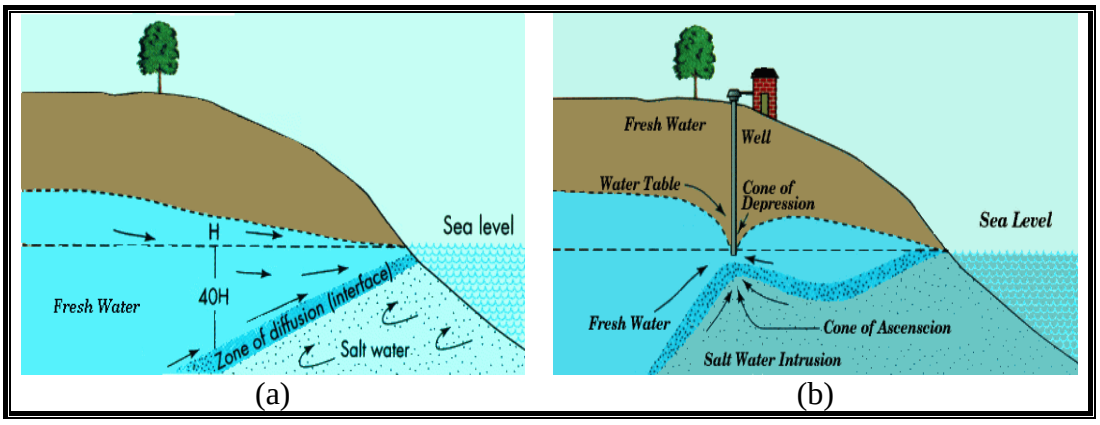

Figure 2.1 Interaction between fresh groundwater and saline seawater. (a) Undisturbed condition, (b) saltwater intrusion due groundwater pumping

The concept of dispersion zone of the interface is formulated with solute transport equation. Its transport mechanism is mainly advection process in which flow of water due to gravity. If density differences occur and the water is stagnant then the less dense water will float on top of the denser water and a horizontal layering will occur. Flowing fresh and/or saline water will create sloping (density) interfaces. Apart from this, molecular diffusion, a movement of ions occurs that is driven by differences in concentrations to smooth concentration gradients. In the case of an interface between fresh and saline water, a transition zone of brackish water will develop.

Flowing water will create dispersion, a mixing process due to the different magnitude and orientation of the velocity vector of groundwater in the pores. On larger scale irregularities, an aquifer has a similar effect (macro dispersion). The displacement of dissolved matter by the dispersion is proportional to the velocity of the groundwater. Both the dispersion and the diffusion have a smoothing influence on differences in concentration. The dispersion and the diffusion are difficult to be distinguished. The joint effect of diffusion in groundwater is taken into account by means of a hydrodynamic dispersion coefficient.

Fresh groundwater recharge travels from recharge area through permeable formations (aquifers) to the sea or ocean. On its way, it may encounter saline aquifers, replacing or mixing with the saline groundwater. The actual distribution of the fresh and the saline groundwater depends on amongst others hydrogeological parameters and the density differences between the liquids. Climatic changes with different rainfall regimes have also influenced salinity. Seas, oceans, lakes, and rivers act mostly as (outflow) boundaries for groundwater systems, so long-term differences in their levels will interfere in the groundwater system.

A persistent reduction in freshwater flow toward the sea reduces the equilibrium gradient, inducing intrusion of saltwater into the aquifers as the freshwater-saltwater interface moves inland. Therefore, although the development of groundwater supply tends to be cost-effective in the short term, sustained overdraft of groundwater can lead to long-term problem. This phenomenon of seawater movement into fresh water aquifers due to natural processes or human activities is known as *seawater intrusion*. The seawater intrusion is caused by decreases in groundwater levels or by rises in seawater levels. The intrusion can affect the quality of water not only at the pumping well sites, but also at other well sites, and undeveloped portions of the aquifer.

Oude Essink (2001a) summarized the factor affecting coastal aquifer shown in figure (2.2). It can be categorized two main processes, natural processes, and human intervention. Natural processes include sedimentation, tectonic movement, and climate change. Human intervention consist of reclamation of coastal areas, impoldering, extraction of groundwater, artificial recharge of groundwater, lowering of groundwater tables, irrigation and drainage, construction of canals, mining etc. In addition, coastal

aquifers within the zone of influence of mean sea level (MSL) are cautioned by an accelerated rise in global MSL that may more vulnerable than they are threatened today.

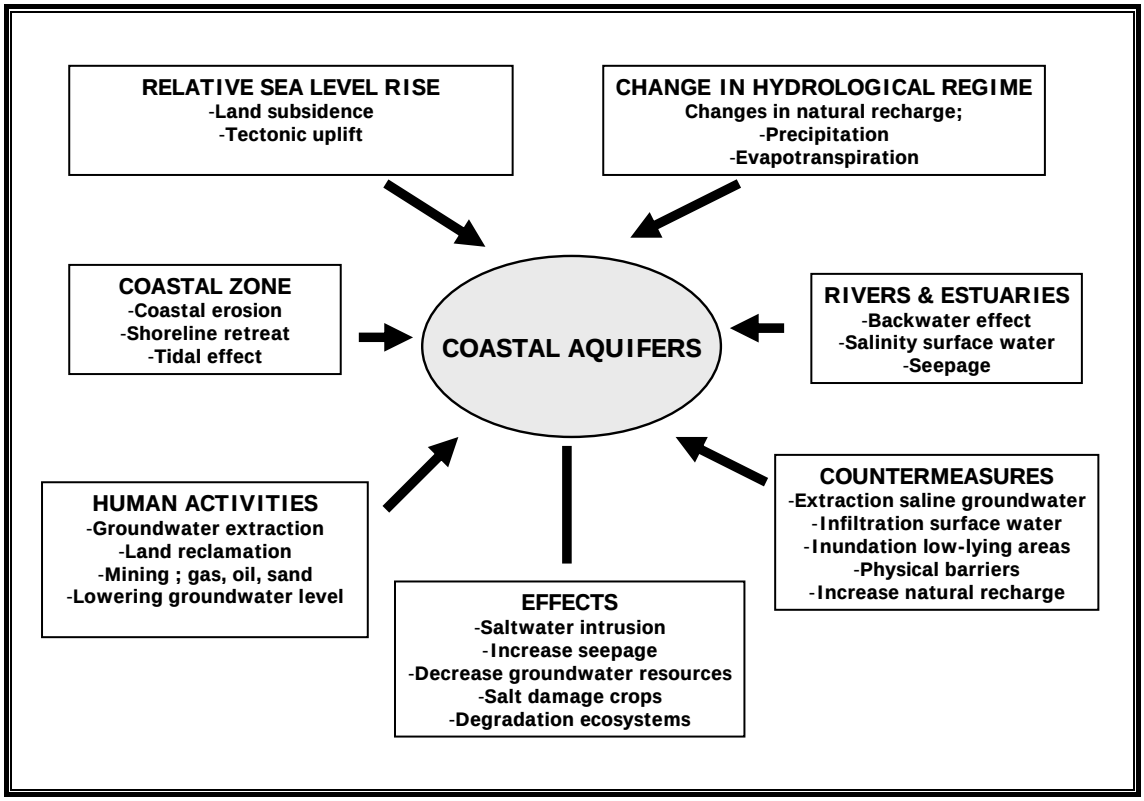

Figure 2.2 Features affecting the coastal aquifers (Oude Essink, 2001a).

2.2.2 Chemical characteristics of water

Mathematical formulation to represent the interface of freshwater-seawater uses density of groundwater. The density is a function of pressure, temperature of the fluid and concentration of dissolved solids stated as follow:

$$\rho = f(p, T, S) \tag{2.1}$$

Where ρ is density [ML^{-3}], p is pressure [MLT^{-2}], T is temperature (^{O}C), and S is salinity or total dissolved solids, TDS, [ML^{-3}].

The influence of pressure can be neglected under the given circumstances for most hydrogeologic systems. Furthermore, the influence of temperature on density is of minor importance with respect to the influence of dissolved solids concentration.

Therefore, the density of groundwater is often only related to the concentration of dissolved solids in the groundwater, whereas the temperature is deliberated to be constant. In general, the quality of groundwater always considers salinity or total dissolved solids (TDS).

The concentration of dissolved solids is subdivided into negative ions (anions) and positive ions (cations). Since chloride (Cl^-) is the predominant negative ion in coastal groundwater, the interest is often focused on its distribution. As a result, simulation of the changes of the chloride distribution means that approximation of all dissolved solids is represented. Obviously, there are vary of classifications of fresh, brackish and saline groundwater based on chloride concentrations. This due to the freshwater term is used according to the purpose of groundwater supply. For instance, the drinking water standard in the European Community equals 150 mg Cl^-/l, the World Health Organization limit to 200 mg Cl^-/l, and Todd gives 100 mg Cl^-/l.

A linear relation between chlorinity and density is mainly stated as follow;

$$\rho(C) = \rho_f \left(1 + \alpha \frac{C_{(i,j)}}{C_s} \right) \qquad (2.2).$$

Where $\rho(C)$ is density of groundwater [ML^{-3}], ρ_f is reference density, usually the density of fresh groundwater (without dissolved solids) at mean subsoil temperature [ML^{-3}], ρ_s is density of saline groundwater at mean subsoil temperature [ML^{-3}], α is $(\rho_s.\rho_f)/\rho_f$ is relative density difference [-], $C_{(i,j)}$ is chloride concentration or the so-called chlorinity [ML^{-3}]. The salinity S is related to the chlorinity C by the formula: C is 0.554 S; C_s is reference chloride concentration [ML^{-3}].

2.3. VARIABLE DENSITY GROUNDWATER FLOW MODEL

2.3.1. Problems of Modeling Dimensions

Numerical modeling of seawater intrusion problem is mainly performed by using two-dimensional (2D) profile model. This 2D-model has been applied for various situations with a number of published papers (Voss and Souza, 1987; Yakirevich et al.,

1999; Sadeg and Karahanoglu, 2001; Sorek et al., 2001; Paritsis, 2005). On undisturbed condition, the groundwater flow perpendicularly to coastline. For such condition, implementation of the 2D-model almost has no shortcoming to produce numerical results accurately. Despite of this 2D-model is quite flexible to apply for various situations; it has some restrictions for practical application.

In groundwater development area, the undisturbed condition has not been existed anymore. A polder area can appear controlling groundwater level yielding a radial flow patterns. Since the 2D-model only cross section that can be simulated, a proper cross section should be carefully selected. For a certain modeling purpose, schematization and modeling by a cross-section may not be allowed any more, but should apply 3D model. However, the 3D model naturally requires even more effort to be understood than the 2D model. The practical application of 3D salt water intrusion model on a broad scale is still at an early stage of development (Oude Essink, 2001b).

The technical problem associated with the 3D-model of saltwater intrusion problem had been highlighted by Oude Essink and Boekelman in Oude Essink, 2001b; Langevin, 2003; Zhang et al., 2004 that are:

1. Problem of data availability.

   A numerical model of seawater intrusion in a coastal hydrogeologic system must be calibrated and verified with available groundwater data to ensure its accuracy and reliability. Simulation by using density dependent flow requires various geological data e.g.: hydraulic conductivity; the effective porosity; the anisotropy; the hydrodynamic dispersion; groundwater extraction rates, and distribution of salinity and piezometric head as a function of space and time. In many cases, reliable and sufficient data are scarce evoking the application of 3D computer codes is restricted seriously. Some common related problems are:

   - The collection of data of hydrogeologic information is mostly obtained from a point source e.g. an observation well (1D) or from a line source (2D), in which must be up-scaled to a 3D distribution of parameters.
   - The calibration of groundwater flow models with salinities changing over time and space is still rather laborious because as a slow process of transport of hydrochemical constituents, it takes some years to monitor the salinity changes.

Unfortunately, these time series are available only occasionally and reliable measurements are scarce in many cases.

2. Problem of computer memory.

   Until some years ago, 3D modeling of salt water intrusion in large-scale coastal hydrogeologic systems was not really possible due to shortcomings in computer capacities. The required number of elements for modeling of large-scale systems is enormous, which may require several hundreds of thousands of elements. However, this situation is changing very fast, by the existing of parallel computation.

3. Problem of numerical dispersion.

   Numerical approximations of the derivatives of the non-linear solute transport equation may introduce truncation errors and oscillation errors (figure 2.3). These errors limit the techniques in solving the partial differential equation. The truncation error has the appearance of an additional dispersion-like term, the so-called *numerical dispersion*, which may dominate the numerical accuracy of the solution. Oscillations may occur in the solution of the solute transport equation as a result of over and undershooting of the solute concentration values. If the oscillation reaches unacceptable values, the solution may become unstable. There is a close relation between numerical accuracy (numerical dispersion) and stability (oscillation). In order to suppress the numerical dispersion and to maintain the stability, the numerical scheme (spatial as well as temporal) should be chosen carefully

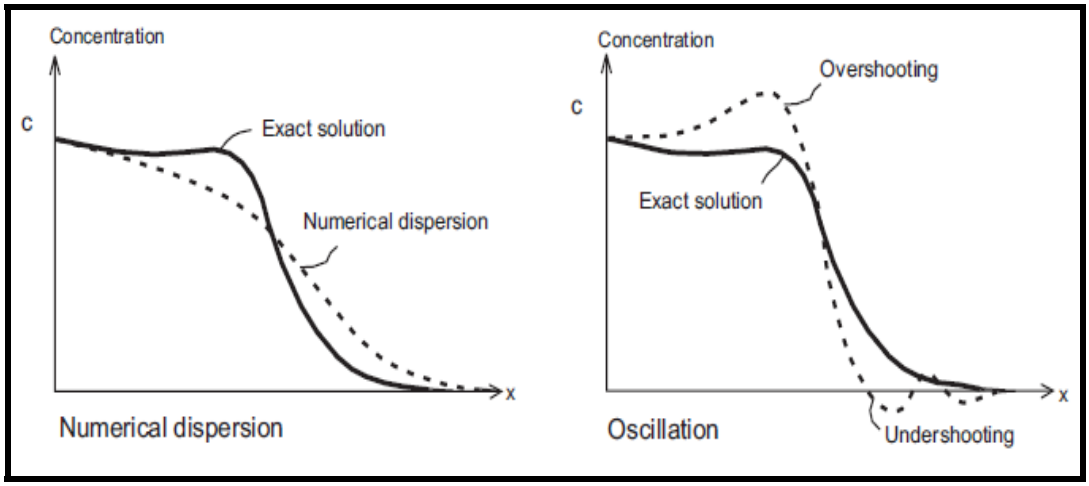

Figure 2.3 Schematisation of numerical dispersion and oscillation (Oude Essink, 2001b)

2.3.2. Some Existing Computer Codes

Reviews of literature of available computer codes and models concerning the fresh and saline groundwater was given by Oude Essink (2001b) based on reviews of Reilly & Goodman ,1985; Custodio *et al.* 1987; and Bear *et al.* 1999. Some reviewed computer codes which can simulate density dependent groundwater flow and solute transport are summarized here.

SUTRA (Saturated Unsaturated TRAnsport) has been applied successfully for the simulation of salt water intrusion in various types of profiles, which is demonstrated in a large number of publications: such as Voss & Souza (1987); Nishikawa (1997); Yakirevich et al., (1998); Sadeg and Karahanoglu (2001). Gradually, SUTRA has become a widely accepted as groundwater flow model throughout the world for simulating two-dimensional of solute transport in density dependent flow at coastal hydrogeologic systems. Basically, this code was developed to simulate density dependent groundwater flow with (thermal) energy transport or chemically reactive (single-species) solute transport. Simulation of groundwater flow system can be done for areal and for cross-sectional modeling of saturated problem, and for cross-sectional modeling of unsaturated flow problem. Numerical approximation employs a weighted residual of Galerkin finite-elements method integrated finite differences method. As SUTRA is a finite element model, the system is represented by nodes and (quadrilateral) elements. The applied temporal discretisation is based on a backward finite-difference approximation for the time derivatives. A unique aspect of SUTRA is the availability of a flow-direction-dependent longitudinal dispersion form (besides the flow-direction-independent form) which allows the longitudinal dispersivity to vary with direction. Nowdays, the new version of SUTRA (Voss and Provost, 2003) has been developed to enhance ability in performing 3D-numerical analysis.

HST3D is a three-dimensional finite difference code that can simulate heat and solute transport. Modelling a large-scale coastal hydrogeologic system with a non-uniform density distribution by using this code seems to be complicated, particularly for small longitudinal dispersivities. Therefore, modeling process requires inserting large dispersivities; otherwise, the solute transport equation does not converge to a solution. As a consequence of simulations with large dispersivities, excessive hydrodynamic

dispersion creates extensive and unrealistic brackish zones which do not agree to the actual situation. For this reason, HST3D is certain to be unsuitable in many cases.

SWICHA is a three-dimensional finite element code for simulating variable density fluid flow and solute transport processes in saturated porous media. The code can be applied from simple one-dimensional to complex three-dimensional problem by coupling flow and solute transport. The governing equations are approximated by the Galerkin technique with employing an implicit Picard iterative scheme to treat the non-linearity of the problems. For a transient simulation, the temporal discretization is handled by using the Crank-Nicolson time step scheme. Spatial discretisation is converged to a solution if a critical Peclet number is exceeded in an element. In order to solve this problem, SWICHA offers a trick to add artificial dispersion to the solute transport equation matrix. This code seems to have difficulty for convergence especially by using small dispersivities.

METROPOL (MEthod for the TRansport Of POLlutants) simulates three-dimensional groundwater flow with varying density and simultaneous transport of contaminants. This code is based on the finite element method developed by the Dutch National Institute of Public Health and Environmental Protection RIVM. The METROPOL has been applied to simulate safety assessments of the geological disposal of radio nuclear waste in (high-brine) salt formations.

SWIFT (Sandia Waste-Isolation Flow and Transport model) is a three-dimensional code for simulating groundwater flow, heat (energy), brine, and radionuclide transport in porous and fractured media. Numerical approximations of the governing equations are solved by using the finite difference method. Modeling with Peclet number greater than 4 may cause problems of oscillations.

FEFLOW is a three-dimensional computer code, which employs the finite element method. The governing partial differential equations describe groundwater flow considering the fluid flow under influence of differences in density. Physical process such as; advection, hydrodynamic dispersion, a simple chemical reactions (e.g. adsorption) are also taken into account.

MOCDENS3D. The three-dimensional computer code MOC3D by Konikow et al.,

1996 is adapted for density differences: MOCDENS3D. This code is applicable to simulate transient model for three-dimensional groundwater flow in a large-scale hydrogeologic systems where non-uniform density distributions occur. The groundwater flow equation is solved by the MODFLOW module of MOCDENS3D. Density differences are taken into account through adding buoyancy terms to the RHS term of the basic groundwater flow equation of MODFLOW. The advection-dispersion equation is solved by the MOC module, using the method of characteristics. An advantage of applying the method of characteristics is that the condition of spatial discretisation is not strict. As a consequence, the displacement of fresh, brackish, and saline groundwater in large-scale hydrogeologic systems can be modeled.

CODESA-3D (COupled variable DEnsity and SAturation) employs a standard finite element Galerkin scheme, with tetrahedral elements and linear basis functions, complemented by weighted finite differences for the discretization of the time derivatives. This code was reviewed by Paniconi et al., 2001. This code uses Crank–Nicolson weighting for both the flow and transport equations, with no mass lumping. Sophisticated algorithms are used to handle the coupling and nonlinearity inherent in the seawater intrusion model and for solving the large sparse systems resulting from discretization and linearization of the model equations. In addition, for computational efficiency dynamic time stepping is implemented to ensure that the code is possibly to use large time steps. The convergence of iterative coupled solution at a given time is provided in term of: fast (time step is increased); intermediate (time step is unaltered); or slow (time step is reduced).

2.4. NUMERICAL SIMULATION OF SEAWATER INTRUSION PROBLEMS

2.4.1. Parametric Study of Seawater Intrusion on Multilayer Aquifers

In order to assess the contamination and plan remedial measures, it is necessary to determine the extent to which ingression of seawater intrusion occurs. Study the phenomenon through field observation is time consuming with a high cost, that in

contrast with performing numerical analysis. The numerical model is capable to predict the interface behavior in the coastal aquifer over a wide range of field condition, in which poses important parameter in developing coastal aquifer management model.

Numerous researches have been done to understand the groundwater behavior and contaminant transport by employing numerical code. It may be performed through a real measured parameter for a specific field problem or general concept of based on parametric studies. However, most of them consider an aquifer as single layer of material, and very few uses multilayer approach. Works of Frind (1982); and Rastogi and Ukarande (2002) can be referred here in which both of them analyzed the phenomena of seawater intrusion based on hypothetical approach employing numerical analysis.

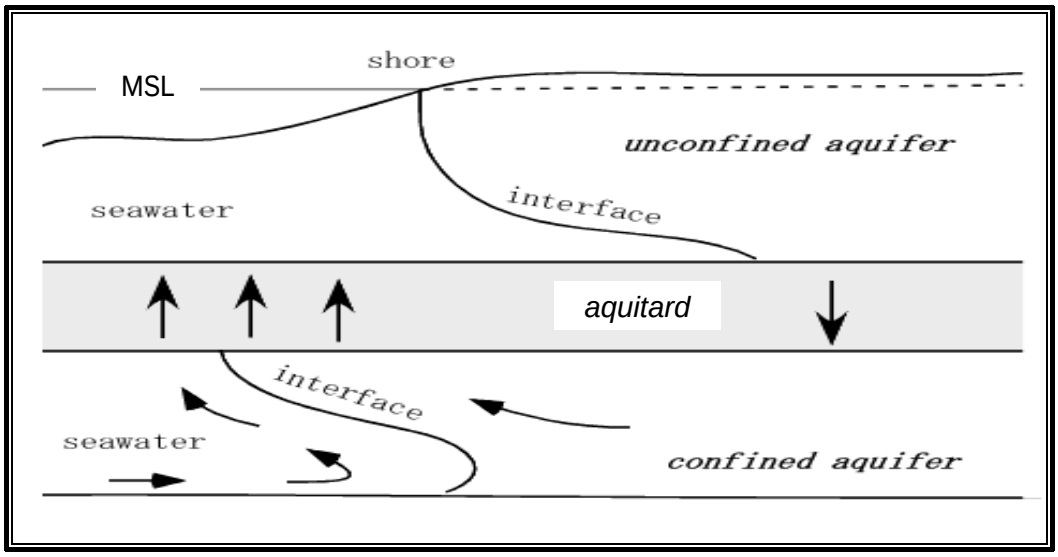

Figure 2.4 Idealized continuous coastal aquifer-aquitard system (Frind, 1982)

Frind (1982) has investigated the influences of aquitard within a continuous system of aquifer-aquitard numerically. Idealized configuration of continuous coastal aquifer-aquitard system is shown in figure (2.4). The system consists of a confined aquifer which is the main water bearing unit, a leaky aquitard, and a thin of unconfined aquifer. Both aquifer and aquitard are continuous and extend under the sea. Permeability contrast between aquifer and aquitard is assumed at least two orders of magnitude, with recharge from landward boundary.

Simulation of this multi-layers aquifer system, Frind showed that the aquitard in a continuous aquifer-aquitard system exerts an important influence in controlling dynamics of the entire system. The influence is most apparent in the large extent of the freshwater discharge face along the aquitard under the sea. The influence of the aquitard also manifests itself in the magnitude of the leakage flux at recharge boundary. Thus, the increase of the hydraulic conductivity of the aquitard resulted in an increase in the total fluid mass circulated through the system.

A difference approach has been also performed by Rastogi and Ukarande (2002) to investigate the effect of field parameters on seawater intrusion in multilayered aquifers. The parameters considered on their study are hydraulic conductivity, dispersivity, molecular diffusion, and hydraulic gradient. Problem domain was taken into consideration is modification of one layer of confined aquifer of the Henry's seawater intrusion problem to be three layers. A number of parameters values were set to observe the interface position. They concluded that except dispersivity all other parameters have significant effect to the seawater intrusion on multi-layered aquifer.

These prior works exhibited that the representation of multi -layer materials arranged the aquifer has a significant influence to result of simulation. However, representation of the complex system by using measured data may become an objection, because the exploration of groundwater measures hydraulic conductivity by pumping test method. This method generalized the aquifer parameter of influence zone to be one value. Therefore, data input to model uses approach values based on literature, and process calibration become very important part to ensure the input data close to field condition.

2.4.2. Prior Works of Field Case Simulation

Seawater intrusion problem has been suffered many area over the world and investigation of the problem has been performed through numerous numerical analysis. Some related prior works in Japan are: Tokaimura coastal plain (Gallardo et al., 2007), in southwestern Kyushu (Don et al., 2005), Konan groundwater basin (Jha et al., 2003), and for other countries can be seen works of Voss and Souza (1987), Yakirevich et al. (1998), Sorek et al. (2001), Zhang et al. (2004), etc. Various different approaches have

been applied to simulate numerical the field problem of the seawater intrusion, from a very simple assumption to a complex model.

By using SUTRA for 2D-model, a number of published numerical results have been presented by Voss and Sousa (1987) such as; variable density flow and solute transport simulation of regional aquifers containing a narrow freshwater-saltwater transition zone. Various field problems have been presented also by using this software with different problem interest from different analysts. The complexity of the hydrogeological system leads to increasing number of studies related to this seawater intrusion modeling.

For most modeling of groundwater flow, representation of the complex hydrogeological system requires to build a conceptual model through a number of simplifications. The effect of the model conceptual design to figure out the interface form was observed by Nishikawa, 1997. Two alternatives of conceptual models for a coastal basin in California were used to test by using a two-dimensional, finite-element groundwater flow and transport model. Both models are characterized by a heterogeneous, layered, and water bearing aquifer. However, the first model is characterized by flat-lying aquifer layers and by a high value of hydraulic conductivity in the basal aquifer layer, which was thought to be a principal conduit for seawater intrusion. The second model is characterized by offshore folding which was modeled as a very near shore outcrop, thereby providing a shorter path for seawater to intrude. The general conclusion from the study that: the aquifer system is best modeled as a flat, heterogeneous, layered system; relatively thin basal layers with relatively high values of hydraulic conductivity are the principal pathways for seawater intrusion; and continuous clay layers of low hydraulic conductivity play an important role in controlling the movement of seawater on that area.

A different approach has been employed by Jha et al., 2003. Their study focused on the effects of tidal fluctuations on groundwater in the Konan groundwater basin of Japan and the methodology for estimating aquifer parameters by the tidal response technique. The field investigation revealed that the two wells near the coastline are significantly affected by seawater intrusion. This study concerned to represent the hydrageological parameter accurately on the modeling to produce a better result. They concluded that

the tidal response technique is effective and reliable for estimating aquifer parameters in the coastal region, and the tidal cycle further triggers the groundwater contamination by seawater intrusion into the basin.

A different view point about the effect of tidal fluctuation has been presented by Zhang et al., (2004) to raise problem of representing of the seaward boundary condition. He argued that management options for controlling seawater intrusion are being explored using numerical modeling, but questions remain concerning the appropriate level of sophistication in models, choice of seaward boundary conditions, and how to accommodate heterogeneity and data uncertainty. The impact of this boundary condition was illustrated for the seawater-intrusion problem in the Gooburrum aquifers. A two-dimensional variable-density groundwater and solute-transport model was constructed using the computer code 2DFEMFAT. Numerical simulations show that the imposition of the commonly used equivalent hydrostatic freshwater heads, combined with a constant salt concentration at the seaward boundary, results in overestimated seawater intrusion in the lower Gooburrum aquifer. Since the imposition of this boundary condition allows water flow across the boundary, a careful check is essential to estimate whether too much mass of salt is introduced. In order to determine the appropriateness of the seaward-boundary condition, the pre-stressed steady-state groundwater condition needs to be achieved with a satisfactory comparison against field evidence. However, obtaining a true steady-state solution for a regional seawater-intrusion problem is computationally expensive. The consideration of the ability of accepting relatively large time-step sizes in selecting a suitable computer code is essential in the modeling. Otherwise, an impractical computational effort or a false steady-state solution may result. However, it is vital to ensure that the true steady-state solution has been achieved to enable to make a correct assessment of the appropriateness of the boundary condition imposed.

Implementation of the 2D modeling in evaluating the groundwater development impact to the aquifer system has been done in many places; two of them are mentioned here in which work of Yakirevich et al. (1999); Sadeg and Karahanoglu (2001); and Sorek et al. (2001). Yakirevich et al. (1999) simulated the effect of the increasing of groundwater abstraction for a certain period at Khan Yunis of the Gaza Strip aquifer. This aquifer is under severe hydrological stress due to over-exploitation, in which excessive pumping

during the past decades has caused a significant lowering of groundwater levels, altering in some regions the normal transport of salts into the sea and reversing the gradient of groundwater flow. Simulations of salt-water intrusion were carried out using a two-dimensional of SUTRA by assuming that pumping rates increase according to the rate of population growth. Numerical simulations show that the results lead to a better understanding of aquifer salinization due to seawater intrusion and give some estimate of the rate of deterioration of groundwater.

Simulation of the field problem is not only performed with the 2D-profile model but also with 2D-areal model. Sorek et al. (2001) presented their study concerning problem of saltwater intrusion in the Khan Yunis portion of the preatic coastal aquifer of Gaza Strip. A two-dimensional (2D) plane model was developed to simulate the groundwater level and the average solute concentration in a 2D horizontal plane, together with the estimation of the saltwater depth. The proposed approach is of particular interest when assessing the effect of different regional pumping scenarios on groundwater level and its quality. By using the calibrated parameter, they investigated predicted results from various regional pumping scenarios using the actual pumping intensity from the year 1985 and extrapolating the increment of pumping rate according to annual population growth. Results showed a considerable depletion of groundwater level and intrusion of seawater due to excessive pumping.

Combination of the 2D-profile and the 2D-areal models has been carried out to assess seawater intrusion problem in Tripoli, Libya (Sadeg et al., 2001). This area suffered from seawater intrusion since 1930s because of groundwater abstraction for the agricultural activity. Hydrogeochemistry of the aquifer system was studied and a numerical assessment of the problem has been accomplished applying a two stage finite element simulation algorithm. First an areal, 2D-model was formulated in order to perform a steady state calibration for the physical parameters and boundary condition of the hydrodynamics system. In the second stage, the mechanism of the seawater intrusion was analyzed using a cross sectional finite element model. Simulation runs have been accomplished to study location of the interface and its temporal migration. Simulation results indicate that the scheme successfully simulates the intrusion mechanism. The simulation can figure out the impact of the continuing of groundwater production policy to migration of the interface leading to a very critical problem.

Improvement of the seawater intrusion modeling was also done by incorporating of hydrogeological process on unsaturated zone. A study focusing on the role of the unsaturated zone in the various mechanisms for surface recharge and in its interaction with the underlying aquifer and the saltwater-freshwater interface at Korba aquifer, Tunisia, has been done by Paniconi et al. (2001). The simulation examined: interplay between pumping regimes and recharge scenarios and its effect on the saline water distribution; and the effects of well location and soil type and the role of the vadose zone in possible remediation actions. This study is basically not pure numerical modeling but integrating with GIS data processing. With the aid of GIS, reasonable and reliable information can be assembled from maps, surveys, and other sources of geospatial and hydrogeological data. Results showed that the GIS and numerical models can be extremely useful tools for water resources management, but require consistent data support, in particular continuous monitoring of relevant parameters and processes.

More complex problem has been analyzed by Don et al. (2005) by incorporating the impact of groundwater extraction with problems of groundwater levels declining, land subsidence, and saltwater encroachment in Shiroishi, Kyushu Area. The study was based on an integration of the modular finite difference groundwater flow model (MODFLOW) and the modular three dimensional finite difference groundwater solute transport model (MT3D). The simulated results from the integrated model show that subsidence rapidly occurs throughout the area with the central prone in the center part of the area. Moreover, seawater intrusion would be expected along the coast if the current rates of groundwater exploitation continue. Sensitivity analysis indicates that certain hydrogeologic parameters such as an inelastic storage coefficient of soil layers significantly contribute effects to both the rate and magnitude of consolidation. In addition, the integrated numerical model is capable of simulating the regional trend of potentiometric levels, land subsidence, and salt concentration.

All above-mentioned problems are corresponded to long term groundwater abstraction. A study concerning the effect of temporary abstraction was evaluated by Gallardo et al. (2007) to investigate the response of groundwater flow and the fresh-saltwater interface in relation to the construction of a particle accelerator at the coastal plain of Tokaimura, Japan. Simulation was done by integrating MODFLOW and MT3DMS to assess the influence the construction on the groundwater flow and the interface zone, covering

three phases of study; analysis of the undisturbed situation, assessment of the effect of groundwater abstraction (dewatering stage); and forecast changes at the transition zone after construction is completed. Numerical results show that the interface has an important migration from predevelopment stage to dewatering phase, and re-establishment of the equilibrium will take 2 years from the end of the dewatering phase. Nonetheless, after construction the accelerator forms a barrier that leads to a sharp rise in piezometric levels and creates a new and long-term disequilibrium in the saltwater wedge. This study made a new contribution to enhance the understanding of the processes occurring in coastal aquifers subjected to anthropogenic influence.

Variable density ground water flow 3D-models are rarely used to evaluate groundwater flow because of limitations in computer speed, data availability, and availability of a simulation tool that can minimize numerical dispersion (Langevin, 2003; Oude Essink, 2001b). However, simulation of the groundwater flow at coastal environment by using 3D-model has also done. Investigation of saltwater intrusion in a three-dimensional large scale coastal aquifer in the northern part of the province Noord-Holland, The Netherlands was presented Oude Essink (2001c). The computer code MOCDENS3D was used to model the displacement of fresh, brackish, and saline groundwater in the hydrogeologic system. The simulation could provide result to gain a better understanding of the problem. It appeared that a severe salinization already occurs that is initiated by the reclamation of the (low-lying) polders during the past centuries. Although seepage quantities decrease in many polder areas due to an increase in salinity, the salt load increases significantly. Langevin, 2003 presented an implementation of the 3D-model by using SEAWAT code, which is a combined version of MODFLOW and MT3D, to estimate rates of submarine ground water discharge to a coastal marine estuary. Hydrologic stresses in the 10-layer model include recharge, evapotranspiration, ground water withdrawals from municipal well-fields, interaction with surface water, boundary fluxes, and submarine ground water discharge to Biscayne Bay. This application demonstrates that regional scale variable density models are potentially useful tools for estimating rates of submarine ground water discharge.

Beside of simulation of the seawater intrusion problem, numerous studies about prevention technique to combat the problem have also done numerically. Sherif and Hamza (2001) investigated a technique to restore the balance between freshwater and

saline water in coastal aquifers. Their design to pumping of brackish water from the dispersion zone and then used to develop green lands in the coastal areas or to irrigate certain types of crops. A two-dimensional finite element model (2D-FEM) of dispersion zone approach has been employed to verify this technique. Simulations were preformed in the vertical view and equi-concentration and equi-potential lines were plotted for different locations of brackish water pumping. In all of the tested runs, the width of dispersion zone has reduced significantly due to brackish water pumping. The quality of the pumped water differs according to the location of pumping.

Narayan et al. (2003) have also investigated numerical of aquifer management practices by including large recharge pits to assist with artificial replenishment of groundwater at Burdekin Delta, North Queensland. The Delta is unique in that it overlies a shallow groundwater system and is close to the Great Barrier Reef. Artificial recharge is used to maintain groundwater levels and subsequently control seawater intrusion. This technique, however, is often costly and ineffective in areas where excessive groundwater pumping occurs. His study was used SUTRA code to define the potential extent of saltwater intrusion in the Burdekin Delta aquifer under various pumping and recharge conditions that was being used in the delta. The results addressed the effects of variations in pumping, and artificial-and-natural recharge rates on the dynamics of saltwater intrusion and showing that the saltwater intrusion is far more sensitive to pumping rates and recharge than aquifer properties such as hydraulic conductivity.

2.5. DISCUSSION

Simulation of the freshwater-seawater interface employing the variable density groundwater flow approach is mainly used in the groundwater modeling. All studies claimed that the performed modeling can established a good representing of the field problem, either the finite element method (FEM) or finite difference method (FDM). However, it seems that the most widely simulation has been carried out by using SUTRA version 1984 that is originally developed for 2D-model either profile or areal model. Nowadays, new version of SUTRA (Voss and Provost, 2003) has been created that is mentioned as SUTRA2D3D in this study, which can be used to simulate problem

of 2D-model and 3D-model. This SUTRA code uses hybridization of the FEM and the FDM gaining advantage to be naturally mass lumping that can avoid oscillatory solution.

Unfortunately, modeling of variable density groundwater flow is well known to suffer easily from numerical dispersion. Analysts come to agreement that it can be suppressed by using a fine mesh. Preparing data of mesh generation to be input of numerical model may take much time, therefore in this study development of new code that can be used to provide data easily and mesh generation can be adjust for short time and simple work. The developed code need to be used to describe the dynamic equilibrium of the modeling area to test the simplicity to perform simulation and the accuracy to represent physical and chemical processes within the system.

REFERENCES

Don, N.C., Araki, H., Yamanishi, H., and Koga, K., 2005, Simulation of groundwater flow and environmental effects resulting from pumping, *Environmental Geology* : 47, pp. 361-374

Frind E.O, 1982, Seawater intrusion in continuous coastal aquifer-aquitard system, *Advanced Water Resources,* Volume 5, pp. 89-97.

Gallardo, A.H., and Marui, A., 2007, Modeling of dynamics of the freshwater-saltwater interface in response to construction activities at a coastal site, *Int. Journal Environmental Sci. Tech.*, 4(3), pp. 285-294.

Jha, M.K., Kamii, Y., and Chikamori, K., 2003, On the estimation of phreatic aquifer parameters by the tidal response technique, *Water Resources Management*: 17, pp. 69-88.

Langevin, C.D., 2003, Simulation of submarine groundwaer discharge to a marine estuary: Biscayne Bay, Florida, *Ground Water*, Vol. 41 No. 6, pp. 758-771

Narayan, K., Schleeberger, C., Charlesworth, P.B., and Bristow, K.L., 2003, Effecto of groundwater pumping on saltwater intrusion in the Lower Burdekin Delta, North Queesland, *CSIRO Land and Water*, Davies Laboratory, Townsville.

Nishikawa, T., 1997, Testing alternative conceptual models of seawater intrusion in a coastal aquifer using computer simulation, Southern California, USA, *Hydrogeology Journal,* Vol. 5, No. 3, pp. 60-74.

Oude Essink G.H.P., 2001a, Improving Fresh Groundwater Supply – problems and solutions*, Ocean and Coastal Management* : 44 pp 429-449.

Oude Essink G.H.P., 2001b, *Density Dependent Groundwater Flow,* Salt Water Intrusion and Heat Transport, Interfaculty Center of Hydrology, Utrech.

Oude Essink, G.H.P., 2001c, Saltwater intrusion in 3D large-scale aquifer: A Dutch Case, *Physical Chemistry Earth (B),* Vol. 26 No. 4, pp. 337-344.

Paniconi, C., Khlaifi, I., Lecca, G., Giacomelli, A., and Tarhouni, J., 2001, Modeling and analysis of seawater intrusion in the coastal aquifer of Eastern Cap-Bon, Tunisia, *Transport in Porous Media,* 43, pp. 3-28.

Paritsis, S.N., 2005, *Simulation of Seawater Intrusion into the Tymbaki Aquifer, South Central Crete, Greece,* Study implemented on behalf of the Department of Management of Water Resources of the Region of Crete, Greece (Report).

Rastogi A.K., and Ukarande S.K., 2002, Parametric studies on the effect of field parameters on seawater intrusion in multi-layered coastal aquifers, *Proceeding of the international groundwater conference on sustainable development and management of groundwater resources in semi-arid region with special reference to hard rocks*, pp. 211-220.

Sadeg, S.A., and Karahanoglu, N., 2001, Numerical assessment of seawater intrusion in the Tripoli Region, Libya, *Environmental Geology,* vol. 40, pp. 1151-1168.

Sherif, M.M., and Hamza, K.I., 2001, Mitigation of seawater intrusion by pumping brackish water, *Transport in Porous Media*, 43, pp. 29-44.

Sorek, S., Borisov, V.S., and Yakirevich, A., 2001, A Two-dimensional areal model for density dependent flow regime, *Transport in Porous Media,* Vol. 43, pp. 87-105.

Voss C.I., and Provost, A.M., 2003, *SUTRA,* A Model for Saturated-Unsaturated Variable-Density Ground-water Flow with Solute or Energy Transport, *Water-Resources Investigation Report* 02-4231, U.S. Geological Survey, published online on internet at http://water.usgs.gov/nrp/gwsoftware.

Voss C.I., and Souza W.R., 1987, Variable Density Flow and Solute Transport Simulation of Regional Aquifers Containing a Narrow Freshwater-Saltwater Transition Zone, *Water Resources Research*, Vol. 23, No. 10, pp.1851-1866.

Yakirevich, A., Melloul, A., Sorek, S., and Shaath, S., 1998, Simulation of seawater intrusion into the Khan Yunis area of the Gaza Strip coastal aquifer, *Hydrogeology Journal:* 6, pp. 549-559.

Zhang, Q., Volker, R.E., and Lockington, D.A., 2004, Numerical investigation of seawater intrusion at Gooburrum, Bundaberg, Queensland, Australia, *Hydrogeology Journal,* Vol. 12, pp. 674-687.

CHAPTER 3

DEVELOPMENT OF NEW NUMERICAL CODE OF VARIABLE DENSITY GROUNDWATER FLOW

3.1. GENERAL REMARKS

This chapter describes development of a new numerical code for simulating couple of groundwater flow and solute transport problems. The groundwater flow problem consists of phenomena at saturated-unsaturated medium, and the solute transport problem emphasize on freshwater-seawater interface. Since these phenomena pose non-linear processes, the numerical dispersion problem becomes main concern in this code development. As a basic requirement to suppress of the numerical problem is that to employ fine meshes in simulation, this code considers to employ a simple mesh generation procedure and directly readable on the groundwater flow code.

In addition, this developed code is going to be applied for a complex problem of hydrogeological system. This due to representation of the complex system by using multilayer aquifer approach will produce a better result of the interface form comparing by simplifying those layers to be single aquifer. For such modeling work, construction of computational grids to represent accurately complex geological structure and stratigraphy poses a formidable task. By incorporating stratigraphy, material properties, boundary conditions, and initial conditions into the numerical model, mesh generation can be more difficult and more time consuming. Moreover, simulation may require modifying the mesh size to represent physical and chemical process without any numerical problem with number of mesh which is able to be supported by the available computer hardware.

Correspond to these aforementioned modeling interests; this research has developed a new FEM code employing Cartesian mesh system. The code development consists of

both automatic mesh generation coding and numerical groundwater flow coding. The automatic mesh generation provides an easy way to input data into the numerical flow code. The numerical flow code is a modification of the SUTRA (Version 2003) software that available online on http://water.usgs.gov/nrp/gwsoftware. The basic code was written by using FORTRAN programming language, but this developed code uses Microsoft visual C++ with numerous modifications to enhance ability in coupling with the mesh generation code. In order to evaluate properness of this developed code, this chapter also demonstrates verification of the numerical groundwater flow code by using several benchmark problems of solute transport.

3.2. MESH GENERATION

3.2.1. Cartesian Mesh System

Since the modeling of the groundwater flow and the solute transport is to solve partial differential equation, continuous physical system of aquifer needs to be discretized into a finite number of points in space. The methods of discretization are usually finite differences, finite volumes, and finite elements, in which use neighboring points to calculate derivatives. In the finite element analysis, the physical domain is mainly meshed with specific shapes of triangles and/or quadrilaterals, without overlapping and gaps. The element connectivity must also be created as requirement on the numerical simulation.

The domain discretization may difficult to fix mesh with a complex real problem. As a result, the complexity is reduced to a manageable geometry. Curved parts of geometry and its boundary may be modeled by using curves and curved surface using high-order elements. However, employing linear elements by using straight lines or flat surface to represent these curves and curved surfaces is most practically approach. The accuracy in representing of the curved parts can be controlled by the number of elements. A finer mesh can give a more accurate representation, but the computer memory demand increases.

A number of researches have been developing meshing techniques to improve accuracy and efficiency. For simplification, the mesh can be summarized into three mesh options shown in figure (3.1).

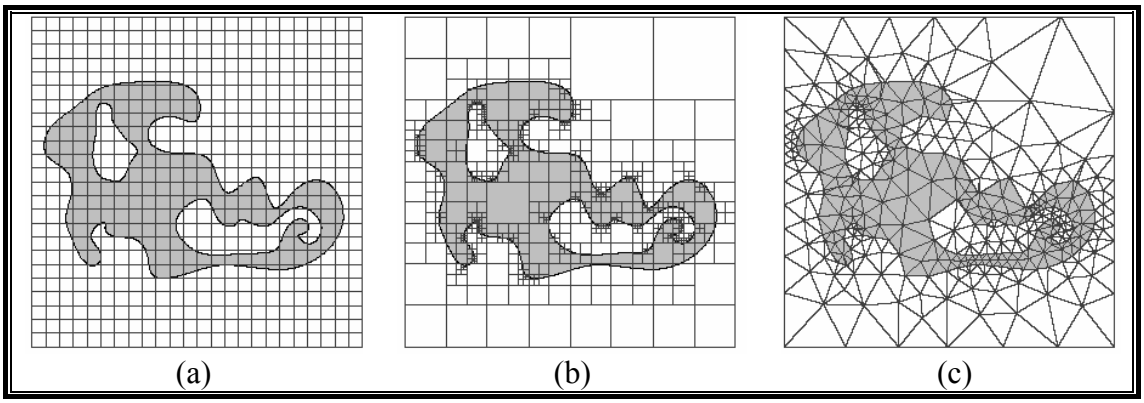

Figure 3.1 Type of mesh for discretization of the distance function and the mesh size function: (a). Cartesian; (b). Octree; and (c) Unstructured mesh (Persson, 2005).

The most simple of mesh type is a Cartesian grid (Figure 3.1a). The advantages of this grid system are very short time for mesh generation time by automatic procedures and simple arithmetic operation. Yet, its disadvantage is incorrect treatment of the geometry shape in a computational domain (Ono et al., 1999). The Cartesian grid locates node points on a uniform grid, and the grid elements are rectangles in two dimensions and blocks in three dimensions.

An alternative is to use an adapted grid, such as an octree structure (Figure 3.1b). The cells are still squares like in the Cartesian grid, but their sizes vary across the region. Since high resolution is only needed close to the boundary, this gives an asymptotic memory requirement proportional to the length of the boundary curve (or the area of the boundary surface in three dimensions). The adapted grid is conveniently stored in an octree data structure. This structured mesh is able to represent the geometry boundary more accurately, but much labor, time consuming and some expertise should be required to make the mesh system with good quality. As a result, this method is not effective for a large size of physical domain.

A third possibility is to discretize using an arbitrary unstructured mesh (Figure 3.1c). This provides the freedom of using varying resolution over the domain, and the

asymptotic storage requirements are similar to the octree grid. An additional advantage with unstructured meshes is that it can be aligned with the domain boundaries, making the projections highly accurate. This can be used to re-meshing an existing triangulation in order to refine, coarsen, or improve the element qualities (mesh smoothing). The unstructured background grid is also appropriate for moving meshes and numerical adaptation, where the mesh from the previous time step (or iteration) is used. The disadvantage of the unstructured mesh system is not always successfully achieved in the practical application, if it is generated by semiautomatic procedures.

The Cartesian grid methods for computational fluid dynamics offer an accurate and robust approach for simulating a complex geometry (Aftosmis, 1997). Because of this flexibility, the quantity of literature devoted to their study has grown substantially in recent years. The Cartesian mesh is not body fitted. Hexahedral cells in the domain consist of a set of right parallelepipeds and the normally orthogonal grid system may extend through solid wall boundaries within computational domain. The method identifies the cells that are completely internal to the geometry, and the remaining cells are considered based on their general volume of elements. The first effort in the computational fluid dynamics relied on structured Cartesian methods focused on the accuracy of spatial operators, and the efficiency of time advancement schemes. There is no embedding meshes and it is frequently used a “stair-cased” description of any geometry in the flow. This scheme is very simple to be implemented.

Most recent implementation focused on representing complex domain accurately. The Cartesian grid is particularly good for implementing level set schemes and fast marching methods. A number of researches have been addressed to this effort, such adaptive mesh refinement, cut mesh, topology optimization, etc. However, in order to solve accurately a complex domain, the entire grid has to be refined. This leads to the number of node points grows quadratically with the resolution (cubically in three dimensions) makes the Cartesian background grid memory consuming for complex geometries. Consequently, this developed mesh generation code uses non-uniform Cartesian grid to reduce the in-accurate treatment of shape boundary.

3.2.2. Structure of Mesh Generation Code

The mesh generation code has been developed by employing Cartesian grid system for 2D and 3D numerical groundwater flow model. The mesh generation code can be integrated with the numerical groundwater flow code by using a loose coupling system. As a loose coupling technique, the mesh code organizes output files according to structure of data requirement of the numerical flow code. Visualization of the generated grid of both 2D and 3D mesh requires GL-View software by using extension file of Virtual Reality Modeling Language (VRML). In addition, the 3D-mesh generation code also provides information for structural contour maps of both top and bottom of each layer of geological material. These structural contour maps are set to be visualized by using Model Viewer software. These supporting software; GL-View and Model Viewer, are available under public domain downloadable on the online internet.

The mesh generation code was formulated under some considerations; such easy and simple in implementation, building and representing volumes from surfaces, distributing nodes within a volume, defining a connectivity of nodes that is compatible with the computational tools being utilized for modeling. It is also provided additional information of initial condition and nodes for assigning boundary conditions.

For simplification of mesh generation process, the code applies concept of background mesh. The idea behind this procedure is simple by storing the function values at a finite set of point x_i (node points) and by using interpolation to approximate the function for arbitrary x. These node points and their connectivity are part of the background mesh. Subsequently, the mesh generation procedure begins by generating a background mesh covering physical domain. Nodes are distributed according to the Cartesian coordinate system (rectangular coordinate system), and connection four nodes (2D-model) and eight nodes (3-D model) in orthogonal direction forms an element. Flow chart for computer coding of this simple procedure is shown in figure (3.2).

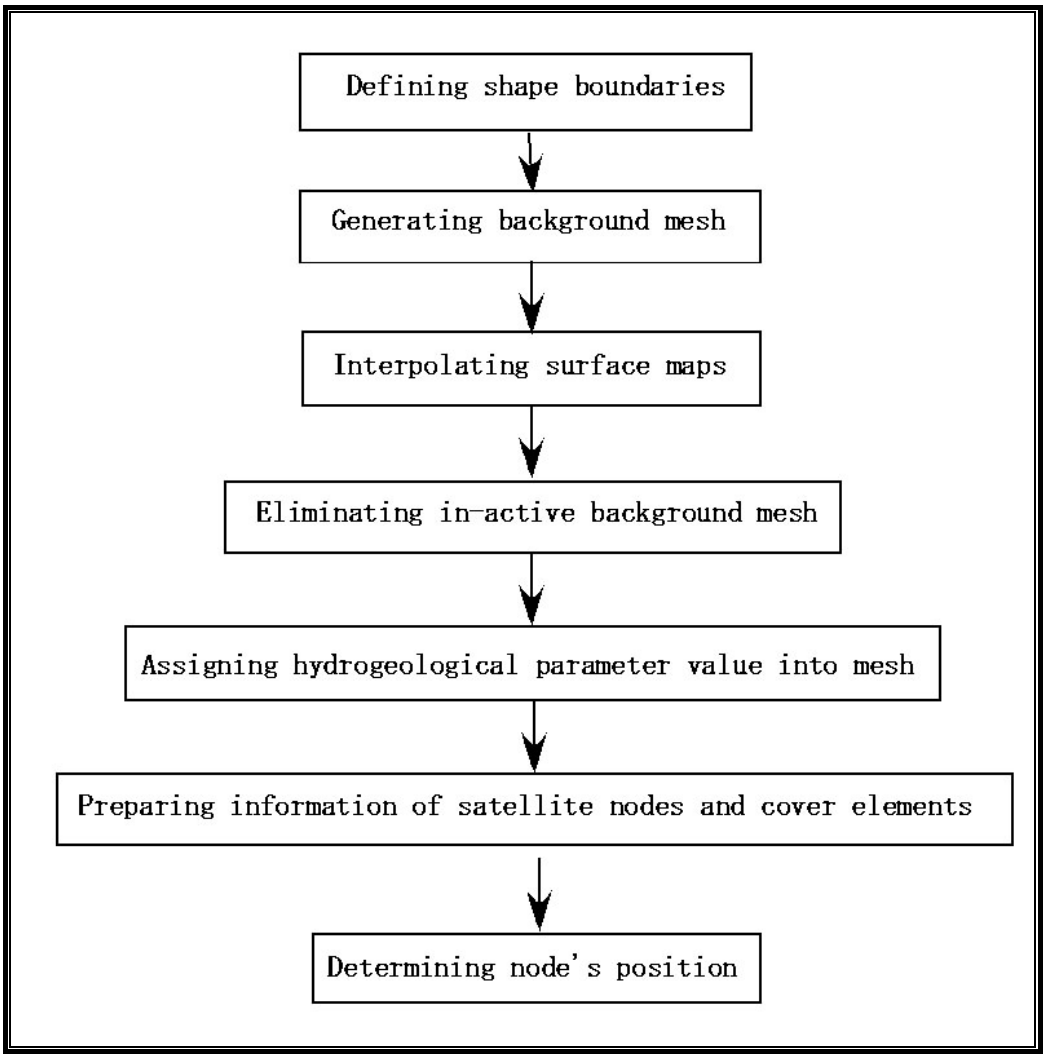

Figure 3.2 Flow chart of mesh generation code.

Defining of background mesh. Background mesh is generated to cover all modeling area or problem domain. The size of mesh needs to be defined at this step. In order to reduce in-accuracy of the Cartesian mesh in treatment shape boundary, the code provides flexibility by allowing the mesh size either in non-uniform or in cubic form, but space on overlapped side must in a same size. User should define the size of background mesh according to modeling requirement. Some additional information, such element connectivity, satellite nodes for each node, nodes within an element, is derived automatically. All these information only a temporary, in which will be modified in the next steps. Application of the three-dimensional Cartesian coordinate system in difference fields, sometimes, emerges a problem. Once the x- and y-axes are specified, they determine the line along which the z-axis should lie, but there are two

possible directions on this line, 'right-handed' and 'left-handed'. This code uses the right-handed system, which is universally accepted.

Surface map generation. After generating background mesh, the next step is to define boundaries of each layer of aquifer. Since the geologic and hydro-geologic information are mostly available in 1D such as well log data, and distributed in an irregular space, the mesh generation requires deriving data of the layers boundaries in a regular space. Deriving the regular data based on the irregular one uses Moving Least Square Method to produce a cross section on the 2D-model, and number structural contour maps of layers boundaries on the 3D-model.

Assignment of hydrogeological parameters. By using Cartesian mesh system, mesh and boundary for every layer cannot be fixed. As a result, it may one mesh covers more than one layer of material. In the input data of these materials, each layer represents a similar hydro-geological values in everywhere within a layer in which may isotropic or anisotropic. In order to assign the hydrogeological parameter on the mesh, space discretization assigns the data requirement of the numerical groundwater flow model by using three approaches: node-wise, cell-wise, and element-wise. The node-wise and the cell-wise are defined at nodes belonging to an element, and the element-wise covers for one element. In simple way, parameter values of each node are determined based on the material type where the node exist, and parameter values of the element-wise depend on position of the central of element. In case an element has one node or two nodes located in outside domain, values of its hydrogeological parameters are assigned as average from other nodes in the same element.

Numerical modeling of the groundwater flow considers representing multi-layer aquifers. Regards to computer memory restriction and data availability, the flow model assumes that the hydrogeological condition of each aquifer layer is homogeneous. Therefore, assigning of hydrogeological parameters in the element-wise just memorize code of material layers to reduce the computer memory demand. Numerous of required hydrogeological parameter in the numerical modeling such as intrinsic permeability (k_{xx}, k_{xy}, k_{xz}, k_{yx}, k_{yy}, k_{yz}, k_{zx}, k_{zy}, k_{zz}), longitudinal dispersivity (αl_{max}, αl_{mid}, αl_{min}), tranversal dispersiivty (αt_{max}, αt_{mid}, αt_{min}), unsaturated parameter, and inclination of material layer (θ_1, θ_2, θ_3) gain a significant in reducing memory demand by this approach, particularly

for a huge number of element. However, the parameters defined by using node (e.g. freshwater pressure head and solute concentration) and cell (e.g. aquifer storativity) approaches are defined for each node.

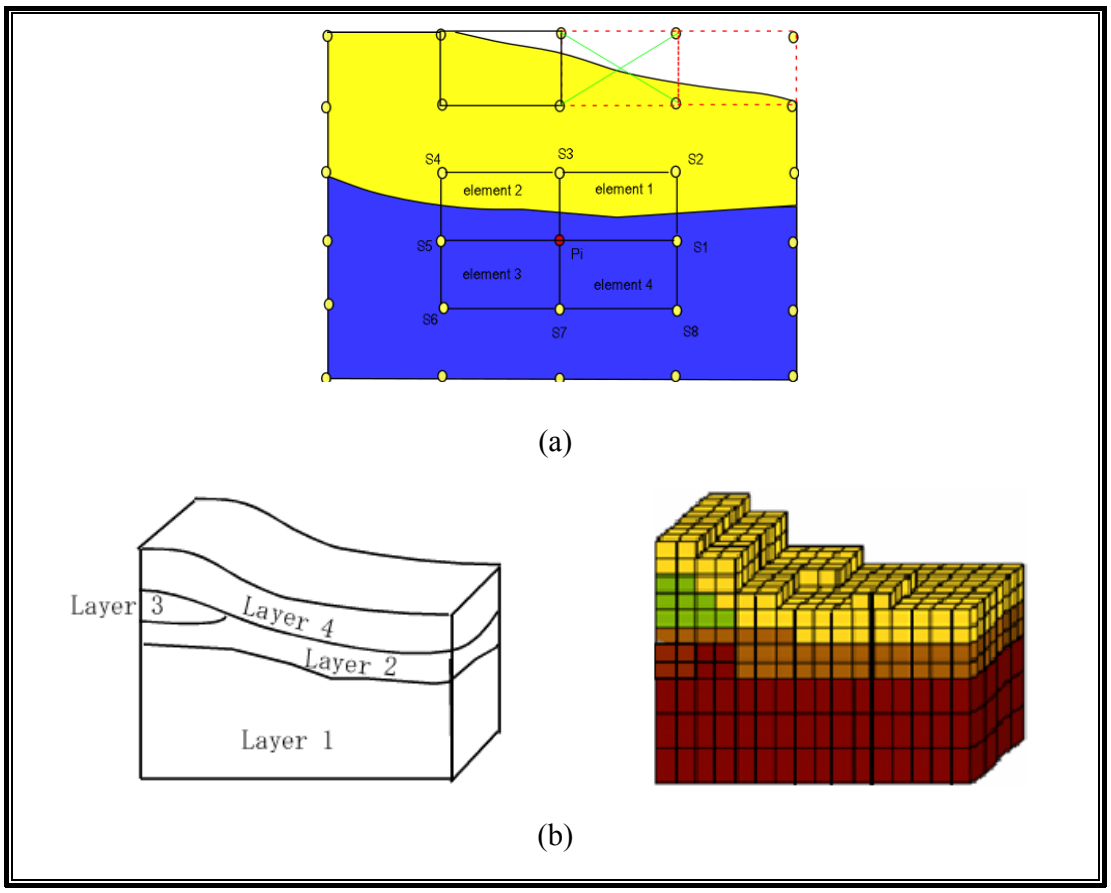

Figure 3.3 An example of generated meshes (a) 2D Mesh (b) 3D Mesh.

Eliminating of in-active elements. After assignment of the hydrogeological parameter to nodes and elements on the background mesh, some nodes and/or meshes may without values then are called in-active nodes and in-active elements. These in-active nodes and in-active elements will be eliminated to reduce memory demand in simulation. The elimination process will be performed automatically.

Fixing of satellite nodes, element connectivity, and nodes information. After eliminating the in-active nodes and the in-active elements, their number is not in a good series. Therefore, the mesh generation code arranges to renumber the active nodes and the active elements. Hence, some action in this part are to re-arrange nodes and elements number, element connectivity, and satellite nodes for each active element.

Preparing of information of boundary nodes. The generated mesh after elimination of the in-active nodes and the in-active elements may form a jagged shape at geometry boundary. As a result, the number of node becomes an irregular series for one direction for physical domain with irregular shape boundary. A big problem will appear in imposition of the essential boundary condition to run the groundwater flow model, in which difficulty to identify the nodes on the boundary. Therefore, this mesh generation code will provide the information in a specific output file to overcome this difficulty. The information is organized into six parts to represent six faces (x, y, z, -x, -y, and –z) of the Cartesian mesh direction.

Implementation of the flowchart at figure (3.2) into computer code is organized into some functions. The main logic flow to the program is straightforward. A schematic diagram of code is shown in figure (3.4). Running this code requires data organized into some input files and output files summarized in table 3.1.

Main function of program code is designed to read input files, to assign output files, and to control mesh generation processes. The functions activated by this main function are gn_info, mt_mesh, nd_cover, and el_active. Descriptions of these functions are;

1. gn_info; The function gives estimation of total of nodes and elements needed to be covered on the computational domain. The estimation is based on the input of modeling area, and the grid space defined by user. When the created nodes and elements over the allocated number on the code, the mesh generation can not be carried out.
2. mt_mesh ; This function generates mathematical mesh or background mesh, and defines nodes at horizontal direction that will be used as control for active grids. The function determines identity number for each node and element, and describes the position of each node and each midpoint of element.
3. nd_cover ; This function assigns output file to describe elements covering each active node defined by the mt_mesh function. The description uses the identity number generated at the background mesh.

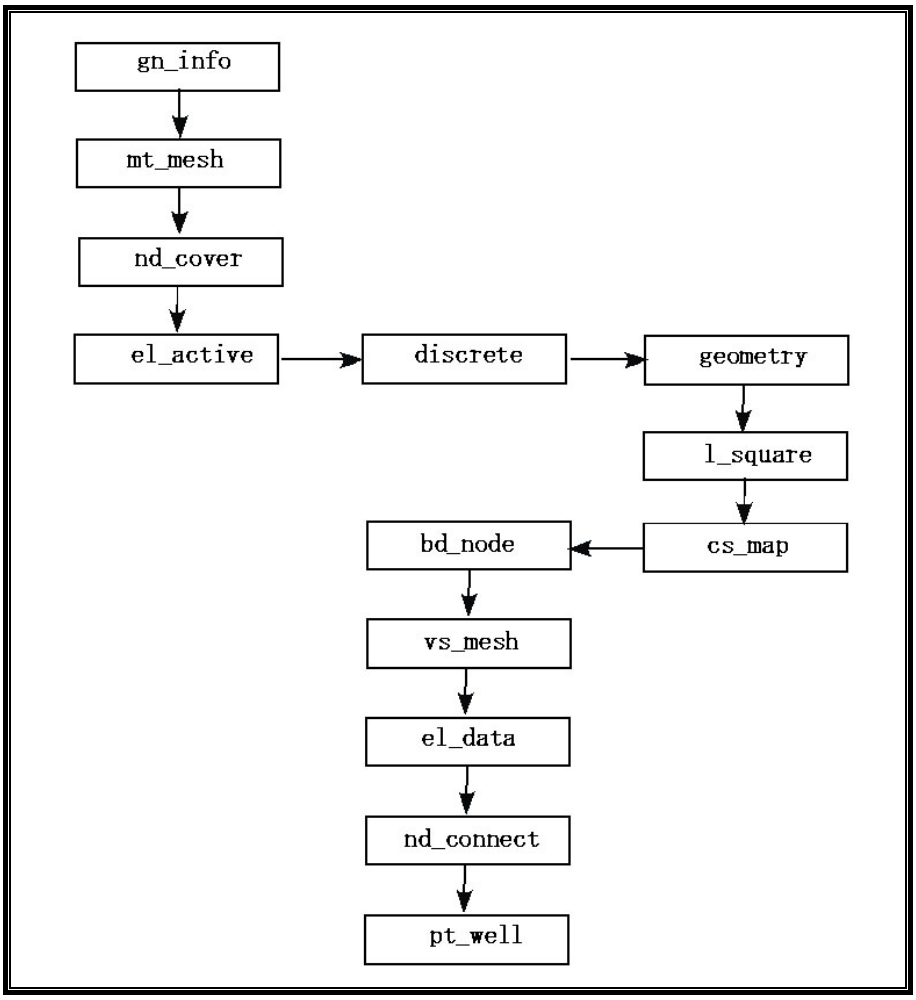

Figure 3.4 Main logic of mesh generation program.

4. el_active ; This function is to organize the active elements and to eliminate the in-active elements, and to re-numbering of the active nodes and the active elements. There are some supporting functions on it described as follow:
   a. discrete; This function fixes the physical domain with the mathematical mesh to define the computational domain. This function activates ;
      - geometry; determines lateral distribution of material layer using linear interpolation based on input data.
      - l_square ; interpolates vertical distribution of material layer by using moving least square method.
      - cs_map ; organizes output data to visualize structural contour maps by using ModView software.

Table 3.1 Summary of input and output files to run the mesh generation code.

File Identity	Functions	Contents
Input files	f_gisfiles f_bground f_mesh	File assignment Background mesh Layer of aquifer's material
Output files	f_well f_info f_grid f_elhd f_incd f_cover f_satl f_bound f_vizual f_map f_obs f_base f_init	Well location General information of the mesh Node position Value of parameter at element Element connectivity Cover for each point Satellite element for each node Node information at shape boundary (3D) Output file for grid visualization Contour of structural map (3D) Fixing well screen position to grid (3D) Node on the lateral distribution (3D) Estimation of initial condition

b. bd_node ; organizes output file containing nodes on boundaries of the computational domain.
c. vs_mesh ; writes output file to visualize generated mesh by using file extension Virtual Real Modeling Language (file.wrl).
d. el_data ; arranges element-wise data required on the groundwater flow model. The information classified into two parts; values of hydrogeological parameter of material of the system, and identity of each element by using material code in the first part.
e. nd_connect ; organizes node incidence data.
f. pt_well ; converts node input of sources and sinks from real position (e.g. well screen position) into fixed points at generated Cartesian mesh on the computational domain.

3.2.3. Moving Least Square Method for Map Generation

The input data of hydrogeologic parameter to model is defined layer by layer. Therefore, surface map for each layer is a necessity to be generated by using data from bore hole. The surface map generation by Moving least square (MLS) method was introduced by Lancaster and Salkauskas for smoothing and interpolating data. The method can be categorized as a method of finite series representation of functions. The MLS method now is a widely used alternative for constructing Mesh Free shape function for approximation. The MLS approximation has two major features that make it popular:

1. The approximated field function is continuous and smooth in the entire problem domain, and
2. Capability produces an approximation with the desired order of consistency.

The moving least square method is employed in the development of mesh generation code to define each layer boundaries creating cross-section for the 2D-model, and yielding structural contour maps for the 3D-model.

Implementation of the moving least square method within a domain *(Ω)* is done by defining *u(x)* to be a function of the field variable, and the approximation of *u(x)* at point *x* is denoted $u^h(x)$. MLS approximation of the field functions is stated as;

$$u^h(x) \approx L_x u(x) = \sum_{i=1}^{n} a_i(x) p_i(x) = p^T(x) a(x) \tag{3.1}$$

Where *n* is the number of terms of monomials (polynomial basis), and *a(x)* is a vector of coefficients given by;

$$a^T(x) = \{\ a_o(x)\ \ a_1(x)\ \ .....\ \ a_n(x)\ \} \tag{3.2}$$

The *p(x)* in equation (3.1) is a vector of basis functions that consists most often of monomials of the lowest orders to ensure minimum completeness. Enhancement functions can be added to achieve better efficiency or to produce stress fields of special characteristics. A complete polynomial basis of order m in 2D space is given by;

$$p^T(x) = p^T(x, y) = \{1, x, y, xy, x^2, y^2, ..., x^n, y^n\} \tag{3.3}$$

Furthermore, the vector of coefficients *a(x)* in equation (3.1) is determined using the function values at a set of nodes that are included in the support domain of *x*. A support domain of a point *x* determines the number of nodes that are used locally to approximate the function value at *x*.

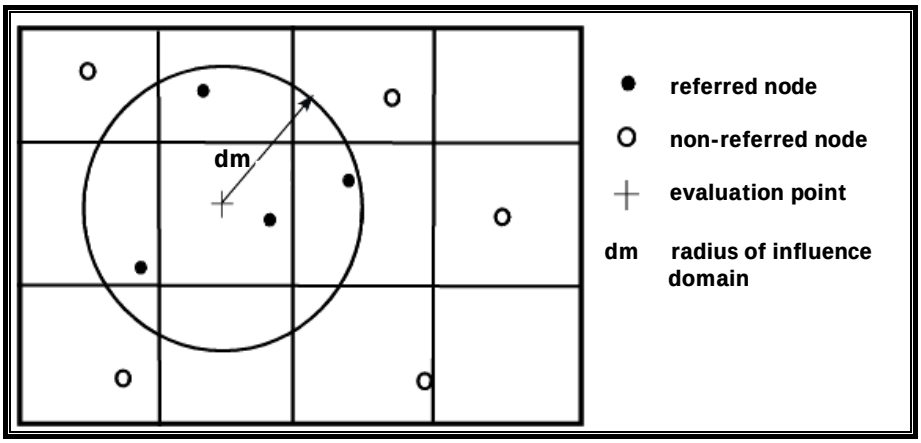

Figure 3.5 Support size of MLS interpolation

Given a set of n nodal values for the field function u^1, u^2, ..., u^n, at *n* nodes x^1, x^2, .., x^n that are in the support domain. Equation (3.1) is then used to calculate the approximated values of the field function at these nodes;

$$u^h(x, x_i) = p^T(x_i)a(x), \qquad i = 1,2,...,n \tag{3.4}$$

Note that *a(x)* here is an arbitrary function of *x*. A functional of weighted residual is constructed by using the approximated values of the field function and nodal parameters, $u_i = u(x_i)$ that are shown in figure (3.6) and formulated as follow;

$$J = \sum_i^n W(x - x^i)\left[u^h(x, x_i) - u(x_i)\right]^2$$

$$= \sum_i^n W(x - x_i)\left[p^T(x_i)a(x) - u_i)\right]^2 \tag{3.5}$$

Where; $W(x-x_i)$ is a weight function, and u_i is the nodal parameter of the field variable at node *i*.

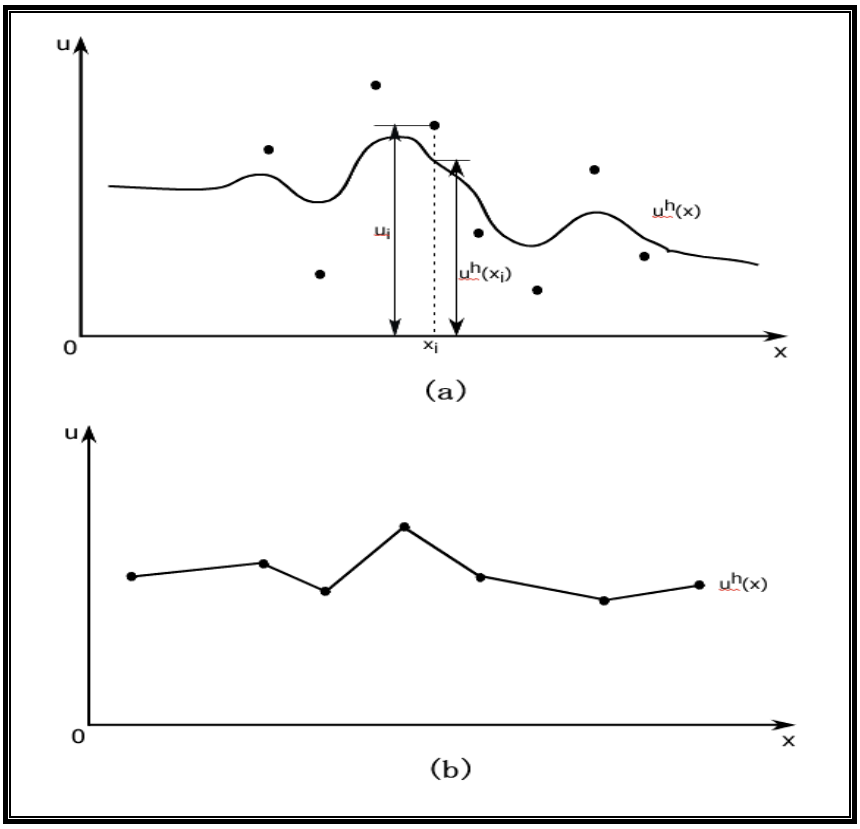

Figure 3.6 The approximation function $u^h(x)$ and the nodal parameters u_i in the MLS approximation.

The weight function used in equation (3.6) plays two important roles in constructing MLS shape functions. The first is to provide weightings for the residuals at different nodes in the support domain. We usually prefer nodes farther from x to have small weights. The second role is to ensure that nodes leave or enter the support domain in a gradual (smooth) manner when *x* moves. The second role of the weight function is very important manner, because it makes sure that the MLS shape functions to be constructed satisfy the compatibility condition.

In the MLS approximation, at arbitrary point *x, a(x)* is chosen to minimize the weighted residual. The minimization condition requires

$$\frac{\partial J}{\partial a} = 0 \tag{3.6}$$

Where the results in the following linear equation system;

$$A(x)a(x) = B(x)U_s \tag{3.7}$$

Where A is called the (weighted) moment matrix given by

$$A(x) = \sum_{I}^{n} W_I(x)\, p(x_I)\, p^T(x_I) \tag{3.8}$$

Where

$$W_I(x) = W(x - x_I) \tag{3.9}$$

In equation (3.7) where the matrix B has the form of;

$$B(x) = \left[B_1, B_2, ..., B_n\right] \tag{3.10}$$

$$B_I = W_I(x)\, p(x) \tag{3.11}$$

And U_s is the vector that collects the nodal parameters of the field variables for all the nodes in the support domain;

$$U_s = \{u_1, u_2, ..., u_n\}^T \tag{3.12}$$

Solving equation (3.7) for *a(x)*, we obtain;

$$a(x) = A^{-1}(x)B(x)U_s \tag{3.13}$$

Substituting the above equation back into equation (3.5) leads to;

$$u^h(x) = \sum_{i}^{n}\sum_{j}^{m} p_j(x)(A^{-1}(x)B(x)_{jI}u_I \tag{3.14}$$

Or

$$u^h(x) = \sum_{I}^{n} \phi_I(x)u_I \tag{3.15}$$

Where the MLS shape function is defined by;

$$\phi_I(x) = \sum_j^m p_j(x)(A^{-1}(x)B(x))_{jI} = p^T A^{-1} B_I \tag{3.16}$$

Note that m is the number of terms of polynomial basis *p(x)*, which is usually much smaller than *m*, which is the number of nodes used in the support domain for constructing the shape function. The requirement of *n>>m* prevents the singularity of the weighted moment matrix, so that A^{-1} exists.

Equation (3.15) can also be written in the following matrix form;

$$u^h(x) = \Phi(x)U_s \tag{3.17}$$

Where *Φ(x)* is the matrix of MLS shape function corresponding to *n* nodes in the support domain;

$$\Phi([x]) = [\phi_1(x), \phi_2(x), ..., \phi_n(x)] \tag{3.18}$$

Some conditions need to be considered in constructing the weight functions given by Monaghan, 1992 (Liu, 2003) as follow;

1. $W(x-\xi, h) > 0 over \Omega$ positivity (3.19)

2. $W(x-\xi == 0 outside \Omega$ compact (3.20)

3. $\int_\Omega W(x-\xi, h)d\xi = 1$ unity (3.21)

4. *W* is a monotonically decreasing function (decay) (3.22)

5. $W(s,h) \longrightarrow \delta(s) ash \longrightarrow 0$ (Delta function behavior) (3.23)

The common of weight functions used in the mesh free method consists of functions; the cubic spline, the quartic spline, and the exponential. The developed code employed the quartic spline weight function that is written as follow;

$$W(x-x_I) \cong W(d) = \begin{cases} 1-6d^2+8d^3-3d^4 & for \quad d \le 1. \\ \\ 0 & for \quad d > 1 \end{cases} \tag{3.24}$$

Where, $$d = \frac{|x-x_I|}{d_W} = \frac{d}{d_w} \tag{3.25}$$

3.2.4. Implementation of the Mesh Generation Code.

An application example of the mesh generation code for 3D model is given in this part through discretizing the coastal aquifer of Bali area, Indonesia. We chose this area because its morphology shows an irregular coastline as physical boundary, a relative uniform of slope gradient to the coast, and simple hydrogeological setting of the system. These conditions bring an easy way to show properness of the implementation of this mesh generation code.

The area has a relatively low level morphology and to the north consists of fairly high mountain range. Geological condition is mainly composed of Bujan-Bratan and Batur volcanic deposits, and small alluvium deposits around shoreline. Based on geological information of 32 bore holes on the area, the hydrogeological system can be simplified within three layers of material characteristics; lower aquitard, aquifer, and upper aquitard. The hydrogeological parameters values are assigned for each layer as a homogeneous medium. If the each layer consists of vary of the parameters values, the layer may separated into two layers or more. This example assumed each layer has similar value everywhere within a layer of material.

Discretization of this hydrogeological system creates four maps, bottom of the lower aquitard, top of the lower aquitard or bottom of the aquifer, top of the aquifer or lower of the upper aquitard, and land surface or top of the upper aquitard. These four maps are shown in figure (3.7) – (3.10). Discretized domain into 3D Cartesian mesh is shown in figure (3.11). Observation of the produced grid shows that this code could mesh the modeling area in accurate result, particularly to represent boundary for each layers. The inclination of the layer can be represented clearly.

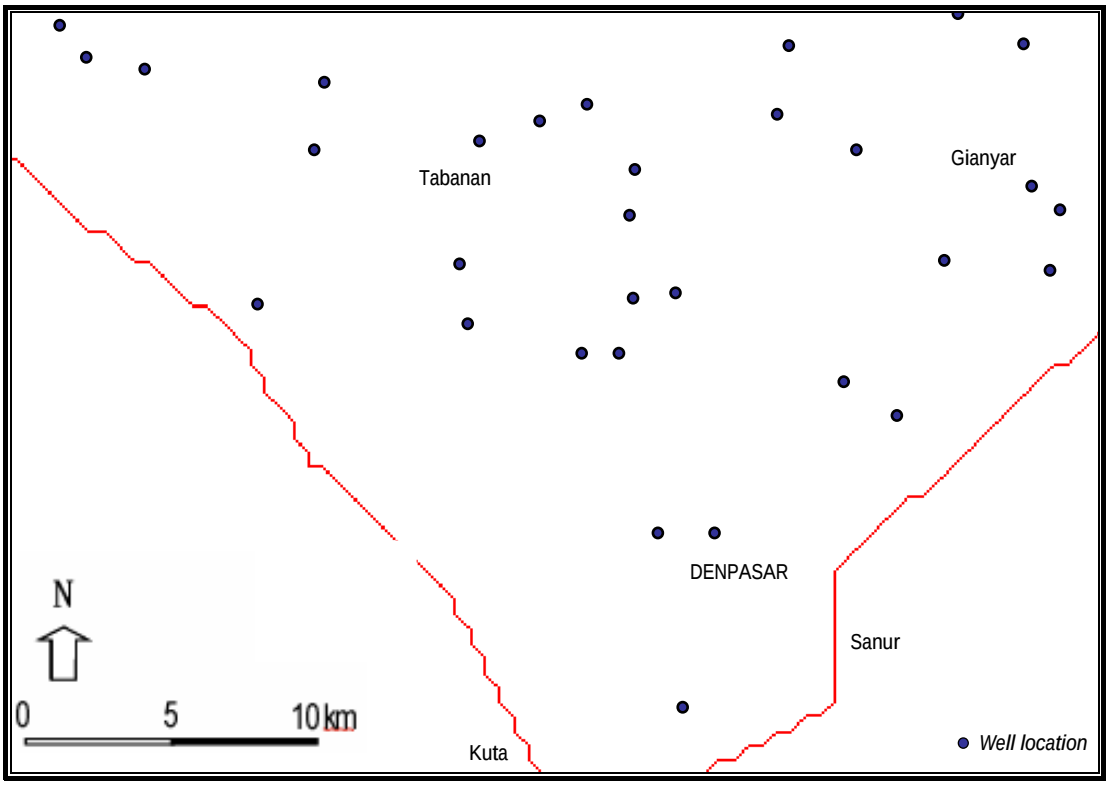

Figure 3.7 Contour map of bottom of lower aquitard.

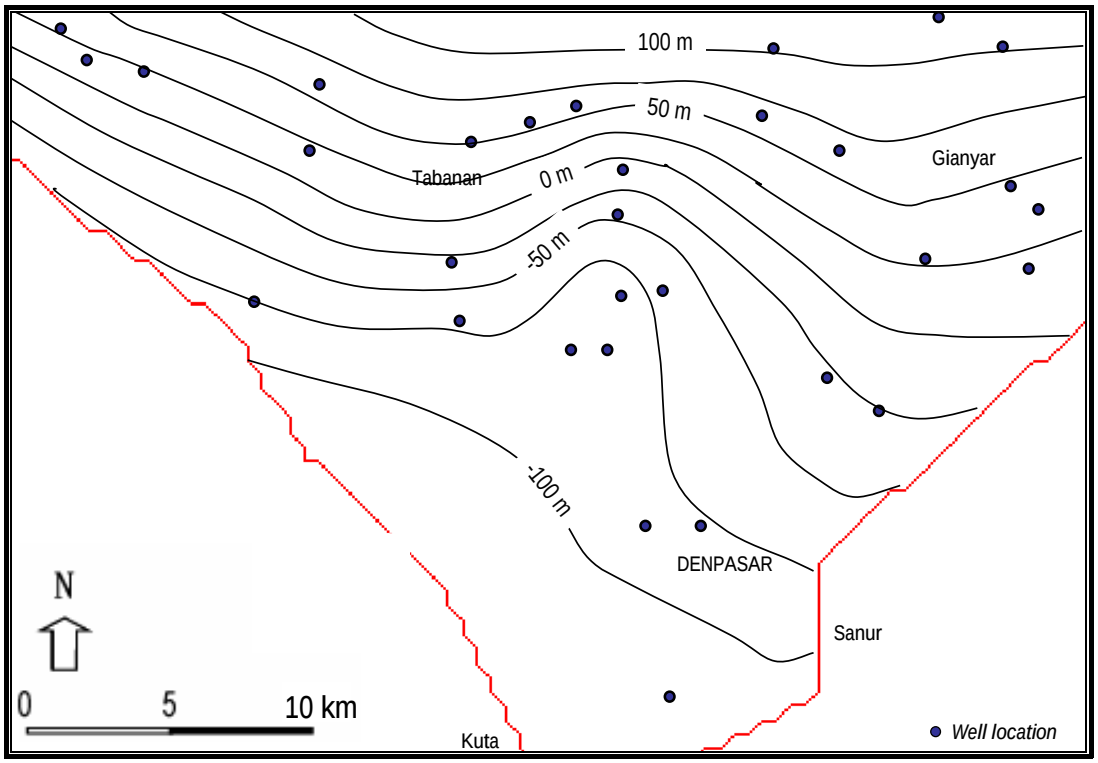

Figure 3.8 Contour map of bottom of aquifer.

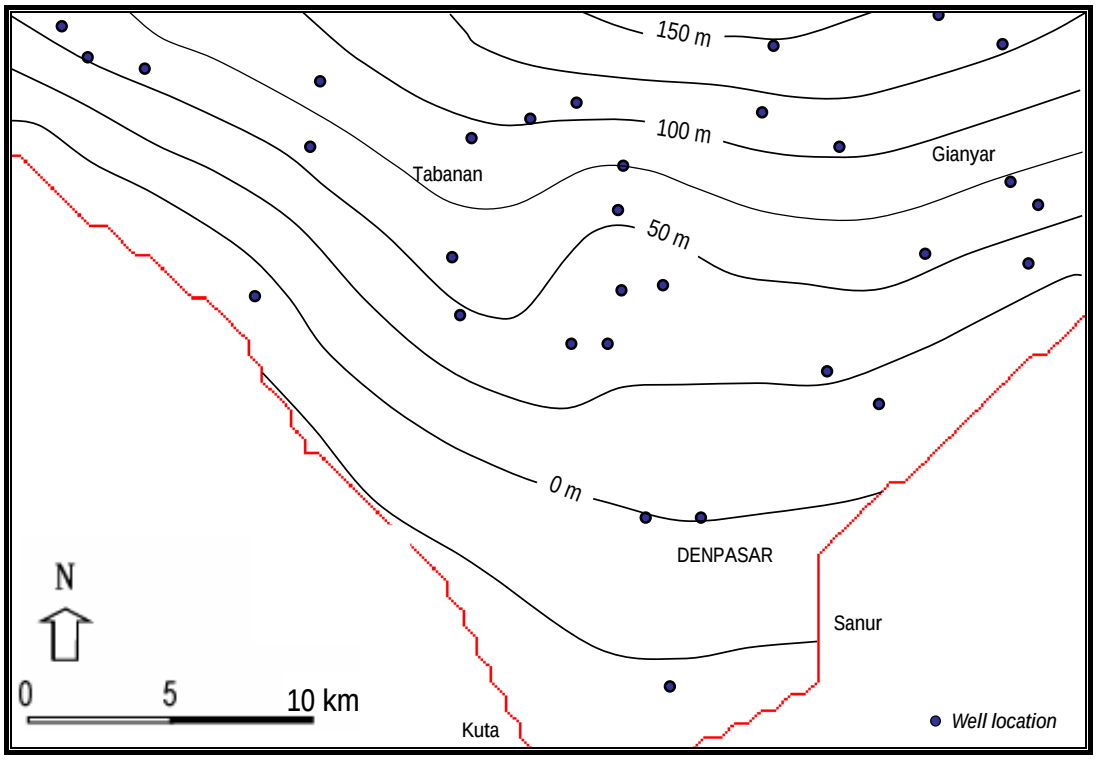

Figure 3.9 Contour map of top of aquifer

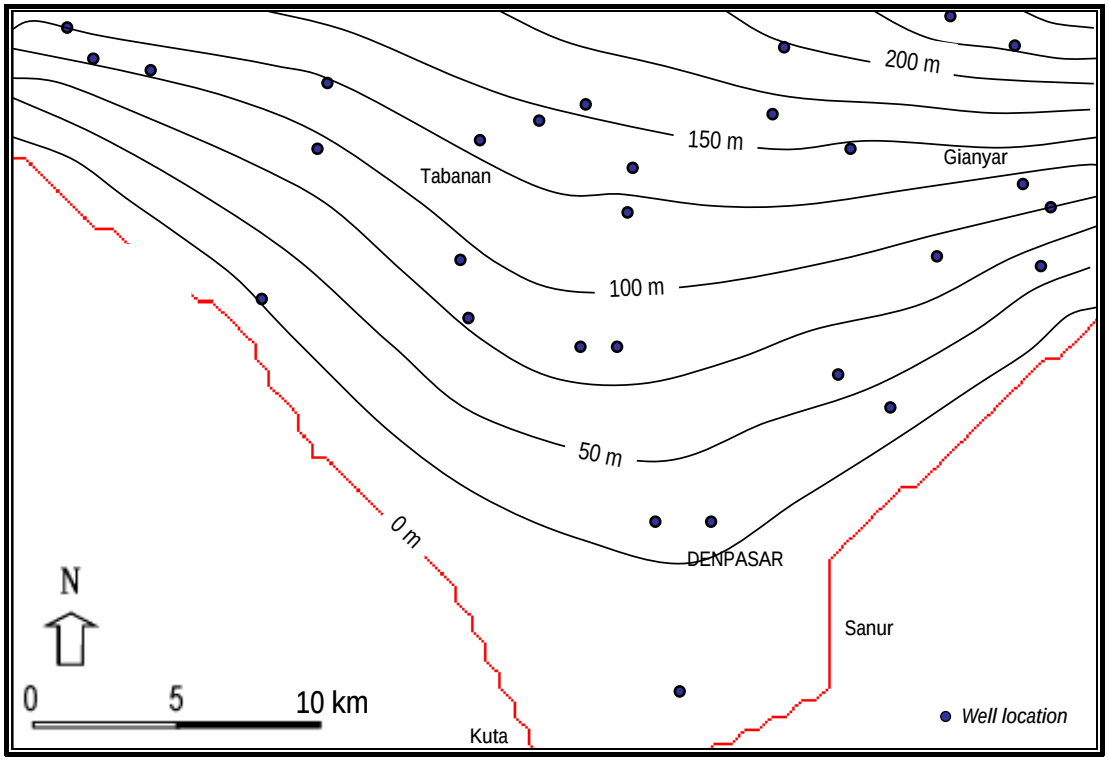

Figure 3.10 Contour map of land surface.

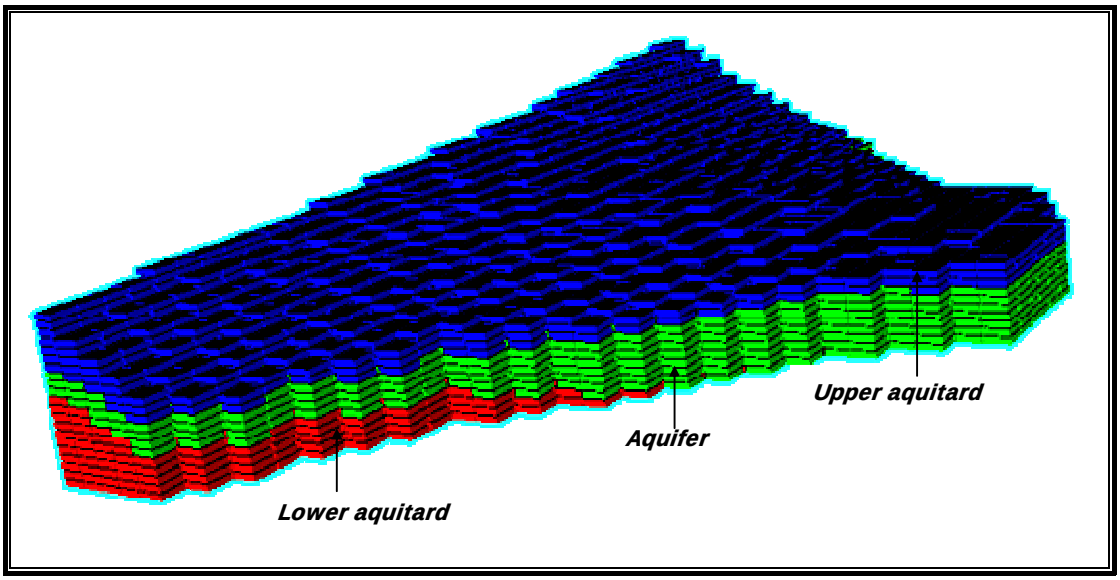

Figure 3.11 Three dimensional grid of Bali coastal aquifer.

3.3. NUMERICAL CODING OF VARIABLE DENSITY FLOW

SUTRA software (Voss and Provost, 2003) has been chosen as a basic of code development. The code is upgraded version of well established SUTRA for 2D modeling by improving capability to simulate 3D problem, so that in this thesis, this new version is mentioned as SUTRA2D3D. This code employs a hybridization of finite element and finite difference method to approximate the governing equations. The equations describe two interdependent processes consisting of:

1. fluid density dependent saturated or unsaturated groundwater flow;
2. either transport of solute in the groundwater or transport of thermal energy in the groundwater and solid matrix of the aquifer.

The governing equation of the original code has been simplified by excluding variables of the transport of thermal energy. Then, the modified code is only applicable for solving problem of fluid density dependent saturated or unsaturated and solute transport in groundwater flow, emphasizing into freshwater-seawater interface. The governing equations and numerical formulations employed on the modified code are summarized and simplified from the SUTRA2D3D manual (Voss and Provost, 2003).

3.3.1. Governing Equations

Modeling of variable saturated-density of groundwater flow requires solution of two partial differential equations representing fluid flow and solute transport. Mathematical model is expressed here in terms of equivalent freshwater pressure head, fluid mass balance, and solute mass balance.

3.3.1.1. Concept of Equivalent Freshwater Pressure Head

Simulation of groundwater flow is, mostly, assumed that density of the groundwater is spatially and temporally constant. However, this assumption is not valid for groundwater in coastal area because seawater contains a higher concentration of dissolved salt than rainfall in which primarily source of aquifer recharge. Formulating of the groundwater flow uses term of hydraulic head will results cumbersome expressions involving density and its derivatives, and no computational advantage is gained. Therefore, respect to problem interest, the governing equations apply concept of fluid pressure. The concept of the fluid pressure is freshwater pressure head or equivalent freshwater pressure head in a non-fresh groundwater environment, figure (3.12), that can be formulated as;

$$h_f = \frac{P_N}{\rho_f g} + Z_N \tag{3.26}$$

where: h_f is equivalent freshwater head [L], P_N is pressure at point N [$ML^{-1}T^{-2}$], ρ_f is fluid density [ML^{-3}], g is acceleration due to gravity [LT^{-2}], and Z_N is elevation of point N above datum [L].

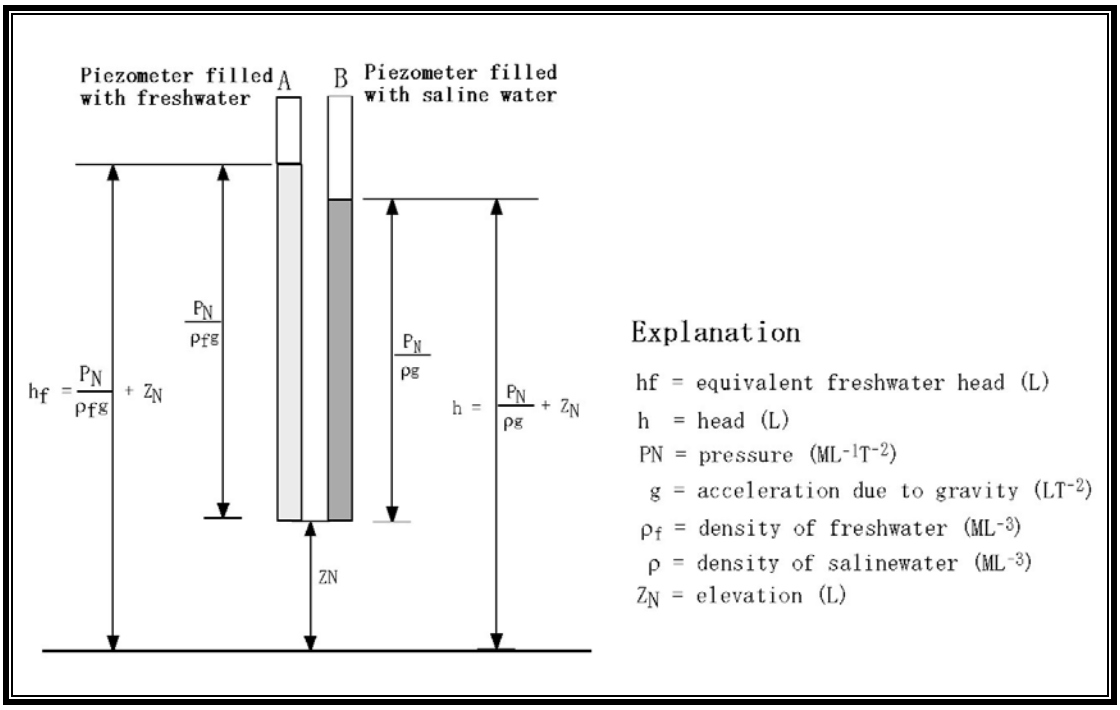

Figure 3.12 Concept of fluid pressure for two piezometers, one filled with freshwater and the other with saline water.

Hydraulic head (h) on the aquifer varies not only as do pressure and elevation, but also as water density. Thus, at two points having equal pressures and the same elevation but different water densities, the hydraulic head will be recorded in different values. Variation in fluid density, aside from fluid pressure differences, will drive flows that it must be counted by considering the effects of gravity acting on fluids. The actual flow velocities of the groundwater from point to point in an aquifer may vary, and is usually too complex to be measured in real systems. Thus, an average velocity is commonly used to describe flow in porous media that is based on Darcy's law written as follow;

$$v = -\left(\frac{kkr}{\varepsilon S_w \mu}\right)(\nabla p - \rho g) \tag{3.27}$$

where v is average fluid velocity [LT^{-1}], k is solid matrix permeability [L^2], k_r is relative permeability to fluid flow (assumed to be independent of direction), ε is porosity (%), S_w saturation degree (%), μ is viscosity [$ML^{-1}T^{-2}$], ρ is water density [ML^{-3}], and g is gravitational acceleration [LT^{-2}]. The gravity vector is defined in relation to the direction in which vertical elevation is measured:

$$g = -|g|\nabla(elevation) \tag{3.28}$$

Where $|g|$ is the magnitude of the gravitational acceleration vector.

Equation (3.27) shows that fluid velocity, even for a given pressure and density distribution, may take on different values depending on mobility of the fluid within the solid matrix. The mobility depends on the combination of permeability, relative permeability, and fluid viscosity. Permeability is a measure of the ease of fluid movement through interconnected voids in the solid matrix when all voids are completely saturated. Relative permeability expresses what fraction of the total permeability remains when the voids are only partly fluid-filled and only part of the total interconnected void space is connected by continuous fluid channels. Viscosity directly expresses ease of fluid flow; a less viscous fluid flows more readily under a driving force. The fluid viscosity is a weak function of pressure and concentration, and is primarily depend on fluid temperature. The viscosity in this study is assumed to be a constant value of 1.0×10^{-3} $kg.m^{-1}.s^{-1}$.

The average fluid velocity is the velocity of fluid with respect to the stationary solid matrix. The velocity is referred to as an "average", because true velocities in a porous medium vary from point to point due to variations in the permeability and porosity of the medium at a spatial scale smaller than that at which measurements are made. It is also commonly used term of Darcy velocity is $q = \varepsilon S_w v$. This value is always less than the true average fluid velocity. The Darcy velocity is not being a true indicator of the speed of water movement, but is actually a 'flux' of fluid representing the volume of fluid crossing an area of porous medium per time.

3.3.1.2. Fluid Mass Balance Equation

Estimation of the fluid mass balance is actually a calculation of the amount of fluid mass contained within the void spaces of the solid matrix changes with time. In a particular volume of solid matrix and void space, the fluid mass may change due to ambient groundwater inflow or outflow, injection or pumping wells, changes in fluid density, or changes in saturation. The fluid mass balance per unit aquifer volume at a point in the aquifer is formulated by assuming that the contribution of solute dispersion

to the mass average flux of fluid is negligible. Thus, the fluid mass balance is expressed as;

$$\frac{\partial(\varepsilon S_w \rho)}{\partial t} \cong -\nabla(\varepsilon S_w \rho v) + Q_p + \gamma \tag{3.29}$$

Where Q_p [$ML^{-3}T^{-1}$)] is fluid mass source (including pure water mass plus solute mass dissolved in source water), γ [$ML^{-3}T^{-1}$] is solute mass source (e.g., dissolution of solid matrix or desorption), t is time [T], and other parameters has been described on the above equations.

The fluid mass balance is the sum of pure water and pure solute mass balances for a solid matrix in which there is negligible net movement (i.e., no subsidence and no compaction). The term on the left of the equation (3.29) can be recognized as the total change in fluid mass contained in the void space with time. The term involving ∇ represents contributions to local fluid mass change due to excess of fluid inflows over outflows at a point. The fluid mass source term, Q_p, accounts for external additions of fluid including pure water mass plus the mass of any solute dissolved in the source fluid. The pure solute mass source term, γ□, may account for external additions of pure solute mass not associated with a fluid source. In most cases, this contribution to the total mass is small compared to the total pure water mass contributed by fluid sources、so it is neglected in the fluid mass balance.

The actual amount of total fluid mass contained depends solely on fluid pressure (p) and solute concentration (C). A change in total fluid mass can be expressed as follow;

$$Vod(\varepsilon S_w \rho) = Vo\left[\frac{\partial(\varepsilon S_w \rho)}{\partial p} dp + \frac{\partial(\varepsilon S_w \rho)}{\partial C} dC\right] \tag{3.30}$$

Since the saturation (S_w) is entirely dependent on fluid pressure, and the porosity (ε) does not depend on concentration, so the equation (3.30) can be derived;

$$Vod(\varepsilon S_w \rho) = Vo\left[\left(S_w \frac{\partial(\varepsilon\rho)}{\partial p} + \varepsilon\rho \frac{\partial S_w}{\partial p}\right) dp + \varepsilon S_w \frac{\partial \rho}{\partial C} dC\right] \tag{3.31}$$

Under fully saturated condition, the factor $\partial(\varepsilon\rho)/\partial p$ correspond to aquifer storativity defining as follow (Bear, 1979; Voss and Provost, 2003);

$$\frac{\partial(\varepsilon\rho)}{\partial p} \equiv \rho S_{op} \tag{3.32}$$

$$Sop = (1-\varepsilon)\alpha + \varepsilon\beta \tag{3.33}$$

Where S_{op} is specific pressure storativity, α is porous matrix compressibility $[ML^{-1}T^{-2}]^{-1}$, and β is fluid compressibility $[ML^{-1}T^{-2}]^{-1}$.

In order to express each mechanism represented by terms of variable p and C, the time derivative of equation (3.31) may be expanded from equation (3.32) and (3.33) as follow;

$$\frac{\partial(\varepsilon S_w \rho)}{\partial t} = \left(S_w \rho S_{op} + \varepsilon\rho \frac{\partial S_w}{\partial p} \right)\frac{\partial p}{\partial t} + \left(\varepsilon S_w \frac{\partial \rho}{\partial C} \right)\frac{\partial C}{\partial t} \tag{3.34}$$

While the concepts upon which specific pressure storativity, S_{op}, is based, do not exactly hold for unsaturated media, the error introduced by summing the storativity term with the term involving $(\partial S_w/\partial p)$ is insignificant as $(\partial S_w/\partial p) >>> S_{op}$.

The exact form of the fluid mass balance is obtained from (3.29) by neglecting γ, substituting (3.34):

$$\left(S_w \rho S_{op} + \varepsilon\rho \frac{\partial S_w}{\partial p} \right)\frac{\partial p}{\partial t} + \left(\varepsilon S_w \frac{\partial \rho}{\partial c} \right)\frac{\partial c}{\partial t} + \nabla(\varepsilon\rho v) = Q_p \tag{3.35}$$

And employing Darcy's law for v;

$$\left(S_w \rho S_{op} + \varepsilon\rho \frac{\partial S_w}{\partial p} \right)\frac{\partial p}{\partial t} + \left(\varepsilon S_w \frac{\partial \rho}{\partial C} \right)\frac{\partial C}{\partial t} - \nabla\left[\left(\frac{k k_r \rho}{\mu} \right)(\nabla p - \rho g) \right] = Q_p \tag{3.36}$$

where ρ is fluid density $[ML^{-3}]$, S_{op} is specific pressure storativity $[ML^{-1}T^{-2}]$, p is the pressure $[ML^{-1}T^{2}]$, C is the solute concentration of fluid as a mass fraction $[M_s M^{-1}]$, ε is

aquifer volumetric porosity [-], v is fluid velocity [LT^{-1}], and Q_p is a fluid mass source [$ML^{-3}T^{-1}$].

Considering of saturated and unsaturated medium, such as in the SUTRA2D3D, it uses only a type of porosity in which some instance need to distinguish between effective porosity and total porosity. The fraction of total volume filled by fluid is εS_w. When $S_w = 1$, the void space is completely filled with fluid (fully saturated), and $S_w < 1$ is unsaturated. The changes of saturated to unsaturated may be understood with a drop of fluid (gauge) pressure below zero. The drop of the pressure may not be directly replaced by air, but air may enter suddenly when a critical capillary pressure is reached. This pressure is the entry pressure (or bubble pressure) expressed with p_{cent} [$ML^{-1}T^{-2}$)] shown in figure (3.13). Typical values for p_{cent} range from about 1.0 x 10^3 kg/(ms^2) for coarse sand to approximately 5.0 x 10^3 kg/(ms^2) for fine silty sand.

The relation between fluid saturation and capillary pressure in a given medium is typically determined by laboratory experiment, and except for the portion near bubble pressure, tends to have an exponential character (Figure 3.13a). Different functional relations exist for different materials as measured in the laboratory. In addition, a number of general functions with parameters to be fitted to laboratory data are available. Because of the variety of possible functions, no particular function is set. Any desired function may be specified for simulation of unsaturated flow. For example, a general function with three fitting parameters is (Van Genuchten, 1980):

$$S_w = S_{wres} + (1 - S_{wres})\left[\frac{1}{1 + (ap_c)^n}\right]^{\left(\frac{n-1}{n}\right)} \tag{3.37}$$

Where S_{wres} is a residual saturation below which saturation is not expected to fall (because the fluid becomes immobile), and both a and n are parameters. The values of these parameters depend upon a number of factors and these must be carefully chosen for a particular material.

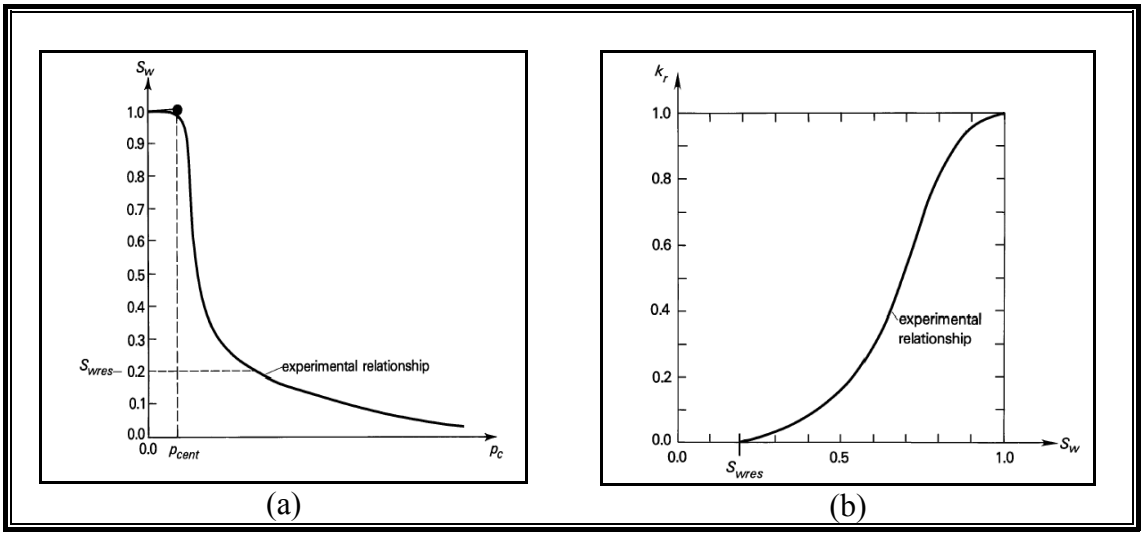

Figure 3.13 Hydrogeology parameter for unsaturated zone. a). Saturation-capillary pressure scheme, S_w is saturation, S_{wres} is residual saturation, and r_{cent} is air entry pressure, b). Relative permeability-saturation schematic, k_r is the relative permeability.

The factor, $\partial S_w/\partial p$, is obtained by differentiation of the chosen saturation-capillary pressure relation. For the example function given as;

$$\frac{dS_w}{dp} = \left[\frac{a(n-1)(1-S_{wres})(ap_c)^{(n-1)}}{(1+(ap_c)^n)^{(2n-1)/n}} \right] \tag{3.38}$$

3.3.1.3. Solute Mass Balance Equation

Solute-transport simulation is accounted for single species mass stored in fluid solution as well as solute and species mass stored as adsorbate on the surfaces of solid matrix grains. The accounted process is formulated as;

$$\begin{aligned} &\frac{\partial(\varepsilon S_w \rho C)}{\partial t} + \frac{\partial[(1-\varepsilon)\rho_s C_s]}{\partial t} \\ &= -\nabla(\varepsilon S_w \rho v C) + \nabla[\varepsilon S_w \rho (D_m I + D)\nabla C] + \varepsilon S_w \rho \Gamma_w + (1-\varepsilon)\rho_s \Gamma_s + Q_p C^* \end{aligned} \tag{3.39}$$

Where D_m is apparent molecular diffusivity of solute in solution in a porous medium including tortuosity effects [L^2T^{-1}], I is identity tensor (1 on diagonal, 0 elsewhere), D is dispersion tensor [L^2T^{-1}], Γ_w is solute mass source in fluid due to production reactions [$M_s.M^{-1}T^{-1}$], C^* is solute concentration of fluid sources [M_sM^{-1}], C_s is specific

concentration of adsorbate on solid grains [$M_s.M_G^{-1}$], ρ_s is density of solid grains in solid matrix [$M_G L_G^{-3}$], Γ_s is adsorbate mass source due to production reactions within adsorbed material itself [$M_s.M_G^{-1}T^{-1}$], and L_G^3 is the volume of solid grains.

Application of the equation (3.39) to simulate the phenomena of transport for mixing freshwater and saltwater can be simplified by excluding the solute mass source from the production reactions. Thus, the equation (3.39) becomes;

$$\frac{\partial(\varepsilon S_w \rho C)}{\partial t} = -\nabla(\varepsilon S_w \rho v C) + \nabla[\varepsilon S_w \rho (D_m I + D)\nabla C] + Q_p C^* \qquad (3.40)$$

The term of fluid velocity represents average advection of solute mass into or out of the local volume. The term of molecular diffusivity of solute (D_m) and dispersion tensor (D) express the contribution of solute diffusion and dispersion to the local changes in solute mass. The last term accounts for dissolved species mass added by a fluid source with concentration, C^*.

Relation between density and concentration is given as a linear function;

$$\rho = \rho(c) \cong \rho_0 + \frac{\partial \rho}{\partial c}(c - c_0) \qquad (3.41)$$

Where ρ_0 is fluid density at base solute concentration [ML^{-3}], and $\partial\rho/\partial c$ is constant of proportionality for each solute. ρ_0 [M/L^3_f] base fluid density at $C=C_0$, C_0 [M_s/M] base fluid solute concentration. The ρ_0 is the base fluid density at base concentration, Co. (Usually, Co = 0, and the base density is that of pure water.) The factor $\partial\rho/\partial C$ is a constant value of density change with concentration. For example, for mixtures of freshwater and seawater at 20°C, when C is the mass fraction of total dissolved solids, Co = 0, and ρ_0 = 998.2 (kg/m^3), then the factor, $\partial\rho/\partial C$, is approximately 700 (kg/m^3).

3.3.2. Numerical Formulations

Numerical formulation of the governing equation is quite complex because:

1. density-dependent flow and transport requires two interconnected simulation models;

2. fluid properties are dependent on local values of concentration;
3. geometry of a field and distributions of hydrogeologic parameters may be complex;
4. hydrologic stresses of the system may be distributed in space and change with time.

This requires great computational effort, and considerable numerical intricacy is required to minimize it. The mathematical elegant finite element and integrated finite different hybrid method employed in the code allows a great numerical flexibility in describing processes and characteristic of flow and transport in the hydrologic system.

3.3.2.1. Spatial Discretization

By adopting technique of the SUTRA2D3D code, regardless the code is applied as a 2D-model and 3D-model, the region of space is to be simulated is defined in three spaces dimension. The 2D model divides the aquifer into a single layer of contiguous blocks, and the 3D model organizes a set of contiguous blocks in layers. The blocks are not done simply in manner that creates one block (element) for each portion of the aquifer system that has unique hydrogeological characteristics. Each hydrogeologic unit is in fact divided into many elements, giving the subdivided aquifer region the appearance of a fine mesh.

The type of element employed for 2D simulation is a quadrilateral that has a finite thickness in the third space dimension. Thus, the element is restricted to single layer. The x-y plane bisects each of the edges parallel to z is referred to an element, and the midpoint of each z-edge is a node. Differ with 2D mesh, 3D mesh of SUTRA2D3D the six faces of the element no need to be planar, and none of twelve edges need be parallel to the z-coordinate direction. However, the 3D mesh must be logically rectangular that means even though the geometry may be irregular, the nodes must be connected in the same manner with regular mesh. This can be thought of as consisting of rows, columns, and layers of elements, with each row, column, and layer containing its full complement of elements. This condition has been modified in this study.

Hydrogeologic parameters that vary from point to point in an aquifer are defined in element or set of element employs three approaches; element-wise, node-wise, and cell-wise. Aquifer parameters and coefficients are either assigned a particular constant value in each node may discretized in two possible way (node-wise and cell-wise), or

assigned a particular value in each element is discretized as element-wise. Description of these three approaches is given in figure (3.14) below.

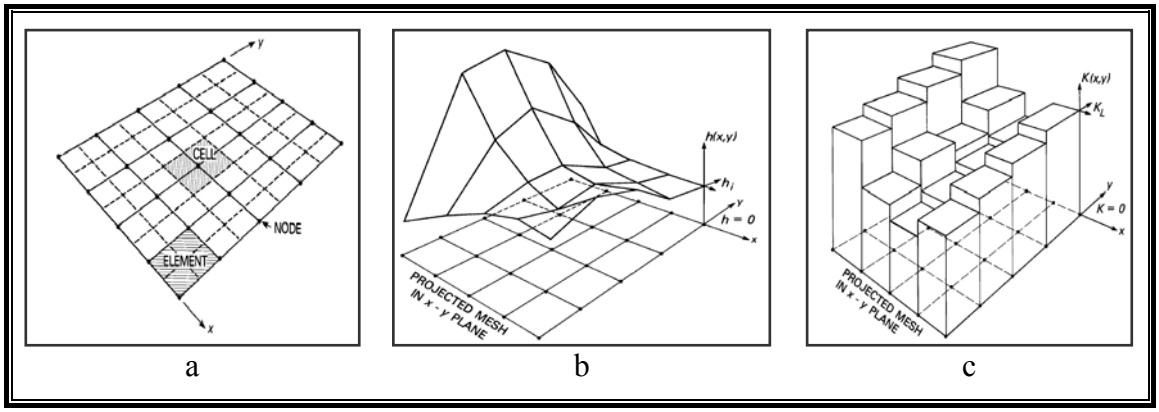

Figure 3.14 *Approaches in space discretization (Voss and Provost, 2003). a). Nodes, cells and elements in 2D FE-mesh, b). Node-wise, c). Element-wise.*

Aquifer parameters discretized as node-wise are pressure head and solute concentration, as element-wise are hydraulic conductivity and dispersivity, and cell-wise is storativity. The element-wise, node-wise, and cell-wise discretization can be expressed, respectively, as follow;

$$K(x,y,z) \approx \sum_{e=1}^{ne} K_e(x,y,z) \tag{3.42}$$

$$h(x,y,z,t) \approx \sum_{i=1}^{nn} h_i(t)\phi_i(x,y,z) \tag{3.43}$$

$$S_o(x,y,z) \approx \sum_{i=1}^{nn} S_i(x,y,z) \tag{3.44}$$

3.3.2.2. Fluid Mass Balance

By clearing the integral constants and applying the Green's theorem at the governing equation of the fluid mass balance written on equation (3.36), the weighted residual can be formulated as follow;

$$AF_i \frac{dp_i}{dt} + CF_i \frac{dC_i}{dt} + \sum_{j=1}^{NN} p_j(t) BF_{ij} + v_{p_i} p_i = Q_i + v_{p_i} p_{bc_i} + q_{IN_i} + DF_i \tag{3.45}$$

Where;

$$AF_i = \left(S_w \rho S_{op} + \varepsilon \rho \frac{\partial S_w}{\partial p} \right)_i V_i \tag{3.46}$$

$$CF_i = \left(\varepsilon \rho \frac{\partial \rho}{\partial C} \right)_i V_i \tag{3.47}$$

$$BF_{ij} = \int_x \int_y \int_z \left\{ \left[\langle\langle k \rangle\rangle \left\langle \frac{k_r \rho}{\mu} \right\rangle \right] \nabla \phi_j \right\} \nabla \omega_i dz dy dx \tag{3.48}$$

$$DF_{ij} = \int_x \int_y \int_z \left\{ \langle\langle k \rangle\rangle \left[\left\langle \frac{k_r \rho}{\mu} \right\rangle \right] \langle \rho g \rangle^* \right\} \nabla \omega_i dz dy dx \tag{3.49}$$

For 2D simulations, (3.48) and (3.49) are written as

$$BF_{ij} = \int_x \int_y \left\{ \left[\langle\langle k \rangle\rangle \left\langle \frac{k_r \rho}{\mu} \right\rangle \right] \nabla \phi_j \right\} \nabla \omega_i B dy dx \tag{3.50}$$

$$CF_{ij} = \int_x \int_y \left\{ \langle\langle k \rangle\rangle \left[\left\langle \frac{k_r \rho}{\mu} \right\rangle \right] \langle \rho g \rangle^* \right\} \nabla \omega_i B dy dx \tag{3.51}$$

The form of the discretized fluid mass balance implemented as follows:

$$\sum_{j=1}^{NN} \left[\left(\frac{AF_{ij} \delta_{ij}}{\Delta t_{n+1}} \right) + BF_{ij}^{n+1} + v_{p_i} \delta_{ij} \right]$$

$$= Q_i^{n+1} + v_{p_i} p_{bc_i}^{n+1} + DF_i^{(n+1)^*} + \left(\frac{AF_i^{n+1}}{\Delta t_{n+1}} \right) p_i^n + \left(CF_i^{n+1} \right) \left(\frac{dC_i}{dt} \right)^n \tag{3.52}$$

Where δ_{ij} is the Kronecker delta:

$$\delta_{ij} = \begin{cases} 0 & if \quad i \neq j \\ 1 & if \quad i = j \end{cases} \tag{3.53}$$

3.3.2.3. Solute Mass Balance

The weighted residual of solute mass balance is:

$$\frac{\partial(\varepsilon S_w \rho C)}{\partial t} = -\nabla(\varepsilon S_w \rho v C) + \nabla[\varepsilon S_w \rho (D_m I + D).\nabla C] + Q_p C^* \tag{3.54}$$

By combining and rearranging the evaluations of integrals, the following *NN* spatially discretized weighted residual relations are obtained in 3D:

$$AT_i \frac{dC_i}{dt} + \sum_{j=1}^{NN} C_j(t) DT_{ij} + \sum_{j=1}^{NN} C_j(t) BT_{ij} + Q_i C_i(t) + Q_{bc_i} C_i(t)$$

$$= Q_i C_i^* + Q_{bc_i} C_{bc_i} + \psi_{in_i} \tag{3.55}$$

Where;

$$AT_i = [\varepsilon S_w \rho] V_i \tag{3.56}$$

$$DT_{ij} = \int_x \int_y \int_z \left[\langle \varepsilon \rangle \langle S_w \rho \rangle \langle v \rangle^* \nabla \phi_j \right] \varpi_i \, dz dy dx \tag{3.57}$$

$$BT_{ij} = \int_x \int_y \int_z \left\{ \langle \{\rho\} \rangle \left[\langle \varepsilon \rangle \langle S_w \rangle \langle D_m I + D \rangle \nabla \phi_j \right] \right\} \nabla \phi_i \, dz dy dx \tag{3.58}$$

For 2D simulations, (3.57) and (3.58) reduce to

$$DT_{ij} = \int_x \int_y \left[\langle \varepsilon \rangle \langle S_w \rho \rangle \langle v \rangle^* \nabla \phi_j \right] \varpi_i B \, dy dx \tag{3.59}$$

$$BT_{ij} = \int_x \int_y \left\langle\left\{\rho\right\}\right\rangle\left[\left\langle\varepsilon\right\rangle\left\langle S_w\right\rangle\left\langle D_m I + D\right\rangle\nabla\phi_j\right]\nabla\phi_i B dy dx \tag{3.60}$$

The form of the discretized solute mass balance equation, which is implemented, is as follows:

$$\sum_{j=1}^{NN}\left\{\left(\frac{AT_i^{n+1}\delta_{ij}}{\Delta t_{n+1}}\right) + DT_{ij}^{(n+1)*} + BT_{ij}^{n+1} + \left[v_i + \left(Q_i^{n+1} + Q_{bc_i}^{n+1}\right)\right]\delta_{ij}\right\} C_j^{n+1}$$

$$= \left(Q_i^{n+1} C_i^{(n+1)*} + Q_{bc_i}^{n+1} C_{bc_i}^{n+1}\right) + v_i C_{bc}^{n+1} + \psi_{in_i}^{n+1} + \left(\frac{AT_i^{n+1}}{\Delta t_{n+1}}\right) C_i^n \tag{3.61}$$

Where δ_{ij} is the Kronecker delta.

3.3.2.4. Fluid Velocity

Fluid velocity defined by equation (3.27) poses a relation strictly holds true at a point in space. In order for the relation to hold true when discretized, the terms ∇p and ρg must be given the same type of spatial variability. A consistent evaluation of velocity is required by the transport solution and in the evaluation of the dispersion tensor, where velocity is required in each element, in particular, at the Gauss points for numerical integration. In addition, a consistent evaluation of the ρg term is required at the Gauss points in each element for the fluid mass balance solution in the integral that is shown in equation (3.49 or 3.51).

The coefficients for calculation of velocity are discretized as follows: *Permeability*, k, is discretized elementwise; *porosity*, ε, is discretized nodewise. *Unsaturated flow parameters*, k_r and *Sw*, are given values depending on the node-wise discretized pressure. To complete the discretization of velocity, values in global coordinates at the Gauss points are required for the term (∇p - ρg). Whenever this term is discretized consistently in local element coordinates (ξ, η [,ζ]), a consistent approximation is obtained in global coordinates for any arbitrarily oriented quadrilateral (2D) or hexahedral (3D) element. The remainder of this section presents a consistent approximation for this term.

Consistent discretization in local coordinates is obtained when the spatial dependence of $\partial p/\partial \xi$ and $\partial p/\partial \eta$ [and $\partial p/\partial \zeta$] is of the same type as that of $\rho g\xi$ and $\rho g\eta$ [and $\rho g\zeta$]. Because the discretization for $p(\xi, \eta [,\zeta])$ has already been chosen to be bilinear (2D) or trilinear (3D), it is the discretization of the ρg term, in particular, that must be adjusted. First, in the following, a discretization of the ρg term is presented which is consistent with the discretization of ∇p in local coordinates, and then both ∇p and ρg are transformed to global coordinates while maintaining consistency. The development is presented for the 3D case. In 2D, the summations are performed over four (instead of eight) nodes and only terms not involving z or ζ are relevant.

The pressure gradient within a 3D element in local coordinates is defined in terms of the derivatives with respect to the local coordinates:

$$\frac{\partial p}{\partial \xi}(\xi,\eta,\zeta) = \sum_{i=1}^{NN} p_i \frac{\partial \Omega_i}{\partial \xi} \tag{3.62}$$

$$\frac{\partial p}{\partial \eta}(\xi,\eta,\zeta) = \sum_{i=1}^{NN} p_i \frac{\partial \Omega_i}{\partial \eta} \tag{3.63}$$

$$\frac{\partial p}{\partial \zeta}(\xi,\eta,\zeta) = \sum_{i=1}^{NN} p_i \frac{\partial \Omega_i}{\partial \zeta} \tag{3.64}$$

A local discretization of ρg with a spatial functionality that is consistent with the local pressure derivatives is

$$(\rho g)_\xi(\xi,\eta,\zeta) = \sum_{i=1}^{8} \rho_i g_{\xi_i} \left|\frac{\partial \Omega_i}{\partial \xi}\right| \tag{3.65}$$

$$(\rho g)_\eta(\xi,\eta,\zeta) = \sum_{i=1}^{8} \rho_i g_{\eta_i} \left|\frac{\partial \Omega_i}{\partial \eta}\right| \tag{3.66}$$

$$(\rho g)_\zeta(\xi,\eta,\zeta) = \sum_{i=1}^{8} \rho_i g_{\zeta_i} \left|\frac{\partial \Omega_i}{\partial \zeta}\right| \tag{3.67}$$

where the vertical bars indicate absolute value, ρ_i is the value of ρ at node i in the element based on the value of C at the node through relation (3.40), and $g_{\xi i}$, $g_{\eta i}$, and $g_{\zeta i}$

are the ξ, η, and ζ components of g at node i, respectively. The gravity vector components in local coordinates at a point in the 3D element are obtained from the global gravity components as:

$$\begin{Bmatrix} g_\xi \\ g_\eta \\ g_\zeta \end{Bmatrix} = [J] \begin{Bmatrix} g_x \\ g_y \\ g_z \end{Bmatrix} \tag{3.68}$$

Where *[J]* is the Jacobian matrix.

The derivatives of pressure in local coordinates, and the consistent density-gravity term components in local coordinates are transformed to global coordinates for use in the evaluation of the integrals in which they appear by

$$\begin{Bmatrix} \frac{\partial p}{\partial x} \\ \frac{\partial p}{\partial y} \\ \frac{\partial p}{\partial z} \end{Bmatrix} = [J^{-1}] \begin{Bmatrix} \frac{\partial p}{\partial \xi} \\ \frac{\partial p}{\partial \eta} \\ \frac{\partial p}{\partial \zeta} \end{Bmatrix} \tag{3.69}$$

$$\begin{Bmatrix} \langle \rho g \rangle^*_x \\ \langle \rho g \rangle^*_y \\ \langle \rho g \rangle^*_z \end{Bmatrix} = [J^{-1}] \begin{Bmatrix} (\rho g)_\xi \\ (\rho g)_\eta \\ (\rho g)_\zeta \end{Bmatrix} \tag{3.70}$$

Where $(\langle\langle g\rho \rangle\rangle^*)_x$, $(\langle\langle g\rho \rangle\rangle^*)_y$, *and* $(\langle\langle g\rho \rangle\rangle^*)_z$ are the consistently discretized density-gravity term components in global coordinates, and $[J]^{-1}$ is the inverse Jacobian matrix.

3.3.3. Structure of Numerical Code

Such aforementioned that this development of numerical code has chosen the SUTRA2D3D software code as basis code. The original code has been modified with four considerations;

(1) Problems that can be solved has been simplified for groundwater flow and solute transport only, in which the variable of thermal process available on the basis code has been excluded;
(2) Simulation can be carried by discretizing of hydrogeological system employing either the Cartesian grid system or the FEM mesh;
(3) The data is arranged to provide input of numerical flow model with an efficient memory demand particularly for 3D-simulation by designing that input of parameter values into elements just memorizes the identity of material type;
(4) Numerical solver for approximation of the governing equation uses Pre-conditioned bi-conjugate gradient method.

The first consideration has not given a significant change to the code structure, therefore there is no important work had been done need to be described here. The modification was done by excluding the hydrogeological parameters and the numerical code related to the thermal process. However, several parts of the basis code required modifications concern to the last three considerations.

A brief description of the SUTRA2D3D in this present work is given here. The SUTRA2D3D software is upgraded version of a well established SUTRA code developed by Voss, (1984) for 2D problem. This upgraded version is to improve ability to solve 3D problem. Both these codes employed finite element and finite difference method to approximate the above mentioned of governing equations. By using hybridization of both methods, it is gained advantages in which it is naturally mass lumping, in contrast to common formulation of the finite element method, which requires mass lumping to avoid oscillatory solutions. In addition, the hybrid finite element and finite difference methods has all the ability of finite element method to handle irregular geometries and complex boundary conditions.

The SUTRA2D3D was designed to perform simulation with finite element mesh in which 2D-mesh may regular or irregular form, but 3D-mesh only support block-wise mesh. This research has designed a code that can be used to simulate a groundwater flow problem by using either the Cartesian mesh system or the finite element mesh. In addition, in order to solve couple of the fluid mass balance and the solute transport, the hydraulic head and the solute concentration are calculated through a synchronous time-

stepping approach either explicit or implicit coupling. The explicit coupling assigns fluid densities in the fluid mass balance equation in a lagged approach. This coupling calculates the fluid densities by using solute concentration from the previous time step. Advective fluxes from the fluid mass balance solution for the current time step are, then, used in current solution to the solute mass balance. This cycling mechanism results in an explicit coupling of equations for the fluid mass balance and solute mass balance. With the implicit coupling method, solutions to the fluid mass balance and solute mass balance are repeated, and concentrations and densities are updated within each time step until the maximum difference in fluid density at a single cell for consecutive iterations is less than a convergence criterion specified by user.

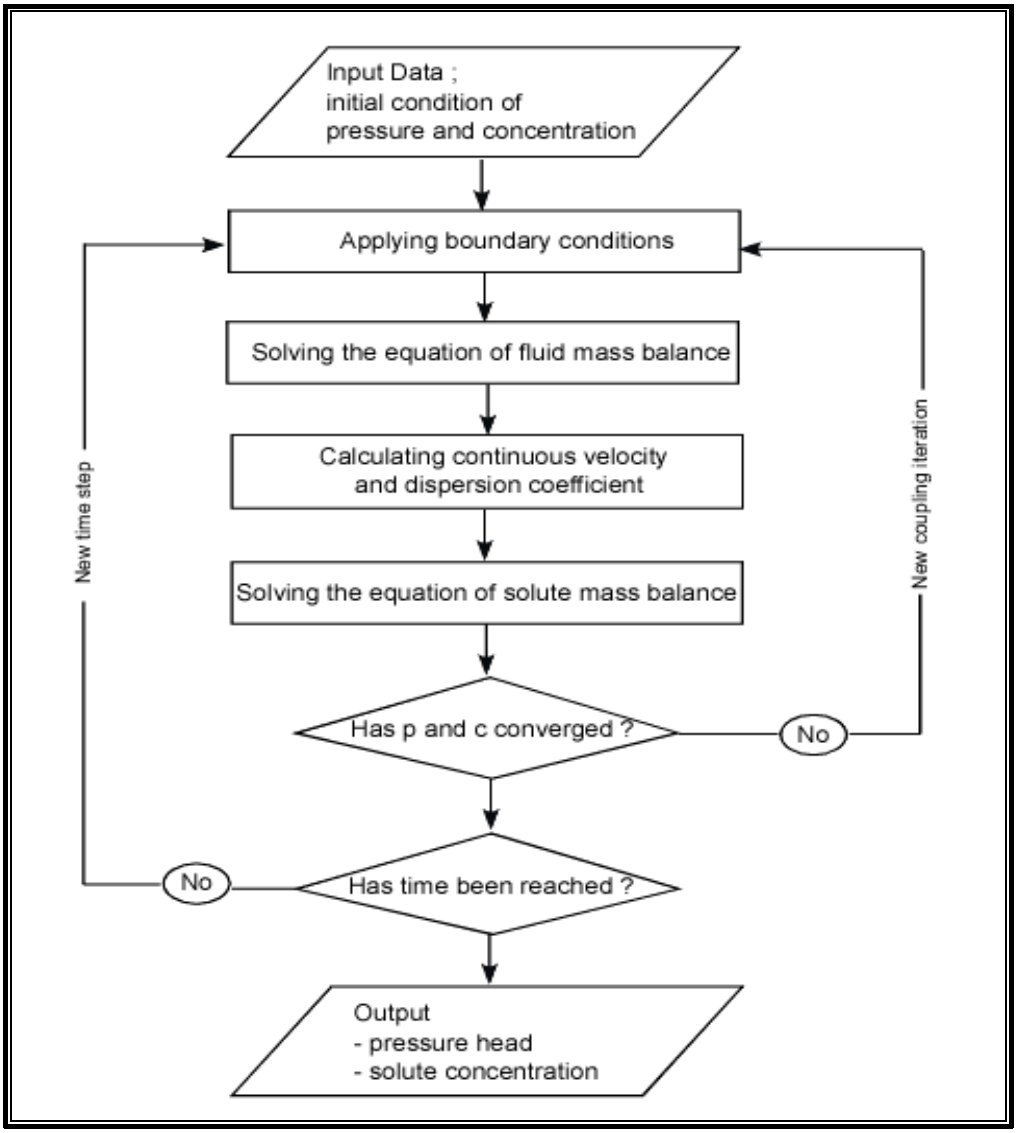

Figure 3.15 Flowchart of coupled fluid mass balance and solute mass transport.

The developed code employing the Cartesian grid system requires additional information of satellite nodes for each node. Construction stiffness matrix is only storage the component that has possibility non-zero value by using indexed storage of spare matrix system. Therefore, the memory requirement for conductance matrix is only N x 9 for 2D model and N x 27 for 3D model.

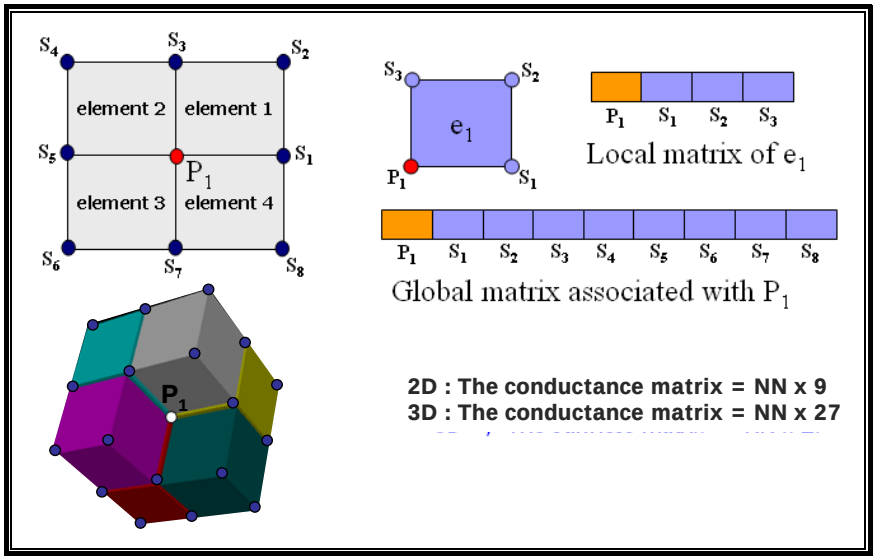

Figure 3.16 Interconnectivy of nodes with elements and matrix storage system.

Implementation of the flowchart at figure (3.15) into computer code is translated into some functions. The main logic flow to the program is straightforward. A schematic diagram of code is shown in figure (3.17). Running this code requires data organized into some input files and output files that is summarized in table 3.2.

Main function of program code is designed to read input files, to assign output files, and to control numerical the groundwater flow and the solute transport simulation. Some functions activated by this main program are described as follow;

1. Data_input ; to read main input data consisting of reading input files and defining output files.
2. Surf ; reads node incidence data.
3. Initial ; reads initial freshwater pressure head and solute(salt) concentration
4. Source ; reads node numbers, the pressure values, and the solute concentration of specified source and/or sinks.

5. Bound ; reads node numbers of specified the freshwater pressure head and/or the solute concentration, the pressure values and the solute concentration values.
6. Product ; creating output files.
7. O_node ; prints the pressure head, the solute concentration, and the saturation degree at nodes.
8. O_elem ; prints elementwise output of velocity vector of groundwater flow.
9. O_obsv ; prints the freshwater pressure head, the solute concentration, and the saturation degree at the observation points.
10. O_maps ; prints the pressure head, the solute concentration, and the saturation degree of the simulation result at cross sections defined by user.
11. O_rstr ; prints the simulation output of the pressure head and the solute concentration according to format of data input of initial condition. This file is prepared for simulation at next time step.
12. F_model ; calculates numerically the governing equation of the groundwater flow and the solute transport. Supporting functions are;
    a. Init_flo; organizes new initial pressure and solute concentration for each time step.
    b. Shp_flo ;
        - dat_flo ; reads hydrogeological parameter for each element
        - basis ; calculates values of basis functions, weighting function, their derivatives, Jacobians, and coefficient at a point in a hexahedral element for 3D meshes and in a quadrilateral for 2D meshes.
        - flo_ele ; carries out all elementwise calculation associated to pressure head required in the matrix equation, and to calculate element centroid velocities.
        - sol_ele ; carries out all elementwise calculation associated to solute concentration required in the matrix equation. This function call dispers3 to transform a symmetric tensor between two Cartesian coordinate systems
        - bd_flo; implements the specified pressure head node conditions in the matrix equation and assembles all nodewise and cellwise terms in the matrix equation.

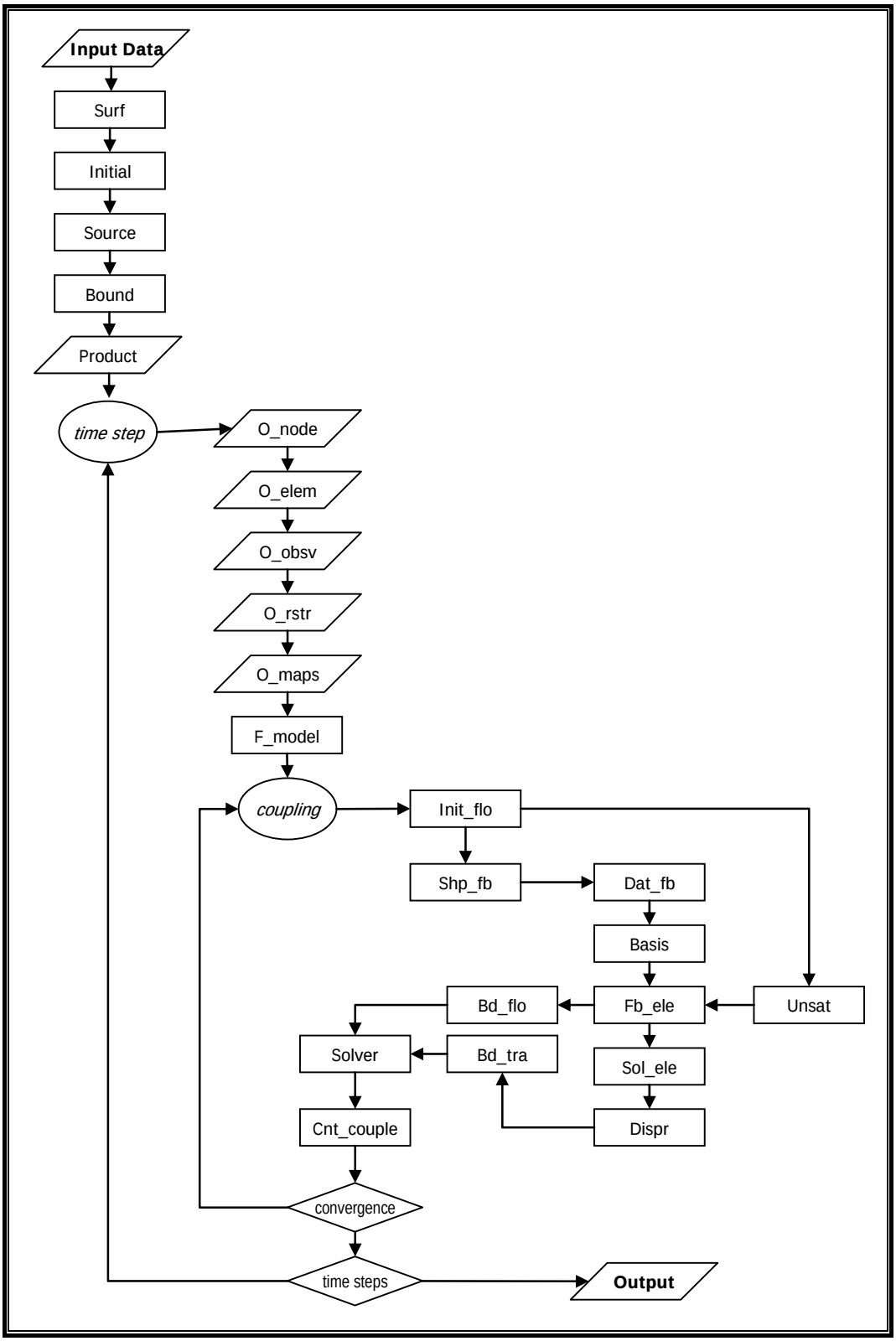

Figure 3.17 Main logic of the numerical groundwater flow program

- bd_tra; implements the specified concentration node conditions in the matrix equations and assembles all nodewise and cellwise terms in the matrix equation.
- unsat ; unsaturated flow functions. This function requires modification by user to fix with the modeling area. In this seawater intrusion code, it is used van Geneutchen parameter defined on SUTRA model.
- solver ; linearisasi governing equation using pre-conditioned bi-conjugate gradient. Explain more detail later.

c. cnt_couple ; to control coupling process. If standard of convergence criterion has not achieved the re-calculation is required for implicit coupling option.

Table 3.2 Summary of input and output files for the groundwater flow model.

File Identity	Functions	Contents
Input Files	Modfiles F_grid F_phidro F_pcov F_node F_satl F_ctrl F_obsv F_source F_bc F_initp F_initu	Assignment files input Node information Values of hydrogeological parameter Elements cover nodes Nodal information Satellite node Parameter standard of model Observation points Nodes for sinks and sources Nodes for specified p & C Initial freshwater pressure head Initial solute concentration
Output files	F_modv F_eleo F_obso F_preo F_cono f_maps	Nodewise output Elementwise output Observation output Pressure output Concentration outp Map of pressure, concentration, and saturation

3.3.4. Numerical Solver

Numerical solver supported by SUTRA2D3D are DIRECT (banded Gaussian elimination), CG (IC-preconditioned conjugate gradient), GMRES (ILU-preconditioned generalized minimum residual), and ORTHOMIM (ILU-preconditioned orthomim). In our developed code is employed PBCG (preconditioned bi-conjugated gradient) supported by indexed storage of sparse matrix. Both methods are described as follow.

Indexed storage of sparse matrices. Using the tri- or band-diagonal matrices can store in a compact format that allocates storage only to elements which can be nonzero, plus perhaps a few lasted locations to make the bookkeeping easier. However, for more general sparse matrix of dimension $N \; x \; N$ that only contains a few times N nonzero elements, it is surely inefficient and often physically impossible to allocate storage for all N^2 elements. Even if one did allocate such storage, it would be inefficient or prohibitive in machine time to loop over all of it in search of nonzero elements. Therefore, an indexed storage scheme is required that stores only nonzero matrix elements. This numerical code employs the *"row-indexed sparse storage mode"*.

Pre-Conditioned Bi-conjugate Gradient. The conjugate gradient (CG) method, first introduced by Hestenes and Stiefel, has recently become popular for solving Finite Different or Finite Element discretization of the groundwater flow equation. The attractiveness of the CG methods for large sparse systems is that they reference *stiffness matrix* only through its multiplication of a vector, or the multiplication of its transpose and a vector. Therefore, these operations can be very efficient for a properly stored sparse matrix.

The simplest, "ordinary" conjugate gradient algorithm solves only in the case that stiffness matrix (***A***) is symmetric and positive definite. Generalization of this "ordinary" conjugate gradient algorithm to solve linear function but not necessarily positive definite or symmetric may be called as the *bi-conjugate gradient method*. Applying of the bi-conjugate gradient method increases the number of iterations required. In order to allow the algorithm to converge in fewer steps, it is required to apply preconditioned form to in the original equation;

$$A.x = b \tag{3.71}$$

The simplest ordinary conjugate gradient algorithm solves only in the case that A is symmetric and positive definite. It is based on the idea minimizing the function;

$$f(x) = \frac{1}{2} xA.x - bx \tag{3.72}$$

This function is minimized when its gradient:

$$\nabla f = A.x - b \tag{3.73}$$

is zero, which is equivalent to equation (3.71).

In order to solve linear problem but not necessarily positive definite or symmetric, a different generalization of bi-conjugate gradient method is important. In addition to allow convergence in fewer steps, the preconditioned is applied with general form as follow;

$$\left(\widetilde{A}^{-1} A\right)x = \widetilde{A}^{-1} b \tag{3.74}$$

The matrix $\widetilde{A}$ is called a *pre-conditioner.*

Implementation of this numerical solver into our code by simplifying the code is written by Anne Greenbaum that available on *Numerical Recipes; The art of scientific computing,* to be fixed with this code. The original code provides two options in defining convergence criterion that are;

$$\frac{|Ax - b|}{|b|} < tol \tag{3.75}$$

$$\frac{\left|\widetilde{A}^{-1}(A.x - b)\right|}{\left|\widetilde{A}^{-1} b\right|} < tol \tag{3.76}$$

Where *tol* is input quantity of convergence tolerance defined by user.

3.4. MODEL VERIFICATIONS

Due to a complexity of the numerical algorithm and the computer code, each developed code requires verification to ensure its ability in solving an interest problem in certain of accuracy. The code verification refers to comparison of the numerical solution obtained by the model with one or more analytical solution or with other numerical solutions. Several benchmark problems exist for verification of numerical model of variable density groundwater flow includes spatial and temporal variation of density. However, except of the Henry's problem there is no other analytical solution available, so the verification is mainly performed by comparing with obtained results from some other numerical code.

3.4.1 Vertical Interface between Fresh and Saline Groundwater

Verification model by using problem of vertical interface is aimed to observe groundwater flow due to density differences in a simple geometry for 2D model. Problem domain is considered as a homogeneous aquifer with saline water at the right and freshwater at the left part. The domain dimension is 0.5 m in vertical, and 1.0 meter on horizontal direction. To carry out simulation, the domain was discretized by using a uniform element of 0.0125 m x 0.0125 m. A node on the left boundary at z = 0.25 m is described as a Dirichlet boundary condition (constant freshwater head equal to 0.0 m), and other nodes are no-flow boundary. Numerical simulation was performed in period of time of 1440 minutes with time step 1 minute. The boundary conditions and the initial condition of the domain are illustrated on figure (3.18), and the hydrogeological parameters of the system are summarized in the table (3.3).

Table 3.3. Physical parameters of the vertical interface problem

Parameter	Unit	Value
Hydraulic conductivity *(k)*	ms^{-1}	$1.0.10^{-3}$
Porosity *(ε)*	-	0.1
Freshwater density (ρ_f)	$kg.m^{-3}$	1,000
Saline water density (ρ_s)	$kg.m^{-3}$	1,025
Longitudinal dispersivity (α_L)	m	0.0
Transversal dispersivity (α_T)	m	0.0
Effective molecular diffusion (D_m)	m^2s^{-1}	0.0

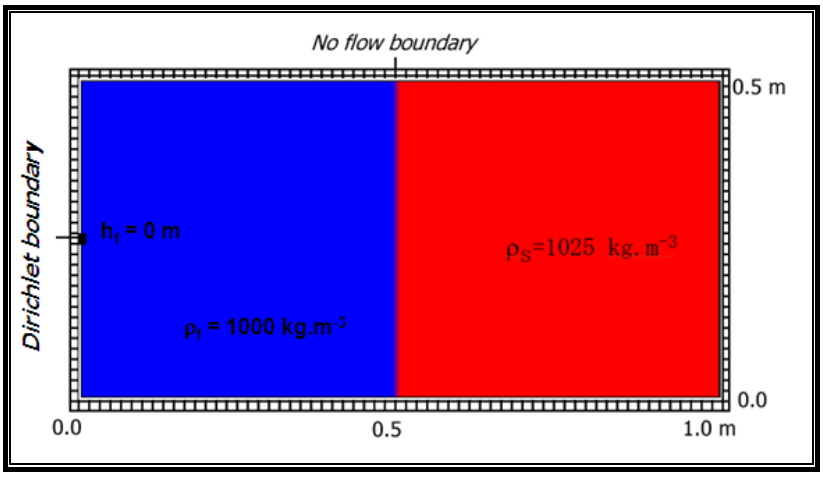

Figure 3.18 Geometry of the vertical interface problem

Numerical solution results shown that the model can figure out the groundwater flow of the system without any numerical problem. Consistency of groundwater movement to a new equilibrium is shown on figure (3.19). As a function of time, the initial vertical interface is moving towards a horizontal position.

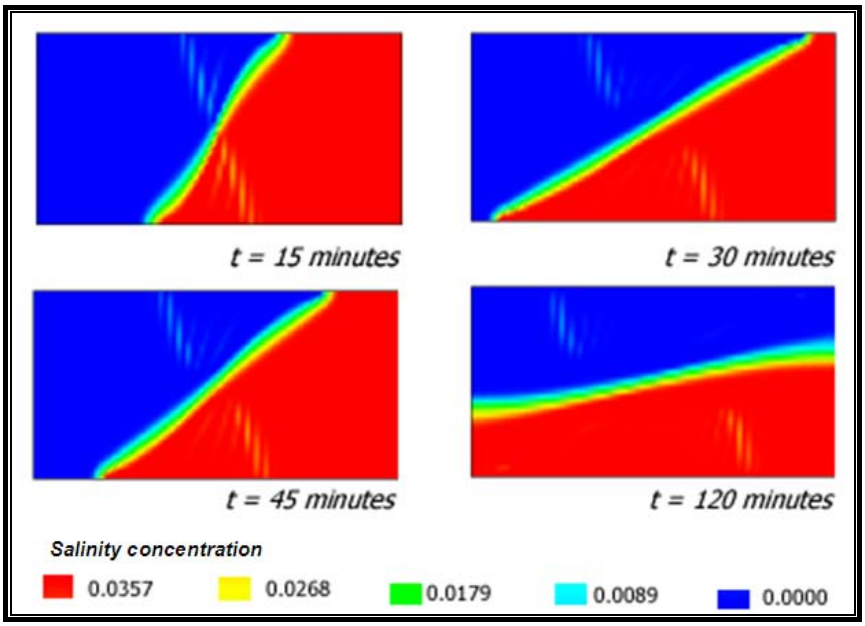

Figure 3.19 Evolution of the interface between fresh and saline groundwater.

3.4.2. Saltwater Pocket in a Fresh Groundwater Environment

Simulation of the saltwater pocket problem is to investigate the groundwater flow with density difference under influence of gravity for 2D model. The saltwater mix with freshwater is caused by hydrodynamic dispersion. Dimension and boundary conditions of the problem are shown on figure (3.20), and the hydrogeological parameters of the system are summarized in table (3.4). The simulation was performed to observe the characteristic of the mixing process on the system in a different mesh size. Three type of mesh size employed in the problem domain are 20 x 10, 40 x 20, and 80 x 40 in lateral and vertical direction respectively.

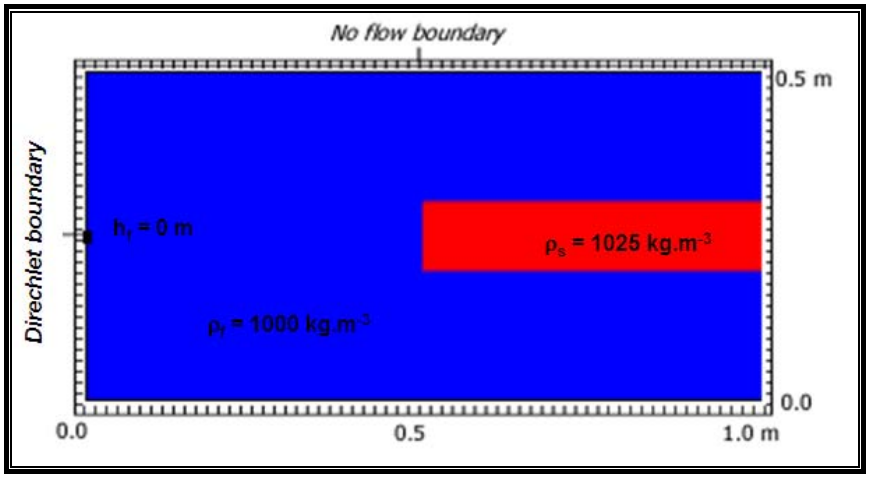

Figure 3.20 Geometry of the saltwater pocket problem

Table 3.4 Physical parameters of the saltwater pocket problem

Parameter	Unit	Value
Hydraulic conductivity *(k)*	ms^{-1}	1.0×10^{-3}
Porosity *(ε)*	-	0.1
Freshwater density *(ρ_f)* at C=0	$kg.m^{-3}$	1,000
Saline water density *(ρ_s)* at C=35000	$kg.m^{-3}$	1,025
Longitudinal dispersivity *(α_L)*	m	1.0
Transversal dispersivity *(α_T)*	m	0.1
Effective molecular diffusion *(D_m)*	m^2s^{-1}	1.0×10^{-9}

Outputs of numerical simulation demonstrate the evolution of saltwater pocket on the freshwater environment such as figure (3.21). The numerical results show the saltwater movement reaches bottom of domain after 60 minutes of elapsed time. This problem of saltwater pocket is quite sensitive to the mesh size, in which a small mesh shows the salinity mixing go faster than a big mesh size. These phenomena refer to the stability of the code from numerical dispersion problem. However, for modeling application, time and space discretization has important effect to the numerical results, so that both variables should be chosen carefully particularly for a very low of the groundwater flow velocity.

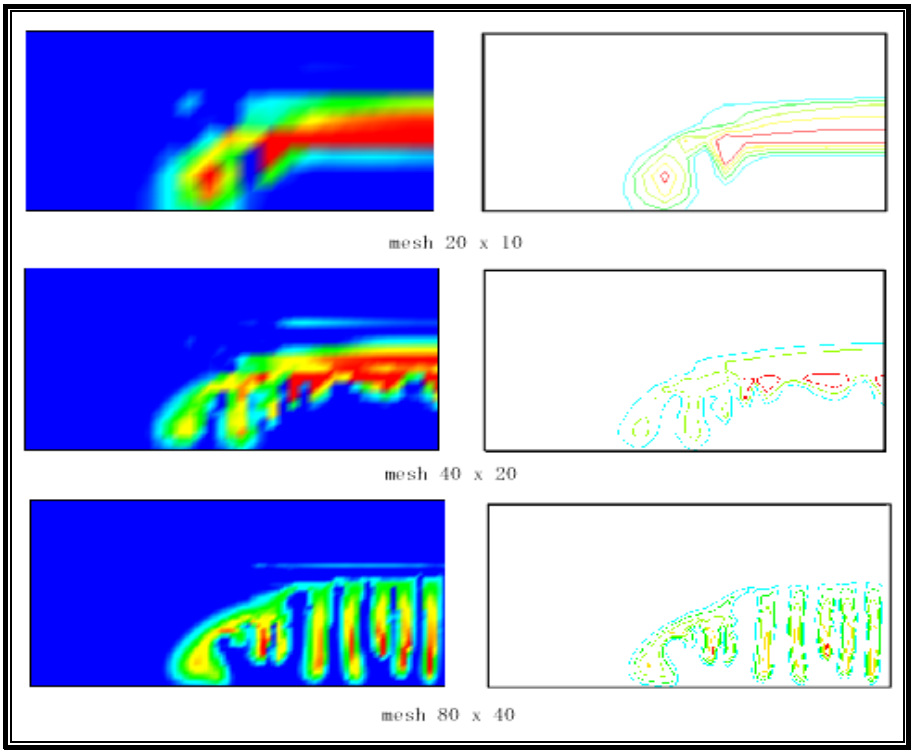

Figure 3.21 Evolution of salt pocket on freshwater environment after 60 minutes

3.4.3. Henry's Seawater Intrusion Problem

The Henry problem is the one of the analytical solution for density dependent groundwater flow in combination with hydrodynamic dispersion. The problem is unique because more than 40 years of research, there have a lot of discussions about the reproducibility and quality of Henry's analytical solution, which is rather controversial.

The Henry problem caused further confusion among the modeling community because some modelers attempting to verify numerical codes calculated an erroneous value for molecular diffusion that did not correlate with the original value used by Henry (Voss and Sousa, 1987). However, in the literature, the problem is always used as benchmark of variable density models (Simpson and Clement, 2003). Since the Henry's solution is rather controversial, the verification approach is mainly to compare against published numerical solution.

Geometry of the Henry's problem was formulated for seawater intrusion in a homogeneous, isotropic, confined, and rectangular aquifer. The aquifer has dimensions of height *(d)* = 100 cm by length *(l)* = 200 cm. The top and bottom boundaries are impermeable (no-flow boundaries), with a constant freshwater flux *(Q)* = $6.6.10^{-2}$ kg/sec entering the aquifer along the vertical at x = 0, and the seaside boundary at x = 200 cm is a constant saltwater head. The boundary conditions are summarized in figure (3.22). Hydrogeological parameters of the aquifer are that the hydraulic conductivity *(K)* is 1 cm/sec, the effective porosity is 0.35, the coefficient of molecular diffusion *(Dm)* is $6.6.10^{-6}$ m^2s^{-1}, and the specific storage *(Ss)* is set to zero. Reference density (ρ_0) is 1,000 $kg.m^{-3}$, and brine density (ρ_s) is 1,025 kgm^{-3}. Figure (3.22) shows the geometry of the Henry's problem and boundary conditions.

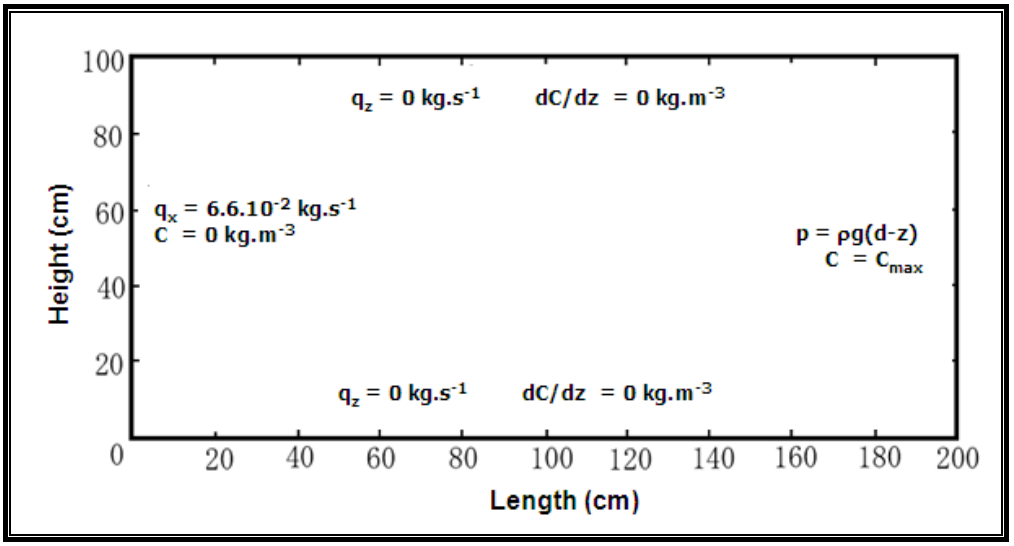

Figure 3.22 Geometry and boundary conditions applied on the Henry's seawater intrusion problem

This Henry's problem is used to study seawater intrusion in a cross section under steady state. The simulation was performed by using a regularly aquifer discretization with 231 nodes (21 horizontally and 11 vertically). Initial condition of the problem was composed of freshwater at time zero, and then saltwater begins to intrude the freshwater system by moving under the freshwater from the sea boundary. The intrusion is caused by the greater density of the saltwater. The time step for the simulation was gradually increased 60 seconds, with starting time at 0 second. In the SUTRA2D3D software, it is simulated 100 minutes to reach steady state. Using our developed code, the steady state is obtained by applying the maximum change in pressure head was less than 1.0 $kg.m^{-1}.s^{-2}$ and concentration was less than $1.0.10^{-4}$ kg. The convergence criterion of numerical solver uses 1.0 $x10^{-10}$ for both flow and solute transport. To reach steady state, it is required 95 minutes of elapsed time. Comparison of the numerical result with SUTRA2D3D result and Henry's analytical solution is shown at figure (3.23) for iso-chlor 25%, 50%, and 75 % of seawater salinity.

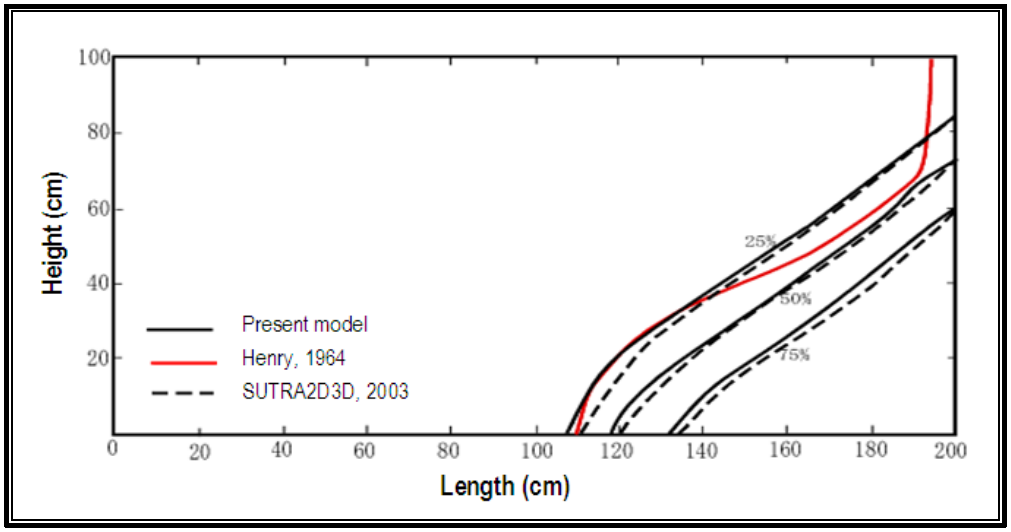

Figure 3.23 Comparison of calculated iso-chlor with SUTRA and Henry's solution for original boundary conditions

Several authors have modified the original boundary conditions to make the problem more realistic that is started by work of Segol (Simpson, 2003). Modification of the original boundary condition has been done at seaside boundary, at x = 200 cm, to combine a partial of freshwater (20% upper part) and partly seawater boundary (80 % lower part). Result of simulation by applied this modified boundary conditions

are shown in figure (3.24) to compare with the result of Simpson and Clement (2003) and Frind (1982).

Using quite different approximation methods, a number of authors obtained similar results. However, the mystery of Henry's solution is that no numerical model so far has been able to produce closely his analytical result, so verification is done to against other numerical results. Verification the model with other models shows a good agreement for iso-chlor 0.25, 0.50, and 0.75. Using the modified Henry's problem results in good agreement for iso-chlor 0.25 and 0.50, but iso-chlor 0.75 shows a different result with the obtained work of Simpson (2003). Applying the model to solve both the original and the modified Henry's problem, it is shown that toe of seawater intrudes more deep into aquifer with the modified boundary condition than with the original one.

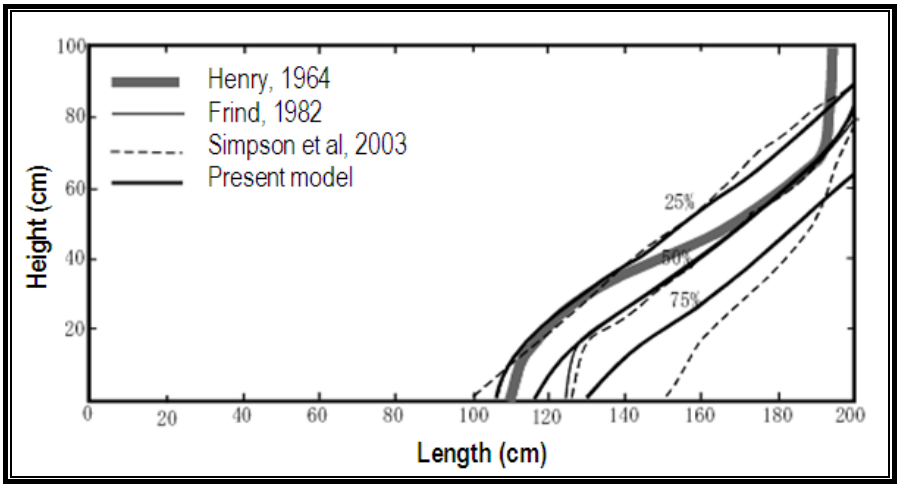

Figure 3.24 Comparison of the simulated result with other solution for modified boundary conditions

In addition, simulation with a different initial condition for the original Henry's problem, initially fresh and initially salty, were performed. Computational time to reach steady state for the initial fresh is faster than initial salty, with 97 and 320 minutes respectively. The iso-chlor 0.50 at a certain time both numerical results are shown in figure (3.25).

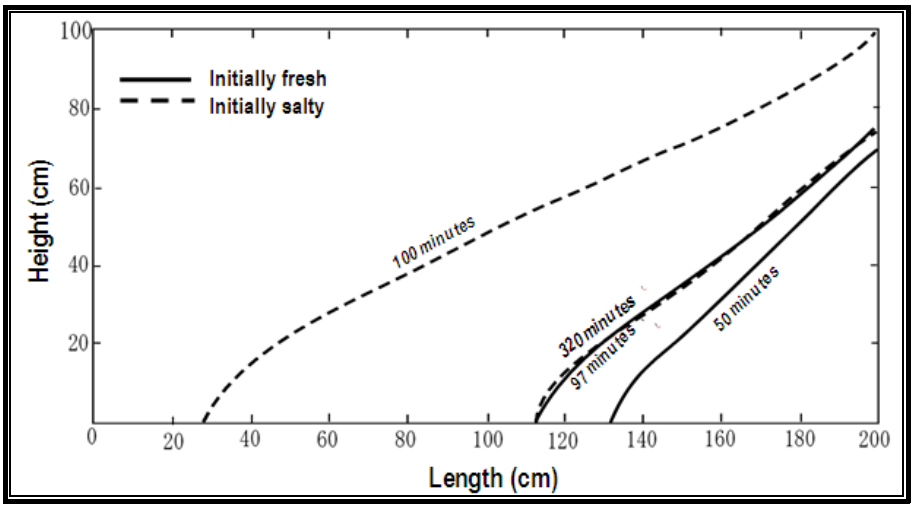

Figure 3.25 Approach to solution steady state from initially fresh and initially salty condition for the Henry's problem

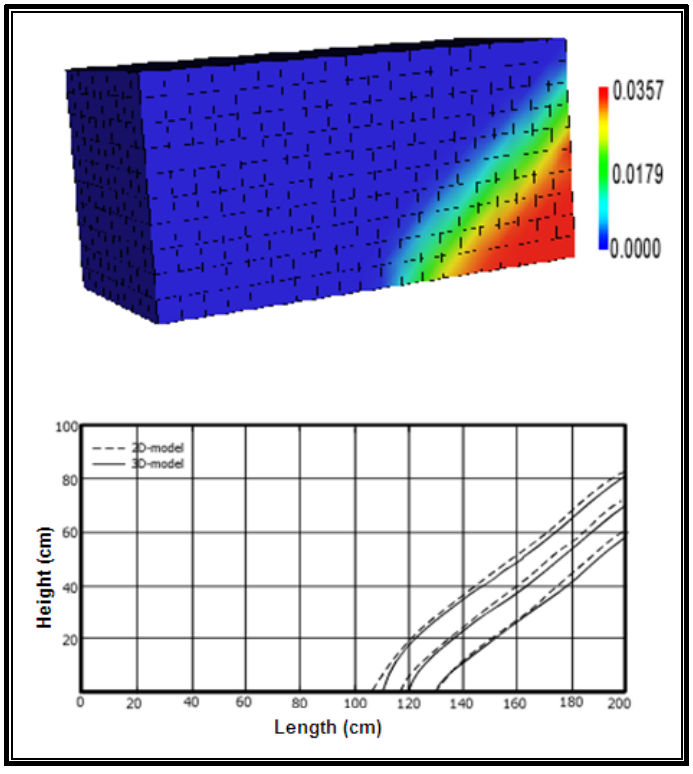

Figure 3.26 Simulation results for extension of the Henry's problem. The 3D visualization (upper) with bar chart describes salinity concentration) and comparison of numerical results between 3D and 2D model (lower).

The original Henry's problem is a two-dimensional model. Since the developed code include 3D model, the problem is extended into 3D model. Numerical result of chloride concentration and pressure head distribution are shown on figure (3.26). The result refers that a reasonable interface of freshwater-seawater is formed which is has a good agreement with 2D model.

Furthermore, in order to investigate the effect of jagged form of mesh to the numerical results the vertical seaside of original geometry of Henry's problem is modified to be a slope boundary. A coastal slope is created by prolong the bottom of layer until 1 meter at seaside boundary. To compare the numerical simulation results the model was run by discretizing the problem domain with the FEM mesh and the Cartesian mesh. Both mesh system is set to produce a same number of 300 elements. Numerical results shown in figure (3.27) have a good agreement for iso-chlor of 25 %, 50 %, and 75 % for both type of mesh.

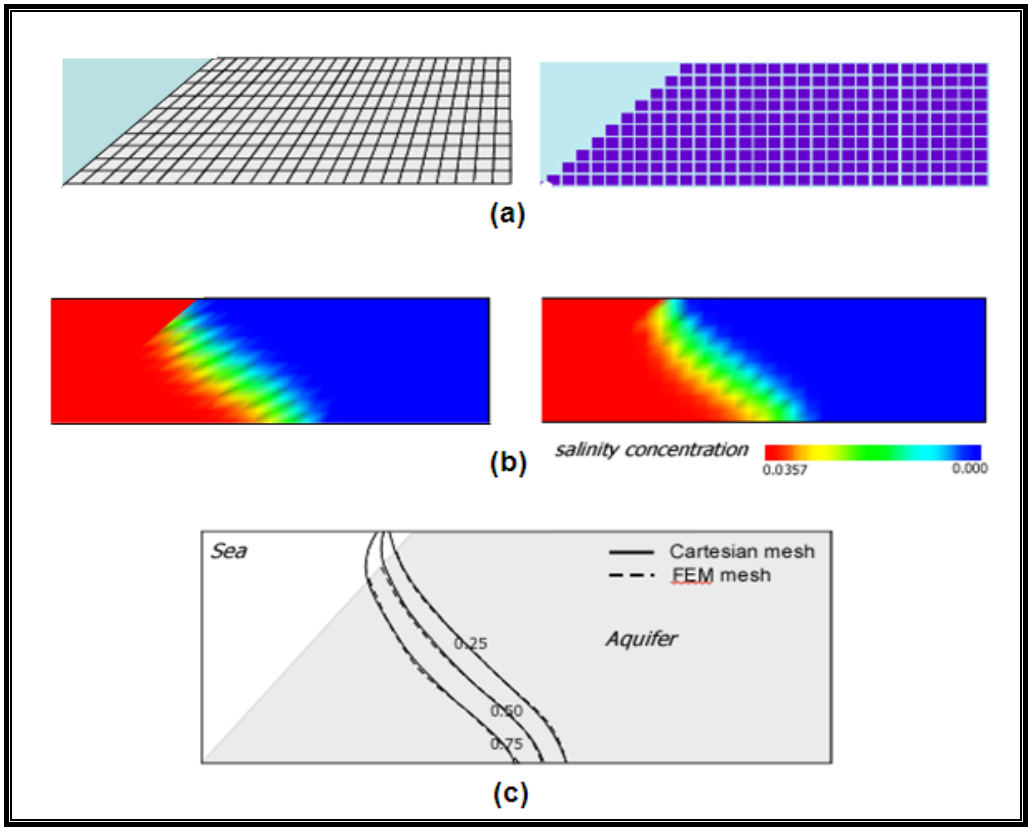

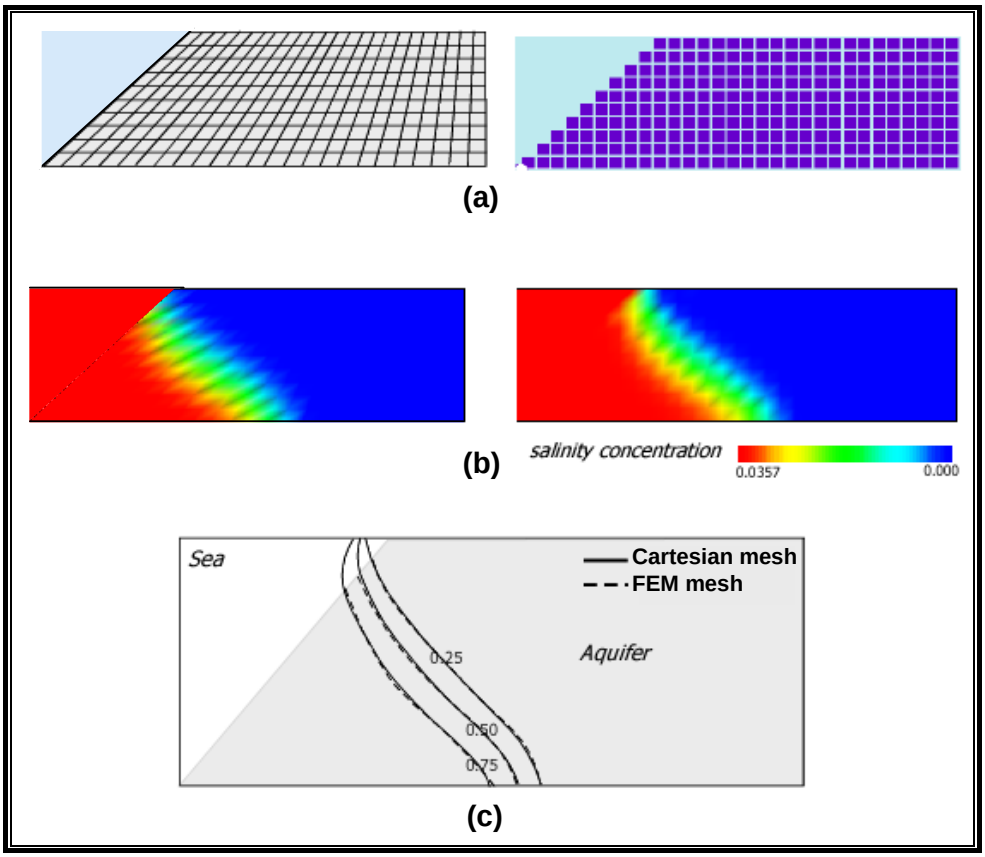

Figure 3.27 *Simulation result of extension of Henry problem with slope at seawater boundary. (left side as the FEM analysis, and right side by this developed code.*

3.4.4. Elder Convection Problem

Elder problem is a free convection problem concerning laminar fluid flow in a closed rectangular box modeled in cross section. The flow within the box was initiated by a vertical temperature gradient, and thermally induced density gradients caused a complex pattern of fingering of the denser water to mix through the box. This problem was studied both physically in the laboratory with the use of Hele-Shaw cell as well as being numerically reproduced. Since the laboratory conditions restricted the fluid flow to laminar conditions, Elder also developed a modified problem with parameters suited to porous media flow where the density dependence was caused by solute variations. This modified Elder problem is another standard benchmark problem used for testing several density-dependent flow codes. This problem is referred as the Elder salt-convection problem (Simpson and Clement, 2003).

The domain and boundary conditions for the Elder salt convection problem describe a closed aquifer, a zero pressure head is maintained at the two upper corners of the domain (Figure 3.28). The aquifer properties and solute transport characteristics are summarized in Table (3.5). Elder (Voss & Souza, 1987) employed a standard finite different method to represent the governing equations for vorticity, stream function, and thermal energy balance. The equations were solved sequentially with a forward temporal difference. The Elder's grid consists of 80 nodes laterally, and 40 nodes vertically, and time discretization 20 steps to reach 1 year of elapsed time. Basically, the system can be modeled by using only a half of the domain (left side or right side), but performing simulation entire box is aimed to check the ability of model to produce a symmetric vortices.

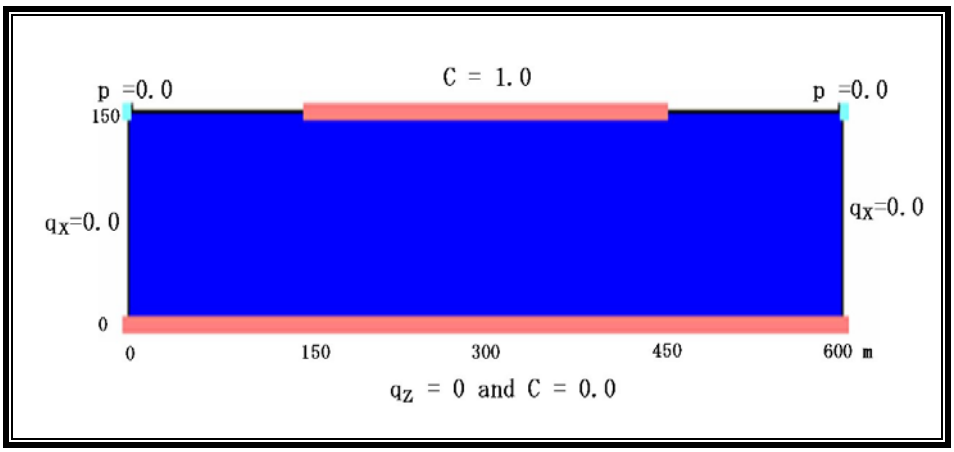

Figure 3.28 Boundary conditions for Elder problem

Table 3.5 Aquifer and transport properties used for the Elder problem

Parameter	Symbol	Unit	Value
Coefficient of molecular diffusion	D_m	m^2s^{-1}	3.565×10^{-6}
Magnitude of gravitational acceleration	g	ms^{-2}	9.81
Intrinsic permeability	k	m^2	4.845×10^{-13}
Maximum density ratio	β_{max}	-	1.2
Specific storage	Ss	m^{-1}	0.0
Porosity	ε	-	0.1
Dynamic viscosity	μ	$kgm^{-1}s^{-1}$	1.0×10^{-3}
Reference density	ρ_o	kgm^{-3}	1000
Brine density	ρ_{max}	kgm^{-3}	1200

Similar to the Henry's problem, there are several published profiles available for the Elder salt convection problem. For example, previously published by Voss and Souza (1987) and Elder are compared to the present numerical result. Comparing these profiles one could draw to conclusions, firstly the current model is capable of reproducing the solute concentration patterns reasonably well. Secondly, the comparison shows that the difficulty in quantitatively benchmarking the Elder problem. Unfortunately, benchmarking the Elder results can be a tedious task as the solutions available in the literature can differ dramatically depending upon the numerical discretization and level of modeling sophistication used to generate results. For, example Kolditz et al (1998) showed that the Elder problem depend upon the level of modeling sophistication chosen for the numerical representation of the density dependent flow and transport processes. Furthermore, their work incorporated a mesh-refinement procedure to show that the results can be quite sensitive to the level of discretization used in the numerical representation of the problem.

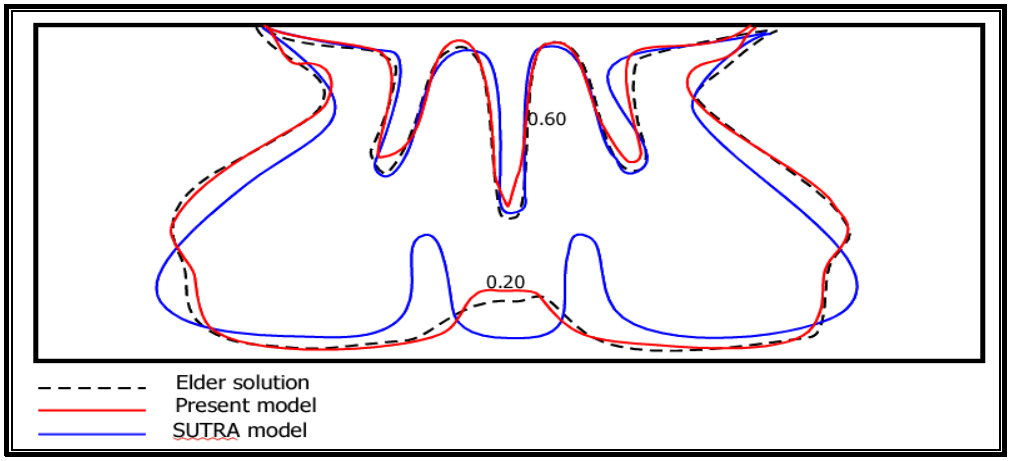

Figure 3.29 Comparison of numerical solution for Elder problem and prior results after 10 years of elapsed time.

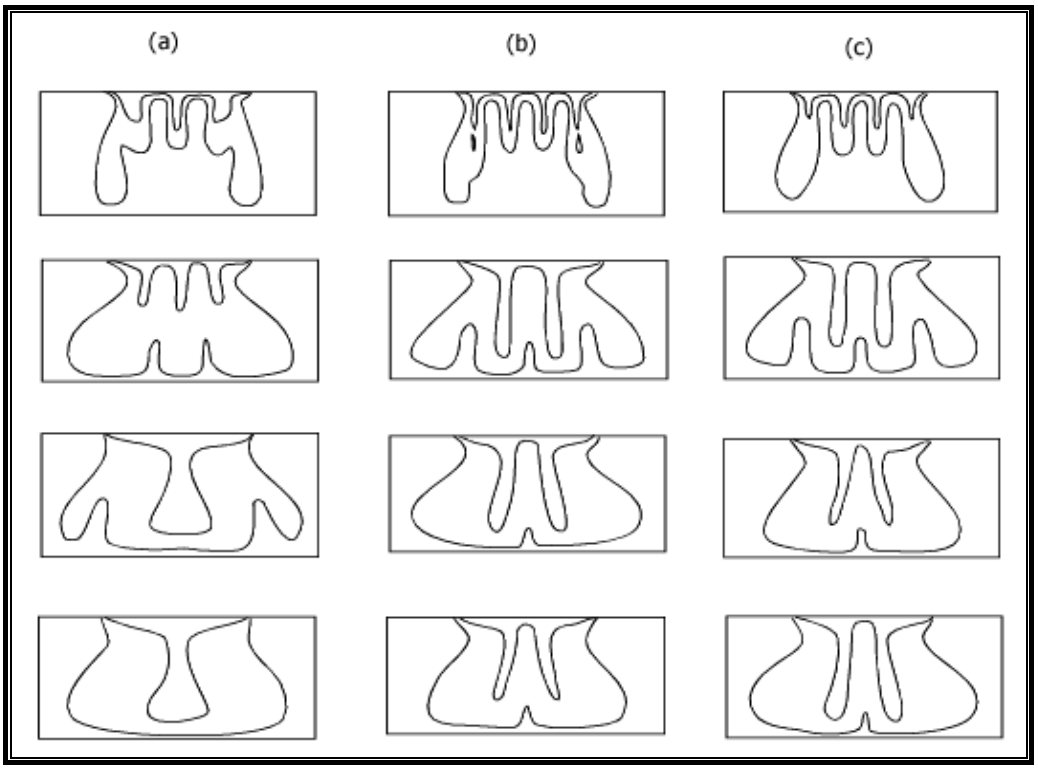

Figure 3.30 Sensitivity of Elder problem to the mesh size shown salinity evolution at 4,10,15 and 20 years for 0.20 and 0.60 iso-chlor.(a) Coarse mesh (1170 elements), (b) fine mesh (4400 elements), (c) very fine meshes (9900 elements) (Kolditz et al, 1998)

Another point of interest with the Elder salt convection problem was shown with work of Boufadel et al (1999), in which the problem was simulated using linear triangular finite elements. They showed that the problem is sensitive to mesh-induced anisotropy when discretized with regularly aligned linear triangular elements and that the mesh had to be refined to overcome these problems. Therefore, given the range of solutions presented in the literature, at best the analyst can only show a qualitative comparison to demonstrate that the profiles generated by the new algorithm capture the essential features of the problem. This is why only a qualitative comparison between the profiles in figure (3.31) and (3.32) is possible for the benchmarking of the current numerical algorithm. In spite of this difficulty, the results from the present model captures the essential features of the fluid flow and the solute profiles are similar to those reported in the literature.

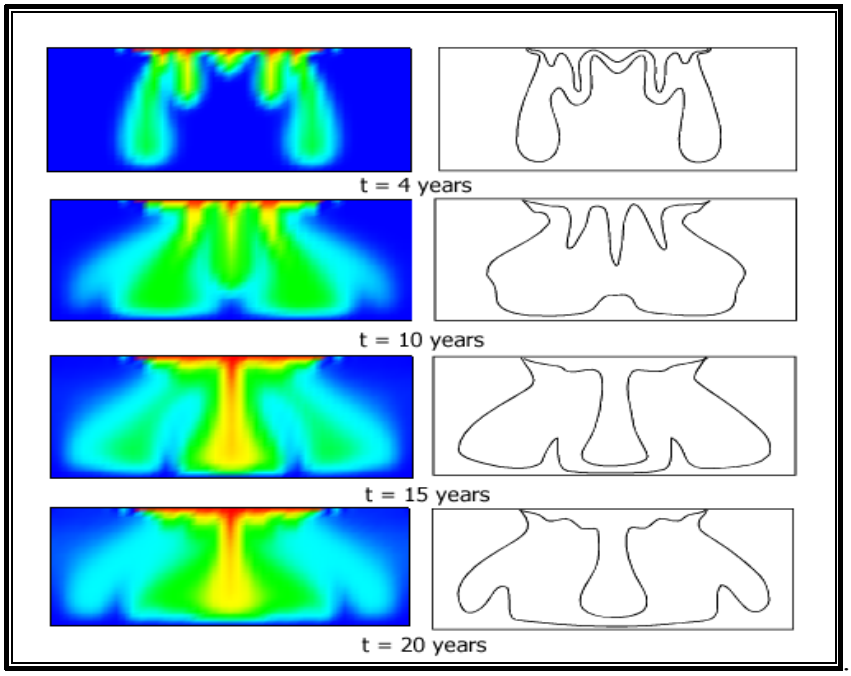

Figure 3.31 *Numerical results for Elder problem, with contour line at 0.2 and 0.6 of concentration with t is elapsed time of simulation.*

In this study, the domain is regularly discretized using 1170 nodes and 1100 linear rectangular elements. The temporal discretization was maintained at a constant interval of one month (2.6298 x 10^6 second), and the iterative coupling between the groundwater flow and the solute transport equations was considered complete when the maximum change in the freshwater pressure head between iteration less than 500 kg. A fully implicit temporal weighting scheme was used to approximate the transport equation. The distribution of the coupled flow and transport characterized was determined after; 4, 10, 15, and 20 year of simulation

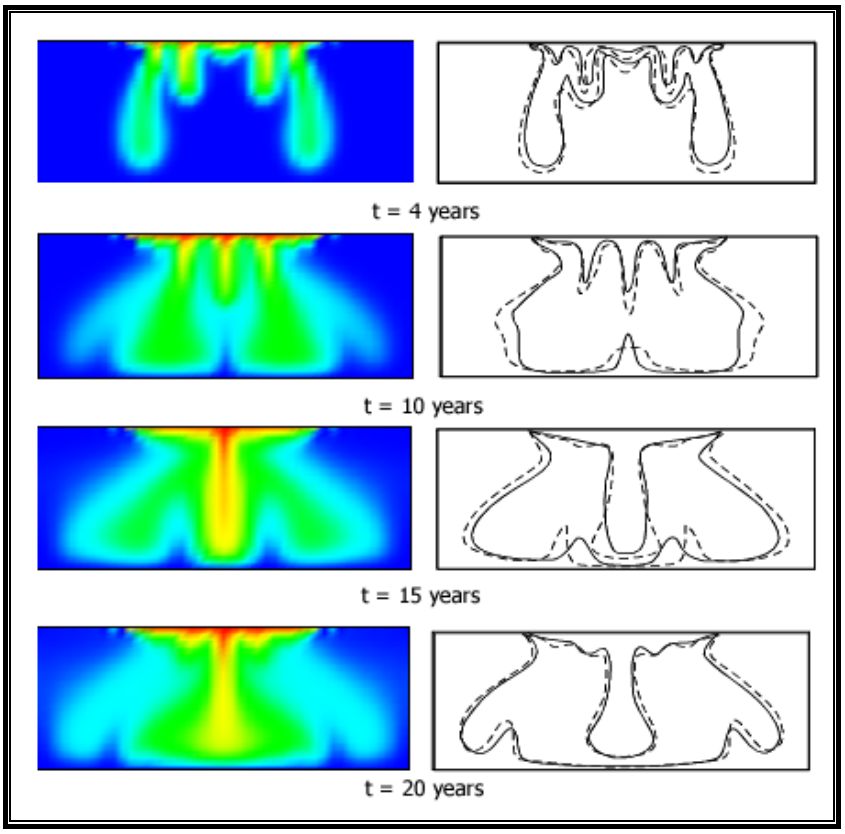

Figure 3.32 Visualization and contour iso-concentration of simulation result for 3D-model of Elder Problem. Dashed line represents the obtained 2D model and solid line for 3D model.

3.4.5. Circular Island Problem

Verification of developed code for problem of variably density groundwater flow at saturated-unsaturated medium uses Circular island problem. This problem used Voss and Provost (2003) to compare the numerical simulation result obtained by performing simulation with 2D radial mesh with the well established SUTRA code and fully 3D mesh with SUTRA2D3D code. The accuracy of numerical result by employing the Cartesian mesh was investigated in this study to figure out both the saturation degree on unsaturated zone, and salinity distribution on the groundwater.

This circular island problem concerns simulation of the post-drought recharge and restoration of the lens. The aquifer on the island is unconfined with both unsaturated and saturated zones and the material properties are generally homogeneous but

permeability is anisotropic. The problem poses flow in the sea undergoes a prolonged drought, and all ground water beneath the island becomes saline. Then, fresh rainwater recharge to the island begins and continues at a constant rate, raising the water table on the island, flushing out seawater, and eventually establishing a stable freshwater lens and a diffuse saltwater-freshwater interface.

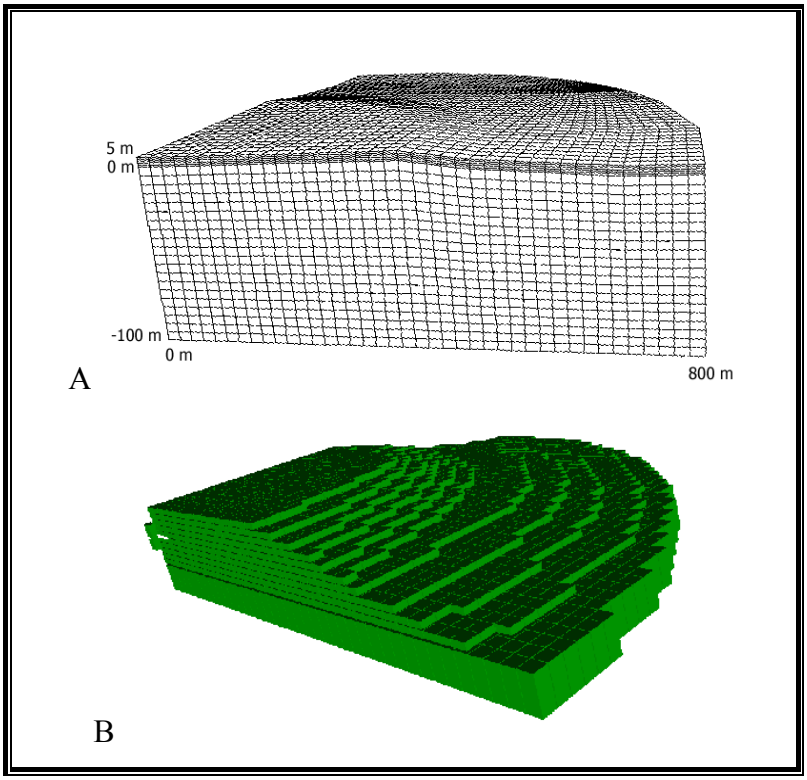

Figure 3.33 *Mesh employed on the simulation of the circular island problem. a). FE mesh employed by the SUTRA2D3D code, b). Cartesian mesh employed by developed code showing mesh from -15 m below sea level to top surface.*

Voss and Provost (2003) simulated the problem by representing only one fourth of the entire island to reduce size of simulation, taking some advantage of radial symmetry of the 3D solution. The finite-element mesh employed on the simulation does not inherently favor a radial symmetric even though the solution is radial symmetric. The 3D mesh consist of 40 by 40 elements horizontally and 25 elements vertically, giving 43,706 nodes and 40,000 elements. The horizontal direction is discretized with 20 m spaces, vertically 5 m except 5 meter from top surface with 1 m. By using the Cartesian mesh, it is used grid space of 20 meter horizontally, and 5 m vertically

except from top surface to 5 m below sea level with 1 m. The discretization gives 33,218 nodes and 29,800 elements within the domain after eliminating the empty background mesh.

Table 3.6. Hydrogeological parameter of model of circular island problem

Parameter	Symbol	Unit	Value
Compressibility of matrix	α	ms^2/kg	1.00×10^{-8}
Compressibility of fluid	β	ms^2/kg	4.47×10^{-10}
Porosity	ε	-	0.01
Fluid viscosity	μ	kg/ms	1.00×10^{-3}
Freshwater density	ρ_0	kg/m^3	1000.00
Seawater density	ρ_{sea}	kg/m^3	1024.99
Horizontal intrinsic permeability	k_h	m^2	5.00×10^{-12}
Lateral intrinsic permeability	k_v	m^2	5.00×10^{-13}
Molecular diffusivity	D_m	m^2/s	1.00×10^{-9}
Longitudinal dispersivity	α_L	m	10.0 and 2.5
Transversal dispersivity	α_T	m	0.10
Rainfall recharge	Q_{IN}	kg/m^2	2.3776×10^{-5}
Seawater salinity concentration	C_{sea}	-	0.0357
Residual fluid saturation	S_{wres}	-	0.3
Van Genutchen soil parameters	a	ms^2/kg	5.0×10^{-5}
	n	-	2

Boundary conditions of the hydrogeological system may be set that there is no flow crosses the inner boundary (the axis of radial symmetry, $r = 0$) and the bottom boundary (z = -100 m). Along the vertical outer boundary (r = 800 m) is specified as hydrostatic seawater pressure. Along the top boundary, nodes above sea level (r <= 500 m) receive freshwater recharge (equivalent to 75.0 cm/yr) totaling 18.6658 kg/s of recharge for the entire circular island. The amount of recharge at each node is determined by the surface area of its cell on the top surface. At nodes below sea level, the pressure is specified to be hydrostatic seawater pressure. Any fluid that enters at points of specified pressure has the concentration of seawater. Values of hydro-geological parameter of model are shown on table (3.6). Initial condition of salt concentration is set as seawater, and initial pressures are obtained through an extra simulation. The extra simulation was carried out

by setting boundary condition that no recharge at the surface and specified pressure head along the sea bottom and the outer boundary.

Under transient condition, the model was run to approximate both pressure and concentration using the time step of 6311520.0 second (0.2 year). The modeling achieves a new steady state after 100 time steps (20 year). The numerical results was analyzed by using the output obtained by using the SUTRA2D3D with the FEM mesh and by using this developed code with the Cartesian mesh. Results are reported 20 years after recharge begins, by which time the system has nearly reached a new steady state. Results of both simulations are compared in figure (3.34), (3.35), and (3.36). Small biases are found from both figures around the top surface boundary. This can be understood due to representation of slope surface of the Cartesian mesh is less accurate than the finite element mesh. However, it can be accepted that the simulations provide consistent saturated-unsaturated, variable-density fluid flow and solute transport results. Both results exhibit a good agreement to produce concentration distribution on groundwater and saturation degree on unsaturated zone.

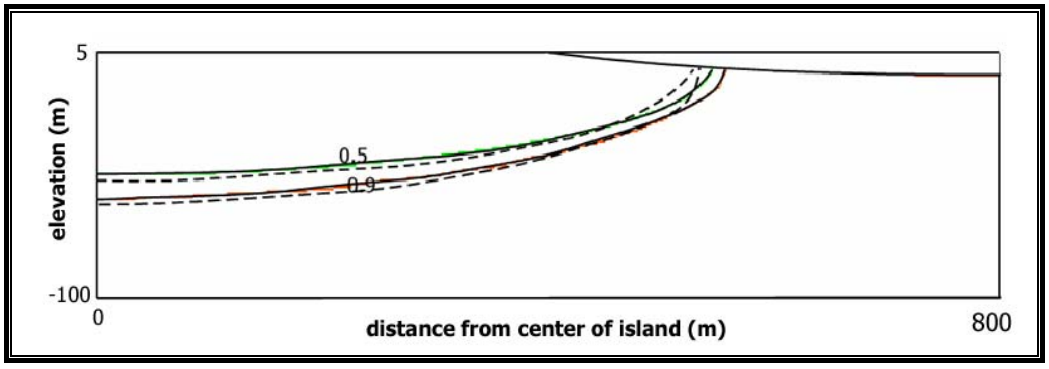

Figure 3.34 Comparison of result from the sutra and the developed code of the circular island problem. Concentrations at t = 20 years.

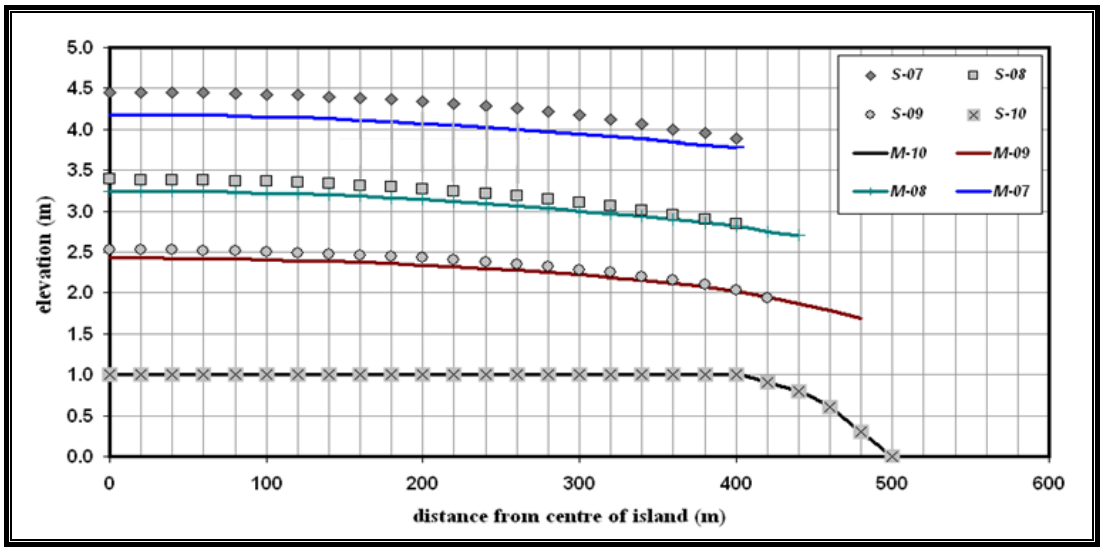

Figure 3.35 *Comparison of water saturation results from sutra and our developed code of the circular island problem at simulation time of 20 year. Thick dashed line indicates sutra results, and solid line the developed code*

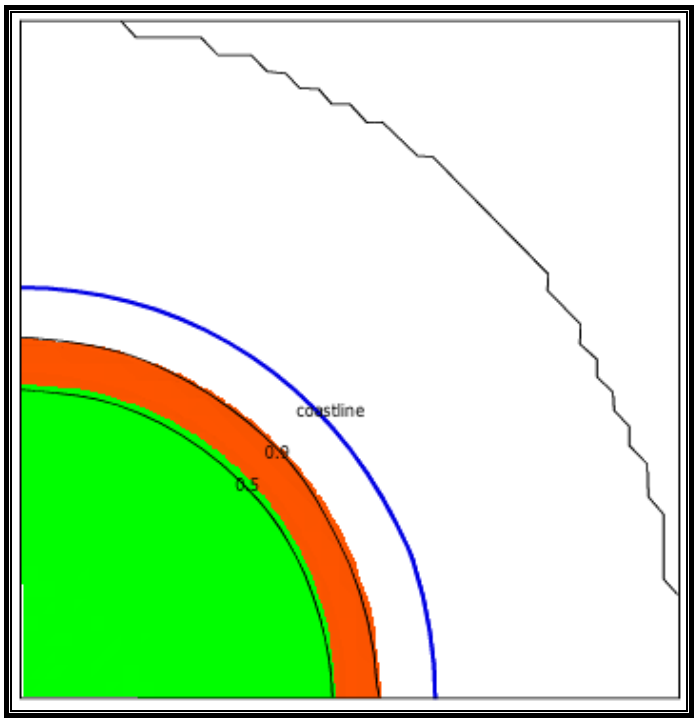

Figure 3.36 *Areal view result from the 3D model of the circular island problem, solute concentration at 35 m below seawater level at t=20 year. Concentration is expressed as the fraction of seawater concentration. Colorfull area is calculated by SUTRA and solid line by this developed code.*

3.5. DISCUSSION

A new numerical groundwater flow code employing the Finite Element Method with the Cartesian mesh has been developed. The developed code is designed to simulate the phenomena of the groundwater flow on saturated-unsaturated medium (variable saturated) and the solute transport (variable density). Even though this study emphasized to the implementation of the Cartesian mesh by considering its simplicity, this code is also applicable to the computational domain discretized by using the FEM mesh. This numerical groundwater flow code is supported with a mesh generation code to provide an easy way in mesh generation process. The mesh generation code consists of 2D and 3D model in which both these codes use moving least square technique for surface interpolation data. The mesh generation code and the groundwater flow code are integrated with loose coupling system, in which the mesh generation code provides some output files readable with the numerical groundwater flow code.

The numerical groundwater flow code approximates the governing equation by applying a hybridization of Finite Difference Method and Finite Element Method adopted from the SUTRA code. Two non-linear equations of fluid mass balance and of solid mass balance can be solved by either implicit or explicit scheme. In order to reduce computer memory demand in storing the stiffness matrix, the row-index sparse storage matrix is adopted, and data input to elements are designed to recognize type of material instead of defining all parameters to each element. The numerical approximation is linearized by using Pre-Conditioned Bi-Conjugate Gradient method.

The developed groundwater flow code is verified by using benchmark problems of variable saturated-density flow. These problems are vertical interface problem, the saltwater pocket problem, the Henry's seawater intrusion problem, the Elder salt-convection problem, and the circular island problem. The obtained numerical results show a good agreement with some others published numerical result.

This developed code using Cartesian mesh system in which has weakness to represent the irregular shape boundary. By using irregular size of the Cartesian mesh system, the problem of representing shape boundary can be reduced. For a certain modeling purposes, representing with similar size may be become simple technique but it will

required a huge number of element. For such kind modeling effort, implementation of parallel computation becomes a necessity.

The numerical code of groundwater flow applies concept of the equivalent freshwater pressure head. Therefore, implementation of this code can be more flexible, which can be used to simulated problem not only for seawater intrusion phenomena, but also for another type of groundwater pollution. However, defining of the contaminant to the model should know pollutant density. In addition, regarding to issue of rise water level due to global warming, this code adopt it easily. In the model verification, it showed that this code could provide a satisfactory result for irregular surface boundary of modeling area. Therefore, assigning the invasion of the seawater on surface area can be done easily by take concern to the equivalent freshwater pressure head.

REFERENCES

Aftosmis, M.J., 1997, Solution adaptive Cartesian grid methods for aerodynamic flows with complex geometris, *Computational Fluid Dynamics*, von Karman Institute for Fluid Dynamics.

Anderson MP., and Woessner MW., 2002, *Applied Groundwater Modeling*, Simulation of flow and advective transport, Academic Press, INC, New York.

Babuska I., and Melenk J.M., 1997, The Partition of Unity Method, *International Journal for Numerical Methods in Engineering,* Vol. 40, pp.727-758.

Belytschko T., Krongauz Y, Organ D., Fleming M., Krysl P., 1996, Meshless Methods; An overview and recent developments, *Computational Method in Applied Mechanics and Engineering*, Vol. 139, pp.3-47.

Boufadel, M.C., Suidan, M.T., and Venosa, A.D., 1999, A numerical model for density-and-viscosity-dependent flows in two-dimensional variably saturated porous media, *Journal of Contaminant Hydrology:* 37, pp. 1 -20

Breuck W.D., 1991, *Hydrogeology of Salt Water Intrusion*; A selection of SWIM Papers, International Association of Hydrogeologists, Verlag Heinz Heise, Vol. 11, Hannover.

Dolbow J., and Belytschko T., 1999, Numerical Integration of the Galerkin Weak Form in Meshfree methods, *Computational Mechanics,* Vol. 23, pp. 219-230.

Fetter, C.W., 1992, *Contaminant Hydrogeology,* Macmillan Publishing Company, New York.

Filipiak, M., 1996, *Mesh Generation*, Edinburgh Parallel Computing Centre, The University of Edinburg.

Forrer, H., and Jeltsch, R., 1998, A higher-order boundary treatment for cartesian-grid methods, *Journal of Computational Physics: 140*, pp. 259 – 277.

Fries T.P., and Matthies H.G., 2003, *Classification and Overview of Meshfree Methods,* Institute of Scientific Computing, Technical University Braunschweig, Brunswick.

Ge, Y., and Boufadel, M.C., 2005, Solute transport in multiple-reach experiments : Evaluation of parameters and reliability of prediction , *Journal of Hydrology;* Article in press, pp. 1-14.

Ingram, D.M., Causon, D.M., and Mingham, C.G., 2003, Development in Cartesian cut cell methods, *Mathematics and Computers in Simulations :* 61, pp. 561-572.

Jin C., Suzuki K., and Ohtsubo H., 2000, Linear Structural Analysis Using Cover Least Square Approximation*, Journal of Applied Mechanics*, Vol. 3.

Kolditz O., Ratke R., Diersch H.G., and Zielke W., 1998, Coupled Groundwater Flow and Transport; 1. Verification of variable density flow and transport models, *Advances in Water Resources*, Vol. 21, No. 1, pp. 27-46.

Lancaster P., and Salkauskas K., 1981, Surface Generated by Moving Least Square Methods*, Mathematics of Computation*, Vol. 37 no. 155, pp.141-158.

Liu G.R., 2003, Mesh Free Methods, *Moving Beyond the Finite Element Method*, CRC Press Ltd, New York.

Ono K., Fujitani K, Fujita H., 1999, Application of CFD Using Voxel Modeling to Vehicle Development, *Proceedings of the 3rd ASME/JSME Joint Fluids Engineering Conference*, San Fransisco.

Park S.H., and Youn S.K., 2001, The Least-Square Meshfree Method**,** *International Journal for Numerical Methods in Engineering*, 52, pp. 997-1012.

Persson P.O., 2005, *Mesh Generation for Implicit Geometries*, PhD Thesis Massachusetts Institute of Technology.

Petersen, S.B., Rodrigues J.M.C., and Martins, P.A.F., 2000, *Automatic Generation of Quadrilateral Meshes for the Finite Element Analysis of Metal Forming Processes*, Finite Elements in Analysis and Design, Vol.35 Issues 2,p. 157-168.

Press, W.H., Teukolsky, S.A., Vetterling, W.T., and Flannery, B.P., 1992, *Numerical Recipes in C,* The art of scientific computing, Second edition, Cambridge University Press, Cambridge.

Schwartz F.W., and Zhang H., 2003, *Fundamental of Groundwater*, John Wiley & Sons, Inc, New York.

Simpson, M.J., and Clement, T.P., 2003, Theoritical analysis of the worthiness of Henry and Elder problem as benchmarks of density-dependent groundwater flow models, *Advances in Water Resources:* 26, pp. 17-31.

Voss C.I., and Provost, A.M., 2003, *SUTRA,* A Model for Saturated-Unsaturated Variable-Density Ground-water Flow with Solute or Energy Transport, *Water-Resources Investigation Report 02-4231*, U.S. Geological Survey, published online on internet at http://water.usgs.gov/nrp/gwsoftware.

Voss C.I., and Souza W.R., 1987, Variable Density Flow and Solute Transport Simulation of Regional Aquifers Containing a Narrow Freshwater-Saltwater Transition Zone, *Water Resources Research*, Vol. 23, No. 10, pp.1851-1866.

Wang H.F., and Anderson, MP., 1982, *Introduction to Groundwater Modeling*, W.H Freeman and company, San Fransisco.

Wesseling P., 1992, *An Introduction to Multigrid Methods*, John Wiley & Sons, Chisheter.

Yagawa G., 2004, Node-by-Node Parallel Finite Elements; a virtually meshless method, *International Journal for Numerical Method in Engineering*, Vol. 60, pp. 69-102.

Zalik B., Clapworthy G., and Oblosenk C., 1997, An Efficient Code-Based Voxel-Transversing Algorithm, *Computer Graphics Forum*, Vol. 16, no. 2, pp. 119-129.

CHAPTER 4

SIMULATION OF THE INTERFACE DYNAMICS AT SEMARANG AQUIFER

4.1. GENERAL REMARKS

Dynamics of the freshwater-seawater interface is related to recharge and discharge of groundwater in a coastal area. When the recharge increase the interface is pushed out to seaward reducing groundwater salinity around coastline. Otherwise, when the discharge increase the interface moves inland, increasing the groundwater salinity. This interface movement is recognized as seawater intrusion that is mainly affected by groundwater abstraction.

Many published reports have explained this phenomenon due to over exploitation in the groundwater development area. The non-similarity of geological and hydrogeological condition seems to become a hindrance to be standardized this problem for all groundwater development area. With a number of reasons, the complexity of the geological setting is mostly studied by simplifying to be a single layer of aquifer. However, this kind of simplification may not acceptable for some conditions especially for inter-layering of aquifer and aquitard system. Simulation of the groundwater flow on multi layer of aquifers is provided in this research with case study at Semarang coastal aquife.

Regarding to the three side effects of environmental problem due to groundwater exploitation, the seawater intrusion and the land subsidence have been reported in this city, yet the degradation of groundwater quality by contaminant leaching from city's infrastructure has not been well investigated. We limit scope of this chapter with concern to the seawater intrusion problem. The investigation was performed by numerical modeling analysis by using the two-dimensional (2D) model and the three-dimensional (3D) model. This simulation was addressed to learn behavior of the

freshwater-seawater interface due to the effect the existing groundwater development system on the Semarang aquifer. Due to lack and inconsistency of observation data, the simulation was mainly done for interpretive purpose. In order to show the accuracy of result, the simulation period was set up to cover time-period of the existing field observation data.

4.2. HYDROGEOLOGICAL SYSTEM OF SEMARANG AQUIFERS

4.2.1. Geological and Hydrogeological Setting

The modeling area is located in centre of Semarang city, the capital town of Central Java Province, Indonesia. The area is a flat terrain with average surface elevation about 5.0 m above mean sea level and becoming gently undulating in the southern part. Numerous rivers originating in the mountain flow almost parallel to the Jawa Sea in the north. There are two seasons for a year cycling a wet and a dry season with the latter continuing from June to September. The mean annual precipitation is about 2644 mm.

Geological condition of the area is composed two type of geological formation; Alluvium (Qa), and Damar Formation (Qtd) shown in map at figure (4.1). The Alluvium consists of coastal plain, river, and lake deposits. The materials arrange structure of alternating layers of medium grained sand with clayey materials, with 50 m thick or more. Sand deposit commonly forms a river-mouth deposit as reservoir with thickness of about 10 m in depth about of 60 m. The Damar formation is composed tuffaceous sandstone, conglomerate, and volcanic breccia. The formation outcrop appears in the hill area south of Semarang City.

Based on drilling records, the geological units can be interpreted and classified into the following aquifers;

1. Shallow aquifer. The depth of phreatic (unconfined) aquifer is about 4 – 10 m below ground surface. Groundwater in this aquifer is being abstracted with numerous dug wells for domestic water supply. Water level fluctuates 2 m – 5 m, and some wells have salty quality water with electric conductivity 4000 μohms/cm.
2. The Delta Garang aquifer consists of sand layers. This aquifer is referred to as the deep aquifer system or confined aquifer with average depth of 60 m. This layer

spreads relatively continuously through the coastal plain. Groundwater exploitation via deep wells is concentrated on this aquifer, and affected declining of hydraulic head continuously.

3. The Damar formation composed of a low permeability layer causing this formation has not being exploited effectively.

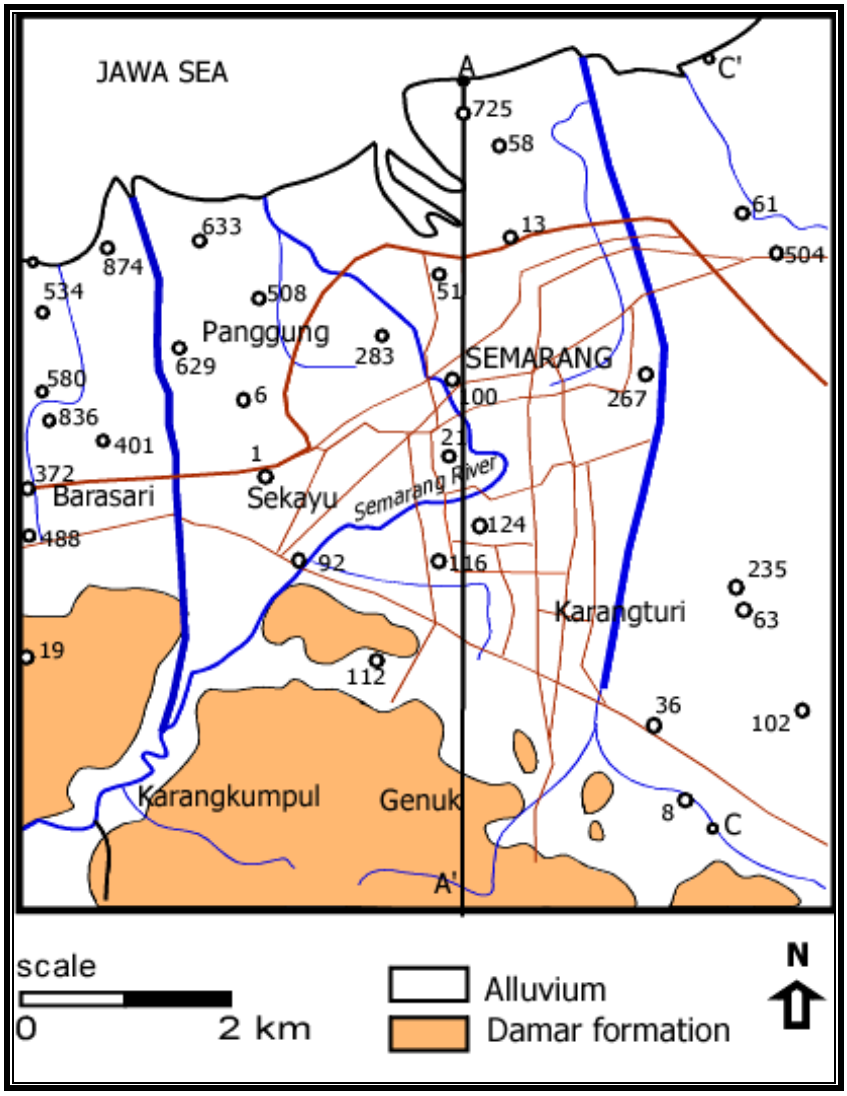

Figure 4.1 Geological map of Semarang – Indonesia (Mulyana et al., 1996)

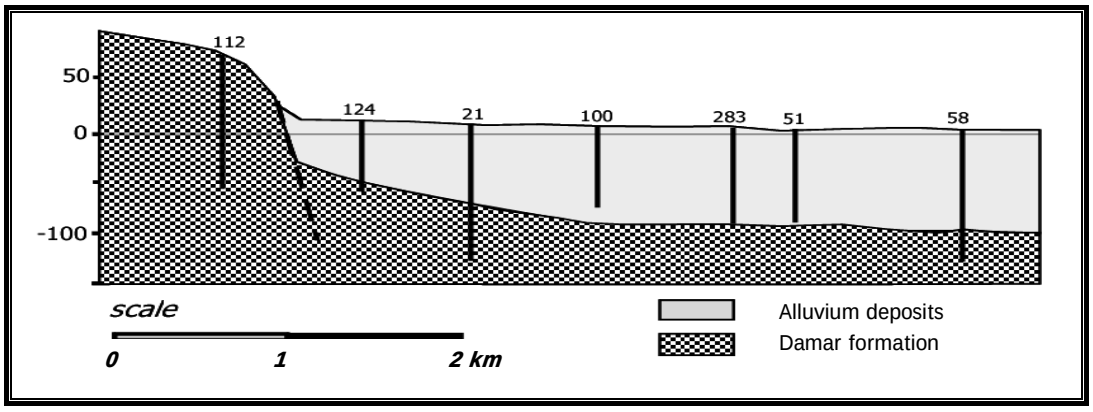

Figure 4.2 Geological cross section at Semarang area

The groundwater system in the aquifer characterized with coastal area interacts with hilly area. Water infiltrating to recharge area in the mountain then enters the aquifer system is found in the coastal plain. In the mountain area, a fault follows along the hills close to Semarang from west to east. Several previous investigations indicate that the fault does not act as a barrier between groundwater at the mountain area and the coastal plain. Therefore, the subsurface lateral flow into the model area in the inland part is considered as flux boundary.

4.2.2. Groundwater Balance

The groundwater flow in coastal belt along North Jawa has a similar pattern. Rainwater infiltrates mountains area in southward and flows to the north to the Jawa Sea. In the eastern part of Semarang City is originated with a wide river delta plain, and the groundwater flows from southeast to northwest. This groundwater flow patterns is also similar with pattern of surface water flow. The amount of groundwater extracted through dug wells does not produce a significant water level drawdown. However, water table fluctuation is dominated by the alternating scheme of wet and dry season (Spitz, 1989). Observation of piezometric head on the confined aquifer on 1980, before intensive groundwater exploitation commenced, indicates undisturbed flow pattern. It was recorded that the piezometric head up to 5 m above mean sea level on the well located close to hill area.

Observation on 28 wells on 1941 by Van Bemmelen shown all wells are artesian. Since 1990, the intensive groundwater exploitation has not remained unaffected the

piezometric head. The aquifer response reveals itself by a decline of the piezometric heads. The hydraulic heads are now below of the land surface covering large area. The increasing of groundwater production wells that has been registered on Directorate of Environmental Geology (DEG) is shown on figure (4.3) below.

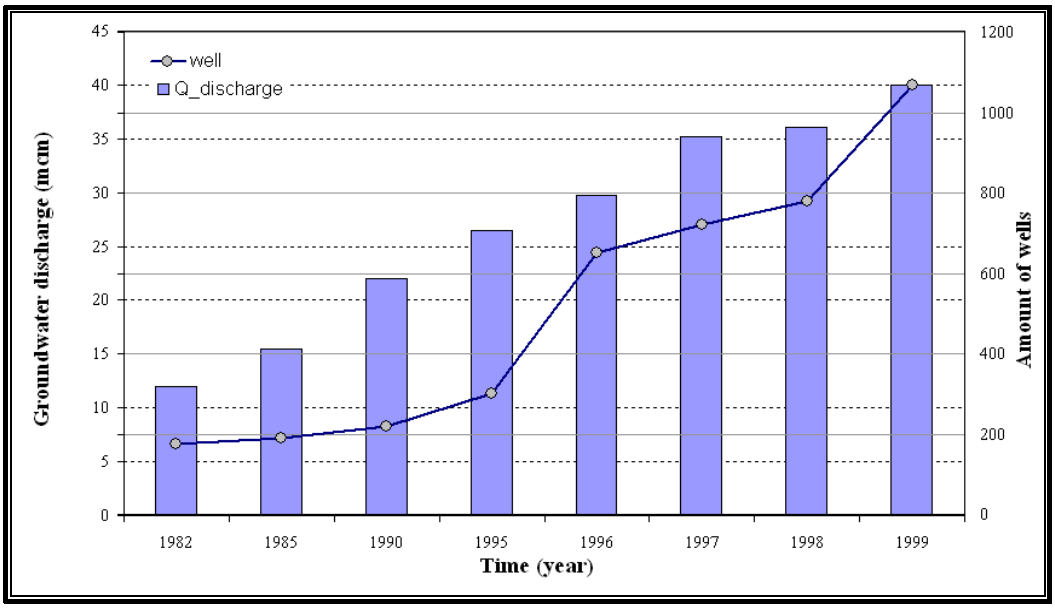

Figure 4.3 Groundwater abstraction and amount of wells at Semarang aquifer. (Sihwanto and Iskandar, 2000)

Study of groundwater recharge in this area has been done by Pudjihardjo (1995). The estimation was based on concept of water balance of the Schincht and Walton method uses formula;

$$Qt = Qq + Qs + Et + Qu \pm Sm \pm Sg \qquad (4.1)$$

where; *Qt* is rainfall intensity, *Qq* is infiltration, *Qs* is run off, *Et* is evapo-transpiration, *Qu* is underflow, *Sm* is soil moisture change, and *Sg* is change of storage. Using equation (4.1) based on observed data of 1986-1992, the groundwater resource in this city was estimated 6,545 m^3/sec (Pudjihardjo, 1995).

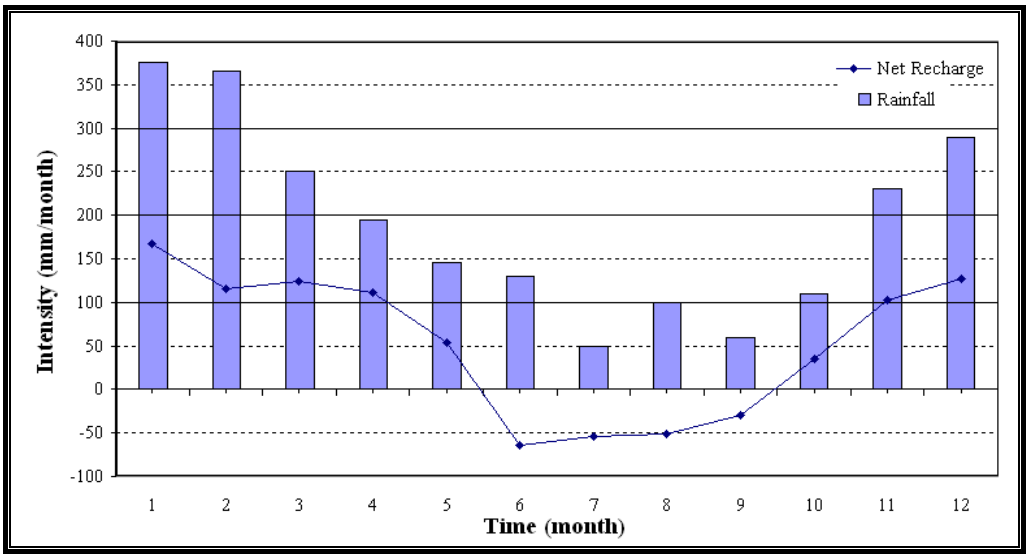

Figure 4.4 Average monthly rainfall and recharge net over the year

There are some water resources available in this city to support human demand: surface water, springs, and groundwater. Investigation report of water usage form these sources on 1990 (Mulyana and Widharto, 1996) documented that the surface water provided approximately 50,112 m^3/day, the springs was 24,192 m^3/day, the groundwater from unconfined aquifer was abstracted by dug wells is 63,000 m^3/day, and groundwater abstraction on confined aquifer through deep wells was 44,064 m^3/day. At the time, the groundwater extraction by dug wells was higher than by deep wells.

Modeling process requires the groundwater extraction in a certain series of time. Since the data of groundwater abstraction from unconfined aquifer through dug-wells are not available, so that the trend of exploitation was interpolated with a linear increment of 1.17 % according to population growth. Whereas, extrapolation of the groundwater abstraction through deep wells from confined aquifer exhibits a parabolic curve. This extrapolation line is based on data from industrial companies as main user of those deep wells. The trend of the groundwater exploitation in 1982-2010 for both unconfined and confined aquifer is shown in figure (4.5) and (4.6), respectively.

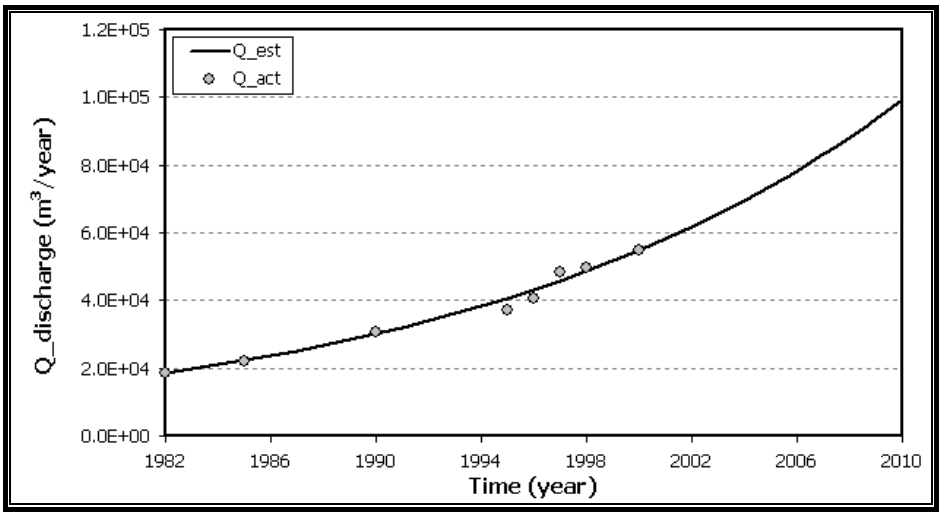

Figure 4.5 Estimated and actual discharge of groundwater pumping of confined aquifer.

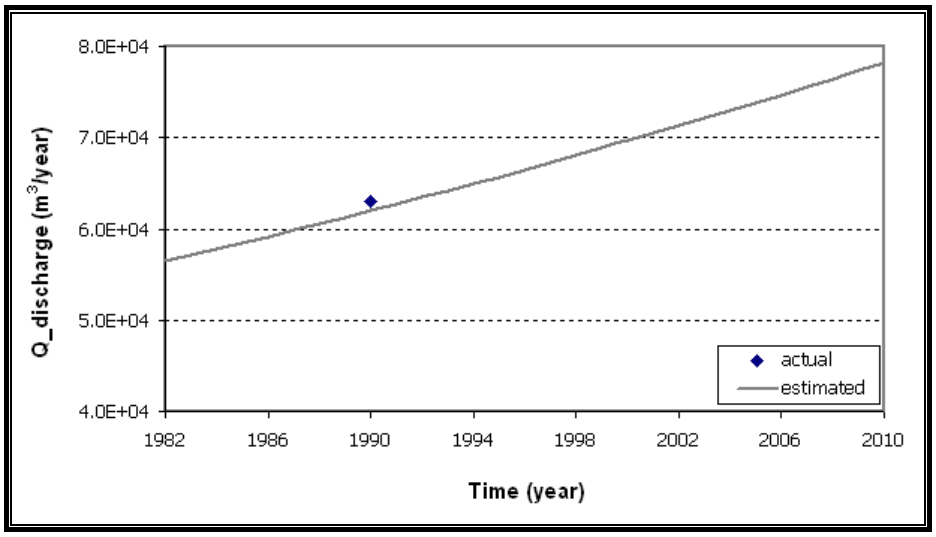

Figure 4.6 Estimated and actual discharge of groundwater pumping of unconfined aquifer

Observed water table or piezometric head both aquifers in 1989 (Spitz, 1989) and 1992 (Pudjihardjo, 1995) are shown in maps of figure (4.7) to (4.10). The groundwater exploitation within this period has no significant effect to the water table on the unconfined aquifer. On the confined aquifer, the cone depression occurs. In 1989, the cone depression maximum 2 meter below mean sea level (MSL) in the central part of Semarang City (figure 4.9), and then reach 20 meter below MSL in 1992 (figure 4.10). This phenomenon indicates over exploitation of the confined aquifer.

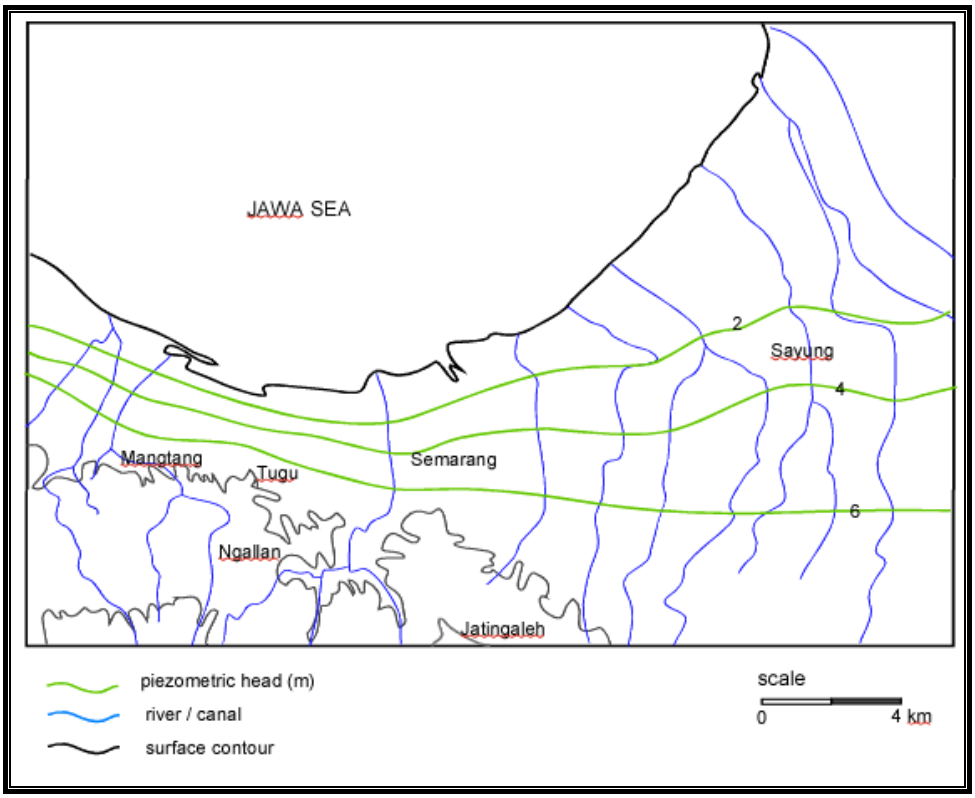

Figure 4.7 Water table map in 1981 on unconfined aquifer.

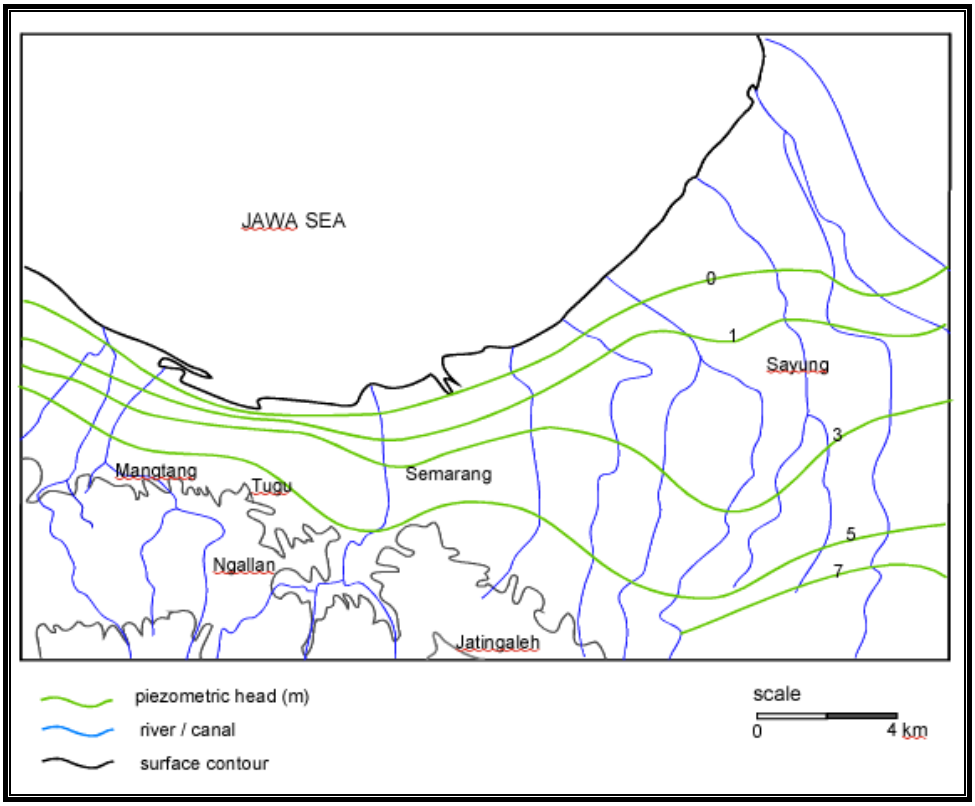

Figure 4.8 Water table map in 1992 on unconfined aquifer

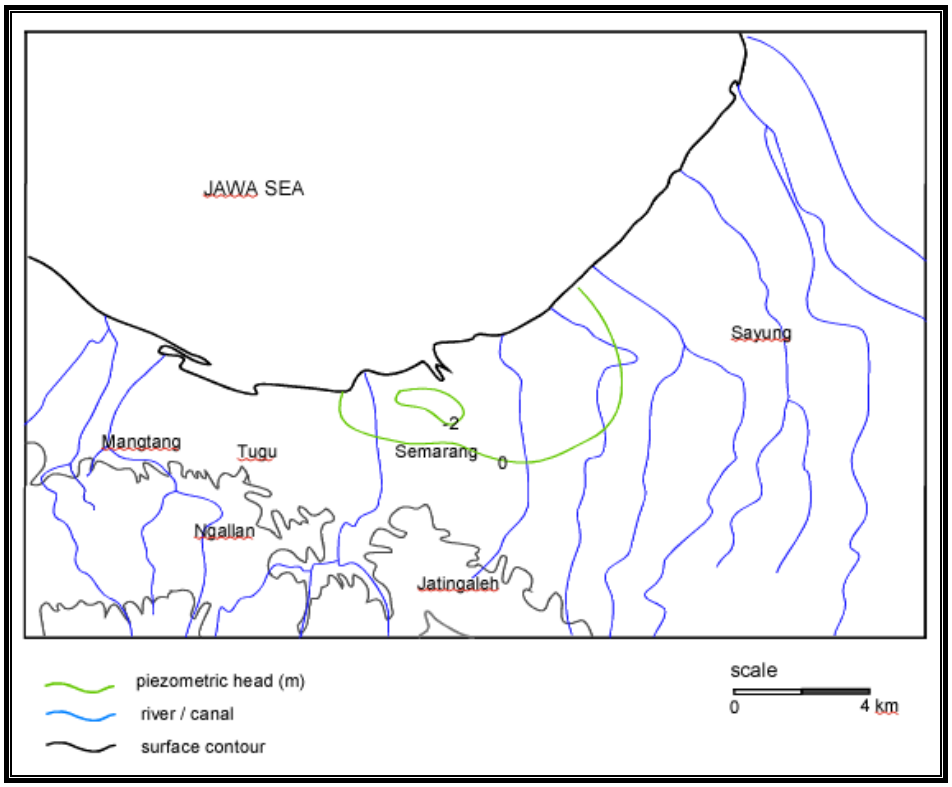

Figure 4.9 Piezometric head of groundwater on confined aquifer in 1989.

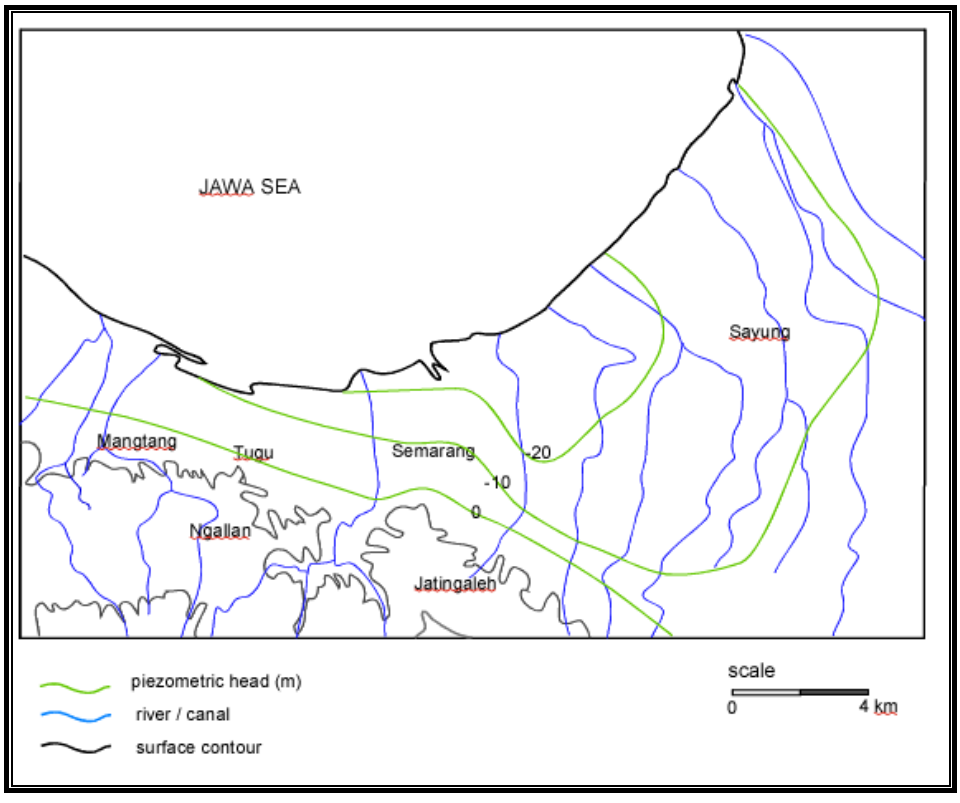

Figure 4.10 Piezometric head of groundwater on confined aquifer in 1992.

4.2.3. Groundwater Quality

Groundwater quality is controlled by some factors, such as; depositional environment of geological material, interaction of the groundwater with surface water, and chemical dissolution of minerals composing the geological material of the aquifer. These three factors may also affect the groundwater salinity. To ensure the salinity source of the groundwater in this area, Sihwanto and Iskandar (2000) studied using distribution of chemical concentration within the aquifer. Analysis based on Chloride-Bicarbonate Ratio, DM Ratio, and Molar Ratio methods indicate that the salinity is caused by seawater encroachment.

Measured the groundwater quality in a certain period denotes the groundwater development on this area has been emerging degradation of the groundwater quality. In the era 1980's, the groundwater exploitation was not recognized to have a negative impact to groundwater quality and to elevation of piezometric head. In contrast with the era 1990's, contour line of piezometric head had fallen deeper than 10 m below mean sea level and shown an invasion of seawater into aquifer. The worst groundwater deterioration has been observed in two monitoring wells of W-629 and W-764 located on the west part of study area. The groundwater on W-629 had electrical conductivity (Ec) of 695 μmhos/cm in 1994, and then increased to 4970 μmhos/cm in 1995. At observation well of W-764, the electric conductivity of groundwater increased from 2930 in 1994 to 11600 μmhos/cm in 1995.

Generally, the groundwater quality in Semarang aquifers can be categorized in a good quality for drinking water. Some dug wells may be contaminated seawater particularly near coastline and the old river. Since the dug wells penetrate only unconfined aquifer, there is no consistency of the quality degradation occur. The groundwater on the confined aquifer exhibits increasing values of electric conductivity. Compilation of observed data carried out by Directorate of Environmental Geology (DEG) of Indonesia produces maps of electric conductivity that is shown in figure (4.11). There are two maps, observed data in 1992 – 1993, and in 1989 – 1999. These maps may not precisely figure out the real condition because screen position of the observation well is not in the same depth. However, the maps can provide acceptable information for general

condition. The interface of freshwater-saltwater has no exhibited meaningful invasion to inland, but indicates increment of the electrical conductivity of groundwater.

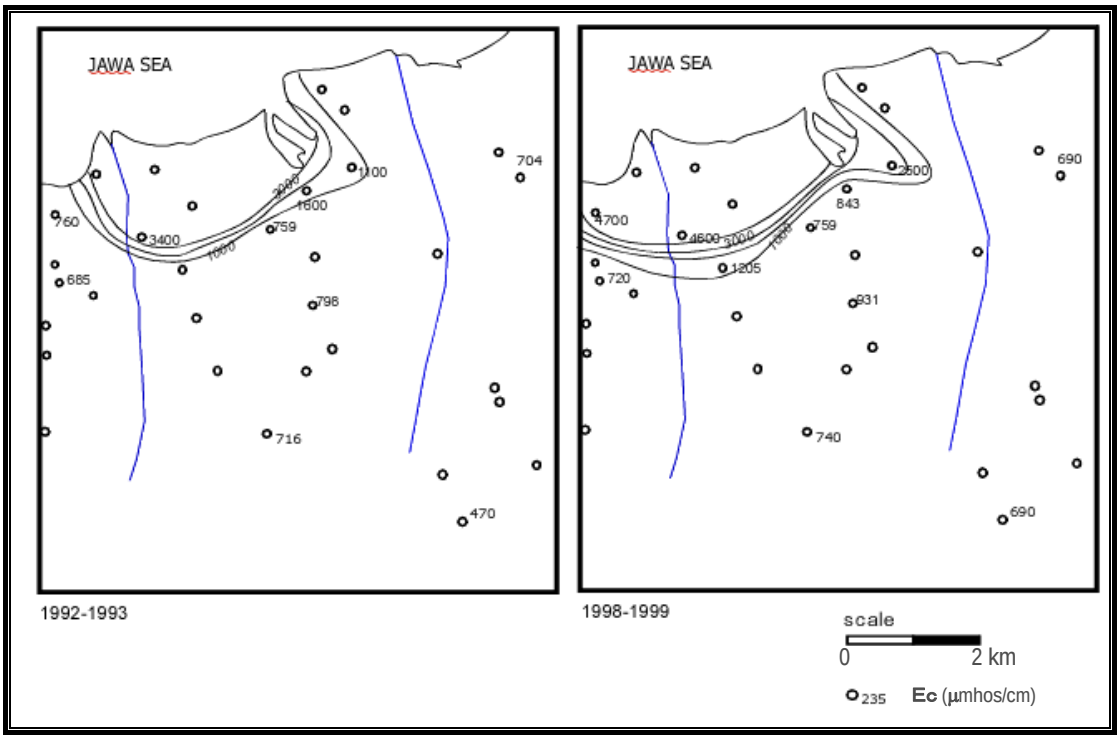

Figure 4.11 Maps of the groundwater electric conductivity

4.3. TWO-DIMENSIONAL PROFILE MODELING

A two-dimensional profile model was developed at the local scale to simulate dynamic of the freshwater-seawater interface at Semarang aquifer. This model was aimed to achieve two objectives: to help facilitate development of 3D model, and to simulate the groundwater flow and solute transport patterns in detail with a fine level of spatial resolution. Despite of the profile model simulates flow and solute transport only in two dimensions problem, the model is better suited for calibrating certain aquifer parameters and performing a comprehensive sensitivity analysis.

4.3.1. Model Conceptual and Design

A common method for orienting two-dimensional model is to align the horizontal axis with a linear or curving groundwater flow line. This method relies on the definition of a

flow line, which does not allow groundwater to flow across the line. Groundwater, therefore, can be simulated in two dimensions, one along the flow line and the other in the vertical direction. This is the general approach used cross-sectional model built in this study. For this purpose, the groundwater maps were drawn based on measured data on 1989 and 1992.

A cross section extent from inland to offshore past location of observation wells in which salinity concentration were measured. The two-dimensional profile model was constructed along groundwater flow lines toward central of Semarang city shown in figure (4.1) at line A-A'. The cross section extends from inland boundary at 7,000 meter of coastline to sea boundary at 500 m of coastline. The profile covers from topographical surface to depth 85 m below mean sea level. This physical domain is discretized vertically 5 meter for area below mean sea level (MSL), and 1 m above the MSL. In lateral direction, the physical domain is discretized 20 m from seaside to 3,800 m inland, and 25 m from 3800 m to inland boundary. The discretization produces four types of mesh size, distributes 9410 nodes, and employs 9.024 elements.

This profile model was designed to simulate average groundwater flow and solute transport condition from 1982 to 1998. This period of time was selected because it corresponds with the period of field data were available for this study. This periods of simulation time then to extend 2010 to have general idea the interface movement due to the groundwater exploitation policy.

To simulate successfully problem of variable density groundwater flow, an adequate spatial discretization should be adopted. The appropriateness of the spatial discretization can be evaluated by using a mesh peclet number, in which is formulated as;

$$Pe_m = \frac{|v|\Delta_s L}{D_L} = \frac{|v|\Delta_s L}{\left(D_m + \alpha_L |v|\right)} \tag{4.2}$$

Where $\Delta_s L$ is the local distance between sides of element measured along the local flow direction, $|v|$ is the magnitude of local velocity, and D_L is the total longitudinal dispersion coefficient in equation (4.2).

The mesh Peclet number is a measure of the amount of local advective transport relative to the local amount of hydrodynamic dispersion. Since the molecular diffusion (D_m) is small relative to the mechanical dispersion ($D_L \approx \alpha_L |v|$), the mesh Peclet number can be simplified (Voss and Sousa, 1987) as;

$$Pe_m \approx \left(\frac{\Delta_s L}{\alpha_L} \right) \tag{4.3}$$

When the mesh Peclet number is high, centered finite difference and Galerkin finite element approximation can give values of concentration, which oscillated in space. The Peclet number should be designed as small to ensure a stable numerical solution. Voss and Sousa (1987) described that oscillation do not occur when the mesh Peclet number is approximately four or less ($Pe_m < 4$) in direction along flow, and is approximately less than 10 perpendicular to flow line. It means that grid along flow line is smaller equivalent forth of longitudinal dispersion ($\Delta_s L > 4\alpha_L$), and grid perpendicular flow line is smaller equivalent tenth of tranversal dispersion ($\Delta_s T > 10\alpha_T$).

In this profile modeling, it was used two spaces in lateral direction of 20, and 25 meter. By using value of the longitudinal dispersion is 50 m, the mesh Peclet number is 2, and 2.5. In the perpendicular flow line (vertical direction), it is meshed with space of 1.0 and 5.0 meter. With value of the transversal dispersion of 10 m, the grid size results the mesh Peclet number of 0.1 and of 0.5.

The geological materials composed the area are classified into three types; tuffaceous sand, sandy clay, and silt & sand. Based on the characteristic of these materials, hydrogeological system of the model area can be conceptualized into three aquifers: an unconfined aquifer and two confined aquifers; and one aquitard. The unconfined aquifer is composed silt and sand material. The confined aquifers are composed silt and sand material, and tuffaceous sand in which often is mentioned as Delta Garang aquifer, and Damar formation aquifer, respectively. Between the unconfined aquifer and Delta Garang aquifer exists a sandy clay aquitard. Conceptualized and discretized of aquifer stratification is exhibited on figure (4.12).

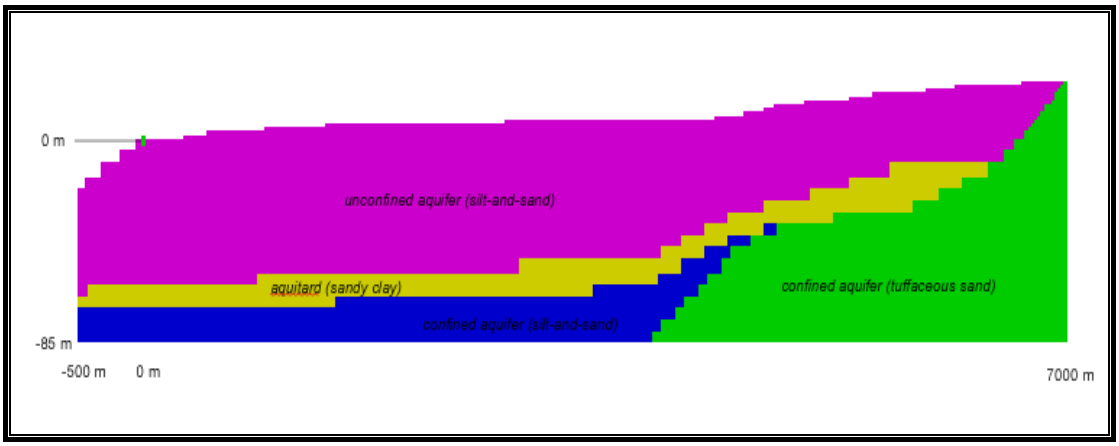

Figure 4.12 The discritized model area employing 2D-Cartesian mesh system

4.3.2. Model Boundaries

The boundary conditions applied in this modeling is exhibited on figure (4.13) consisting of specified flux & concentration, no-flux, and specified pressure head and concentration boundaries.

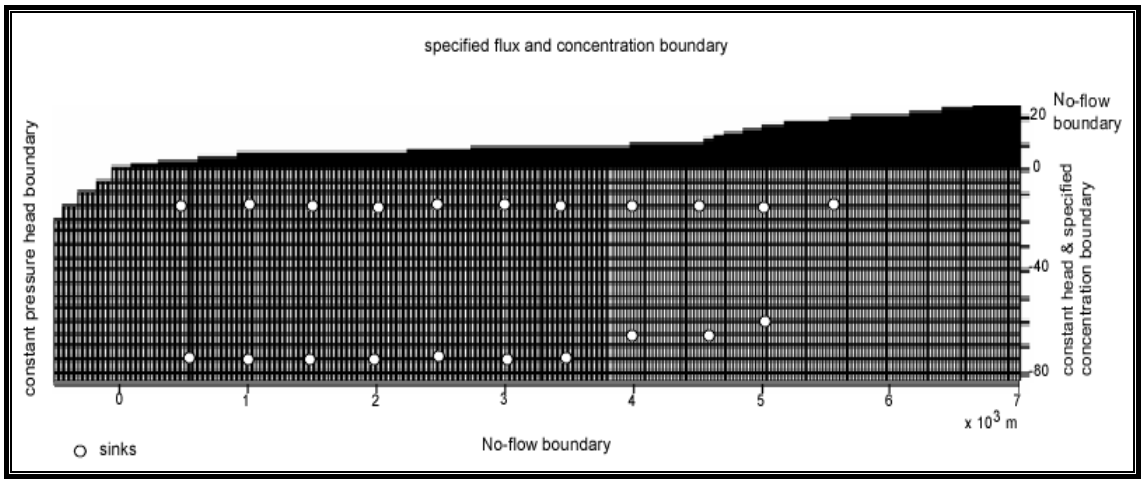

Figure 4.13 Boundary conditions are applied in the modeling

Specified flux boundary; A Neumann type of no-flux boundary condition was assigned to the bottom of the aquifer, and the part of the inland boundary above groundwater table (unsaturated zone). It is assumed that there is no flow from 5 meter above means sea level to the surface in inland boundary.

A Neumann influx boundary condition was assigned at the land surface. The averaged water flux values as net recharge value of 3.5 x 10^{-4} m/day (equivalent to 4.0 x 10^{-6} kg/sec) and salt concentration is 9 mg/liter (UGM, 1997 in Sihwanto and Iskandar, 2000).

Specified pressure head boundary; A Dirichlet type of boundary condition was assigned to the below mean sea level at seaward boundary, and below 5 m at inland boundary. On the seaside boundary, the constant pressure head was prescribed at this boundary by assuming the salt concentration of seawater is 35.7 kg/m^3. On inland boundary, the pressure head is set equal to pressure head 5 m above mean sea level, with salt concentration is 9 mg/liter (0.9 kg/m^3).

To simulate the effect of pumping stress on the aquifer, several internal sinks were assigned on figure (4.13). Each the internal sink does not act for actual position of production well in the field, but to represent a group of well around the sinks. This is caused by difficulty to have data of all wells around the transaction line since many wells are not registered on the government office. In order to represent the group of wells into a point, a graph of relation between relative pumping to distance from coastline (figure 4.14) was made. Combination between this graph (figure 4.14) with the graph of extrapolation for pumping discharge in figure (4.5) for confined aquifer and figure (4.6) for unconfined aquifer, the discharge for each internal sink can be counted.

In the real fact, the groundwater flows in three-dimensional system. Assigning this pumping discharge into the 2D-profile modeling requires an adjustment to bring into a line. Therefore, the approximated discharge of every sink is divided by effective wide of aquifer affected by the extraction. In this numerical simulation task, the effective wide to represent the groundwater development area in Semarang aquifer is approximated 8,000 m. This simulation was performed within time period of 1982-2010 with assumption that the pumping discharge is annually constant.

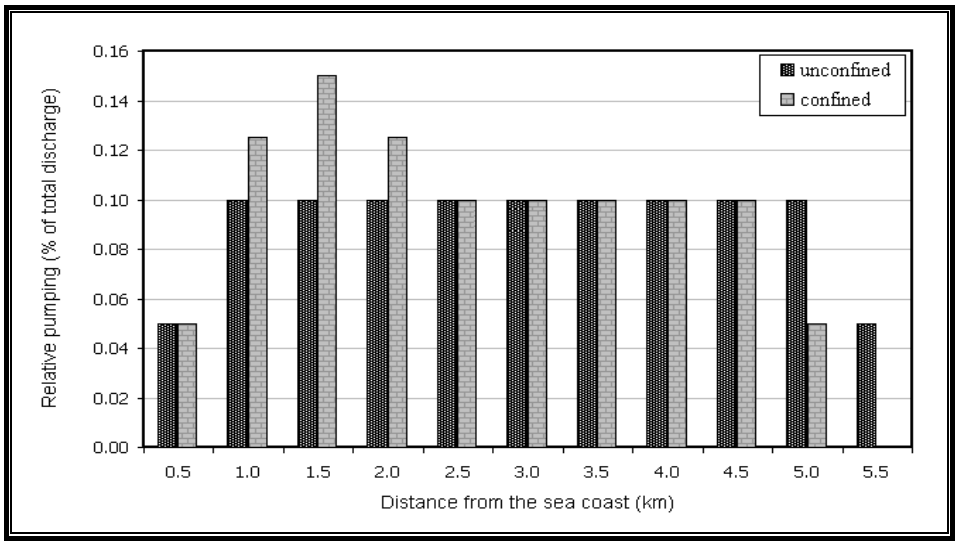

Figure 4.14 Relation between relative pumping and distance from coastline

4.3.3. Initial Condition

Modeling of the groundwater flow on coastal aquifer should solve equations of the groundwater flow and the solute transport under transient condition. For this purpose, initial condition is required, yet this kind of information mostly has not available. Therefore, modelers have to make approximation by considering some conditions to represent the initial condition of the hydrogeological system. In this modeling work, the initial condition was obtained after long time simulation under transient condition to achieve steady state. In order to achieve this requirement, two extra simulations were performed by modifying of above mentioned boundary conditions.

First, the model was run with no pumping discharge was assigned into the model, and recharge from rainfall is set to be zero. The initial condition for this first run is arbitrary freshwater pressure head and 0.9 kg/m^3 of groundwater salinity within the system. The simulation used time step of one month, and the simulation was defined to reach convergence criterion when change of the freshwater pressure head less than 1.0 x 10^2 kg/m^2, and solute transport is less than 1.0 x 10^{-4} kg/m^3 with the increment of simulation time. The second run is to continue simulation by using the pressure head and the salinity distribute obtained on the first run as the initial condition. In this running, boundary conditions are set by defining the pumping discharge to sinks according to data on 1982, and assigning the recharge rate on the top surface boundary. The

simulation was carried out to achieve steady state with changes of the freshwater pressure head and the salinity concentration that is similar applying in the first run. The final result of this second running is considered as initial condition on 1982.

4.3.4. Model Calibration and Simulation Results

This profile model was calibrated by adjusting the boundary stress and the aquifer parameters, within a range of reasonable values, until simulated conditions generally matched with the conditions observed in the field. In this 2D-model, aquifer parameters for each layer of material are represented by a homogeneous distribution rather than a more complex heterogeneous distribution. Results obtained from this method for calibrating the profile model are then used for simulating 3D problem.

The model was calibrated to data, which is collected from monitoring wells located on or near the model transect. The data values used in the calibration are presented in table (4.1). For monitoring wells that are not located directly on a model transect, the horizontal distance was specified as the approximate distance of the monitoring well from the coastline. This method for projecting the monitoring wells into a model axis assumes that contours of head and salinity are parallel to the coastline and perpendicular to the model cross section. This assumption may limit confidence in the calibration if actual contours of salinity and head are not parallel to the coast. In addition, the elevation of the screen centre was used to locate the measurement of head and salinity within the vertical section of the model. Most of the well screen is 5 - 10 m length, which means that heads and salinity values measured at the wells were vertically averaged over the distance.

Comparison of the observed data (O) and the simulated results (S) of the hydraulic head and the salinity concentration are shown on figure (4.14) and (4.15). The observation data are available at 1984 (O-84), 1986 (O-86), 1988 (O-88), 1990 (O-90), 1992 (O-92), and 1998 (O-98). Since these data were measured in the deep wells (confined aquifer), and there is no record available for dug wells (unconfined aquifer), consequently this matching explain to condition of the hydraulic head and the salinity concentration on the confined aquifer. Even though the calibration was not be carried out for the unconfined aquifer, these results can be accepted because based on the two maps of the water table

shown in figure (4.7) and (4.8) almost there is no change on the transect line. In addition, several investigation in this area described that the water table position and the salinity concentration too much depend on season; dry and rainy season.

Table 4.1 Calibrated parameter values used for Semarang aquifer

Parameter	Value	Unit
Intrinsic permeability (silty sand)	1.02×10^{-11}	m^2
Intrinsic permeability(sandy clay)	1.02×10^{-17}	m^2
Intrinsic permeability (silty sand)	3.57×10^{-11}	m^2
Intrinsic permeability(tuffaceous sand)	4.08×10^{-12}	m^2
Porosity of aquifer	0.30	-
Porosity of aquitard	0.40	-
Viscosity	0.001	$m\ s^{-2}$
Gravity	9.81	$kg\ m^{-2}$
Longitudinal dispersivity	50	m
Transversal dispersivity	10	m
Molecular diffusion	3.565×10^{-3}	$m^2\ s^{-1}$
Tortuosity	1	-
Density of freshwater	1000	$kg\ m^{-3}$
Density of seawater	1025	$kg\ m^{-3}$
Compressibility of water	4.47×10^{-10}	$m\ s^2\ kg^{-1}$
Compressibility of soil matrix	1.00×10^{-8}	$m\ s^2\ kg^{-1}$

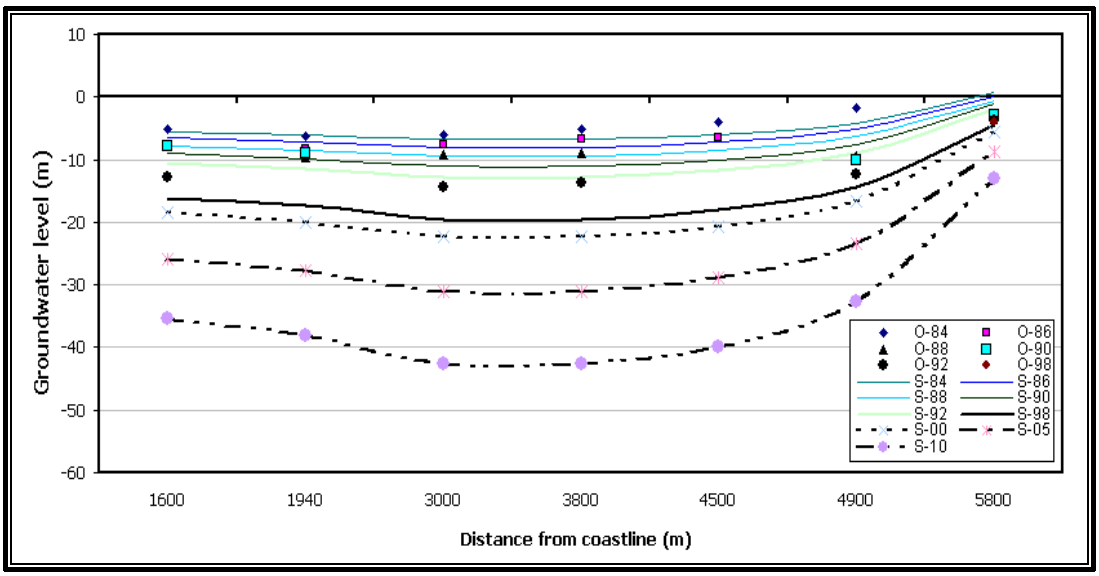

Figure 4.15 Comparison of simulated and observed hydraulic head of groundwater on confined aquifer. (O = observed hydraulic head; S = simulated hydraulic head)

Simulation results obtained by running model with calibrated parameters generally match with field observation data of both the hydraulic head (figure 4.15) and the salinity concentration (figure 4.16). The transition zone appears to be in a reasonable width, and the simulated piezometric head closes to elevation of measured groundwater levels.

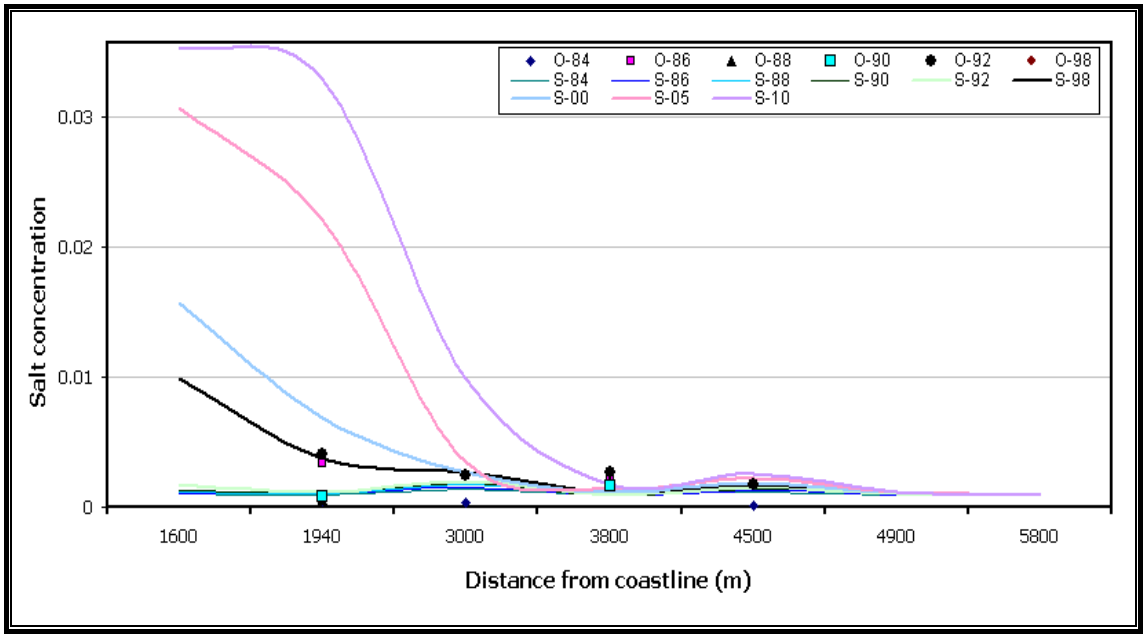

Figure 4.16 Comparison of estimated with observed salinity of groundwater on confined aquifer.(O = observed salinity; S = simulated salinity)

In order to have an idea of the interface dynamic due to groundwater abstraction for future, the simulation period was also extended to 2010. By using calibrated parameter value, and assumption of the above mentioned pumping discharge of wells, simulation results demonstrate a drastically change of the hydraulic head and the groundwater salinity; and the interface invades too far inland. Unfortunately, monitoring data within this period does not available yet, emerging difficulty to obtain its accuracy. If this simulation result is over estimated, the lack of accuracy may be influenced by over estimation of well discharge, representation of pumping discharge for each zone, and recharge estimation from top surface and inland boundary. However, this drastically change can be interpreted a critical condition of the aquifer that is required mitigation efforts. Representation of the numerical results is shown in figure (4.17) for 1990, 2005, and 2010.

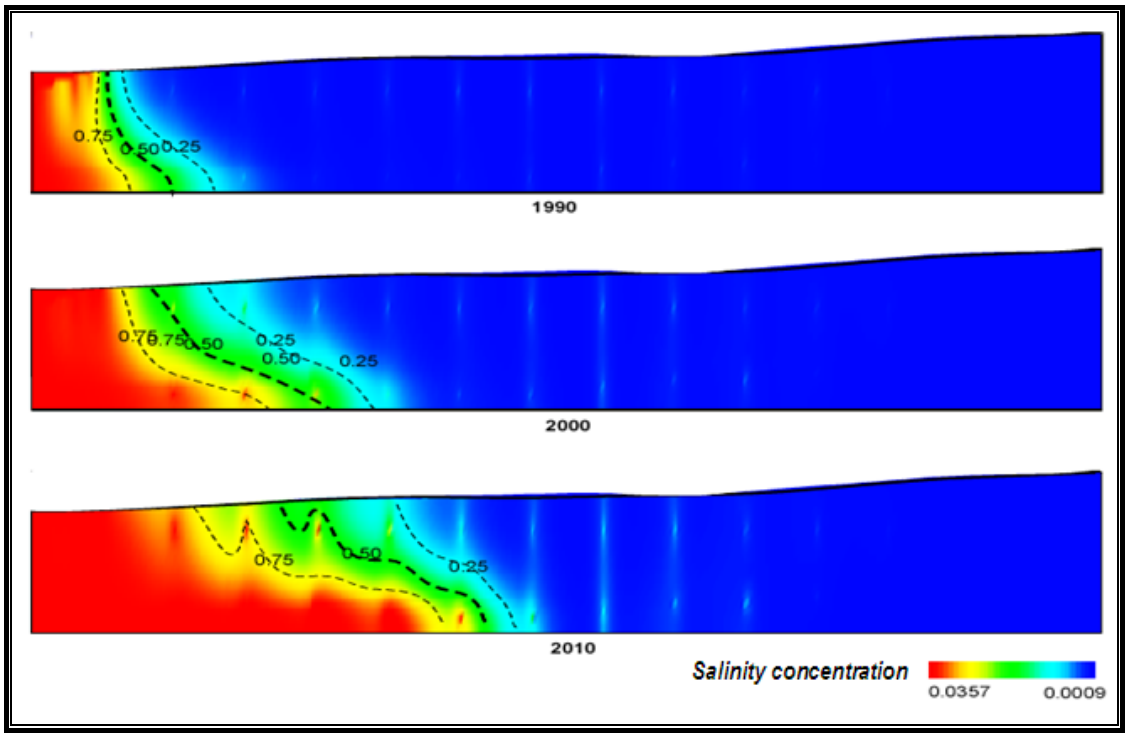

Figure 4.17 Evolution of simulated seawater intrusion into aquifers

4.3.5. Sensitivity Analysis

A sensitivity analysis was performed to evaluate the effects of the different aquifer parameters and boundary conditions on the simulated groundwater heads and salinities. In this sensitivity analysis, the simulation done by using the calibrated parameters that is referred to as base case. For each sensitivity run, only one parameter or the boundary condition was examined by adjusting from the valued used in the calibrated model. The model was run under transient condition, and the increment of pumping discharge was also applied according to the above interpolation. For each model, the effect of each parameter will be described qualitatively based on the simulated salinities and hydraulic heads.

Modification of the boundary conditions and the aquifer parameters investigated on this run were; groundwater recharge (infiltration) rate, longitudinal dispersivity, transversal dispersivity, and hydraulic conductivity of those aquifer and aquitard. In order to investigate response of the system to the changes of parameters values, it was simulated both higher and lower than the base value. Explanation of the interface shape is, then,

made by drawing salinity contour of 25 %, 50%, and 75 % from seawater salinity, for simulated evidence on 1990, 2000, and 2010. The dash lines represent the base condition, and the intact lines describe simulated results as effect of modification of the aquifer parameters or the boundary conditions.

The first run was done by increasing the infiltration rate twice and by reducing a half. The hydraulic heads and salinities produced by this run are shown in figure (4.18) and (4.19). In the beginning, when the infiltration rate increases, simulated head increase and salinity contours move to inland. This evidence is clearly observed on unconfined aquifer. However, in the end of simulation contour of 25 % match with the base condition, but contour of 50 % and 75 % move into aquifer. The opposite results are shown with the decreasing of the infiltration rate. This phenomenon affects both aquifers, in which the salinity contours move seaward. This evidence can be understood that the infiltration rate has significant impact to protect seawater intrusion for both aquifers.

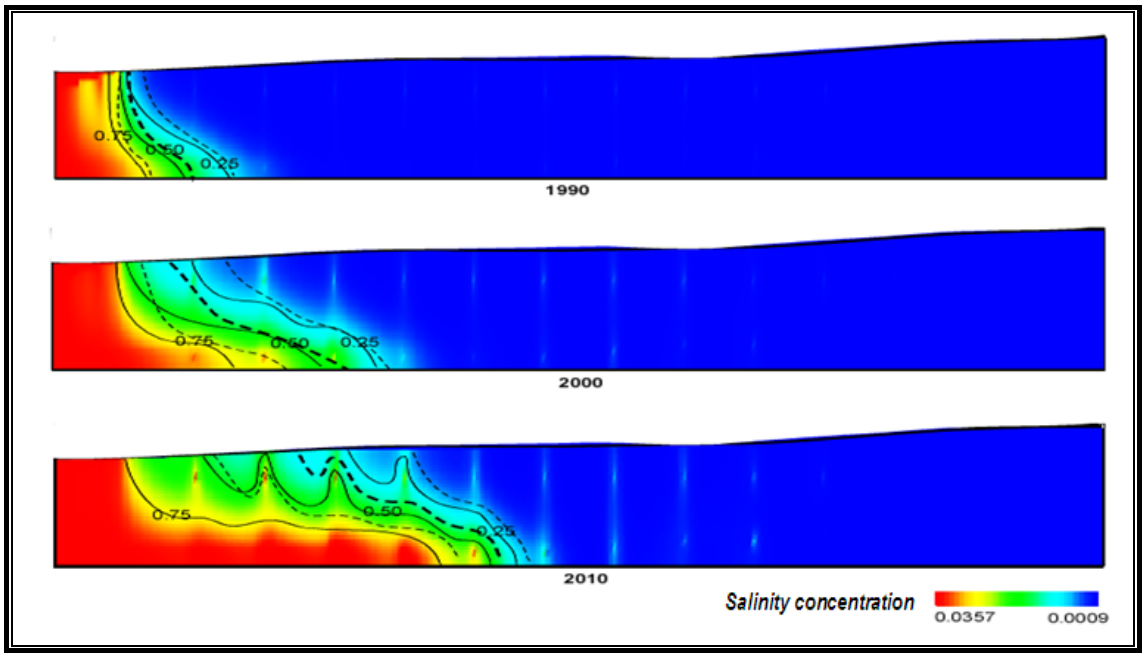

Figure 4.18 The simulated interface form with infiltration rate of 8.0 x 10^{-6} kg/m/sec

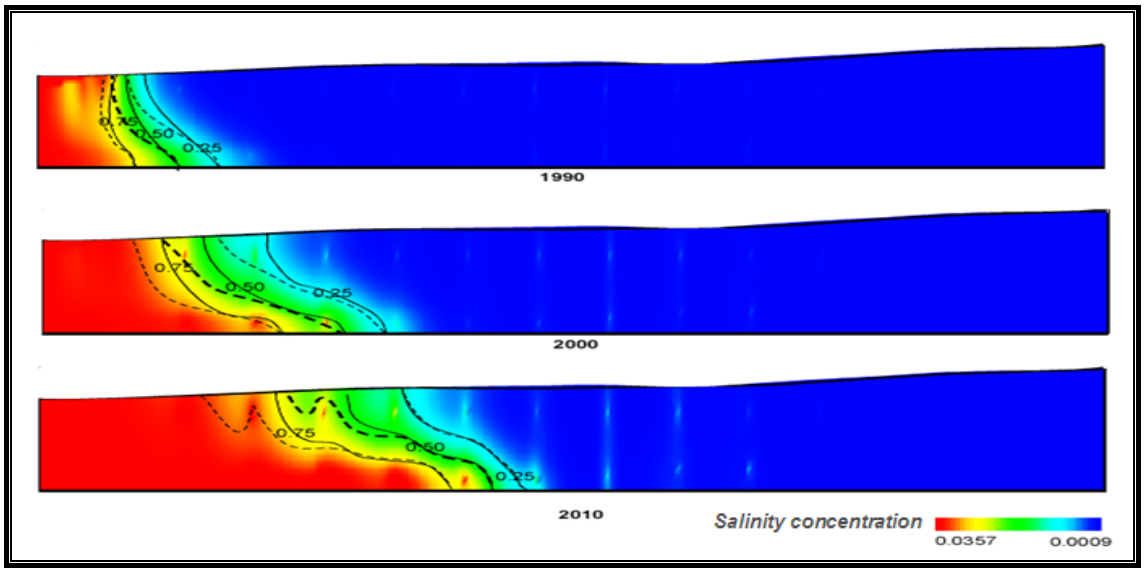

Figure 4.19 The simulated interface form with infiltration rate of 2×10^{-6} kg/m/sec.

The second run was done by increasing the transversal dispersivity twice and by reducing a half. The simulated interface form shown in figure (4.20) and (4.21) exhibits that increasing and decreasing of the transversal dispersivity has no significant effect. The salinity contour of the base condition represented by dash line almost overlap with the salinity contour of both modification value.

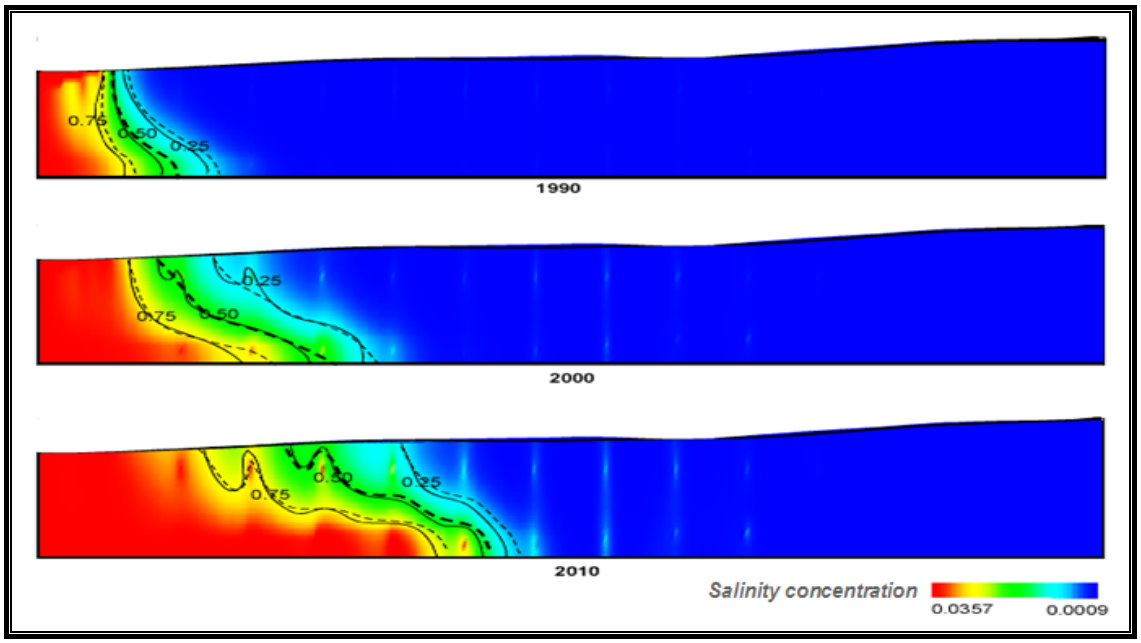

Figure 4.20 The simulated interface form with value of transversal dispersivity of 20 (twice of the base value).

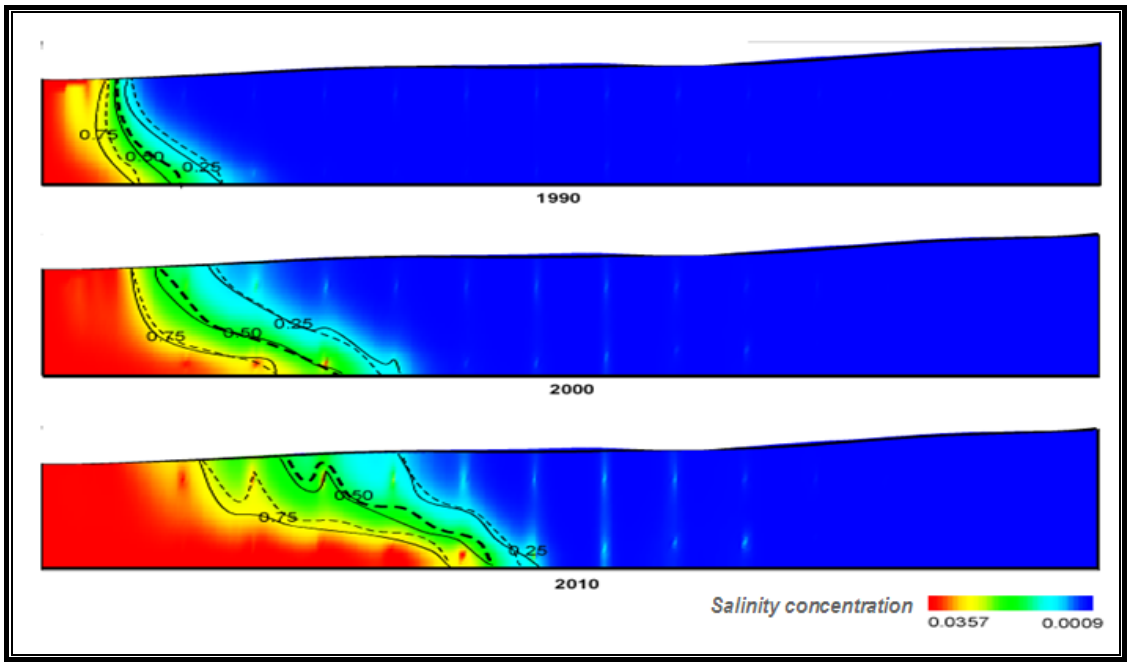

Figure 4.21 The simulated interface form with value of transversal dispersivity of 5 (a half of the base value).

The third run was done by increasing twice and by reducing a half of the longitudinal dispersivity. This parameter has also no affected the simulated interface form shown in figure (4.22) and (4.23). Salinity contours both those conditions have a similar pattern and almost match each other.

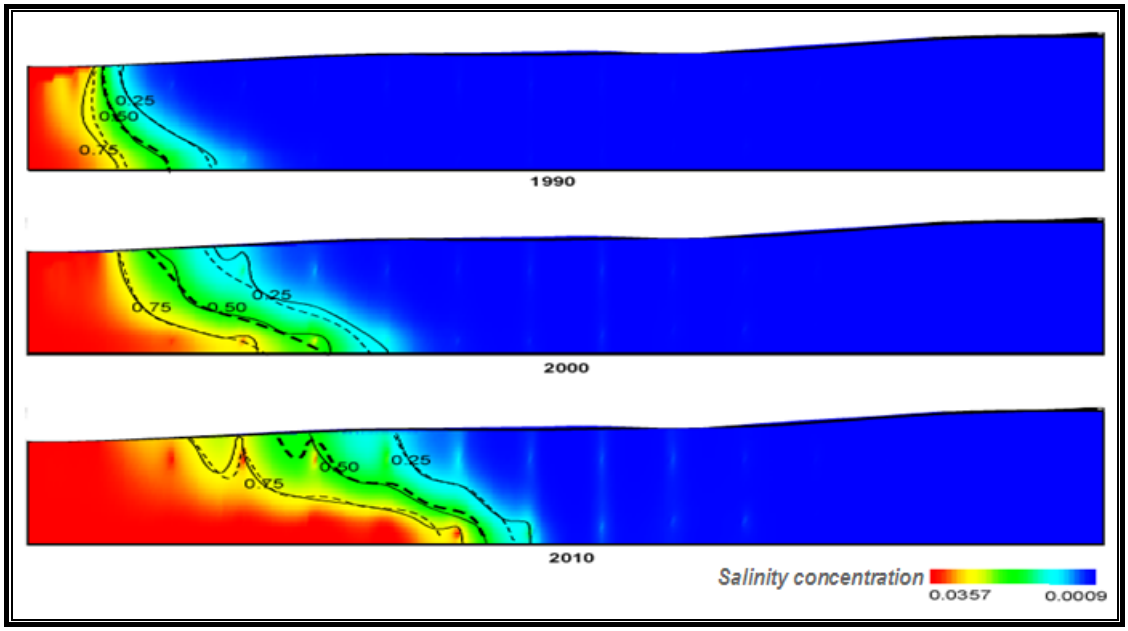

Figure 4.22 Numerical results for value of longitudinal dispersivity 100 (twice of the base value).

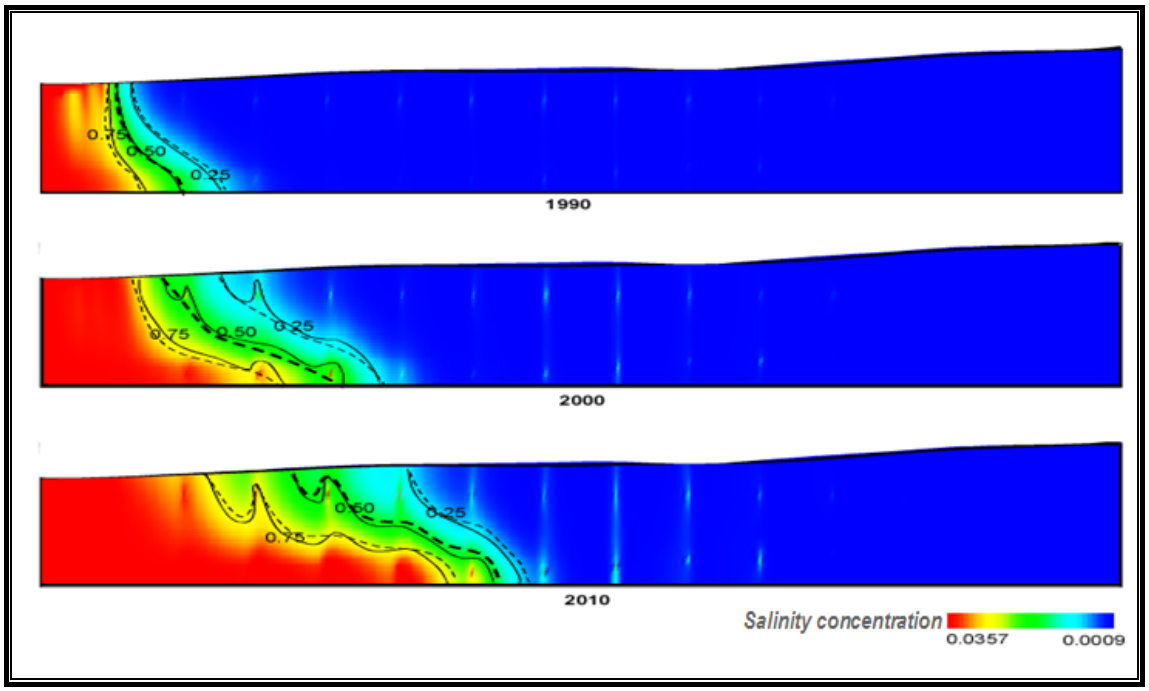

Figure 4.23 The simulated interface form for value of longitudinal dispersivity of 25 (a half of the base value) .

The forth run was done by increasing the hydraulic conductivity of the unconfined aquifer ten times and by reducing one tenth. The form of simulated interface is shown in figure (4.24) and (4.25). With the increasing hydraulic conductivity, the simulated head decreases and salinity contours move to inland. This evidence is clearly observed on both the unconfined and the confined aquifer. Consecutively the increment of pumping discharge, the salinity contour is than overlap for these both conditions. However, the decreasing of the hydraulic conductivity value increases hydraulic head, and the interface move seaward. This effect occurs on both these aquifers. And consecutively to increment of the pumping discharge, with elapse of time, the low salinity contour to be close for both conditions. The influence of this parameter to the interface can be categorized moderate.

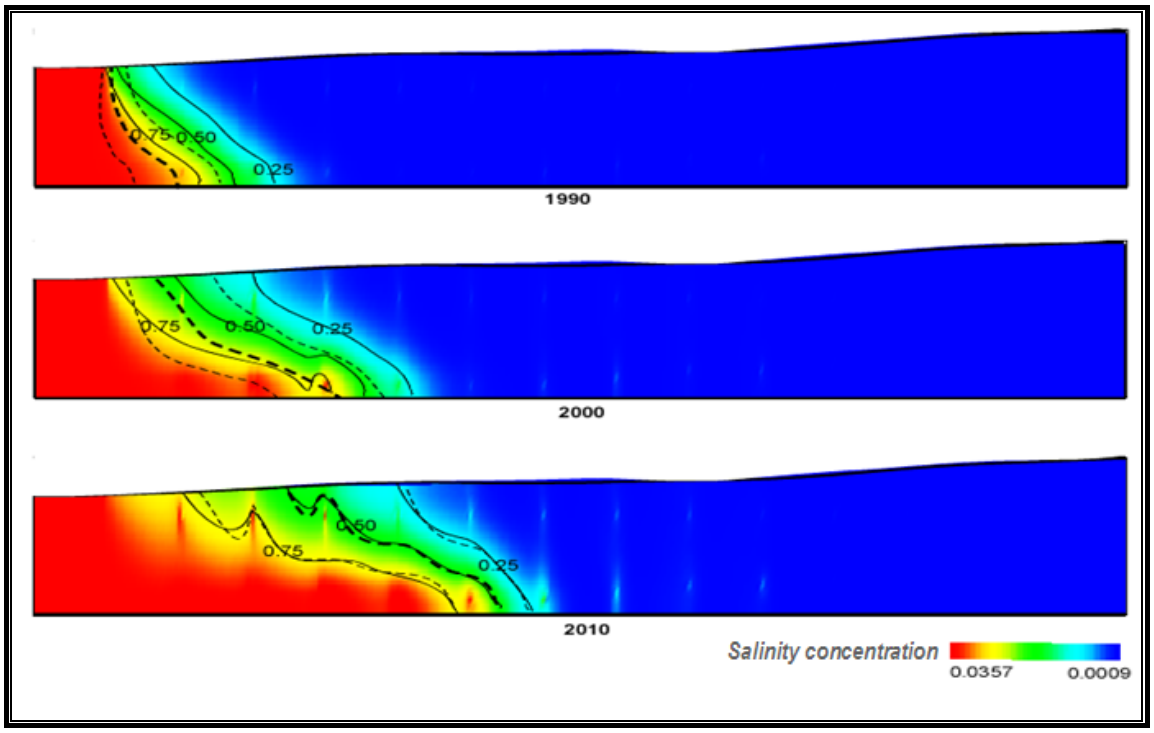

Figure 4.24 *The simulated interface form with hydraulic conductivity of the unconfined aquifer is set to be ten times of the base value.*

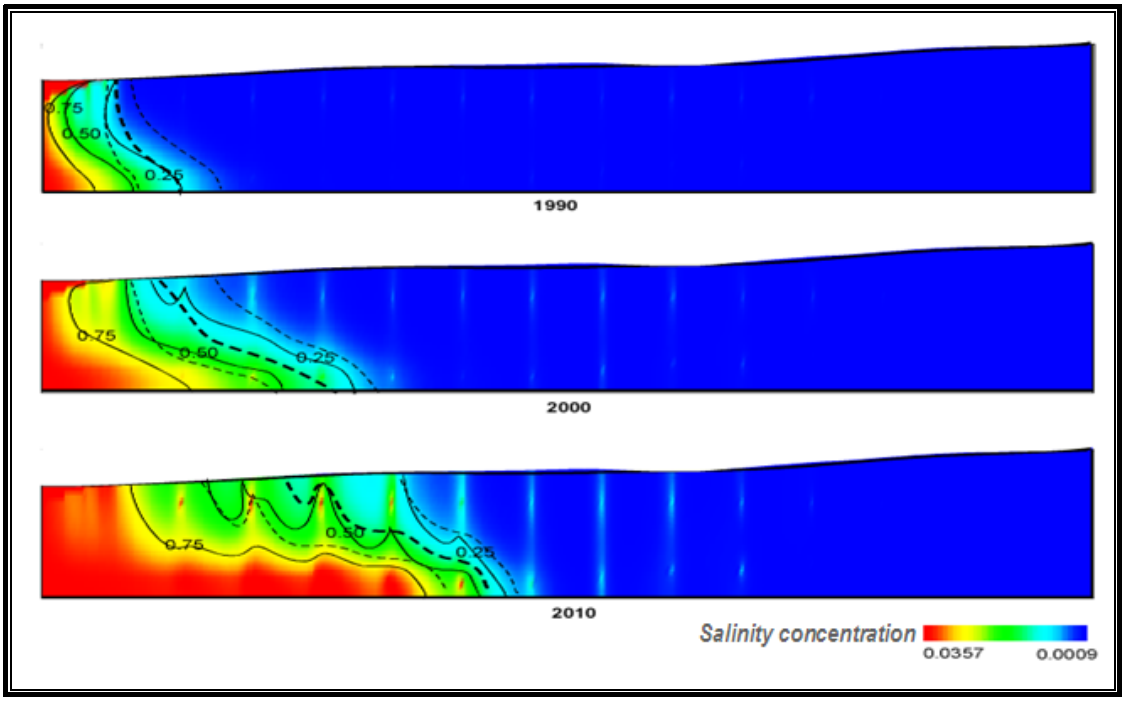

Figure 4.25 *The simulated interface form with hydraulic conductivity of the unconfined aquifer is set to be one tenth of the base value.*

The fifth run was done by increasing the hydraulic conductivity of the confined aquifer ten times and by reducing one tenth. The simulated interface form is shown in figure (4.26) and (4.27). Increasing the hydraulic conductivity decreases the hydraulic head and the seawater move inland. This evidence is occurred in both aquifers. Consecutive to the increment of pumping discharge, the interface become wider. The decreasing of the hydraulic conductivity moves the interface seaward.

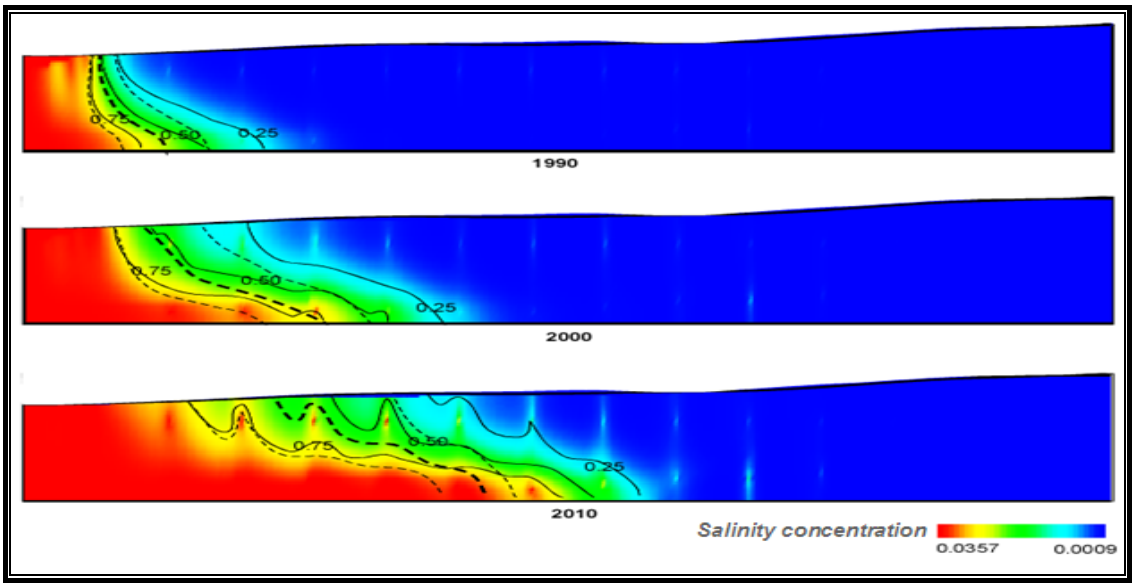

Figure 4.26 *The simulated interface form with hydraulic conductivity of the confined aquifer is set to be high of ten times of the base value*

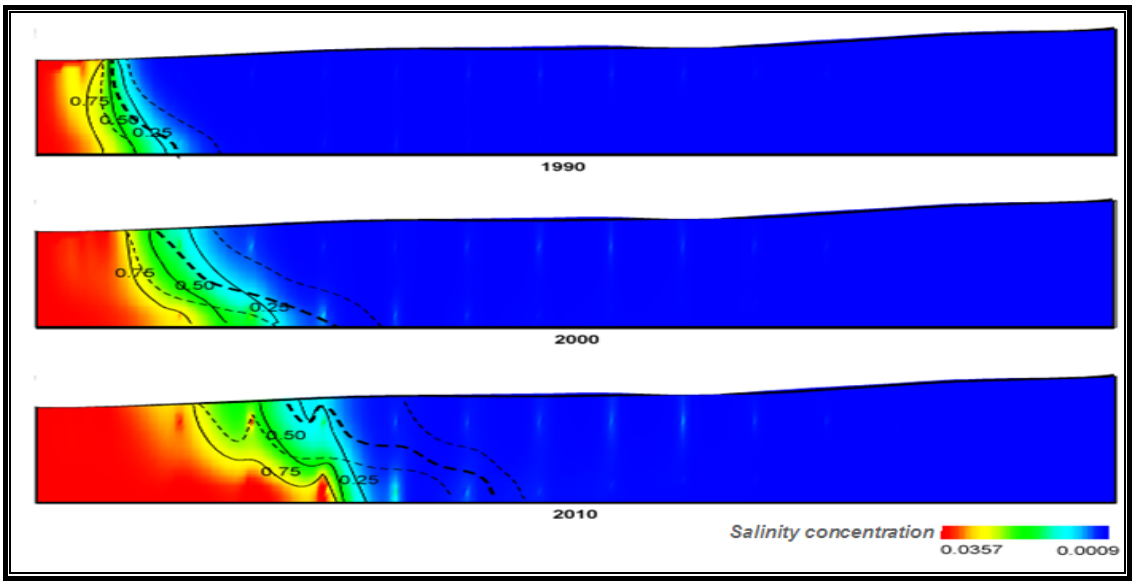

Figure 4.27 *The simulated interface form with hydraulic conductivity of the confined aquifer is set to be small of one tenth of the base value*

The sixth run was done by increasing the hydraulic conductivity of the aquitard ten times and by reducing one tenth. The simulated interface form is shown in figure (4.28) and (4.29). The increasing of hydraulic conductivity decreases hydraulic head, and the interface move inland. The opposite occurs with the decreasing the hydraulic conductivity, in which the interface move seaward. This can be categorized small effect.

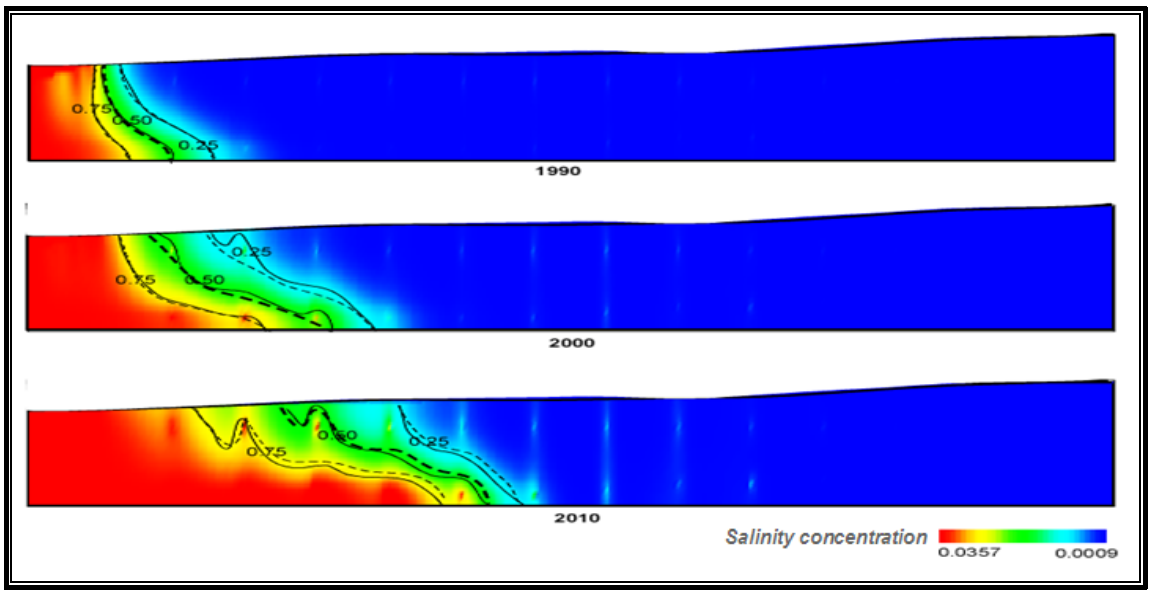

Figure 4.28 *The simulated interface form with hydraulic conductivity of aquitard is set to be ten times of the base value*

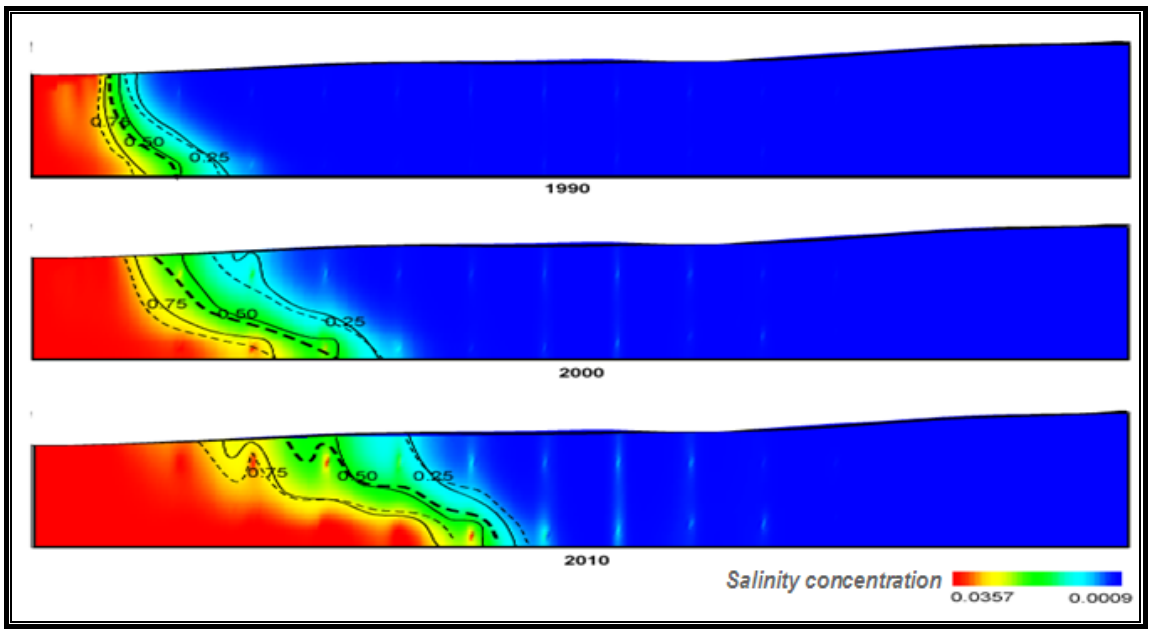

Figure 4.29 *The simulated interface form with hydraulic conductivity of aquitard is set to be one tenth of the base value.*

The seventh run was done by increasing and by reducing recharge rate of underground flow. Since the underground flow is represented as specified constant pressure head and constant concentration, the modification is done by increasing and reducing the pressure head in which equivalent to 1 m of different hydraulic head. With this boundary conditions, form of simulated interface shown in figure (4.28) and (4.29) exhibit a movement of the interface seaward with the increasing the underflow, and a movement to inland with decreasing the underflow. The numerical results exhibited a small influence.

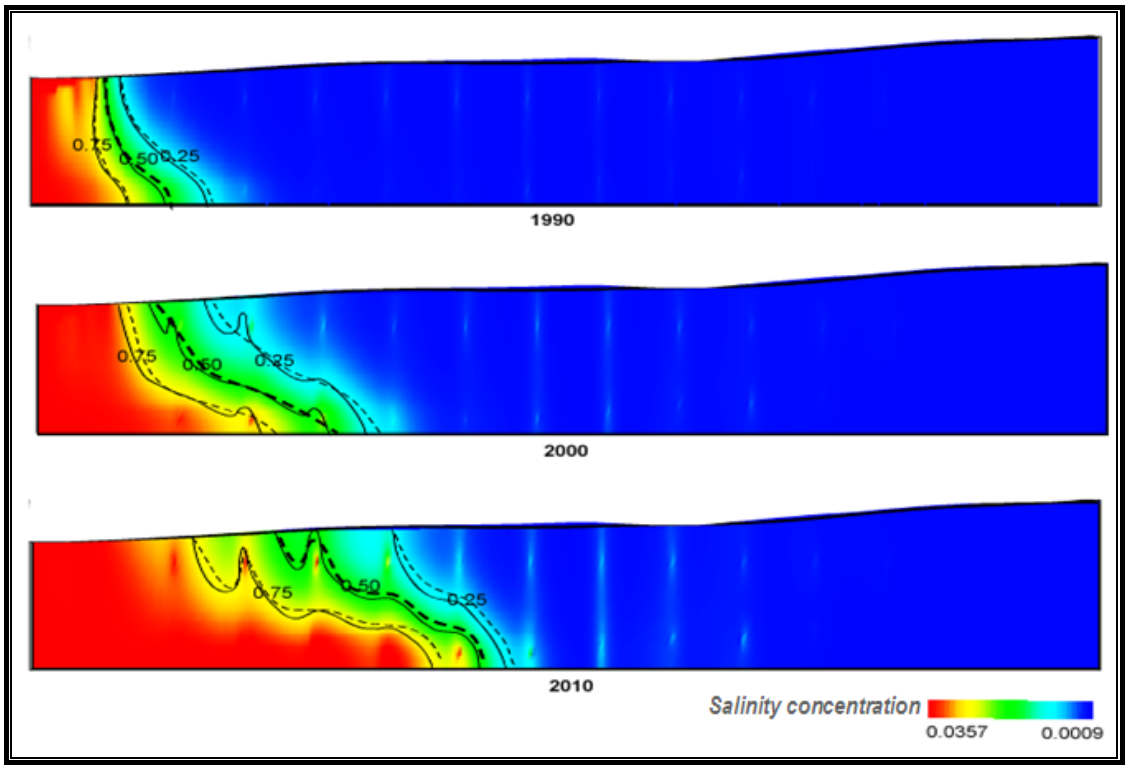

Figure 4.30 *The simulated interface form with underflow recharge is set to be higher than base value.*

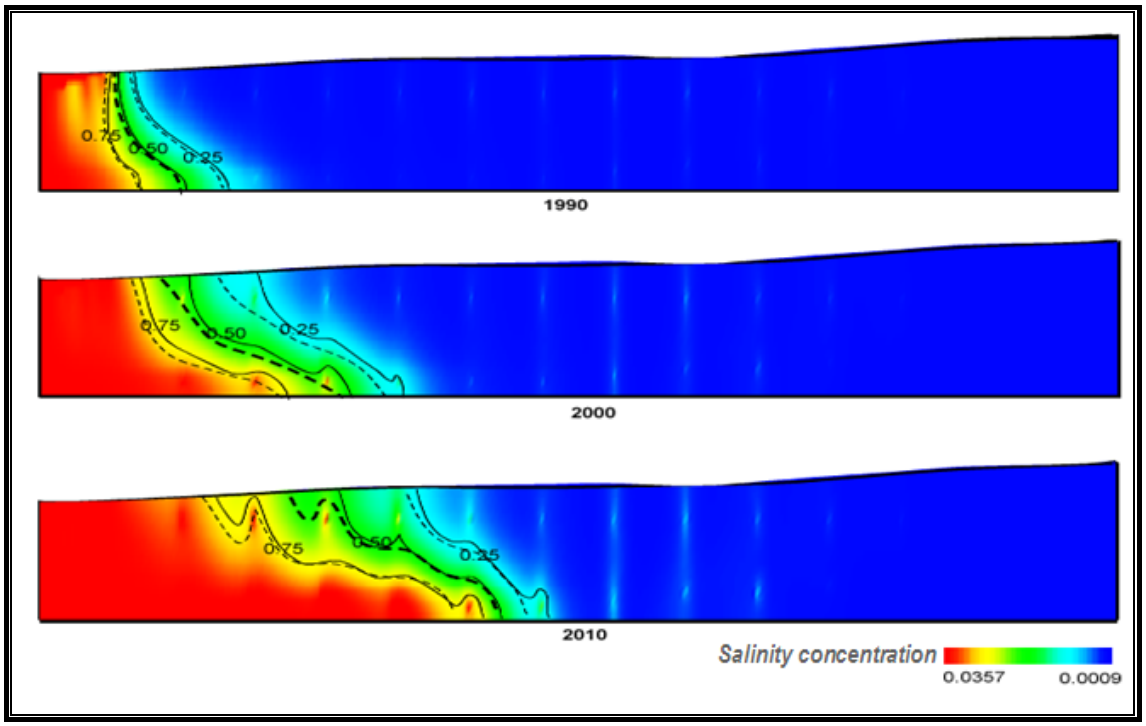

Figure 4.31 The simulated interface form with underflow recharge is set to be smaller than the base value

Changing the flux at the inland boundary has a small effect on model result. The effect is nearly opposite to changing of hydraulic conductivity. When the flux is decrease, salinity contours move inland and the hydraulic heads decrease. When the hydraulic conductivity is decrease, salinity contours move seaward. Many different combinations of hydraulic conductivity and flux may produce the same hydraulic head and salinity distribution, but flow pattern may be different.

4.4. THREE-DIMENSIONAL MODELING

The two-dimensional model of groundwater flow and solute transport is the most common effort to understand the phenomena of seawater intrusion problem. Although they can be applied in various situations, the practical application is rather limited such as: requires a proper cross section to represent a hydrogeological system, and need a proper way to represent abstraction wells on the cross section. For a better simulation approach, 3D-model should be applied.

Obviously, 3D model naturally require even more effort to be understood, implemented and utilized effectively than 2D models. The practical application of 3D salt water intrusion models on a broad scale is still at an early stage of development. Main problems often arise in the practical modeling are; the data availability, the computer memory, and the numerical dispersion problem (Oude Essink, 2001). Mostly reliable and sufficient data are scarce. The availability of enough reliable data is obviously even more pinching for 3D models than for 2D models. For such kind problems, application of 3D computer codes is restricted seriously. To minimize this problem, it is required up-scaling data from 1D and 2D to 3D. In addition, the solute transports is a long time process, consequently a long time observation to detect salinity changes is needed. Another serious problem is computer memory in which is required a huge number of elements to represent 3D system and to avoid numerical dispersion. Correspond to above mentioned problems, combination of the 2D-Model and 3D-Model may give an important contribution to understand the phenomena of the seawater intrusion.

A three-dimensional (3D) model was carried out to simulate the groundwater and the freshwater-seawater interface from January 1982 to December 2010. The 3D-model simulated theses problem by conceptualizing hydrogeological system based on the 2D-model. Restriction of computer memory did not allow representing the hydrogeological system with a fine mesh such as the 2D-model. The hydrogeologic stresses included in the model are flows from lateral boundaries, effective recharge, and groundwater withdrawals. Numerical results are visualized with a number of cross sections and maps that is more communicative than the 3D visualization. User can determine location and position of the cross-sections and maps applied in this developed code.

4.4.1. Spatial and Temporal Discretization

The 3D-model for simulating groundwater flow at Semarang aquifers employed a regularly spaced of Cartesian grid system, in which the x-axis of the grid would roughly parallel the coast. In the horizontal plane, each cell is 300 m by 75 m that has produced 27 columns and 121 rows. In the vertical direction (z-axis), it was used spaces of 2 m and 5 m. An area between mean sea level (MSL) and land surface was discretized in 2 m space, and below the MSL to bottom boundary of the modeling area was discretized in 5 m. In this vertical direction was divided into 30 grids. As result, after eliminating

non-active background mesh, the computational domain consists of 61,421 nodes and covers 55,358 elements.

Assignment of model parameter to these meshes and these nodes employed three approaches: element-wise, node-wise, and cell-wise described in chapter 3. Input data into this 3D-model used the calibrated parameters obtained by the 2D-model. However, up-scaling of the 2D-model data to the 3D-model data is required to represent a more reliable condition of the hydrogeological system. In this 3D-model, each groundwater production well can be located more accurately than the 2D-model.

The modeling area consists of three types of material: silt & sand, sandy clay, and tuffaceous sand. These materials builds four different layers of hydrogeological unit; silt & sand of unconfined aquifer, sandy clay of aquitard, silt & sand of confined aquifer, and tuffaceous sand of confined aquifer. These material layers incline to north-west, so that the unconfined aquifer becomes thicker on seaward boundary.

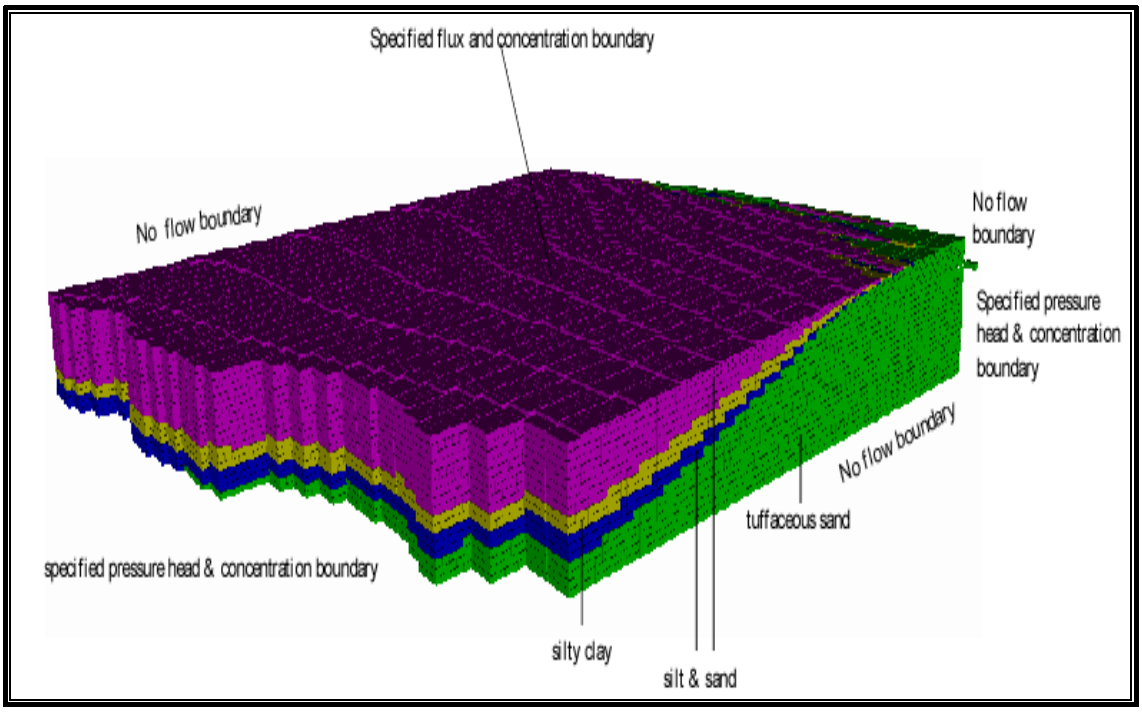

Figure 4.32 The 3D Cartesian grid of Semarang aquifer

Time discretization of this simulation is one month in which equivalent to 2.6298 x 10^6 seconds. Simulation was run within 29 years of time-period, in which each period was

divided into 12 time steps. Numerical analysis investigated the groundwater flow and the interface behavior in 1982 – 2010. Within this simulation period, numerical results can be calibrated with the available data on 1984 – 1998, and make a prediction of the impact of groundwater development policy on the modeling area to the hydraulic head declining and seawater intrusion invasion.

4.4.2 Boundaries and Initial Condition

For most simulations of groundwater flow, boundaries of the model are extended to locations in the aquifer where hydrogeologic boundaries reside. Ideally, these hydrogeological boundaries are persistent flow liner, impermeable barriers, or areas that can be represented do not exist for the inland portion of the model domain. For this reason, boundaries at east, south, and west were extended to be outside of the area of problem interest. The eastern and western boundaries were represented with now-flow boundary. The southern and northern boundaries were defined as specified (constant) pressure head and specified (constant) concentration boundary.

Seaward boundary. Contact between modeling area with Jawa Sea in the northern part was specified with a constant pressure head and constant concentration boundary. The pressure head is obtained 0.0 $kg.m^{-2}.s^{-1}$, and the concentration is used seawater salinity of 0.0357.

Inland boundary. To represent lateral flow of groundwater to or from the inland perimeter of the model, a specified pressure head and concentration boundary was assigned to each node in the southern boundary. The hydraulic head on this boundary was assumed that the boundary would not be affected by withdrawal due to the groundwater exploitation in the hydrogeological system. The assignment of equivalent freshwater pressure head were interpolated based on the water table and the piezometric maps in which variably from east to west side of the model area. The salt concentrations for this boundary were assumed constant throughout the simulation periods by setting this value to 0.9 kg/m^3. In addition, the rest of upper part of this side, unsaturated zone, was considered as no-flow boundary.

Lower model boundary. The lower model boundary represents the base of the Semarang aquifer. This boundary was assigned as an impermeable part or no-flow boundary. Although, there may be upward the vertical groundwater flow from deeper aquifer into the modeling area, there is no evidence related to this boundary to suggest that necessary to include in the modeling calculation.

Upper model boundary. The upper model boundary represents water recharge due to rainfall occurrence. The general procedure for defining recharge values used average recharge net through simulation period that was already calibrated in the 2D-model. Therefore, in this 3D-model, the recharge rate was assigned on upper boundary based on the calibrated rate on the 2D-profile model. This rate was assumed constant within the simulation period.

Initial condition. Initial condition of the model was determined through a number of time steps of extra simulation with two running systems such as employed in the 2D-profile model. The extra simulation with the first running system began to reach steady state condition through long-term transient simulation from arbitrary initial condition. The run was performed by applying above-mentioned boundary conditions with exceptions that the upper boundary was set to be zero for recharge value. In this first running there was no pumping discharge assigned in modeling area. By using one month of time discretization, the run was considered to reach steady state when changes of the freshwater pressure head less than 1.0×10^{2} kg/m^2, and of the salinity concentration less than 5.0×10^{-4} with the increment of time step. This obtained result was, then, used as initial condition for the second run. The second run is to simulate by defining the recharge rate on the upper boundary and by assigning pumping discharge on the wells. This simulation was done for 5 years of time period by setting the input data equal to observation data at 1982. The results of this second running were assigned to be initial condition for this 3D-model simulation in order to learn the dynamic equilibrium of the freshwater-seawater interface in this area.

4.4.3. Simulation Results

Calibration work is, in general sense, one requirement in the groundwater modeling to represent the physical and chemical system accurately. However, the limitation of data

availability and the uncertainty of data emerge difficulties and time-consuming work to do it. Therefore, this procedure, sometimes, is not become a necessity to be done for all modeling effort (Anderson and Woessner 2002). Based on its purposes, the modeling is classified into three types: interpretive, generic study, and predictive. The modeling applied for the predictive purpose requires calibration, and for the interpretive and the generic study, the calibration is not so important.

Calibration is a procedure of adjusting input parameters until the model is a reasonable representation of the physical system. In 2D model, calibration was achieved by adjusting the input parameters for the model within a reasonable range, in which the simulated results of head, net recharge, and position of saltwater interface close to the observed data. Since the input parameter of this 3D-model used the calibrated parameter of 2D-model, no calibration effort had been performed in this 3D simulation. A different approach has been done in assignment pumping discharge to the model, in which in 2D-model converted the well discharge to a line by dividing with wide of aquifer interest, yet such kind assignment is not required in this 3D-model. The pumping discharge was assigned on the model according to the estimation of average the groundwater production from each well.

This modeling was mainly applied for interpretive purpose that is used as a framework for studying system dynamics and/or organizing field data. Despite of this application type does not necessarily require calibration, both the simulated and observed head and salinity concentration were matched ensuring that the input parameter are able to represent the system close to the real condition. Special attention was paid for the salinity distribution simulated within the observation time. Figure (4.33) shows a comparison between the simulated and the observed salinity concentration.

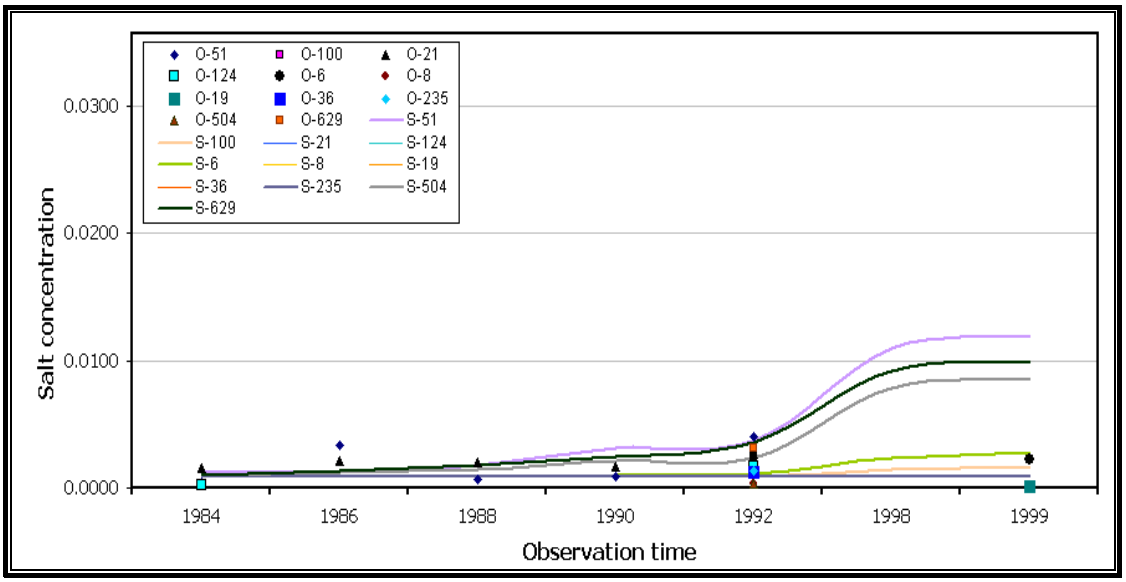

Figure 4.33 Comparison of observed and simulated salinity of 3D-model (O = observed salinity; S = simulated salinity)

In the figure (4.33), the observed groundwater salinity data available at wells of 112 (O-112), 116 (O-116), 124 (O-124), 21 (O-21), 100 (O-100), 51 (O-51), 13 (O-13), 58 (O-58), 8 (O-8) , and 625 (O-625). The graph show reasonable agreement between both observed and measured salinities. The observation data are available from 1982 to 1999. The most difficult problem in the calibration process is non-continuity monitoring activity. However, within the observation periods, simulation is able to produce measured data to ensure the accuracy in representing the physical and the chemical process within this hydrogeological system.

Numerical simulation results are visualized with three cross sections and one map. The cross sections are located on x axis: 1500, 3900, and 6000 with coordinate of 0.0; 0.0 at west side at inland boundary. The map represents salinity distribution at depth of 35 m below mean sea level. Obviously, the model reasonably simulates the position of the saltwater interface. Three numerical results are visualized in figure (4.34), (4.35), and (4.36) demonstrate the simulated salinity distribution on 1985, 1995, and 2010, respectively. The figure (4.34) shows contour line of 75 % of seawater salinity that almost overlaps with the seawater salinity or coastline, and the salinity degrades uniformly inland. This can be interpreted that there is not seawater intrusion problem appear in 1985.

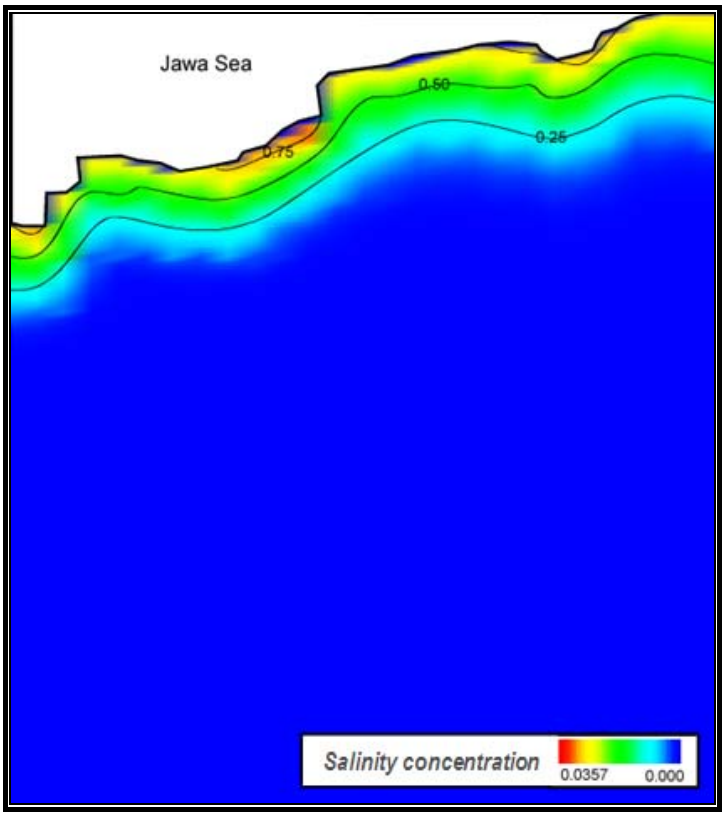

Figure 4.34 The simulated interface form in 1985 at depth of 35 m below MSL

Figure (4.35) reflects a movement of seawater intrusion inland in 1995. The figure shows invasion of the seawater into aquifer at east side deeper than west side. This pattern differs from the simulated interface shown at figure (4.34) that has trend to be uniform along coastline. Prediction of condition at 2010 by using assumption that the groundwater discharge increase according to the trend of the groundwater pumping increment of 1982-1999, shows that the interface move far enough inland. The predicted interface has similar pattern that happened in 1995. These simulation results can be understood that a severe of the seawater intrusion problem will occur if the groundwater is continuously exploited without mitigation efforts.

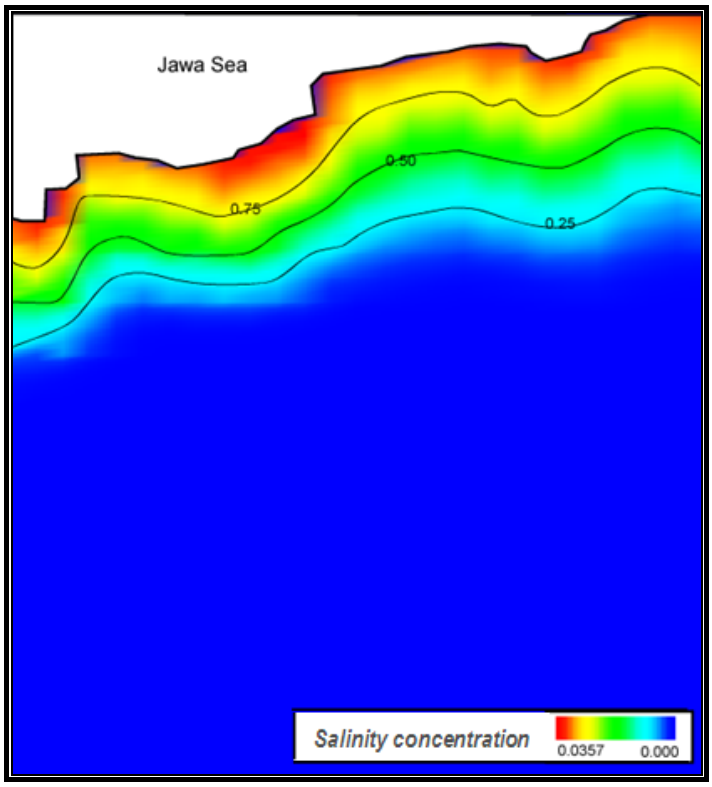

Figure 4.35 The simulated interface form in 1995 at depth of 35 m below MSL

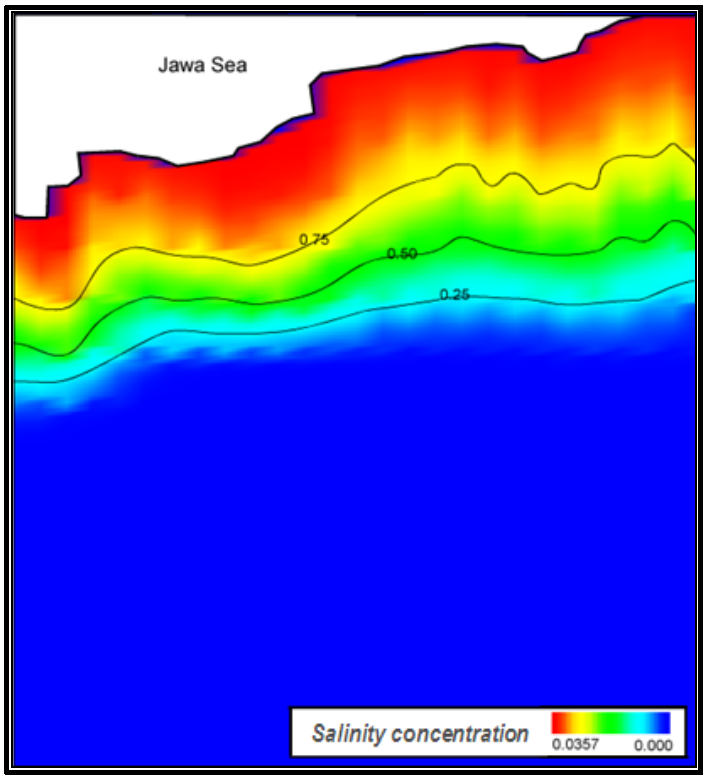

Figure 4.3 The simulated interface form on 2010 at depth of 35 m below MSL

Visualization by using cross section shown in figure (4.37), (4.38), and (4.39) demonstrate simulation results in 1985, 1995, and 2010, similar with the above maps. In 1985, salinity contour of 75 % is close or almost overlaps with coastline, and this contour has trend to move inland with elapsed time. The cross sections depict that east the cross section tends to invade deeper than the other side, particularly at bottom of the confined aquifer. Yet, the movement the interface at west cross section tends shorter but its movement is almost uniform from bottom to top of aquifer. This phenomenon appears at confined and unconfined aquifer.

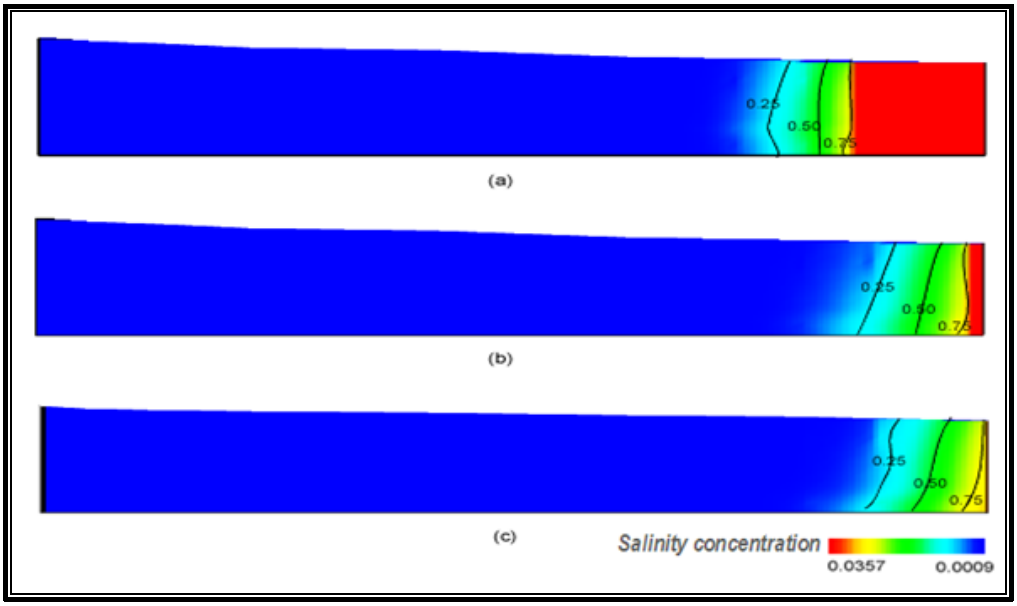

Figure 4.37 Profile of simulated interface in 1985 (a) West cross section, (b) Centre cross section, (c) East cross section

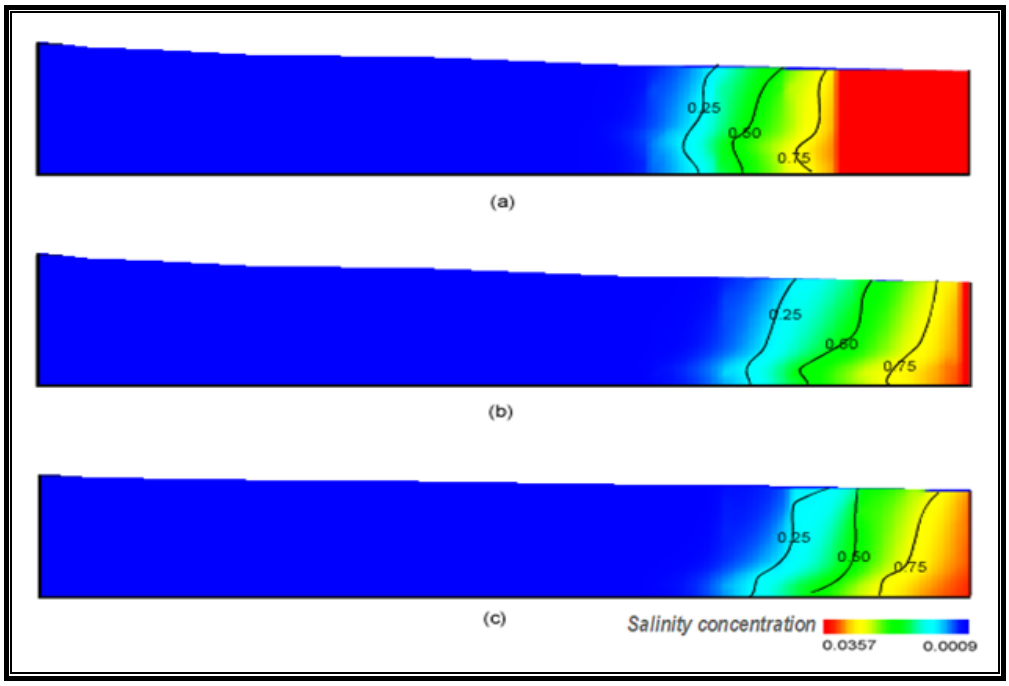

Figure 4.38 Profiles of simulated interface in 1995. (a) West cross section (b) Center cross section, (c) East cross section.

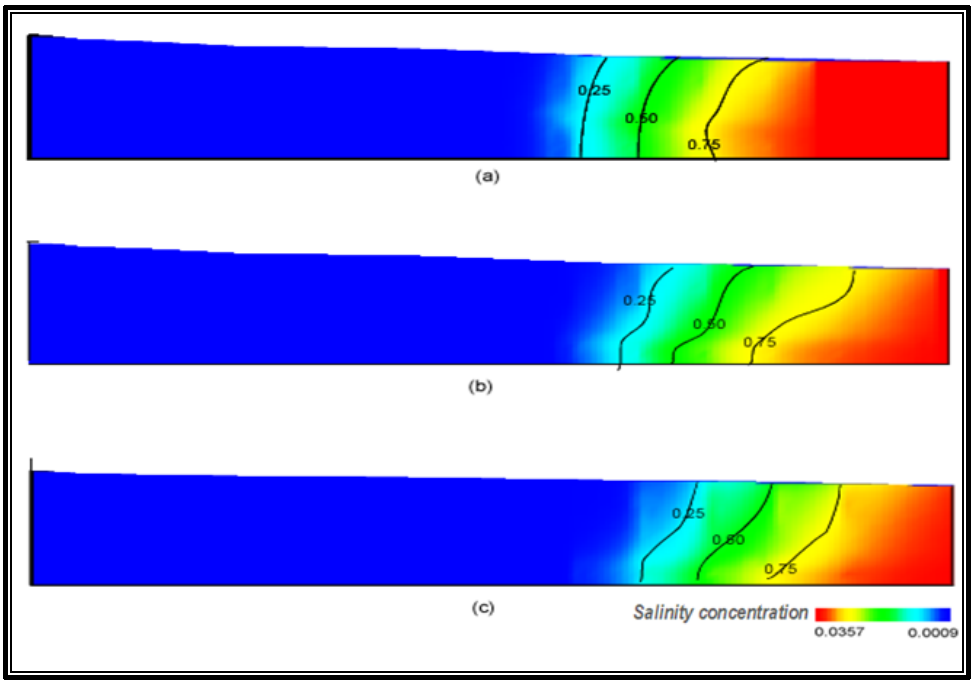

Figure 4.39 Profile of simulate interface in 2010 (a) West cross section, (b) Centre cross section, (c) East cross section.

4.4.4. Model Limitations

The 3D numerical models of the groundwater flow and the solute transport are limited in their representation of the physical system because they contain simplifications and assumptions that may or may not be valid. Result from the groundwater flow simulation has a degree of uncertainty primarily because detailed three-dimensional distribution of aquifer parameters that are rarely available. Result from the solute transport model has more uncertainty because it depends on groundwater velocities calculated from flow models and other uncertain parameters specific to solute transport.

Modeling of freshwater-seawater interface at Semarang aquifer faces also problem of these uncertainties. Possible explanations for this uncertainty correspond to lack of data and grid size. Unavailability the aquifer parameters and detail data of pumping wells are main difficulty in this 3D modeling. The aquifer parameters value was adopted from 2D-model in which is also approximated by literature approach. While, the in-complete information of groundwater production wells was represented by distributing a number of nodes with uniform space and define same discharge for those nodes. Combination these two approaches may produce significant bias to real field condition. However, in order to support interpretive application type, this simplification acceptable to figure out the dynamic process within the aquifer.

Employing the Cartesian mesh system has also contribution to discrepancy between the simulated with the observed hydraulic head and groundwater salinity. This discrepancy is closely related to size of mesh, because an observation point will be defined into the nearest node. Therefore, picked simulated the hydraulic head and the salinity does not represented real position of the field observation point.

4.5. DISCUSSION

Implementation of the developed code integrating FEM with the Cartesian mesh system to a field problem is demonstrated in this chapter. The Semarang aquifer was chosen in the study that was simulated the groundwater flow and the interface behavior with the 2D-model and the 3D-model. This modeling effort was applied for interpretive purpose

to understand the dynamic of the freshwater-seawater interface within the system. The 2D-model was developed to simulate the groundwater flow and the solute transport pattern in detail with a fine level of spatial resolution, and to facilitate development of 3D-model. The 3D-model was performed to overcome limitation of the 2D-model in representing influence of the pumping discharge. Results of both methods are then compared to explain the dynamic of the interface.

The 2D-model was performed trough a cross section passing central of Semarang City with inland boundary at 7000 m to coastline. The profile was extended to 500 m seaward. The simulation was carried out by using lateral space of 20 and 25 meter, and vertically 1 and 5 meter. The final calibration of the 2D-model could produce accurately the hydraulic head and the groundwater salinity compared with the observed data of 1982-1998. Sensitivity analysis was also done in the 2D-model in which the interface position is highly controlled by hydraulic conductivity, and is small effect by underflow recharge. The other parameters seem to have almost no influence to the interface form. By using the calibrated parameter of the 2D-model, the 3D simulation produced reasonable form of the freshwater-seawater interface if we compare with the observed data in 1982-1999. Extension the simulation periods to 2010 estimated that the interface invades too far inland particularly with the 2D-model. With the 3D-model, the thickness of aquifer triggers seawater intrusion into aquifer.

Numerical results both the 2D-model and the 3D-model have a similar pattern of the change of interface form for extended period of simulation from the available observation data. By applied the estimated pumping discharge according to the trend of the groundwater abstraction to the system, the groundwater salinities change drastically. Even though, this applied discharge may be overestimated, yet the ability of the model to represent the physical process within the system is acceptable and reasonable. These numerical results can be interpreted that by continuing the existing groundwater development policy, the groundwater in this aquifer is at critical condition. In order to sustain groundwater supply, a prevention effort should be applied.

The numerical result established form this modeling may represent some data with less accuracy, particularly for recharge rate from surface and underground flow. These entire data requirement are associated with a high uncertainty may produce some bias with the

observed field data. The surface recharge rate used in this modeling was taken from previous study that is counted with a simple recharge estimation method. Therefore, to ensure that representation of the system can produce the measured variable with certain of accuracy, the modeling performed calibration that was done by adjusting the recharge rate and of the hydraulic conductivity. Setting both the recharge rate and the hydraulic conductivity to produce the hydraulic head and the contaminant concentration is a very difficult and time-consuming task, and too much user dependent. Kinzelbach (2002) suggested that since large scales of the hydraulic conductivities values are usually known with even less accuracy than the recharge rate, the model calibration quantity is better for the hydraulic conductivity, and the recharge rate must come from other methods.

Another possibility in producing miscalculation is representing underground flow recharge at boundary. This underground flow recharge was assigned as specified (constant) head and concentration boundary condition. This assignment technique is very simple because the specified values is interpolated from the water table/piezometric map and assuming the boundary would not affected by physical and chemical process on the system. Running model with long time simulation may difficult to control relation between boundary and process on the system. Therefore, assigning the boundary condition by using the concept of groundwater level fluctuation seems more reliable. Furthermore, less accurate simulated result may also come from assigning the boundary condition at seaside. This modeling used specified pressure head and concentration by considering the seawater level in constant position (mean sea level). In the real fact, the seawater level fluctuates under tidal effect. Incorporating of this seawater level fluctuation will produce better modeling results.

REFERENCES

Anderson MP., and Woessner MW., 2002, *Applied Groundwater Modeling,* Simulation of flow and advective transport, Academic Press, INC, New York.

Arifin, M.B., and Wahyudin., 2000, *Investigation of Groundwater Resources at Semarang and Ungaran Basins, Central Jawa,* Directorate of Environmental Geology, Bandung.

Breuck W.D., 1991, *Hydrogeology of Salt Water Intrusion*; A selection of SWIM Papers, International Association of Hydrogeologists, Verlag Heinz Heise, Vol. 11, Hannover.

Frind E., 1980, Seawater intrusion in continuous coastal aquifer-aquitard system, *The Third International Conference on Finite Elements in Water Resources at the University of Missisipi*.

Kinzelbach W., 2002, A survey of methods for groundwater recharge in arid and semi-arid regions, *United Nations Environment Programme,* UNEP/DEWA/RS.02-2.

Langevin, C.D., 2003, Simulation of submarine groundwater discharge to a marine estuary: Biscayne Bay, Florida, *Ground Water*, Vol. 41. No. 6, pp, 758-771

Langevin, C.D., Thorne, D.T., Dausman, A.M., Sukop, M.C., and Guo, W., 2008, *SEAWAT Version 4: A computer Program for Simulation of Multi-Species Solute and Heat Transport*, U.S. Geological Survey, Virginia.

Mulyana., and Widharto, T., 1996, *Quartenary Geological Map of The Semarang Quadrangle, Jawa,* Geological Research and Development Center, Bandung.

Ohnishi Y., Ohtsu H., Nishioka T., Naka Y., Yasuda T., and Takahashi K., 2003, Observational method for tunnel construction considering environmental impact to groundwater, *Groundwater Engineering* – Recent Advances, Balkema, pp. 17-24.

Oude Essink G.H.P., 2001, Improving Fresh Groundwater Supply – problems and solutions, *Ocean and Coastal Management* 44 pp 429-449.

Pudjihardjo, H., 1995, *Study of Impact of Groundwater Exploitation to Seawater Intrusion on Semarang Area*, Directorate of Enviromental Geology, Bandung.

Said, H.D., 2000, *Hydrogeological Map of Semarang*, Scale 1 : 250.000, Directorate of Environmental Geology, Bandung. (in Indonesian)

Scanlon B.R., and Healy R.W., 2002, Choosing appropriate techniques for quantifying groundwater recharge, *Hydrogelogy Journal* Vol. 10; pp. 18-39, Springer-Verlag.

Schwartz F.W., and Zhang H., 2003, *Fundamental of Groundwater*, John Wiley & Sons, Inc, New York.

Sihwanto., and Iskandar, N., 2000, *Grounwater Conservation on Semarang Area*, Directorate of Environmental Geology, Bandung.

Spitz, K., 1989, *Groundwater Flow Modeling, Semarang-Central Jawa*, Directorate of Geology and Mineral Resources for Indonesia, Bandung.

Utomo E.P., and Sudarsono U., 2003, Groundwater resources in Java island, Indonesia, *Proceeding of the International Symposium on Safe and Sustainable Exploitation of Soil and Groundwater Resources in Asia*, Okayama University, pp. 61-76.

Voss C.I., and Provost, A.M., 2003, *SUTRA*, A Model for Saturated-Unsaturated Variable-Density Ground-water Flow with Solute or Energy Transport, *Water-Resources Investigation* Report 02-4231, U.S. Geological Survey, published online on internet at http://water.usgs.gov/nrp/gwsoftware.

Voss C.I., and Souza W.R., 1987, Variable Density Flow and Solute Transport Simulation of Regional Aquifers Containing a Narrow Freshwater-Saltwater Transition Zone, *Water Resources Research*, Vol. 23, No. 10, pp.1851-1866.

Wang H.F., and Anderson, MP., 1982, *Introduction to Groundwater Modeling*, W.H Freeman and company, San Fransisco.

CHAPTER 5

MITIGATION OF SEAWATER INTRUSION PROBLEM AT SEMARANG AQUIFER

5.1. GENERAL REMARKS

Tremendous increasing population along coastal zone associated with increase human activities will impose additional water demand. Development of groundwater as a main resource to supply water demand disturbs equilibrium of the interface. As a result, the intensive groundwater exploitation exceeding recharge rate has been emerged severe seawater intrusion problem in many cities over the world. In contrast with the concept of sustainable development by *World Commission on Environment and Development* in which implies meeting the need of the present without compromising the ability of future generations to meet their need.

The sustainable development of water resources refers to a holistic approach to development, conservation, and management of water resources, that considers all components of the hydrologic system. In the field of groundwater research, the concept of sustainable development remains debatable issue. The early approach is concept of safe yield considering water balance in a groundwater basin. Despite of this method has been used for long time, yet it has been criticized by Sophocleous (2002) for not taking surface water into consideration. Integration of the surface water and groundwater is not easy to be analyzed. Therefore, the idea of groundwater development that is proposed here is in a frame of hydrodynamic equilibrium of the freshwater-seawater interface.

This chapter describes hydro-dynamics of the freshwater-seawater interface on the groundwater development area as effects of designing prevention techniques of the seawater intrusion. The hydro-dynamics investigated by using the 2D-model based on the calibrated modeling parameter described in chapter (4) is used as a base condition representing the effect of the existing groundwater development policy.

5.2. PREVENTION METHODS OF SEAWATER INTRUSION

Prevention of seawater intrusion into coastal aquifer is quite expensive. Some techniques have been successful to control the seawater intrusion. The most direct effort is to reduce the pumping rates, probably by introducing other water resources such as: treated wastewater, desalted water, and recycled industrial water. Land use may also implement with specific reference to cultivation practices in coastal regions. Some crops such as rice and sugarcane need huge amount of water that can be infiltrated into the ground surface and recharge the underlying aquifer. Such agricultural activities can be applied to adjust water tables and/or piezometric heads in coastal aquifers.

Artificial recharge of groundwater represents another alternative for seawater intrusion mitigation. The artificial recharge is done by infiltrating surface water into ground that is commonly at rates and quantities many times in excess of natural recharge. Two methods in this category are basin spreading and hydraulic barrier. The basin spreading is to infiltrate surface water into aquifer by through surface depression. The water flows to a deeper layer by natural process in which hydraulic parameter of the rock/soil is main control of this recharge rate. In some area, this system has been applied by collecting the surface water into number dug wells. Another method for the artificial recharge is hydraulic barrier. The hydraulic barrier is to construct a series of injection well into aquifer along coastline. This technique attempts to establish groundwater elevations greater than or equal to the original elevation.

In some regions, the artificial recharge may be difficult to be applied due to a lack of surface water. The requirement of imported water to be injected into aquifer may cause the design reach its life expectancy, increasing demands of well, and replacement budget. Therefore, some alternative studies such slurry walls, grout curtains, air injection, and bio-walls have been developing. The slurry walls are build with a ditch is then backfilled with a mixture of soil-bentonite, a mixture of cement-bentonite, or plastic concrete materials, to form an impervious barrier to seepage. The grout curtains are constructed by drilling holes along a single line or multiple parallel lines. Grout is then injected into the holes under pressure to fill the surrounding soil pores or rock fractures. By placing these holes on a tight enough spacing, a grout barrier of variable thickness is created. The grout curtains can be installed to most any depth and can be

surgically injected to treat specific zones. The air injection is used in the development of oil and gas fields and during tunneling to cutoff the flow of water. Adopting this technique attempts to cause a piezometric rise in water level that can be used to alter groundwater gradients and flow directions. Air entrained in soil pores causes an overall decrease in the permeability of the aquifer, which could be used to reduce flow across specific zones. The bio-wall technology involves the injection of starved bacteria cultures into the pores of the aquifer media to develop a biological subsurface plug. This method uses microbial growth to fill the void space found in all soils, thus decreasing its permeability. The wall is maintained by periodic injection of nutrients to feed the bacteria in specific zones.

Other technique that can be practiced to combat the seawater intrusion is pumping of brackish groundwater. The pumping of brackish water will reduce pressure head of the seawater. Since the invasion of the seawater depends on the equilibrium between the pressure head of the seawater and the freshwater, reducing the pressure head of the seawater will allow abstracting a more the freshwater from aquifer. However, in order to provide a stagnant interface, well of brackish water abstraction at some distance from the shore requires a careful design. In-accurate design may trigger the seawater intrusion.

This study deals with the artificial recharge as tools to mitigate and control seawater intrusion problem into Semarang aquifer. Unlike most of the available investigations, the simulation was carried out to understand the behavior the groundwater flow and the solute transport as effect on implementation of prevention scheme while the freshwater pumping to supply water demand is run on. In addition, most previous analysis employed the sharp interface, but this investigation applied concept of variable density of the interface.

5.3. THE INTERFACE DYNAMICS DUE TO PREVENTION SCHEMES

Condition of the seawater intrusion in a coastal aquifer depends on many factors. These factors are among others the type of aquifer (confined, unconfined, leaky, or multilayer) and its geological setting, water table and/or piezometric head, seawater concentration

and density, natural rate of flow, capacity and duration of water withdrawal or recharge, rainfall intensity, land use, geometry and hydraulic boundaries, tidal effect, variation of barometric pressure, and wave actions. This complex variable creates a specific characteristic of the interface for each groundwater development area. To analyze such kind problem, the numerical model is an important tool in which can be as 2D-model and 3D-model. Both of models were applied to investigate the dynamic of the freshwater-seawater interface at Semarang aquifer by considering the existing groundwater development policy. Unfortunately, the simulation results showed that this area in very high risk to suffer from seawater intrusion. Therefore, mitigation effort should be introduced to sustain the groundwater supply. In order to find an effective prevention method, the response of aquifer system was observed through the 2D-profile model.

The interface's response to proposed prevention techniques were analyzed by concerning to the base condition at chapter (4) that was run using the calibrated parameter. An interesting phenomenon was investigated here is a mitigation scheme applied on a unique hydrogeological system, in which a combination of unconfined and confined aquifer that separate at around coastline but connect each other at inland part. The effect of prevention scheme to the seawater intrusion is then explained qualitatively by using term of high, medium, and small category.

Two techniques of the artificial recharge; surface recharge and hydraulic barrier, has been investigated here. It is used terms of surface recharge to mention artificial recharge that can be injected through dug wells, and hydraulic barrier for infiltrating water through deep injection wells. Frame of study is to investigate the effectiveness of these methods to control the seawater intrusion into aquifers. Description does not cover technical design each prevention method. With assumption that each method can work properly, in-efficiency of these methods to flowing water due to imperfect construction were neglected. Since the lack of observation data, these numerical results are mainly characterized by application of interpretive category.

Periods of simulation begin from 2001 to 2010 with time steps of 1 month. The initial condition was obtained from simulated result of 2000. This 2000 is used as initial condition because the data availability is reported on that time. This simulation scenario

considers learning the dynamic equilibrium affecting by the prevention technique as long as 10 years. In order to evaluate the effectiveness of the proposed scheme, the model was run with 10 years simulation time without introducing a prevention scheme. This result produced from simulation performed on chapter (4) that is aimed to figure dynamic equilibrium of the interface due to the existing development policy.

The effectiveness of each prevention scheme is visualized every two years progress with two graphs: one graph for groundwater salinity on the unconfined aquifer, and other graph for the confined. The graphs are constructed by using estimated groundwater salinity at node with interval 100 meters, and within a zone of 1 km from coastline. Two depths of observation point are assigned; at depth 20 m below MSL for the unconfined aquifer, and depth of 65 m below MSL for the confined aquifer. Descriptions of these numerical results are compared with the groundwater salinity produced by simulation without prevention technique. For graphs below, the red color describes the groundwater salinity after running model of 10 years with the existing groundwater development system, and blue color to figure out the initial condition used on this simulation. Five black color lines represent the groundwater salinity changes due to the implementation of prevention scheme for every two year of elapsed time.

Scheme One.

A prevention scheme of the seawater intrusion problem was designed by increasing of natural recharge rate on the land surface or shallow depth aquifer. Implementation of this design scheme on the numerical modeling is to assign desired recharge rate on the top domain boundary. For practical construction, the artificial recharge is injected through numbers of dug wells. Simulation of the interface dynamic on chapter (4) established the calibrated rate of natural recharge was 4.0×10^{-6} kg/m^2/sec or equivalent with 0.344 mm/day. The estimated result is used in the analysis that is drawn with solid-line.

This prevention scheme is to design the artificial recharge become twice and four time of the calibrated natural recharge rate. This new scenario of recharge rate can be assigned directly into node on the surface boundary of domain without modification of the boundary condition type (figure 4.13). Effect of the increasing of the surface

recharge of twice from the natural rate to the interface condition is represented with groundwater salinity graphs on figure (5.1a) for the unconfined aquifer and figure (5.1b) for the confined aquifer. Both graphs show that the influence of this recharge rate to the interface dynamics can be categorized medium effect on the unconfined aquifer, and small on the confined aquifer. On the unconfined aquifer, the groundwater salinity around the coastline can be maintained since the second year to the end of simulation. The groundwater salinity in the inland part is still increase with similar trend of the effect of the present groundwater development. Fortunately, estimated salinity in the end of simulation has not reached the end simulation with the present development system. Otherwise, the salinity changes on the confined aquifer have a trend that similar with the present system, but degree of the increment is smaller than the present system.

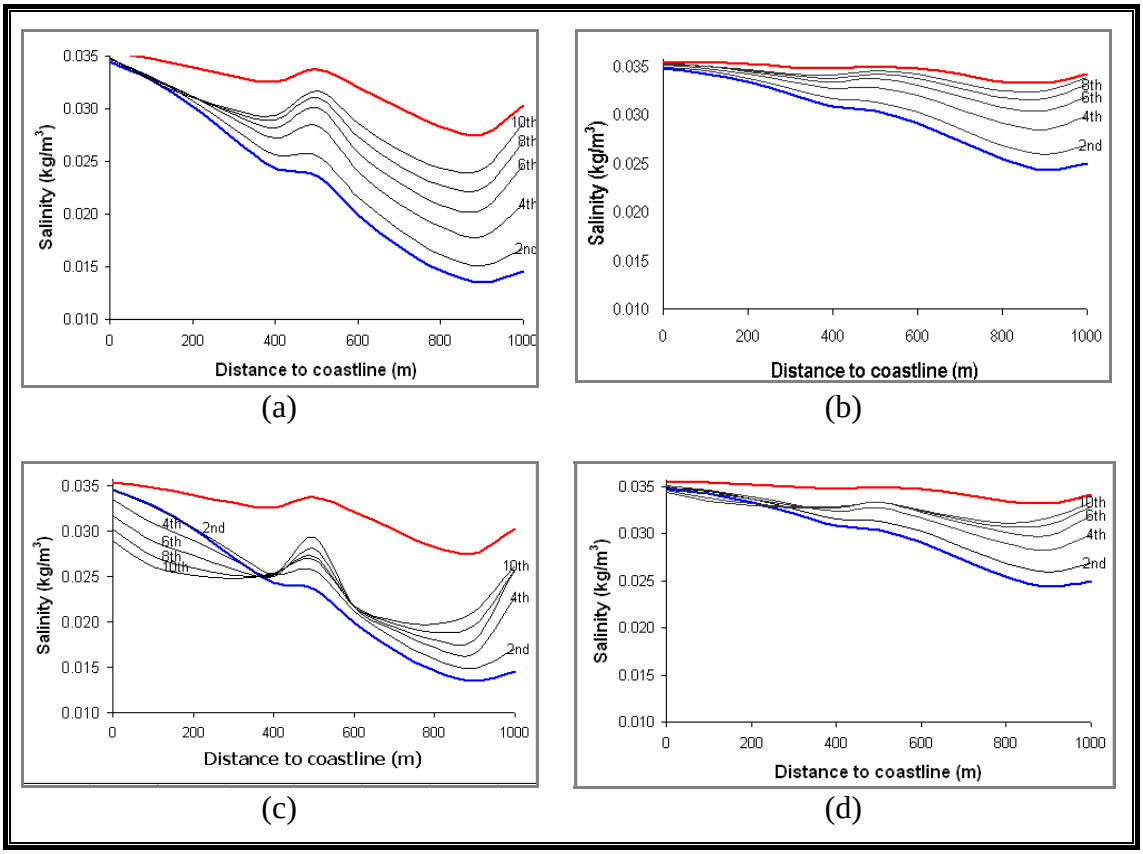

Figure 5.1 *Evolution of the interface due to implementation of scheme one, with (a) and (c) represent unconfined aquifer, (b) and (d) represent confined aquifer.*

The significant impact can be observed on figure (5.1c) and (5.1d) in which describe groundwater salinity changes due to recharge rate of 1.388 mm/day or four times of the

natural recharge rate on both aquifers. The impact of this recharge to the unconfined aquifer can be categorized as high, and to the confined aquifer is a medium. Within zone of 400 m from coastline on the unconfined aquifer, the recharge can maintain the groundwater salinity after 2 years of implementation of the prevention technique, and the groundwater salinity decreases correspond to elapsed time. Yet, on inland part the groundwater salinity successively increase, even though with small increment. The changes have a quite different pattern with the trend of the groundwater salinity due to the present groundwater development. On the confined aquifer, within zone of 300 m from the coastline, it looks to be stagnant. Small increment of the salinity is occurred at the inland part and trend of the increment is same with the present groundwater development.

Scheme Two.

Scheme two is a hydraulic barrier that is designed by injecting freshwater into aquifer around coastline through a series number of wells. Investigation was performed with two scenarios by using two series of wells in which a series at coastline, and a series at 100 m from coastline. Position of well's screen is at depth of 20 m, 40 m, and 70 m below MSL, and the recharge rate is injected into aquifer with recharge of 1.0×10^{-2} kg/sec. Numerical results are shown in figure (5.2) in which graphs a and c represent the groundwater salinity on unconfined aquifer, and the other for confined aquifer. Graphs a and b represent result estimated by injection wells on coastline, graphs c and d represent result from injection well located on 100 meter from coastline.

The graph exhibits that the unconfined and the confined aquifer are affected by the freshwater injection of both schemes above mentioned. The effect is in high category. Placing of injection wells at coastline on unconfined aquifer decreases the groundwater salinity drastically. This effect can be observed within area of 500 m from coastline. This is also occurred on confined aquifer. The groundwater salinity decreases successively with elapsed time of simulation. However, in the inland part, the groundwater salinity increases to be close to the salinity line of the present development system.

The injection well lied on 100 m from coastline can show the decreasing of groundwater salinity drastically on the well position. The effect of this well to lateral direction has no significant impact compared with the scheme one. However, combination of two series of wells gives effect to be more depth into aquifer, particularly for the confined aquifer. On the graphs, the degradation of groundwater is occurred more severe on inland part then the area close to coastline. This is figure out that the groundwater exploitation on this zone is quite intensive.

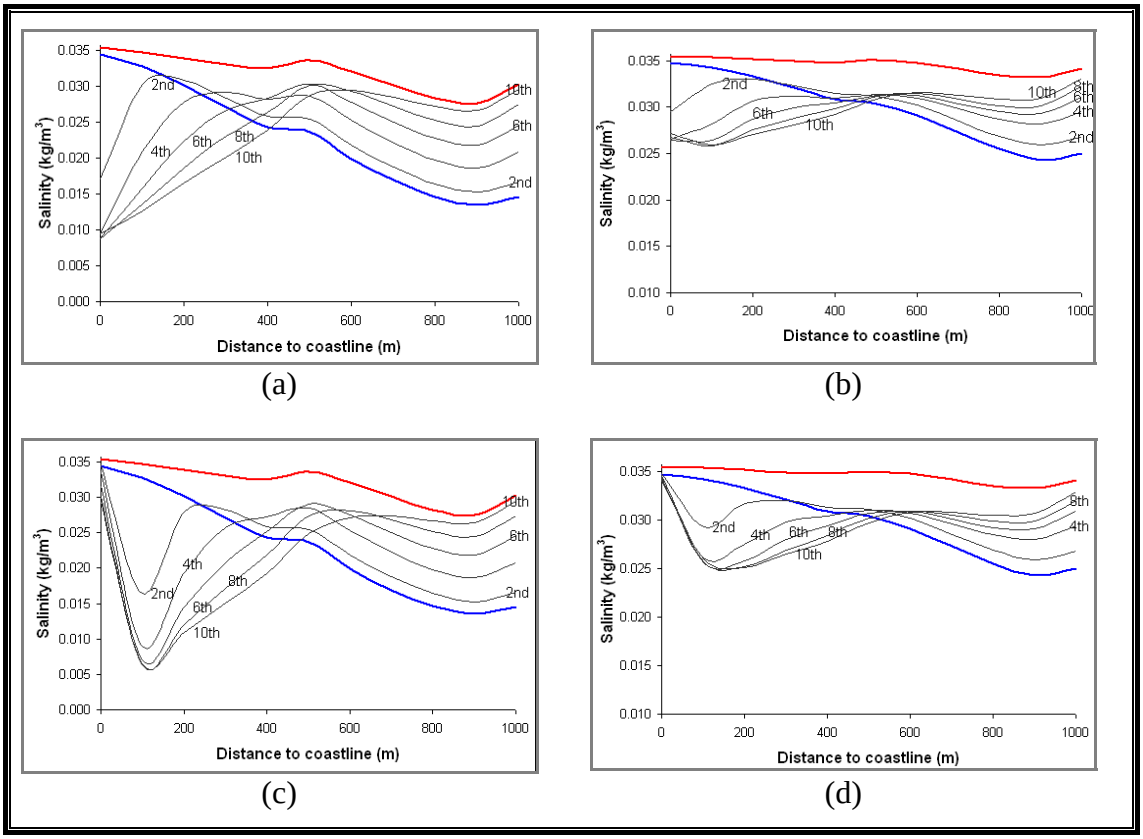

Figure 5.2 Evolution of the interface due to implementation of scheme two, in which (a) and (c) to represent unconfined aquifer; (b) and (d) represent confined aquifer.

Scheme three.

Scheme three consists of a combination between the surface recharge with the hydraulic barrier. The hydraulic barrier is designed to be a line in horizontal direction at depth of 70 m below the mean sea level. Three injection wells designed in this line locates at distance of 100 m, 200 m, and 300 m from coastline. Recharge rate of each deep injection well is 1.0 x 10^{-2} kg/sec. This recharge rate is combined with two different

value of the surface recharge such in scheme one. Scenario 1 is combination with surface recharge rate; 8 x 10^{-6} kg/sec (twice from the natural rate), and scenario two is to combine with surface recharge rate as large as 1.6 x 10^{-5} kg/sec (four times of the natural rate). Numerical result of this scheme are shown in figure (5.3), with graphs (a) and (c) for unconfined aquifer, and graphs (b) and (d) for confined aquifer. Graphs (a) and (b) represent estimated salinity due to scenario 1, and graphs (c) and (d) represent estimated salinity affected by scenario 2.

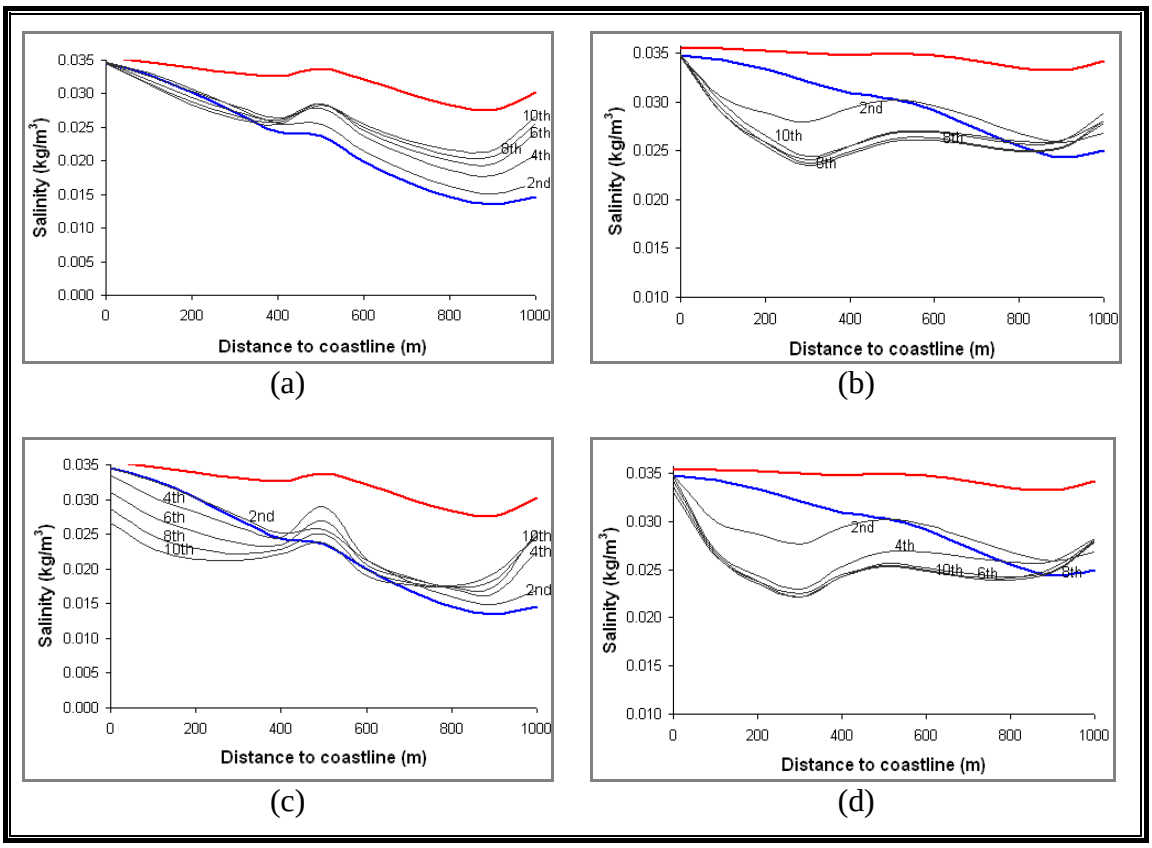

Figure 5.3 *Evolution of the interface due to implementation of scheme three; (a) and (c) represent unconfined aquifer, (b) and (d) represent confined aquifer.*

Scenario 1 provides result with ability to combat the seawater intrusion effectively (figure 5.3a and 5.3b). It can be observed that in the 10^{th} years of simulation with this prevention scheme, the groundwater salinity lines lies quite far from the predicted salinity line by the present development system. On unconfined aquifer, the salinity can be maintained within the simulation period, yet small degradation of the groundwater quality is occurred in the outside of 500 m from coastline. On confined aquifer, the

combination shows a better result, in which the groundwater salinity can be reduced around coastline within the simulation period.

Figure (5.3c) and (5.3d) represent the influence of scenario 2 to reduce groundwater salinity. On unconfined aquifer, from the second year, the groundwater salinity can be maintained without increment from the initial condition. With the elapsed time of simulation, the groundwater salinity decreases to be lower than the initial condition. Groundwater salinity on the confined aquifer has similar pattern with estimated from scenario 1.

Scheme four.

Scheme four composed of the hydraulic barrier and the surface recharge. Unlike with scheme three, the hydraulic barrier in this scheme is to arrange the injection wells in a line for vertical direction for depth of 20 m, 40 m, and 70 m below mean sea level. The injection well is located at distance of 100 m from coastline. The recharge rate of each injection well is 1.0×10^{-2} kg/sec, and the surface recharge infiltrates water with rate twice (scenario 1), and four times (scenario 2) of the calibrated natural rate at the initial condition.

Graph on figure (5.4a) represents the groundwater salinity on the unconfined aquifer and figure (5.4b) for the confined aquifer that are affected by the implementation of the scenario 1 of this prevention scheme. Numerical results show that the salinity lines exhibit drastically decreasing on the location of the injection well, however the end of interface toe the groundwater salinity increases correspond to the simulation time. The similar pattern appears on the confined aquifer but in lower category if it is compared to the effect on unconfined aquifer. These behaviors are also can be observed on the increasing of the surface recharge rate four times than the natural rate (figure 5.4c and figure 5.4d). Small difference this combination with the first one is the increasing of the groundwater salinity on the unconfined aquifer seems to be smaller. Comparing to the scheme three, this combination is less effective in mitigation of the seawater intrusion problem.

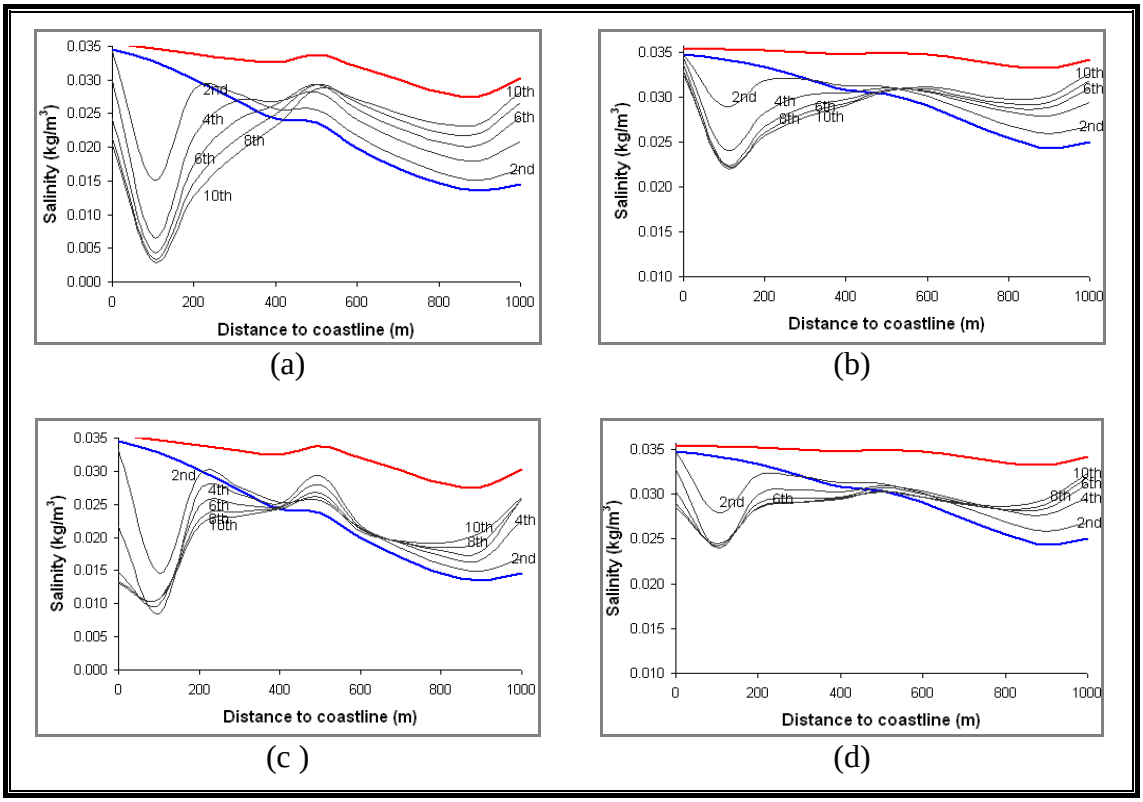

Figure 5.4 *Evolution of the interface due to implementation of scheme four; (a) and (c) represent unconfined aquifer, (b) and (d) represent confined aquifer.*

Scheme five.

Scheme five is to design the seawater abstraction well. Some available studies of brackish water pumping were mainly based on the sharp interface assumption. Study employed dispersion zone approach was done by Sherif and Hamza (2001) for a single layer of aquifer. His research exhibited a successful result. However, he assumed there is no production well that is set to be active. Unlike those approaches, we evaluated the effectiveness this method in multilayer aquifers while the fresh groundwater are being extracted.

The seawater abstraction was designed to locate series of well in two vertical lines. These lines is at shoreline (x = 0 m), and at 100 m to coastline (x = 100 m), with a similar depth of 20 m (z = -20 m), 40 m (z = -40 m), and 60 m (z = -60 m) below mean sea level. The wells extract seawater with discharge rate of 0.1 x 10^{-2} kg/sec equivalent to 10 liter/sec. Defining these extraction wells require modification of the original boundary conditions by adding six nodes for sinks. The model was run to

analyze three pumping schemes; the extraction was carried through the wells on shoreline (scenario 1), the wells on 100 m from the shoreline (scenario 2), and combination both series (scenario 3).

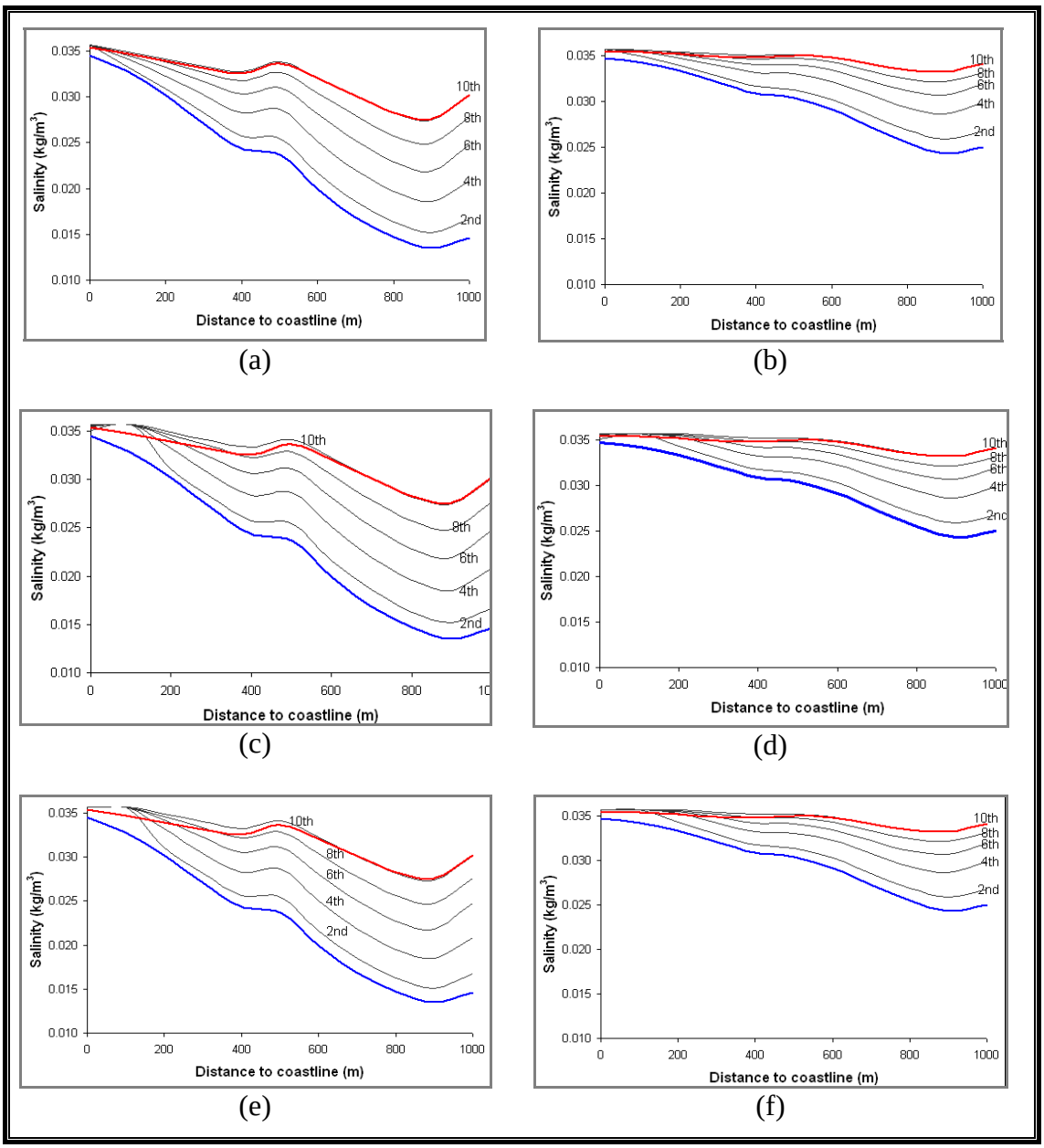

Figure 5.5 *Evolution of the interface due to implementation of scheme five; (a), (c) and (e) represent unconfined aquifer, (b), (d) and (f) represent confined aquifer.*

Numerical simulation results shown in figure (5.5) in which figures (5.5a) and (5.5b) for scenario 1, (5.5c) and (5.5d) for scenario 2, and (5.5e) and (5.5f) for scenario 3. These figures demonstrate that the seawater abstraction cannot be applied to combat seawater

intrusion in these aquifers. In both confined and unconfined aquifers, the abstraction cannot decrease the groundwater salinity. In addition, small increment of the salinity appears around coastline. This graph indicates that the pumping of brackish groundwater become new trigger to the seawater intrusion problem.

Scheme Six

Scheme six is to combine of the hydraulic barrier and the seawater abstraction. The seawater abstraction is located at shoreline, and the hydraulic barrier at distance of 100 m from the coastline. Three points for each line at depth of 20 m, 40 m, and 60 m below the MSL. Recharge rate of the injection wells and the extraction wells is set to 1.0×10^{-2} kg/ sec. With observation points at the same position with other scheme, the numerical results are shown in figure (5.6).

The graphs exhibit this scheme is able to reduce the groundwater salinity to 0.015 in the first year, and then stagnant at 0.009 at the rest of simulation time. In the first year at unconfined aquifer, the salinity is observed within 200 m of the coastline and in the third year at 400 m from the coastline. For confined aquifer, in the first year the salinity degradation occur within 400 m of coastline with maximum change at the injection wells line reach 0.030. Correspond to elapsed time, the salinity decrease to 0.026 at the injection well line, and this effect give influence within 900 m of the coastline.

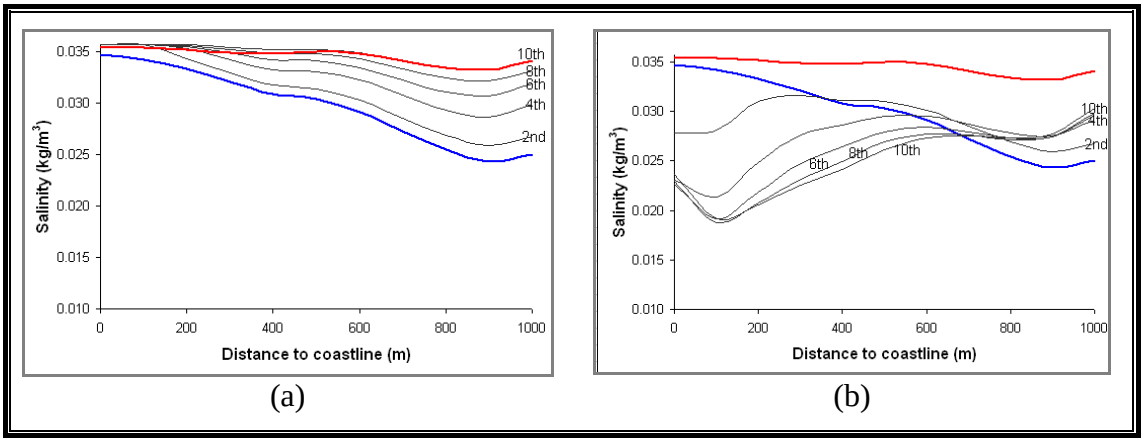

Figure 5.6 *Evolution of the interface due to implementation of scheme six; (a) represent unconfined aquifer, and (b) represent confined aquifer.*

5.4. DISCUSSION

The dynamic of the freshwater-seawater interface due to assignment of prevention techniques on the system has been demonstrated by the two-dimensional profile modeling. The prevention technique concerns to the surface recharge, the seawater abstraction, and the hydraulic barrier yielding six prevention schemes; the surface recharge, the seawater abstraction, the hydraulic barrier, and three types of combination among them. Unlike with some other published research, these prevention schemes were investigated while the groundwater extraction is running on to represent continuity supply of water demand.

Numerical results exhibit that running of the model with 10 years simulation time from the condition of 2000 would cause an extensive seawater intrusion as effect of the existing groundwater development policy. Implementation of the surface recharge and the hydraulic barrier can reduce effectively the seawater intrusion problem. The surface recharge is mainly control the problem on the unconfined aquifer, and a small effect is also occurred on the confined aquifer. In addition, combination this surface recharge with the injection well will provide a better result. This numerical investigation obtained result that sustainable groundwater development can be established by managing of the surface recharge rate and the hydraulic barrier.

Another prevention technique of pumping brackish groundwater located on coastline, but numerical result showed that almost no influence to decrease groundwater salinity on the aquifer. For many cases, this technique has shown successfully in implementation. Therefore, determination of the correct position requires study more detail to integrate this numerical model with optimization model.

REFERENCES

Anderson MP., and Woessner MW., 2002, *Applied Groundwater Modeling*, Simulation of flow and advective transport, Academic Press, INC, New York.

Breuck W.D., 1991, *Hydrogeology of Salt Water Intrusion*; A selection of SWIM Papers, International Association of Hydrogeologists, Verlag Heinz Heise, Vol. 11, Hannover.

Foster S., Lawrence A., and Morris B., 1998, *Groundwater in Urban Development*, Assessing management needs and formulating policy strategies, World Bank Technical Paper No. 390.

Mahesha, A., and Nagaraja, S.H., 1996, Effect of natural recharge on seawater intrusion in coastal aquifers, *Journal of Hydrology*, Vol. 174, pp. 211-220.

Melloul, A.J., and Wollman, S.H., 2003, Qualitatively hydrological and land-use planning tool for the Israel coastal aquif*er, The Science of the Total Environment*: 309, pp. 1 – 17.

Oude Essink G.H.P., 2001, Improving Fresh Groundwater Supply – problems and solutions, *Ocean and Coastal Management:* 44 pp 429-449.

Pinder G.F., 2002, *Groundwater Modeling using Geographic Information System*, John Wiley & Sons, Inc, New York.

Rastogi A.K., and Ukarande S.K., 2002, Parametric studies on the effect of field parameters on seawater intrusion in multi-layered coastal aquifers, *Proceeding of the International Groundwater Conference on Sustainable Development and Management of Groundwater Resources in Semi-arid Region with Special Reference to Hard Rocks*, pp. 211-220.

Sherif, M.M., and Hamza, K.I., 2001, Mitigation of Seawater Intrusion by Pumping Brackish Water, *Transport in Porous Media*, Vol. 43, pp. 29-44.

Sophocleous M.A., 2002, Interactions between groundwater and surface water; the state of the science, *Hydrogeology Journal*, Springer-Verlag.

Storch, K.V., 2004, Reliable groundwater management: the continuous improvement method, *Environmental Geology*, 46, pp. 617-621

Voss C.I., and Souza W.R., 1987, Variable Density Flow and Solute Transport Simulation of Regional Aquifers Containing a Narrow Freshwater-Saltwater Transition Zone, *Water Resources Research*, Vol. 23, No. 10, pp.1851-1866.

Wang H.F., and Anderson, MP., 1982, *Introduction to Groundwater Modeling*, W.H Freeman and company, San Fransisco.

CHAPTER 6

FUTURE STUDY OF ASSIGNMENT OF GROUNDWATER RECHARGE ON BOUNDARY CONDITIONS

6.1. GENERAL REMARKS

Identification of the net groundwater recharge is essential for groundwater modeling and water resources management. The recharge is the most difficult components of the water balance to be measured. In spite of several methods for quantifying groundwater recharge are available, all methods are characterized by large uncertainties associated with a numerous stochastic parameters such as soil properties, topography, rainfall intensity, evapo-transpiration, and depth of water table. Consequently, estimation of recharge by using those methods usually ends with different results. In addition, many empirical formulas have been developed to find out the net groundwater recharge, but none of them has shown to be efficient and accurate result. The groundwater recharge may be also estimated by numerical flow model by using many types of information. This method presents an integrative view, but its disadvantage is that calibration of the model is required. Many combinations of recharge rate and transmissivity can yield the observed head. Therefore, these two parameters cannot be estimated at the same time.

On the groundwater flow modeling practice, the recharge can be as a surface recharge and an underground flow recharge. Since the recharge estimation methods remain debatable issue among hydrologist, this chapter proposes an idea for future studies to represent the recharge on the groundwater flow modeling more accurate than the most common implemented technique nowadays. Since the recharge estimation method by considering groundwater level fluctuation is popular way for hydro-geologists, a recharge estimation method in this criterion of Tank Model is being investigated in this study to be discussed in early stage of implementation.

6.2. OVERVIEW RECHARGE ESTIMATION METHODS

6.2.1. Recharge Estimation based on Groundwater Level.

Groundwater recharge can be defined as the entry into the saturated zone of water made available at the water table surface, together with the associated flow away from the water table within the saturated zone (Freeze and Cherry, 1979). Rushton et al. (2004) distinguishes *actual recharge* estimated from groundwater studies for water reaches the water table, from *potential recharge* estimated surface-water and unsaturated zone studies by considering infiltration water. The infiltrated water may or may not reach the water table because of unsaturated zone processes or the ability of saturated zone to accept recharge. Studies on unsaturated zone is also often use term of *groundwater discharge* for the removal of water from the saturated zone across the water-table surface, together with the associated flow toward the water table within the saturated zone. These two processes are intimately interrelated to a pair of parallel processes in the unsaturated zone.

The complexity process associated with recharge becomes a difficulty to find out the accuracy and the fix method for estimation. Subsequently, choosing an appropriate method is extremely valuable to get information on potential controls on recharge. Scanlon and Healy (2002) gave overview of background information for recharge estimation emphasizing recharge from water infiltration. A conceptual model of recharge on a system need to be developed based on information of climate, hydrology, geomorphology, and geology.

The recharge estimation model is broadly categorized three approaches; the soil-water balance, Darcian, and groundwater level fluctuation (Sopcholeous, 1990). The soil-water balance approach that can be represented with absence of surface run-off by the equation as follow;

$$R = P - ET - \Delta S \tag{6.1}$$

Where R is groundwater recharge, P is precipitation, ET is evapo-transpiration, and ΔS is change in soil-water storage in the vadose zone. This equation refers to that aquifer recharge is dependent on meteorological condition, soil, vegetation, physiographic

characteristics, and properties of the geological material through which water flows. The large data demand and given the nature of routinely available data does not usually provide very accurate result.

The Darcian approach offers the most direct measurement of seepage rates. It is laborious and expensive, requiring specialized field equipment and personnel, and highly site-specific. The soil-water flux is obtained based on potential gradient and unsaturated hydraulic conductivity. The potential gradient can be measured by tensiometer, but accurate determination of the conductivity as a function of water content or pressure head is very difficult.

The groundwater level fluctuation approach is more attractive because groundwater level observations are often available. This method also can give information on temporal and spatial recharge variation. However, this method can be misleading if the water-level fluctuations are confused with those resulting from pumping, barometric, or other causes. The groundwater-level fluctuation method is not reliable unless accurate values of aquifer effective storativity are available. Significant errors may appear in recharge estimations by the use of a constant specific yield for unconfined aquifer with a shallow water table.

However, the recharge estimation based on this observed groundwater level may be the most widely used technique (Healy and Cook, 2002; Xu and Tonder, 2001). Advantages of this method are its simplicity and insensitivity to the mechanism by which water moves through the unsaturated zone. Some estimation method based on this approach are *hybrid water-fluctuation method* (Sophocleous, 1990); CRD method of Bredenkamp (Xu and Tonder, 2001), and *Water table fluctuation* (WTF) method of Meinzer (Healy and Cook, 2002).

The water table fluctuation method is based on assumption that the rise of water table due to the recharge water arriving to the aquifer. Recharge is calculated as;

$$R = S_y dh / dt = S_y \Delta h / \Delta t \tag{6.2}$$

Where S_y is specific yield, h is water table height, and t is time. This equation assumes that water arriving at the water table goes immediately into storage. This assumption is

most valid over short periods of time. This equation may be also applied over longer time intervals (seasonal or annual) to produce an estimate of change in subsurface storage, in which sometimes referred to as net recharge.

In groundwater studies, the concept of specific yield or aquifer storativity is used to transform a change in groundwater level to an equivalent change in water storage and hence recharge. In addition, Kayane introduced the important to distinguish the terms ~*specific yield*' and '*tillable porosity*' (Sophocleous, 1990). Specific yield is the volume of water released from a unit volume of saturated aquifer material drained by a falling water table; tillable porosity is the amount of water that an unconfined aquifer can store per unit rise in water table and per unit area. The *tillable porosity* is smaller than the specific yield, yet its application is not an easy task.

Despite of its simplicity and easy to use, some limitations associated with this method are described Healy and Cook (2002) as follow;

1. The method is best applied to shallow water table display sharp water-level rises and declines. Deep aquifers may not display sharp rises because wetting front end to disperse over long distances.
2. Typically, recharge rates vary substantially within a basin, owing to differences in elevation, geology, land-surface slope, vegetation, and other factors. Wells should be located such that the monitored water levels are representative of the catchments as a whole.
3. The method cannot account for a steady rate of recharge. For instance, if the rate of recharge were constant and equal to the rate of drainage away from the water table, water levels would not change and the WTF method would predict no recharge.
4. Other difficulties relate to identifying the cause of water level fluctuation and calculating a value for specific yield.

6.2.2 Tank Model

Basic Concept

Sugawara et al, 1974, initially developed tank model as a run-off model in field of water resource engineering. Now days, this method has been widely applied for recharge

estimation method through some modifications according to problem interest. The tank model requires recorded data of rainfall and groundwater level that has similarity with the CRD model. Similar with some other recharge estimations method using the groundwater level data, the tank model has simplicity and insensitivity to the mechanism by which water moves through the unsaturated zone (Healy and Cook, 2002; Xu et al 2001).

The tank model is a method of modeling of response of the rainfall – river flow volume in present drainage basin. A conceptual diagram of the tank model is shown in figure (6.1). Rainfall coming into a particular area composes two main components. One is surface runoff occurs immediately after rainfall. The other is the base flow, in which rainwater infiltrated to the underground, and then reappears in surface as groundwater base flow. In order to represent the process in the model, a number of tanks are arranged with arbitrary connections. Each water tank has outlets on its bottom and/or side. Water in a tank flows out through each outlet in proportion to the water depth above the outlet. In this study, the tank model is applied for recharge estimation method emphasizing the volume of rainfall flowing into aquifer.

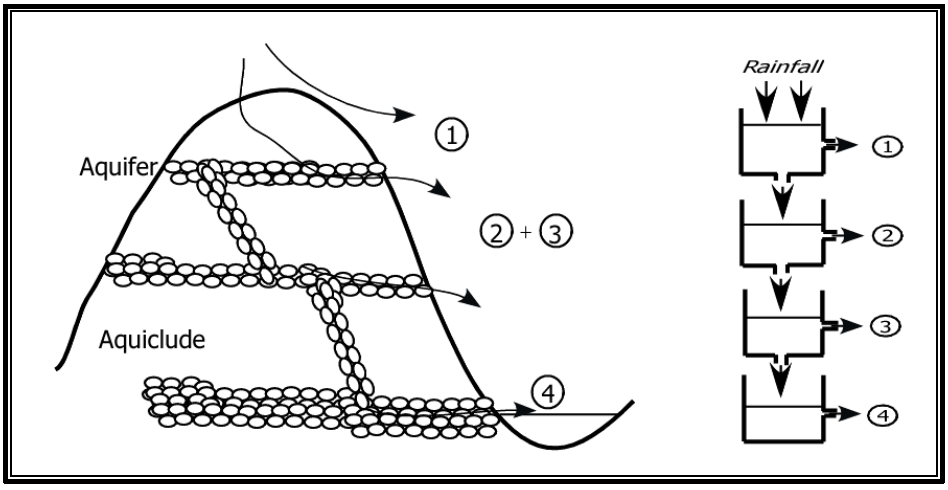

Figure 6.1 Outline of the tank model (JRA in Arai et al, 2003)

Application of the model to quantify recharge rate has been focused on a single tank model. This kind of model composes two layers; upper tank and lower tank, with its configuration and its related coefficient are shown in figure (6.2). The upper tank corresponds to surface runoff and infiltration, and the lower tank to underground flow and groundwater level. Interpretation of the tank model to the physical problem is that

water initially supplied to the top tank by rainfall to the lower tank in connection. By assuming the lower tank is fully saturated, inflow to this tank is considered as recharge. Actual evapo-transpiration is simulated by subtracting from the tank concern starting form the upper tank. If the upper tank is empty, the evaporation will be subtracted form the lower tank for a case of depth of groundwater level is smaller than extinction depth. Storage in each tank is calculated as remainder after addition and deduction of inflow and outflow. All these calculation are performed successively for every time interval.

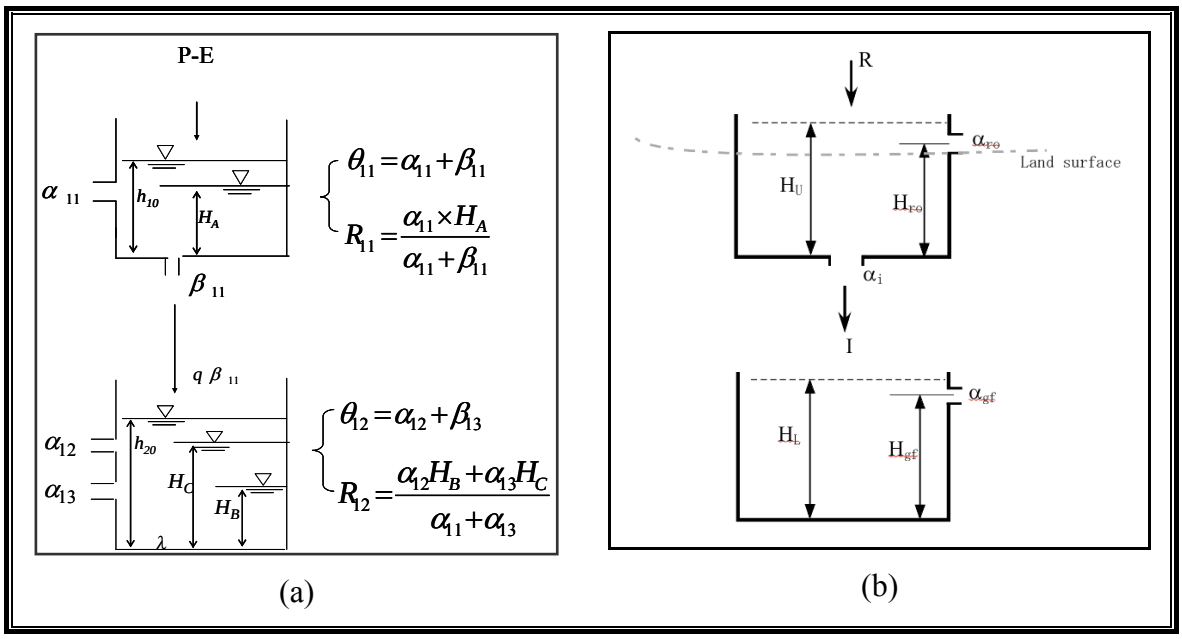

Figure 6.2 Configuration of tank model. (a) The original of tank model, and (b) the modification of tank model.

The figure (6.2a) represents original of the tank model, and figure (6.2b) for modification of the tank model developed in this study. In order to represent the water flowing out from the system, every tank has outlets on its bottom and/or vertical side. In the original of tank model α_{12} and H_C is to represent the intra flow that are avoided in this modification model. Symbols used in this modification model, shown in figure (6.2b), are α_{ro}, α_i, α_{gf} to represent conductance of run-off, infiltration, and groundwater flow, respectively. H_{ro} is head control of run-off (unsaturated zone storage), and H_{gf} for groundwater flow. The I refers to infiltration rate, and R is rainfall intensity. The rate of each component of flow is estimated by multiplying this conductance with gap between water level and height of related outlet. Position of groundwater level is obtained by dividing water height on the lower tank with effective porosity of soil (θ). Comparing

with the recharge estimation purpose, this model is emphasized in generating a number of the Tank Model parameter to reproduce groundwater level fluctuation due to rainfall, and the volume of water comes in to and out from a system.

Formulation

In this study, a code written in C++ has been developed to estimate groundwater level fluctuation on an observation well. Explanation of calculation procedure uses those tank parameters shown in figure (6.2). The calculation is carried out in a time step of the total period of concern. The groundwater level or hydraulic head, H_{Gw}, is counted based on water level in the lower tank, H_L, by the following equation;

$$H_{Gw} = H_{Gw0} + \frac{H_L}{\theta} \tag{6.3}$$

Where H_{Gw0} is the reference groundwater level and θ is effective porosity of material.

Similar to the concept of the CRD method, theory behind this model is water balance on the system. The water stored in tank is equal to the difference between total inflow and total tank outflows. Accordingly, the water level in tank at any time can be constituted as follows;

$$H_U(i) = H_U(i-1) + R(i) - I(i) - q_{ro}(i) \tag{6.4}$$

$$H_L(i) = H_L(i-1) + I(i) - q_{gf}(i) \tag{6.5}$$

Where; i denotes time step, R is rainfall intensity [L], I is portion infiltration [L], q_{ro} is portion of runoff flow [L], and q_{gf} is portion groundwater flow [L]. These last of three parameters are counted by multiply of correspond coefficient and water level gap of each outlets.

Obtaining tank model parameters

There are five unknown parameter of the tank model need to be approximate to produce groundwater level fluctuation due to rainfall. These parameters are determined through trial-and-error procedure to achieve a best fit between observed and estimated hydraulic

head. The best fit can be obtained by minimizing the root means square error (RMSE) and mean error (ME) of those hydraulic heads. Since the fitting process is counted by trial-and-error procedure, the accuracy is specified by user. It is also important to consider time range of a series record data past occurrence in which there is no significant changes in variable affecting the recharge to the slope.

6.3. APPLICATION OF THE TANK MODEL

The proposed method was applied to investigate the changes pore pressure due to rainfall pulse on a slope at Mizusawa,Yamagata Prefecture. This area is well known for heavy snowfall with a number of landslides in the snow-melting season of March to April. Configuration of the investigated slope is shown in figure (6.3) composed two types of geological material; mudstone and colluvial soil. The colluvial soil takes place in upper layer with thickness varying from 10 m in up-hill to 20 m in downhill.

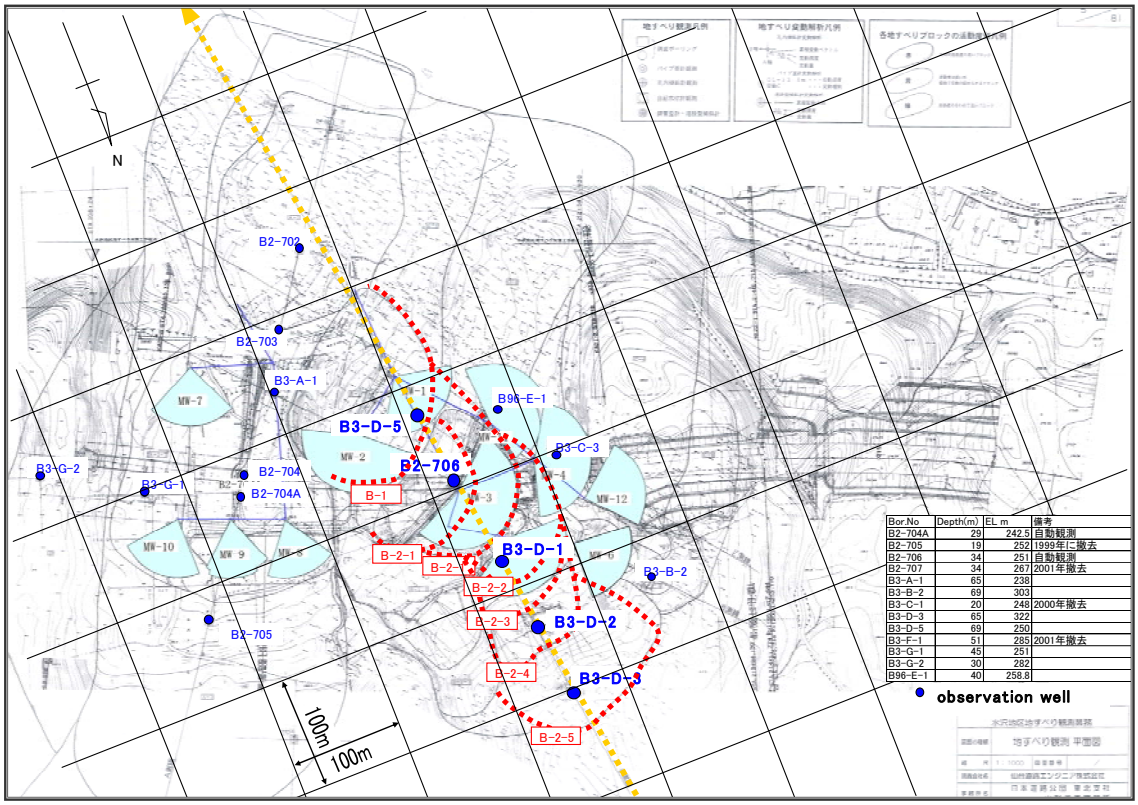

Bor.No	Depth(m)	EL m	備考
B2-704A	29	242.5	自動観測
B2-705	19	252	1999年に撤去
B2-706	34	251	自動観測
B2-707	34	267	2001年撤去
B3-A-1	65	238	
B3-B-2	69	303	
B3-C-1	20	249	2000年撤去
B3-D-3	65	322	
B3-D-5	69	250	
B3-F-1	51	285	2001年撤去
B3-G-1	45	251	
B3-G-2	30	282	
B96-E-1	40	258.8	

Figure 6.3 Map of Misuzawa, Yamagata Prefecture

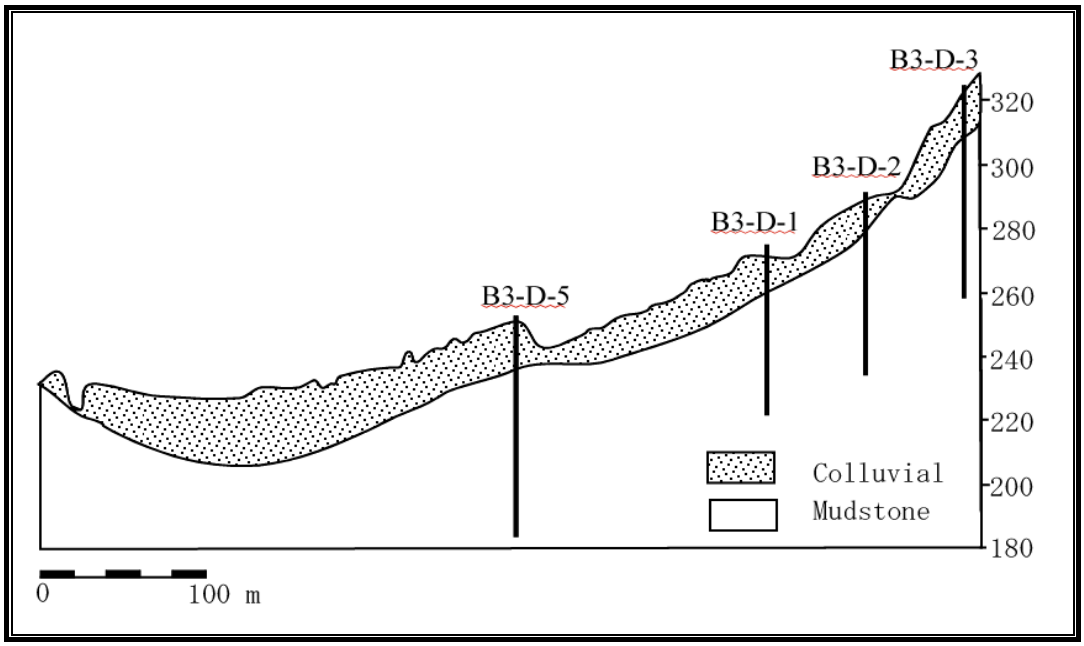

Figure 6.4 Feature of investigated slope at Mizusawa, Yamagata Prefecture.

Four observation wells constructed in this slope, B3-D-1, B3-D-2, B3-D-3, and B3-D-5, were used to investigate reliability of this proposed method. The modeling area covers slope between bore holes B3-D-5 to B3-D-3, which horizontal length of 280 m from surface elevation of 240 – 320 m with lower boundary at elevation of 220 m from mean sea level.

The response of the slope to precipitation intensity was investigated on well of B3-D-5 at downstream boundary, and on well of B3-D-3 at upstream boundary. Analysis was based on data of rainfall intensity and groundwater observation within 183 days (June – November, 1994). The monitoring data of rainfall occurrence is available in one observation point. Since the observed data depict that fluctuation of groundwater level at the well of B3-D-3 is higher than the well of B3-D-5, therefore representation of the hydrogeological parameter into coefficient of tank model has significant difference.

The tank model was applied without considering the component of intra-flow (α_{21} and H_C). This was based on assumption that there is no significant lateral flow occurred from the infiltrated water before reaching water table. Since the position of water table is deeper than the extinction depth and the slope profile and hydraulic gradient shows that the groundwater will flow continuously over time, therefore the H_{gf} also can be set to zero. By using these simplification, unknown variable of the tank model parameters

remain four coefficients: α_{ro}, α_i, α_{gf}, and θ. In order to obtain these parameters, a number of set of approximation values were input to the tank model to estimate hydraulic heads on each well. This is a trial-and-error procedure to find a best match between the observation hydraulic heads with the calculation results. The obtained parameters of tank model is shown in table (6.1), with comparison between the observed hydraulic head (H_obs) with the simulated hydraulic head (H_est) at well of B3-D-3 and of B3-D-5 are shown in figure (6.5) and (6.6), respectively. By using these values, the transient response of the slope to the rainfall pulse can be predicted.

Table 6.1 Obtained value of tank model parameters.

Parameter	**Unit**	**Values at Well**	
		B3-D-5	B3-D-3
Run-off coefficient (α_{ro})	-	0.800	0.850
Infiltration coefficient (α_i)	-	0.750	0.750
Groundwater flow coef (α_{gf})	-	0.075	0.065
Head of outlet of upper tank (H_{ro})	m	0.030	0.020
Effective porosity (θ)	%	0.080	0.015
RMSE	m	0.23	2.39
ME	m	-0.02	-0.43

Estimation of recharge by using the tank model through this procedure is mostly applied for slope seepage problem to predict groundwater fluctuation due to rainfall intensity. This technique is able to represent the water level fluctuation on monitoring wells by considering physical system. As a result, pore water pressure head on the slope can be calculated easily for geotechnical analysis. However, quantification of the recharge is not clearly defined. The similar procedure of recharge estimation can be find in the Cumulative Rainfall Departure (CRD) model, in which to fix the observed head and the estimated head by emphasizing on rainfall fraction entering the aquifer yielding to the groundwater level fluctuation. Therefore, future study is required to calculate the actual recharge entering the hydrogeological system from the surface recharge.

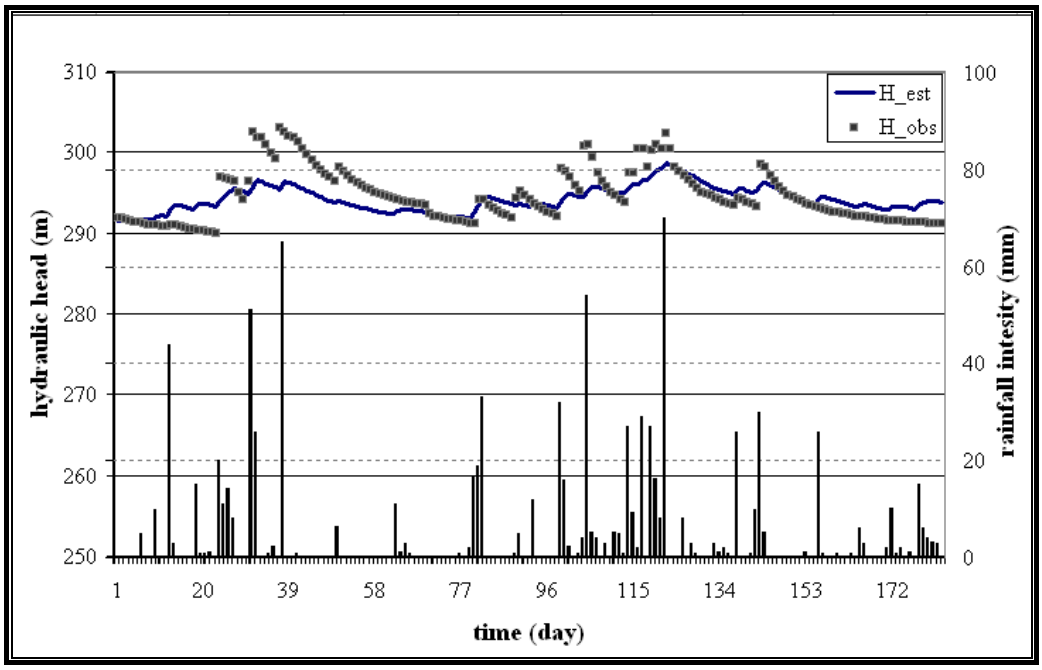

Figure 6.5 *Comparison of observed (H_obs) and estimated hydraulic head (H_est) at bore hole of B3-D-3 by using parameters of tank model at table 6.1.*

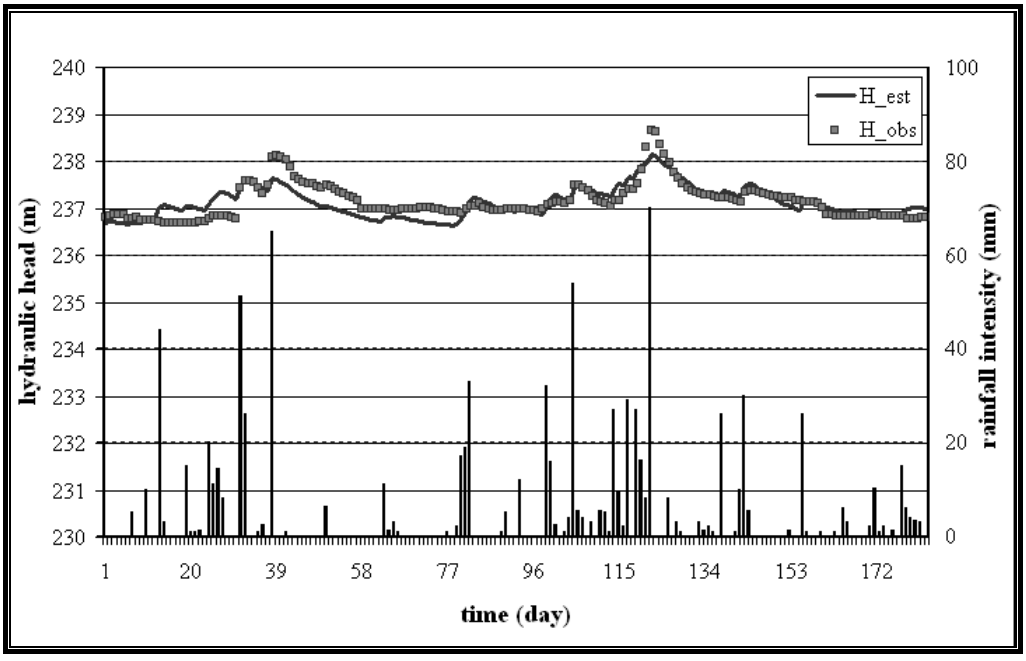

Figure 6.6 *Comparison of observed (H_obs) and estimated hydraulic head (H_est) at borehole of B3-D-5 by using parameters of tank model at table 6.1.*

6.4. COUPLED THE TANK MODEL AND GROUNDWATER FLOW MODEL

In the numerical modeling of groundwater flow practices, the recharge may exist as surface recharge and/or underground flow recharge. These two variables are assigned on the modeling as boundary conditions. Selection of boundary conditions is a critical step in model design and is most subject to error. In steady-state simulations, the boundaries largely determine the flow pattern. Boundary condition influence transient solutions when the effects of the transient stress reach the boundary. In this case, the boundaries must be selected so that the simulated effect is realistic (Anderson and Woessner, 2002).

By considering hydrogeologic conditions, the boundaries can be represented with mathematical statements into three types; (1) Specified head boundaries (Dirichlet conditions), (2) Specified flow boundaries (Neumann conditions), and (3) Head dependent flow boundaries (Cauchy or mixed boundary conditions). For most modeling practice, the surface recharge is generally defined as a specified (pressure) head or specified flow boundaries. However, the underground flow recharge is more complicated, because it can be represented as constant head boundary, specified flux(flow), or head dependent flow boundary. Defining as the constant head boundary is simple way, but too abrupt, and using the specified flux boundary requires an extra simulation leading to an increasing of uncertainty. Therefore, this part describes an integrating of the tank model with the groundwater flow model to investigate representation of the boundaries accurately.

Numerical investigation was carried out for this purpose with case study at Slope of Mizusawa, Yamagata Prefecture. The simulation was carried out by using 2D (two-dimensional) model by considering problem of saturated-unsaturated medium. The governing equation and numerical code development for variable saturated-density flow problem described in the chapter (3), in which become simple for this case because the simulation is only approximated variable saturated and constant density flow. The concept of equivalent freshwater pressure head has advantages to be applied here because the estimated pressure head is similar with pore pressure head used in geotechnical engineering analysis. As result, the developed code taking consideration of freshwater-seawater interface can be easily applied by considering constant density flow

on saturated-unsaturated medium. The numerical groundwater flow model then is integrated with recharge estimation of tank model by using loose coupling system.

The area is discretized with a regularly spaced of Cartesian grid constructed with mesh size of 1.0 by 5.0 m square in the vertical place. The domain discretization results 2979 nodes and 2818 elements shown in figure (6.7). The 183 daily stress periods was simulated to investigate groundwater behavior within slope. For each stress period, the average hydrologic conditions are assumed to remain constant. The simulation was carried by setting boundary conditions as time-dependent boundary condition of fluctuated pore pressure at both vertical sides and of rainfall form top side. The bottom side of the domain was set as no-flow boundary.

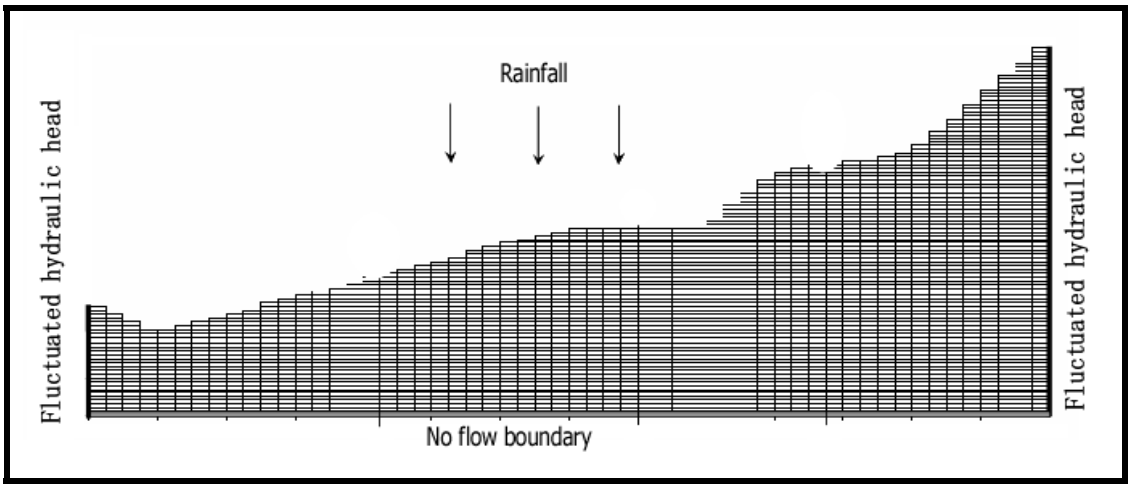

Figure 6.7 Discretization of domain by employing Cartesian grid with mesh size 1 x 5 m, and applied boundary conditions.

To perform simulation, natural initial pore pressure are required to be set everywhere in the aquifer. This value is obtained through an extra initial simulation for steady state case. The time-dependent boundary conditions depicted on figure (6.7) were also modified by using fixed hydraulic head instead of the fluctuated one, and the rainfall is set to be zero. The hydraulic heads on the vertical side boundaries were generated as a linear function from bottom aquifer to top surface.

Assignment of hydrogeological parameter of the system was obtained through calibration procedure of transient problem by employing the boundary conditions such as in figure (6.7). In this step, intrinsic permeability was adjusted to achieve a

reasonable representation of the observed hydraulic head. The estimated hydraulic head was converted to hydraulic head to compare with the observed head from two wells within the model domain. Two monitoring wells with observation data of 183 days were used to compare both hydraulic heads. With a number of simulations, calibrated intrinsic permeability were obtained such as depicted in table (6.3). Matching between the observed and the simulated hydraulic heads produced by using the calibrated parameters are shown in figure (6.7).

Table 6.3 Calibrated Hydrogeological parameter of the evaluated slope

Material	**k_x (m/s)**	**k_y (m/s)**	**Porosity (%)**
Colluviums soil	9.18E-14	9.18E-15	0.30
Mudstone	3.58E-15	3.58E-16	0.25

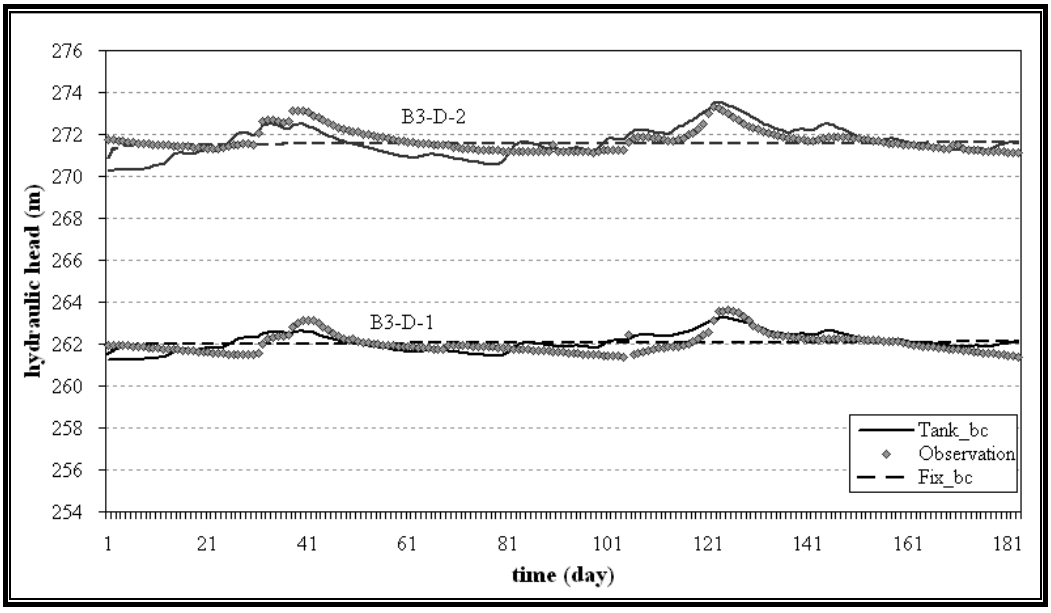

Figure 6.8 Matching observed head (Observation) and estimated head by using tank model (Time_bc) and fixed boundary (Fix_bc) at both vertical side of slope.

In order to investigate the effectiveness of this proposed integration methods, the simulation was run by setting the up-gradient and down-gradient boundary with two difference boundary conditions, fixed and time-dependent hydraulic head, while others

boundaries are set such as shown in figure (6.7). The simulated hydraulic head at two observation points, well of B3-D-1 and B3-D-5, are plotted on figure (6.8). The graph shows clearly that by defining the both vertical sides as fixed hydraulic head (head) boundary, the fluctuation of groundwater level within problem domain can not be represented in both inside wells, even though a same of rainfall intensity is imposed in the top layer to emerge groundwater recharge from infiltration. This means the underflow recharge has a higher influence to hydraulic head changes in the evaluated site than the precipitation. This accurate result of estimation of the hydraulic head produced by this integration models seems to have an important effect to provide a better result of the numerical modeling.

6.5. DISCUSSION

Recharge estimation methods are mainly associated with high uncertainty that is caused by many stochastic parameters required on calculation. Since the estimation based on the groundwater level fluctuation is widely used, Tank Model as a method on this criterion has been observed in this research. By using the most application procedure for the tank model nowadays, this technique can be used to define boundary condition with fluctuated hydraulic head. This method provides an effective way in learning the response of the system than in estimating the net of recharge to the system. Therefore, the underground flow on boundary can be assigned accurately in representing the hydrogeologic condition.

Integrated the recharge estimation model (tank model) with the groundwater flow model to set up boundary condition seems to be useful in improving the accuracy of numerical groundwater flow results. This recharge estimation model can be used to define recharge at boundary condition more accurately comparing by estimating specified flux or assigning constant head boundary. However, this procedure needs to be improved in the future studies particularly to quantify the actual recharge from land surface. By considering estimation technique on the Cumulative Rainfall Departure (CRD) model, the investigation can be focused on the rainfall fraction reaching the groundwater level (saturated zone).

REFERENCES

Anderson MP., and Woessner MW., 2002, *Applied Groundwater Modeling*, Simulation of flow and advective transport, Academic Press, INC, New York.

Arai Y., Ohnishi M., Imai G., Kisanuki T., and Hirayama M., 2003, Preservation countermeasures for groundwater flow against the linear open cut tunnel in low alluvial plain with dissected valley, *Groundwater Engineering* – Recent advances, Balkema, pp. 255-262.

Baalousha H., 2005, Using CRD method for quantification of groundwater recharge in the Gaza Strip, Palestine, *Environmental Geology*: 48, Springer-Verlag, pp. 889-900,.

Butterworth, J.A., Schulze, R.E., Simmonds, L.P., Moriarty, P., and Mugabe, F., 1999, Hydrological processes and water resources management in a dryland environment IV: Long-term groundwater level fluctuations due to variation in rainfall, *Hydrology and Earth System Science:* 3(3), pp. 353-361.

Elhassan A.M., Goto, A., and Mizutani M., 2003, Effect of conjunctive use of water for paddy field irrigation on groundwater budget in an alluvial fan*, Agricultural Engineering International*.

Freeze, R.A., and Cherry, J.A., 1979, *Groundwater*. Prentice Hall Inc.

Healy R.W., and Cook P.G., 2002, Using groundwater levels to estimate recharge, *Hydrogeology Journal*, Springer-Verlag ,Vol. 10, pp. 91-109.

Kinzelbach W., 2002, A survey of methods for groundwater recharge in arid and semi-arid regions, *United Nations Environment Programme*, UNEP/DEWA/RS.02-2.

Koyama, T., Takahashi, K., Ramli, M., and Ohnishi, Y., 2008, Slope stability analysis using coupled tank model and saturated-unsaturated flow simulation, *The 3rd Taiwan-Japan Joint Workshop on Geotechnical Natural Hazards,* Keelung, Taiwan.

Lourenco S.D.N., Sassa K., and Fukuoka H., 2006, Failure process and hydrologic response of a two layer physical model: Implications for rainfall-induced landslides, *Geomorphology :* 73, pp. 115-130.

Moon, S.K., Woo, N.C., and Lee, K.S., 2004, Statistical analysis of hydrographs and water-table fluctuation to estimate groundwater recharge, *Journal of Hydrology:* 292, pp. 198-209.

Ohnishi Y., Ohtsu H., Nishioka T., Naka Y., Yasuda T., and Takahashi K., 2003, Observational method for tunnel construction considering environmental impact to groundwater*, Groundwater Engineering* – Recent Advances, Balkema, pp. 17-24.

Rushton, K.R., Eilers, V.H.M., and Carter, R.C., 2004, Improved soil moisture balance methodology for recharge estimation, *Journal of Hydrology*, article in press, pp. 1-21.

Sanford W., 2002, Recharge and groundwater models: an overview, *Hydrogeology Journal*, Springer-Verlag, 10:110-120.

Scanlon B.R., and Healy R.W., 2002, Choosing appropriate techniques for quantifying groundwater recharge, *Hydrogelogy Journal:* 10, Springer-Verlag, pp. 18-39.

Sophocleous M.A., 1990, Combining the soil water balance and water-level fluctuation methods to estimate natural groundwater recharge; Practical aspects, *Journal of Hydrology*: 124, pp. 229-241.

Sophocleous M.A., 2002, Interactions between groundwater and surface water; the state of the science, *Hydrogeology Journal*, Springer-Verlag.

Tachibana, S., Ohnishi, Y., Nishiyama, S., and Ramli, M., 2006, A New Groundwater Analysis Method with Rainfall for Slope Stability Evaluation, *The 4th Asian Rock Mechanics Symposium*, Singapore.

Tsutsumi A., Jinno K., and Berndtsson R., 2004, Surface and subsurface water balance estimation by the groundwater recharge model and a 3-D two-phase flow model, *Hydrological Sciences*; 49(2), pp. 205-226.

Xu Y., and Tonder G.J., 2001, Estimation of recharge using a revised CRD method, *Water SA* Vol. 27 No. 3.

CHAPTER 7

CONCLUSIONS

7.1. CODE DEVELOPMENT

Modeling of groundwater flow at coastal environment has been performed by using dispersion zone approach to represent the freshwater-seawater interface. Scope of study covers development of new numerical code, assessment of seawater intrusion problem, and mitigation design to combat the problem in order to establish long-term groundwater resources management.

The development of numerical code is concerned to provide a practical and a simple code for application by suppressing the mesh generation problem. It has been chosen SUTRA2D3D as basic code in which employs a hybridization of the finite element method with finite difference method. As a support, a mesh generation code was also developed. The original code of SUTRA2D3D was simplified to be used for simulating variable saturated – density flow on two-dimensional and three-dimensional model only. Simulation of the heat transfer phenomena that available on the original SUTRA2D3D code has been excluded. The governing equations are solved by the Pre-conditioned Bi-conjugate Gradient.

The developed numerical groundwater flow code and the automatic mesh generation code are integrated by using a loose coupling technique in which data transfer is made through input/output model predefined files. Here, the base code has been enhanced ability to simulate the groundwater flow within a domain discretized by employing either the Cartesian mesh or the FEM mesh. Two advantages gained by the new groundwater flow code are the problem mesh generation as principal difficulty in the conventional FEM can be suppressed, and the imposition of the essential boundary condition as deficiency of mesh free method can be done such the conventional FEM.

In-accuracy of the Cartesian mesh to treat shape boundary can be reduced by allowing to generate non-uniform mesh for complex boundaries.

The complexity of the problem has not been able to solve completely in this study. In order to sustain the groundwater development, a vulnerable area requires prevention effort. The end of this research has been investigated numerically dynamic of the interface as a response to a propose prevention technique. A management of the surface recharge, and the injection well (hydraulic barrier) was analyzed to find an effective method to be applied in the field. These two methods were simulated either as an independent or as a combination method. Coupling the surface recharge with the hydraulic barrier shown a satisfactory result to combat seawater intrusion problem. Since the groundwater recharge has important role in modifying the salinity concentration of groundwater, a coupling of numerical flow model with optimization model can be helpful to determine the efficient recharge rate and the effective injection well position.

In addition, the numerical code development requires three more improvements:

1. The application of the developed code employing the Cartesian mesh system for irregular boundaries of domain will produce a jagged boundary. This mesh construction leads to a difficulty in obtaining nodes arranging boundaries. This developed mesh generation code provides output file consisting information of nodes from six directions of the Cartesian mesh. However, the defining parameter values to be imposed in the boundary condition are performed manually. Therefore, development of a graphic user interface to define those variables automatically will gain a significant improvement.
2. Modeling of the freshwater-seawater interface at multi-layer aquifer covering a large area requires a huge number of elements, particularly to avoid numerical dispersion and spurious oscillations problems. In spite of the efficiency of computer memory demand has been improved with hundred thousands element of 3D analysis that can be simulated, but the simulation may need to be carried out with millions element. For this purpose, the parallel computation needs to be implemented.
3. Numerical results may be visualized by using SUTRAPLOT software and ModView Software. The 2D-model visualization can be done easily, but the 3D model cannot be visualized by these softwares if the domain discretization forms a jagged

boundary. The current code may represent the numerical result of the 3D-model with multi cross-sections and maps according to user requirement. For future development, visualization code of the 3-D model is needed.

7.2. NUMERICAL SIMULATION OF DYNAMIC EQUILIBRIUM OF THE INTERFACE

The implementation of the developed numerical code for simulation the groundwater flow at coastal area was demonstrated for field case of Semarang Aquifer, Indonesia. The aquifer system is multi-layer with alternating aquifer-aquitard system. A two-dimensional profile model was constructed by extending the profile 500 m of seaward. The shape of interface reflects the effect of the aquitard. Obtained initial condition through extra simulation produce the interface form with slope that almost similar for both aquifers. However, correspond to the elapsed time a more slightly slope would be formed at the confined aquifer than the unconfined aquifer. This trend was observable for simulation using both calibrated parameter and sensitivity analysis.

The final calibration of the 2D-model could produce accurately the hydraulic head and the groundwater salinity that was compared with the observed data of 1982-1998. By using this calibrated parameter into the 3D-model, numerical results exhibits a similar pattern of the interface form, yet invasion of seawater resulted by the 2D-model deeper than by the 3D-model, particularly in the confined aquifer. This discrepancy was caused by in-accuracy in representing pumping well in the 2D-model and lack data to support the 3D-model. However, combination of these results figures out the important of aquitard between aquifer to the interface form. Extension of the simulation periods to 2010 by using trend of groundwater development in the Semarang City illustrates a critical condition of the aquifer to the seawater intrusion problem that is indicated drastically change of the groundwater salinity after 2000. Sensitivity analysis depicted that the most important parameter to affect the interface form is hydraulic conductivity of the geological stratum. Small influence is caused by underflow recharge and thickness of the aquifer.

7.3. INTEGRATION OF GROUNDWATER FLOW MODEL WITH TANK MODEL.

Since the selection of the boundary conditions is a critical step in model design, and is the most subject to serious error, the assignment of the boundaries requires an accurate representation. However, for most practical modeling, the representation associates with several simplifications yielding to increasing of uncertainty. Therefore, in early stage development for the groundwater flow modeling, the integration of the groundwater model and the tank model is proposed for future studies. The application of this technique for simple field case study in Japan exhibits a satisfactory result in improving the accuracy of numerical results. This integrating model uses a loose coupling system leading to a complicated procedure. Furthermore, this thesis provides only assignment of the boundary condition to define the underground flow recharge. Therefore, a number questions and idea should be explored to find a better procedure of implementation and accurate surface recharge quantification.

REFERENCES

Filipiak, M., 1996, *Mesh Generation*, Edinburgh Parallel Computing Centre, The University of Edinburg.

Katsifarakis, K.L., and Petala, Z., 2006, Combining genetic algorithms and boundary element to optimize coastal aquifers' management, *Journal of Hydrology*, (article in press).

Mantoglou, A., Papantoniou, M., and Giannoulopouos, P., 2004, Management of coastal aquifers based on nonlinear optimization and evolutionary algorithms, *Journal of Hydrology*: 297, pp. 209-228.

Park, C.H., and Aral, M.M., 2004, Multi-objective optimization of pumping rates and well placement in coastal aquifers, *Journal of Hydrology*, 290, pp 80-99.

Xu Y., and Tonder G.J., 2001, Estimation of recharge using a revised CRD method, *Water SA*, Vol. 27 No. 3.